**Distribution Agreement**

In presenting this thesis or dissertation as a partial fulfillment of the requirements for an advanced degree from Emory University, I hereby grant to Emory University and its agents the non-exclusive license to archive, make accessible, and display my thesis or dissertation in whole or in part in all forms of media, now or hereafter known, including display on the world wide web. I understand that I may select some access restrictions as part of the online submission of this thesis or dissertation. I retain all ownership rights to the copyright of the thesis or dissertation. I also retain the right to use in future works (such as articles or books) all or part of this thesis or dissertation.

Signature:

_____          _____
Meghan Elyse Wynne                                              Date

The Mitochondrial Electron Transport Chain Modulates Expression and Secretion of the
Lipoprotein APOE

By

Meghan Elyse Wynne
Doctor of Philosophy

Graduate Division of Biological and Biomedical Science
Neuroscience


_____
Victor Faundez, MD PhD
Advisor


_____
Shannon Gourley PhD
Committee Member


_____
Jennifer Kwong PhD
Committee Member


_____
Steven Sloan PhD
Committee Member


_____
Yoland Smith PhD
Committee Member


Accepted:


_____
Kimberly Jacob Arriola, Ph.D, MPH
Dean of the James T. Laney School of Graduate Studies


_____
Date

The Mitochondrial Electron Transport Chain Modulates Expression and Secretion of the Lipoprotein APOE

By

Meghan Elyse Wynne
B.A., University of California, Berkeley, 2013

Advisor: Victor Faundez, MD PhD

An abstract of
A dissertation submitted to the Faculty of the
James T. Laney School of Graduate Studies of Emory University
in partial fulfillment of the requirements for the degree of
Doctor of Philosophy
in Neuroscience
2023

Abstract


The Mitochondrial Electron Transport Chain Modulates Expression and Secretion of the Lipoprotein APOE

By
Meghan Elyse Wynne

Mitochondria maintain cellular health through several cell-autonomous mechanisms, such as energy production and calcium buffering. While mitochondria are known for these cell-autonomous functions, they can also contribute to cellular homeostasis through non-cell autonomous mechanisms, including modulation of the secretion of proteins and metabolites. Regulation of protein secretion by mitochondria is established for relatively few proteins. These include inflammatory cytokines, growth factor mitokines, plasma protein alpha-fetoprotein, and a small number of mitochondrially-derived peptides. In this dissertation, I test the hypothesis that mitochondrial regulation of protein secretion is more extensive than previously appreciated. I focus on two inner mitochondrial membrane transporters, SLC25A1 and SLC25A4, linked to 22q11.2 deletion syndrome, a strong risk factor for several neurodevelopmental disorders. Genetic disruption of SLC25A1 or SLC25A4 leads to changes in the expression of secreted proteins on par in magnitude with changes in the expression of mitochondrial proteins, supporting the importance of mitochondria in secretome regulation. Loss of either SLC25A1 or SLC25A4 in cell lines caused robust upregulation of the expression and secretion of the lipoprotein APOE. Since APOE is the top genetic risk factor for late onset Alzheimer's disease, I focused on APOE for further study. My work demonstrates that loss of SLC25A1 or SLC25A4 causes APOE upregulation through perturbed electron transport chain assembly. Moreover, direct genetic or pharmacological disruption of electron transport chain complexes I, III, and IV subunits and assembly factors also causes elevated APOE expression and secretion. This APOE upregulation phenotype extends to mitochondrial genes implicated as Alzheimer's risk loci, which encode a complex I subunit and assembly factor. I show that mitochondrial regulation of APOE occurs in iPSC-derived astrocytes, in concert with changes in inflammatory gene expression, supporting the notion that mitochondria can initiate inflammatory signaling in the brain. Together, this body of work supports a new conception for Alzheimer's pathogenesis, in which mitochondria can act upstream of APOE and modulate APOE-dependent disease processes. My findings also add to knowledge of how mitochondria regulate the secretome, providing the first evidence for mitochondria regulating the secretion of a lipoprotein.

Genetic and Pharmacological Disruption of the Mitochondrial Electron Transport Chain
Modulates Expression and Secretion of the Lipoprotein APOE

By

Meghan Elyse Wynne
B.A., University of California, Berkeley

Advisor: Victor Faundez, M.D., Ph.D.

A dissertation submitted to the Faculty of the
James T. Laney School of Graduate Studies of Emory University
in partial fulfillment of the requirements for the degree of
Doctor of Philosophy
Graduate Division of Biological and Biomedical Sciences
Neuroscience
2023

## ACKNOWLEDGEMENTS

**TABLE OF CONTENTS**

# LIST OF FIGURES

**CHAPTER 1: GENERAL INTRODUCTION**

**1.1 Conceptual background and the goals of this thesis**

Understanding pathogenesis mechanisms in neurodevelopmental, psychiatric, and neurodegenerative diseases and disorders continues to be an overarching goal in neuroscience research, since a better understanding of disease mechanisms should lead to more effective treatments. Although neurodevelopmental and neurodegenerative disorders are often conceptualized and thus studied in isolation from one another, recent evidence suggests that these classes of diseases and disorders share genetic and environmental risk factors and cellular mechanisms of pathogenesis (Barnat et al., 2020; Desplats et al., 2020; Hickman et al., 2022; Ivashko-Pachima et al., 2021; Kim et al., 2023; Kovacs et al., 2014; McLaughlin et al., 2017; Modgil et al., 2014; Schor and Bianchi, 2021; Smeland et al., 2021; Van Battum et al., 2015; Vanderhaeghen and Cheng, 2010; Westmark et al., 2016; Wingo et al., 2022). These include exposure to genotoxic agents and immune dysregulation, among other factors (Cheroni et al., 2020; DeMaio et al., 2022; Gauvrit et al., 2022; Gibney and Drexhage, 2013; Hammond et al., 2019; Kisby and Spencer, 2021; Modgil et al., 2014; Patterson, 2009; Shin and Kim, 2023; Tan et al., 2020; Tartaglione et al., 2016). For example, aberrant synaptic pruning mediated by the complement cascade leads to synapse loss and dysfunction and cognitive impairment in models of both schizophrenia and Alzheimer's disease (Bie et al., 2019; Dejanovic et al., 2022; Hong et al., 2016; Sekar et al., 2016; Sellgren et al., 2019; Yilmaz et al., 2021). Furthermore, variations in complement receptor genes are significant genetic risk factors for both diseases in genome wide association studies (GWAS) (Lambert et al., 2009; Naj et al., 2011; Sekar et al., 2016). On the other hand, a deficiency in complement-mediated pruning, leading to an overabundance of synapses, may also play a role in autism spectrum disorders (Mansur et al., 2021; Meng et al., 2022), and a null allele of the complement receptor C4B has been associated with autism (Mostafa and Shehab, 2010; Odell et al., 2005). Complement-dependent synaptic pruning is just one example of how a common mechanism can participate in the etiology of diverse brain

diseases. This information prompted us to measure the extent of molecular overlap between neurodegenerative and neurodevelopmental genes and mechanisms in a systematic manner.

In a collaborative study, we tested the hypothesis that psychiatric and neurodegenerative diseases share a molecular and genetic basis. We assessed how GWAS hits for different diseases correlated with protein abundance in hundreds of human brain proteomes (Wingo et al., 2022). This work identified shared causal proteins and protein-protein interaction networks among psychiatric and neurodegenerative diseases. Gene set enrichment analysis (GSEA) of these shared protein networks implicates synaptic transmission, immune function, and mitochondrial processes as biological processes that play a role across different classes of brain illnesses. These results fall in line with an abundance of evidence demonstrating the importance of synaptic and immune function in brain diseases (Bagni and Zukin, 2019; Barthet and Mulle, 2020; Crabtree and Gogos, 2014; Forrest et al., 2018; Gibney and Drexhage, 2013; Hammond et al., 2019; Lau and Zukin, 2007; Patterson, 2009; Styr and Slutsky, 2018). This work also highlights the need for a better understanding of how mitochondrial biology may influence synaptic and immune function in the brain, in the context of both neurodevelopment and neurodegeneration. While these studies support common pathways in the pathogenesis of neurodevelopmental, psychiatric, and neurodegenerative diseases, they do so by establishing correlations that still need experimental tests. This is the focus of my thesis, where I will test whether mitochondrial genes implicated in 22q11.2 microdeletion syndrome, a neurodevelopmental syndrome arising from haploinsufficiency of genes encoded in the 22q11.2 chromosomal segment, regulate the expression and secretion of the strongest Alzheimer's disease risk factor the lipoprotein APOE.

In the next sections I will introduce 22q11.2 microdeletion syndrome, APOE, and the importance of this lipoprotein to Alzheimer's pathology. This information will provide the landscape that my dissertation navigates.

**1.2 22q11.2 Deletion Syndrome**

We reasoned that a disorder with both neurodevelopmental and neurodegenerative components in which mitochondria are implicated in disease etiology would serve as an excellent model for uncovering novel mitochondrial mechanisms of disease with potential relevance for both neurodevelopment and neurodegeneration. 22q11.2 deletion syndrome is a disorder which fulfills the criteria of having developmental, degenerative, and mitochondrial aspects.

22q11 deletion syndrome is a the most common chromosomal microdeletion disorder, estimated to affect between 1 in 3000 and 1 in 6000 live births (McDonald-McGinn et al., 2015). 22q11 deletion syndrome arises due to meiotic errors in homologous recombination occurring in a genomic region dense with low copy repeats (Edelmann et al., 1999; Saitta et al., 2004). While the size of the 22q11 microdeletion can vary, most individuals with the deletion (80-90%) have the largest variant of the deletion, affecting a region of 3Mb (Edelmann et al., 1999; McDonald-McGinn et al., 2015). This 3Mb deletion creates a haploinsufficiency of 46 protein-coding genes and 17 small regulatory RNAs (Guna et al., 2015). 22q11 deletion syndrome presents as a clinically heterogeneous disorder associated with variable penetrance of cardiac defects, craniofacial malformations, immune deficiency, hypoparathyroidism, gastrointestinal and feeding difficulties, renal anomalies, genitourinary anomalies, and cognitive, social, and affective difficulties (Fiksinski et al., 2021; Jalal et al., 2021; McDonald-McGinn and Sullivan, 2011; Swillen and McDonald-McGinn, 2015; Tang et al., 2014). Individuals with 22q11 deletion syndrome have increased risk for and incidence of a wide array of neurodevelopmental and psychiatric disorders, making it an attractive model for understanding mechanisms of neuropsychiatric disease (Fiksinski et al., 2023; Fiksinski et al., 2018; Jonas et al., 2014; Schneider et al., 2014; Tang et al., 2014; Zinkstok et al., 2019). 22q11 deletion syndrome is most prominently associated with risk for psychosis and schizophrenia (Karayiorgou et al., 1995; Karayiorgou et al., 2010; Murphy, 2002; Schneider et al., 2014; Xu et al., 2008). It is estimated that approximately 25% of those with

22q11 deletion syndrome will develop schizophrenia, and that approximately 1-2% of schizophrenia prevalence can be attributed to 22q11 deletion syndrome (Karayiorgou et al., 2010; Murphy et al., 1999; Owen and Doherty, 2016). In addition to schizophrenia, individuals with 22q11 deletion syndrome are often diagnosed with attention deficit hyperactivity disorder (ADHD), intellectual disability, autism spectrum disorders (ASD), and/or anxiety disorders (Karayiorgou et al., 2010; Schneider et al., 2014; Tang et al., 2014). Interestingly, in addition to the high rates of neurodevelopmental and psychiatric diseases in 22q11 deletion syndrome, the disorder was recently associated with a neurodegenerative condition, early onset Parkinson's disease (Butcher et al., 2013; Mok et al., 2016). Estimates suggest that 22q11 deletion syndrome confers approximately 20 times the risk for early onset Parkinson's disease of that seen in the general population (Zinkstok et al., 2019). These epidemiological facts highlight how 22q11 deletion syndrome is a syndrome that possesses both neurodevelopmental and neurodegenerative etiological components.

## 1.3 Disease mechanisms in 22q11 deletion syndrome

What is known about the molecular and cellular mechanisms thought to be responsible for brain-related phenotypes in 22q11 deletion syndrome? Recent work with mouse models of 22q11 shows the chromosomal deletion causes an array of neurodevelopmental and synaptic defects. These include altered expression of presynaptic and postsynaptic genes (Al-Absi et al., 2020; Nehme et al., 2022), increased spontaneous neuronal excitability (Khan et al., 2020), disordered and reduced axonal outgrowth (Fernandez et al., 2019; Motahari et al., 2020; Mukai et al., 2015; Piskorowski et al., 2016), reduced mushroom dendritic spines and dendritic branching (Al-Absi et al., 2020; Al-Absi et al., 2022; Jeanne et al., 2021; Stark et al., 2008; Xu et al., 2013), increased dendritic spine turnover (Fenelon et al., 2013), deficits in parvalbumin interneuron numbers and migration (Al-Absi et al., 2020; Meechan et al., 2009; Meechan et al., 2012;

Mukherjee et al., 2019; Piskorowski et al., 2016; Toritsuka et al., 2013; Tripathi et al., 2020), changes in short term and long term synaptic plasticity (Al-Absi et al., 2020; Al-Absi et al., 2022; Devaraju et al., 2017; Earls et al., 2010; Fenelon et al., 2013; Khan et al., 2020; Piskorowski et al., 2016; Tripathi et al., 2020), and impaired neurogenesis (Karpinski et al., 2022; Meechan et al., 2009; Paronett et al., 2015). Not surprisingly, 22q11 deletion syndrome mice display defects in neuronal synchronization and function of several circuits important in learning and memory, including hippocampal networks, prefrontal microcircuits, hippocampal-prefrontal circuits, thalamocortical circuits, and thalamus-amygdala circuits (Amin et al., 2017; Choi et al., 2018; Chun et al., 2017; Chun et al., 2014; Earls et al., 2010; Eom et al., 2017; Fernandez et al., 2019; Hamm et al., 2017; Kahn et al., 2020; Loisy et al., 2022; Marissal et al., 2018; Meechan et al., 2015; Mukherjee et al., 2019; Paronett et al., 2015; Piskorowski et al., 2016; Sigurdsson et al., 2010; Tripathi et al., 2020; Zaremba et al., 2017). This phenotypic pleiotropy raises the question of what cellular and molecular substrates are responsible for these alterations.

How does haploinsufficiency of any one of the 46 protein-coding genes, or combinations thereof, in the 22q11 deletion syndrome interval cause synaptic and behavioral defects? To answer this question, many have used a candidate gene approach of targeting singular genes within the 22q11 deletion interval in mice to understand how haploinsufficiency of each gene in the interval affects synaptic and circuit function (Devaraju et al., 2017; Fenelon et al., 2011; Fernandez et al., 2019; Gogos et al., 1999; Harper et al., 2012; Hiramoto et al., 2011; Jeanne et al., 2021; Keser et al., 2019; Mukai et al., 2015; Paronett et al., 2015; Stark et al., 2008; Toritsuka et al., 2013). While this work has produced promising discoveries showing associations of genes with changes in synaptic structure and plasticity and function of cognitive circuits, details about the cellular mechanisms that link these genes to synaptic and cognitive function remain mostly unclear (Motahari et al., 2019; Zinkstok et al., 2019).

**1.4 Mitochondria in models of 22q11 deletion syndrome**

In the pursuit to understand molecular/cellular mechanisms that link 22q11 deletion syndrome to changes in synaptic and circuit function, recent evidence from preclinical models supports an important role for mitochondrial dysfunction in mediating defects in neurodevelopment and synaptic function. Seven genes in the deletion interval (SLC25A1, MRPL40, PRODH, COMT, SNAP29, RTL10, and TXNDR2) code for mitochondrially localized proteins (Rath et al., 2021). Below, we highlight findings related to the mitochondrial ribosome, reactive oxygen species (ROS) regulation, and electron transport function. There is evidence that COMT, PRODH, and SNAP29 contribute to 22q11 deletion syndrome phenotypes but how these proteins participate in mitochondrial functions is less clear (Armando et al., 2012; Crabtree et al., 2016; Gogos et al., 1999; Gothelf et al., 2005; Paterlini et al., 2005).

**1.4.1 TXNRD2 and ROS regulation**

The 22q11 deletion syndrome gene *Txndr2* encodes a mitochondrial thioredoxin antioxidant enzyme, making it important in redox regulation. The LaMantia lab identified a role for this gene in underconnectivity of association cortices, a phenotype often observed in 22q11 deletion syndrome and other neurodevelopmental disorders (Padula et al., 2015; Romme et al., 2017; Schreiner et al., 2017). These associative connections are most often made by projection neurons in layer 2/3 of the cortex and their disruption in mice leads to behavioral deficits (Douglas and Martin, 2007; Fernandez et al., 2019). The LaMantia lab showed that density of layer 2/3 projection neurons is reduced in the *LgDel* mouse model of 22q11 deletion syndrome, and the extent of this neuronal loss correlates with performance on a reversal learning task (Meechan et al., 2015). They followed up on this work recently, showing that differentiation is impaired and

ROS levels are increased in layer 2/3 projection neurons of *LgDel* mice and associated cognitive deficits are modulated by mitochondrial regulation of oxidative stress (Fernandez et al., 2019). Knockdown of the 22q11 deletion syndrome gene *Txndr2* specifically in wild type layer 2/3 neurons phenocopied axonal and dendritic growth and underconnectivity deficits observed in *LgDel* mice. Moreover, increasing expression of TXNDR2 or providing antioxidants pharmacologically rescued growth, underconnectivity, and cognitive deficits in *LgDel* mice. These results provide strong evidence for a role of mitochondrial regulation of oxidative stress in the proper formation and function of cortico-cortical circuits affected in 22q11 deletion syndrome.

### 1.4.2 MRPL40 and mitochondrial ribosomes

Work from our lab and others points to a role for the mitochondrial ribosome (mitoribosome) in phenotypes associated with 22q11 deletion syndrome. The mitoribosome consists of large and small subunits made up of 52 and 30 nuclear-encoded mitochondrial ribosome proteins, respectively, as well as rRNA and one structural tRNA (Ferrari et al., 2021). Within the 22q11 interval, MRPL40 encodes a protein that is part of the large subunit of the mitoribosome. Mitoribosomes are needed to synthesize proteins encoded in the mitochondrial genome. Mitochondrial DNA (mtDNA) encodes only 13 proteins, all of which are essential components of the electron transport chain machinery (Ferrari et al., 2021). Thus, assembly and function of mitoribosomes is crucial for maintaining the health of the electron transport chain. Mutations in mitoribosome subunit and assembly genes cause multisystemic mitochondrial disorders that frequently present with neurological symptoms, such as intellectual disability, seizures, psychosis, language and speech delays, encephalomyopathy, or neurodegeneration (Bulow et al., 2022; Ferrari et al., 2021; Lake et al., 2017; Munoz-Pujol et al., 2023).

Recent work with iPSC-derived forebrain-like excitatory neurons generated from 22q11 deletion syndrome patients and healthy controls showed a role for MRPL40 in supporting

mitochondrial electron transport chain activity in 22q11 deletion syndrome. This study showed that 22q11 deletion syndrome neurons display reduced mitochondrial respiration, ATP levels, and levels of mitochondrially-encoded electron transport chain subunits (Li et al., 2019). They hypothesized this defect arises due to changes in mitoribosome function and generated an MRPL40-deficient iPSC line to test this hypothesis, demonstrating heterozygosity of MRPL40 led to similar defects as those seen in the 22q11 deletion syndrome patient lines (Li et al., 2019). These results support the notion that the mitoribosome is essential in maintaining function of the electron transport chain in neurons and suggest that defective mitoribosome function disrupts oxidative phosphorylation in 22q11 deletion syndrome neurons.

Mitochondrial oxidative phosphorylation plays a key role in fueling neurotransmission, and mitochondrial electron transport chain subunits synthesized locally at the synapse are important for activity-dependent synaptic plasticity (Bulow et al., 2022; Hall et al., 2012; Kuzniewska et al., 2020; Rangaraju et al., 2019). These data imply that impairments to machinery necessary for electron transport chain synthesis, such as haploinsufficiency of a mitoribosome subunit, would adversely affect synaptogenesis and synaptic refinement in response to neuronal activity during development. Our lab analyzed the publicly available BrainSpan and EvoDevo datasets and found that the expression of MRPL40 and other mitochondrial ribosomes differs depending on the stage of neurodevelopment, with mitochondrial ribosome expression being the highest in the period between birth and adolescence (Bulow et al., 2022; Gokhale et al., 2021). This expression pattern suggests mitochondrial ribosomes are likely to modulate this stage of development, which is a window of sensitivity in which disrupted formation and plasticity of cortical circuits may occur to increase risk for schizophrenia and other neurodevelopmental disorders (Hoftman et al., 2017; Meredith et al., 2012; Reh et al., 2020). In line with this assertion, we knocked down MRPL40 expression in developing *Drosophila* via RNAi and saw increases in the numbers and complexity of synaptic boutons at the larval neuromuscular junction and behavioral alterations (Gokhale et

al., 2021). Moreover, these morphological changes coincided with increased amplitude of evoked excitatory junctional potentials at this synapse (Gokhale et al., 2021). Together, these results support the hypothesis that mitoribosomes regulate synaptogenesis.

Another recent study adds to evidence that mitoribosomes are crucial for proper neurodevelopment. A screen of selected 22q11 deletion syndrome genes in zebrafish showed that loss of function mutations in *Mrpl*40 decrease neurogenesis and lead to reduced overall brain size (Campbell et al., 2023). In this zebrafish model, the loss of MRPL40 function also led to impairments in sensorimotor gating in a prepulse inhibition assay (Campbell et al., 2023). Finally, work from the Zakharenko lab on a mouse haploinsufficient for MRPL40 further demonstrates a role for mitoribosomes in synaptic plasticity. They demonstrated that reduction in MRPL40 gene expression results in impaired short-term potentiation and deficits in working memory in adult mice (Devaraju et al., 2017). Their work suggests this phenotype arises in part due to changes in mitochondrial calcium buffering that alter presynaptic $Ca^{2+}$ levels (Devaraju et al., 2017). Importantly, they were able to rescue defective short-term potentiation arising from haploinsufficiency of MRPL40 by overexpressing the mitochondrial adenine nucleotide transporter SLC25A4, a transporter that we have shown interacts with another mitochondrial protein encoded in the 22q11 deleted locus, SLC25A1 (Gokhale et al., 2019). Altogether, the available data support an important role for mitoribosomes in modulation of electron transport chain function and synaptic calcium levels that can affect neurogenesis, synaptogenesis, synaptic plasticity, and circuit function.

**1.4.3 Disruption of the electron chain function and mitoribosomes mediated by SLC25A1**

A final mitochondrial gene that I will focus on in this introduction that resides in the 22q11 deletion syndrome interval is SLC25A1. This gene is beginning to receive attention in the cancer

field. SLC25A1 encodes a carrier channel on the inner mitochondrial membrane that allows the TCA cycle metabolite citrate to move out of mitochondria (Taylor, 2017). Cytoplasmic citrate plays important roles as a precursor in the generation of acetyl-CoA, a molecule needed for lipid synthesis and as a source of acetyl groups for protein post-translational modification (Pietrocola et al., 2015; Taylor, 2017). Mutations in SLC25A1 are associated with two diseases, a severe neurometabolic disease (combined D-2- and L-2-hydroxyglutaric aciduria) and a congenital myasthenic syndrome that can also present with intellectual disability (Balaraju et al., 2020; Chaouch et al., 2014; Nota et al., 2013). Combined D-2- and L-2-hydroxyglutaric aciduria is often fatal early in life and presents with neurological symptoms that include neonatal epileptic encephalopathy and developmental delay (Nota et al., 2013). Mutations in SLC25A1 have also been associated with defective myelin formation (Edvardson et al., 2013; Nowacki et al., 2022).

Our lab became interested in SLC25A1 after uncovering that it was a network hub in the protein expression changes associated with 22q11.2 deletion syndrome. We compared proteomic profiles of fibroblasts of 22q11 deletion syndrome patients with childhood psychosis with those of their unaffected relatives. We also compared these patient proteomes with proteomes from the cortex and hippocampus of the *Df16A(+/-)* 22q11 mouse model and its wild type control. Bioinformatic analyses of these proteomes identified mitochondria as a preponderantly affected organelle and SLC25A1 and SLC25A4 (a gene not in the 22q11 deletion syndrome interval but also previously implicated (Devaraju et al., 2017)) as hub proteins driving disease-associated changes in gene expression (Gokhale et al., 2019). These findings raised the question of what functions mediated by SLC25A1 and SLC25A4 may lead to alterations in neurodevelopment or synaptic function. To begin to answer this question, we used a neuroblastoma cell line where SLC25A1 was FLAG-tagged, paired with mass spectrometry of proteins that precipitate with a FLAG antibody, to identify the proteins that physically interact in complex with SLC25A1. This experiment demonstrated that SLC25A1 interacts with several electron transport chain proteins,

spanning complexes I-V, as well as many other members of the SLC25A transporter family, including SLC25A4. These results support the hypothesis that SLC25A1 regulates the expression of subunits of the electron transport chain, and thus influences electron transport chain function. In support of this hypothesis, we showed that SLC25A1-deficient cells indeed have impaired mitochondrial respiration (Gokhale et al., 2021).

Changes in mitochondrial electron transport chain function downstream of SLC25A1 deficiency suggest SLC25A1 could regulate mitoribosome function. Using biochemical assays, we showed that SLC25A1 physically and genetically interacts with mitochondrial ribosomal proteins including MRPL40, and loss of SLC25A1 is associated with reduced expression of mitoribosome proteins and mitochondrially-encoded transcripts (Gokhale et al., 2021). We showed that reduced expression of SLC25A1 phenocopies reduced mitoribosome expression in morphological analysis of the larval *Drosophila* neuromuscular junction, with reduced expression of SLC25A1 being associated with overgrowth of the NMJ (Gokhale et al., 2021). Furthermore, knockdown of both *Slc25a1* and mitoribosome gene expression concurrently does not exacerbate these phenotypes, supporting the notion that SLC25A1 and MRPL40 act in the same pathway to regulate synaptogenesis and synaptic function.

Since SLC25A1 and SLC25A4 interact, we used the *Drosophila* larval neuromuscular junction to also assess how reduced expression of SLC25A4 affected synaptic development. Similar to knockdown of *Slc25a1* or *Mrpl40*, we observed that reduction in SLC25A4 caused overbranching of *Drosophila* NMJs. This phenotype predicts potential changes in neuronal excitability. We took electrophysiological recordings from the larval NMJ and observed that reduction in SLC25A1 or SLC25A4 is associated with changes in the frequency of spontaneous excitatory neurotransmitter release and, in the case of SLC25A4, reduced paired pulse facilitation (Gokhale et al., 2019). We wondered whether these changes in neuronal excitability could result from changes in mitochondrial calcium buffering. To provide support for this idea, we showed that

the loss of either of these proteins in a lymphoblast cell line is associated with deficient mitochondrial calcium influx (Gokhale et al., 2019). Changes in synaptic development and neurotransmission we observed with loss of SLC25A1 or SLC25A4 suggest these proteins are capable of influencing circuit function and behavior. As sleep is disrupted across many neuropsychiatric illnesses, we used an activity monitoring assay in *Drosophila* mutants to test this hypothesis. Interestingly, we found cell type specific alterations in sleep, with sleep being affected by knockdown of *Slc25a4* specifically in glutamatergic neurons and knockdown of *Slc25a1* specifically in catecholaminergic neurons. Our finding that SLC25A1 and SLC25A4 regulate mitochondrial calcium buffering and physically interact, along with the evidence that SLC25A1 modulates mitoribosome function are interesting in light of findings by the Zakharenko lab in which MRPL40 also regulates mitochondrial calcium buffering. Their work demonstrated that overexpression of SLC25A4 rescued mitochondrial calcium buffering defects mediated by haploinsufficiency of MRPL40 (Devaraju et al., 2017). Together, the current data suggest an intimate association between inner mitochondrial membrane transporters and the mitoribosome in modulation of mitochondrial calcium buffering that can impact synaptic and cognitive function. Further work is needed to understand precisely how these mitochondrial proteins are linked to calcium buffering capacity and whether there are additional mechanisms by which mitoribosomes and mitochondrial inner membrane transporters influence synapses and circuits.

Thus far, the work on mitochondria in 22q11 deletion syndrome, including our own, has focused on cell autonomous effects on mitochondrial function, with an emphasis on bioenergetics and calcium and ROS regulation (Devaraju and Zakharenko, 2017; Motahari et al., 2019). We hypothesize that the effects of haploinsufficiency of mitochondrial genes in 22q11.2 deletion syndrome could also produce non-cell autonomous effects that extend beyond traditional mitochondrial biology. For instance, cell-type specific disruption of mitochondrial function in astrocytes can cause secondary neurodegeneration in neuronal cell types, pointing towards a

non-cell autonomous role for mitochondria in neuronal regulation (Ignatenko et al., 2018; Murru et al., 2019). Moreover, defects in mitochondria can alter the expression of genes with diverse non-mitochondrial functions, including chromatin-modifying genes and genes involved in transmembrane signal transduction pathways (Picard et al., 2015; Picard et al., 2014; Sturm et al., 2023). Furthermore, mitochondria are strong modulators of behavior and cognition (Chandra et al., 2017; Gebara et al., 2021; Hollis et al., 2015; Kasahara et al., 2006; Sharpley et al., 2012). Yet, precise mechanisms that link mitochondria to synaptic structure and circuit function are only beginning to be elucidated (Kanellopoulos et al., 2020, Rosenberg A., 2022 #670; Rosenberg et al., 2022). We believe these data suggest mitochondria are likely to influence synapses through non-cell autonomous mechanisms, in addition to their importance in providing fuel and buffering calcium to regulate synaptic function. Protein secretion is a key aspect of intercellular communication, and mitochondria are known to regulate the secretion of a handful of proteins, such as inflammatory cytokines and growth factor mitokines (Durieux et al., 2011; Lemmon and Schlessinger, 2010; Reichardt, 2006; Riley and Tait, 2020; Tse and Wong, 2019), Thus, we posit that mitochondria are poised to regulate the expression of a number of heretofore unknown secreted proteins capable of modulating synaptic and cognitive function. My thesis will explore this notion of a more extensive regulation of protein secretion by mitochondria in response to dysfunction of genes implicated in 22q11.2 deletion syndrome, the citrate transporter SLC25A1 and adenine nucleotide transporter SLC25A4.

**1.5 Parkinson's disease and 22q11.2 microdeletion syndrome as conceptual guides to the neurobiology of APOE, an Alzheimer's risk factor.**

In this section I will describe the literature that supports the 22q11 microdeletion syndrome as a risk factor for neurodegeneration through increased risk of Parkinson's disease, and I will

present the logic of studying the molecular mechanisms downstream of selected genes located in the 22q11.2 chromosomal locus. In particular, I will focus on the mitochondrial inner membrane transporter SLC25A1 and its interactors.

Studies on brain-related disease mechanisms of 22q11 deletion syndrome have thus far focused almost exclusively on neurodevelopment or phenotypes in adults reminiscent of psychiatric diseases (Sumitomo et al., 2018; Zinkstok et al., 2019). In addition to modulating risk for neurodevelopmental orders, 22q11 deletion syndrome increases risk for a neurodegenerative disorder, early onset Parkinson's disease (PD), by an estimated 20-fold (Mok et al., 2016). Parkinson's disease is a heterogenous neurodegenerative disorder characterized by motor dysfunction due to degeneration of dopaminergic neurons in the substantia nigra pars compacta and their axonal projections to the striatum. Motor symptoms include bradykinesia, hypokinesia, rigidity, resting tremor, and postural instability, but patients frequently experience non-motor symptoms as well, such as depression, cognitive impairment, and sleep problems (Kalia and Lang, 2015). In addition to loss of nigral dopaminergic neurons, another pathological hallmark of Parkinson's disease is the presence of aggregates known as Lewy bodies that contain the protein α-synuclein (Kalia and Lang, 2015). Although the age of onset of motor symptoms is earlier in patients with 22q11 deletion syndrome, the clinical characteristics and responses to Parkinson's disease dopamine replacement therapy appear comparable to cases of idiopathic Parkinson's disease (Boot et al., 2019). One study examined neuropathology in postmortem brain tissue of 3 patients with 22q11 deletion syndrome and Parkinson's disease and found extensive loss of dopaminergic neurons in the substantia nigra in all 3 patients and accumulation of Lewy bodies in 2 of the 3 (Butcher et al., 2013).

What is known about how haploinsufficiency of genes in the 22q11 deletion syndrome interval could lead to Parkinson's disease? Although many mouse models of 22q11 deletion syndrome are available, only one study has looked at Parkinson's disease-related symptomology

in 22q11 deletion syndrome mice. This study found that 22q11 deletion syndrome mice display increased expression of alpha-synuclein and motor coordination deficits in the rotarod test, which are ameliorated by reducing gene dosage of alpha synuclein (Sumitomo et al., 2018). This data supports the notion that preclinical models of 22q11 deletion syndrome can be used to model at least some aspects of Parkinson's disease, but much work is still needed to understand more about the molecular/cellular mechanisms that contribute to Parkinson's disease in 22q11 deletion syndrome. One hypothesis on how 22q11 deletion syndrome predisposes to Parkinson's disease is that changes in levels of dopamine and its metabolites occur due in part to haploinsufficiency of the COMT gene in the interval, which encodes an enzyme involved in the degradation of dopamine and other catecholamines (Boot et al., 2019; Butcher et al., 2017). Another hypothesis is that changes in mitochondrial function due to haploinsufficiency of several mitochondrial genes in the 22q11 interval contributes to elevated Parkinson's disease risk (Boot et al., 2019; Zinkstok et al., 2019). This notion is supported by the fact that multiple mutations that cause or predispose to Parkinson's disease are in mitochondrial genes (Borsche et al., 2021). Moreover, mitochondrial toxins are known to cause parkinsonism in humans and animal models (Borsche et al., 2021; Exner et al., 2012). Interestingly, one case report found that a case of 22q11 deletion syndrome where Parkinson's disease was diagnosed coincided with the patient having a further mutation in the HTRA2/PARK13 gene, a mitochondrial protease (Gambardella et al., 2018). This finding supports the hypothesis that mitochondrial dysfunction contributes to Parkinson's disease pathogenesis in the context of 22q11 deletion syndrome.

Altogether, the presence of both neurodevelopmental and neurodegenerative phenotypes in 22q11 deletion syndrome and changes in mitochondrial function associated with the syndrome suggest it can serve as a good model for uncovering novel mitochondrial mechanisms that have the potential to contribute to a broad range of brain illnesses. Founded on this notion, we used an unbiased transcriptomic and proteomic approach to prioritize targets downstream of two

mitochondrial genes associated with 22q11 deletion syndrome, SLC25A1, which localizes to the 22q11.2 microdeleted segment, and its interactor SLC25A4. We uncovered a novel link between SLC25A1 and SLC25A4 in controlling the steady state levels of subunits and activity of the electron transport chain, which in turn modulates the expression and secretion of the lipoprotein APOE, a protein strongly implicated in Alzheimer's disease. This response is part of a general modification of the secreted proteome which includes inflammatory factors. This suggests a non-cell autonomous response to gene defects in the 22q11.2 segment but, in addition, it reveals a novel mechanism by which cells respond to mitochondrial distress. In this thesis, I use the expression of APOE to measure and dissect this novel pathway. In the following section, I provide the foundation for why I selected APOE to study this mitochondrial mechanism, based on the roles played by APOE in the brain and in Alzheimer's disease. We postulate that SLC25A1, the electron transport chain, and APOE act in sequence to link a neurodevelopmental disorder, 22q11.2 microdeletion syndrome, with pathogenesis mechanisms of a neurodegenerative disease, Alzheimer's, thus expanding the reach of 22q11 deletion syndrome beyond Parkinson's disease.

## 1.6 The neurobiology of APOE and Alzheimer's disease

Apolipoprotein E (APOE) is a main lipoprotein in the brain whose primary function is to transfer lipid and cholesterol between brain cells (Dietschy and Turley, 2001). Interest grew in understanding what roles APOE plays in the brain when it was discovered in the early 1990s that the APOE4 allele of the *APOE* gene is strongly associated with late onset Alzheimer's disease (Corder et al., 1993; Strittmatter et al., 1993). This finding has since been confirmed by several GWAS studies and APOE4 is considered the strongest genetic risk factor for sporadic forms of Alzheimer's disease (Belloy et al., 2019). Besides APOE4, APOE3 and APOE2 are the other common alleles of the gene. APOE2 is protective against Alzheimer's disease and APOE3 is not

associated with a change in disease risk (Belloy et al., 2019; Corder et al., 1994). These associations with risk are also dependent on gene dosage, where having two copies of APOE4 increases risk and decreases age at onset of disease, whereas the opposite is true for those with two copies of APOE2 (Belloy et al., 2019; Farrer et al., 1997).

The main pathological hallmarks of Alzheimer's disease are the deposition of extracellular plaques containing amyloid β (Aβ), generated from amyloidogenic processing of the amyloid precursor protein (APP), and intracellular neurofibrillary tangles composed of hyperphosphorylated tau protein (Association, 2023). Because APOE was found to bind to Aβ when APOE4 was discovered as a risk allele, much of the initial focus on understanding how APOE influences AD pathogenesis centered around modulation of Aβ generation and clearance by APOE (Raulin et al., 2022; Strittmatter et al., 1993). Strong evidence indicates that APOE4 increases Aβ deposition and impairs plaque clearance (Liu et al., 2013; Raulin et al., 2022). Interestingly, APOE4 also increases tau deposition and phosphorylation in humans and iPSC AD patient cell lines (Therriault et al., 2020; Wadhwani et al., 2019).

In addition to influencing the pathological hallmarks of AD, APOE regulates synaptic and cognitive function, neuroinflammation, glucose and lipid metabolism, and mitochondrial function (Bu, 2009; Liu et al., 2013; Martens et al., 2022; Raulin et al., 2022). APOE4 reduces the availability of AMPA and NMDA receptors to be recycled to the cell surface, impairing the ability to modulate synaptic strength (Chen et al., 2010). Dendritic spine density and branching are also reduced in APOE4 knock-in mice that carry a humanized APOE4 allele (Dumanis et al., 2009; Ji et al., 2003; Wang et al., 2005). These synaptic deficits coincide with reduced performance in spatial memory and working memory assays (Bour et al., 2008; Hartman et al., 2001). APOE4 is strongly associated with impaired brain glucose uptake, and reduced glucose uptake is also predictive of progressive cognitive decline in humans (Farmer et al., 2021; Hunt et al., 2007; Reiman et al., 2005; Silverman et al., 2001). APOE is linked to inflammation through modulation

of glia function (Parhizkar and Holtzman, 2022). For instance, the conversion to a particular microglia transcriptomic profile associated with increased cytokine secretion and neurodegenerative disease requires APOE upregulation (Keren-Shaul et al., 2017; Krasemann et al., 2017). APOE4-mediated inflammation may also involve increased breakdown of the blood brain barrier, in part due to isoform-dependent pericyte degeneration (Barisano et al., 2022; Halliday et al., 2016; Montagne et al., 2020).

In addition to the roles discussed above, many studies have demonstrated that APOE isoform influences mitochondrial function. Initial interest in how APOE affects mitochondria came from studies showing that fragments of APOE bind to mitochondrial respiratory complexes and impair respiration, although these studies failed to explain how APOE could make it into mitochondria without having a mitochondrial targeting sequence, which was engineered out for these studies (Chang et al., 2005; Nakamura et al., 2009). Subsequent work has shown that APOE4 is strongly associated with reduced mitochondrial respiration (Area-Gomez et al., 2020; Farmer et al., 2021; Orr et al., 2019; Schmukler et al., 2020; Valla et al., 2010). Mitophagy, the process by which mitochondria are degraded, also appears impaired in the presence of the APOE4 allele, suggesting damaged mitochondria fail to be broken down (Schmukler et al., 2020; Simonovitch et al., 2019). Moreover, APOE4 is associated with increased activity at mitochondria – ER contacts, resulting in increased phospholipid and cholesterol ester synthesis (Tambini et al., 2016). Furthermore, APOE particles transferred to glia from neurons also sequester neurotoxic lipids before they are broken down by the mitochondrial β-oxidation pathway in glia. The abilities to both transfer and metabolize toxic lipids are impaired in the presence of the APOE4 allele (Ioannou et al., 2019; Liu et al., 2017; Qi et al., 2021). Importantly, a declining ability to deal with toxic lipids is associated with increased ROS and inflammation (Liu et al., 2017; Mi et al., 2023; Parhizkar and Holtzman, 2022).

A common thread through all these studies is that the relationship between APOE and mitochondria is studied with the assumption in mind that mitochondria are downstream of APOE, where mitochondria are bystanders reacting to the APOE4 allele. While these studies provide strong evidence that APOE4 is associated with impaired mitochondrial function, no one has tested the hypothesis that mitochondria may influence APOE function. Given that mitochondrial changes are observed very early in AD and are correlated with synaptic and cognitive decline, it seems that the idea that mitochondria can act upstream of APOE would be an important hypothesis to consider (Dragicevic et al., 2010; Galea et al., 2022; He et al., 2019; Mahapatra et al., 2023; Terada et al., 2020; Venkataraman et al., 2022; Yao et al., 2009). Another consideration to the notion that mitochondria could act upstream of APOE is that recent Alzheimer's disease GWAS studies identified a handful of loci where mitochondrial genes are prioritized candidates for the link between the SNP and its resulting effect on changes in gene expression that mediate disease risk. These mitochondrial genes include NDUFS3, NDUFAF7, and COX7C (Bellenguez et al., 2022; de Rojas et al., 2021; Kunkle et al., 2019). NDUFS3 is a subunit of complex I of the electron transport chain, while NDUFAF7 is an assembly factor needed to help the many subunits of complex I come together to form a functional complex. COX7C is a subunit of complex IV of the electron transport chain. Thus, the activity and assembly of the electron transport chain is genetically tied to Alzheimer's risk. Interestingly, one study showed that variation in the mitochondrial uncoupling protein UCP4, which allows the electron transport chain to run without making ATP, modifies AD risk in APOE4 carriers (Montesanto et al., 2016). This finding suggests that the relationship between APOE and mitochondria could in fact be bidirectional. Since both the electron transport chain and APOE are tied to Alzheimer's genetic risk, we postulated that mitochondria could regulate APOE function.

**1.7 Significance of this dissertation research**

In this thesis, I test the hypothesis that mitochondrial dysfunction controls the expression and secretion of APOE. I tested this hypothesis focusing on dysfunction of inner mitochondrial membrane transporters implicated in 22q11.2 deletion syndrome and Alzheimer's genetic risk loci involved in electron transport chain assembly and function. This hypothesis is a departure of the conventional model of Alzheimer's pathogenesis that considers that mitochondria are affected by APOE (Mahley, 2023). My hypothesis upends this idea, as my results suggest that mitochondria are able to act upstream of APOE rather than downstream. This new model has important implications for Alzheimer's disease, which I describe below.

We show that increased APOE expression and secretion occurs in response to impaired function and assembly of the electron transport chain. This APOE upregulation in response to electron transport defects occurred both directly, in response to mutagenesis of Alzheimer's linked genes encoding electron transport chain subunits and assembly factors, and indirectly through mutagenesis of mitochondrial transporters linked to 22q11.2 deletion syndrome that regulate the electron transport chain. These findings demonstrate that diverse mitochondrial proteins can act upstream of APOE, and thus mitochondria are capable of regulating APOE-dependent cellular processes. This result challenges conventional models of Alzheimer's disease where mitochondria are placed downstream of APOE (Mahley, 2023). Instead, our work supports the notion that mitochondria can participate in the disease process in a feedforward loop where disturbances to APOE or other pathology may impact mitochondria but mitochondria can also influence APOE and other disease processes in turn (Fig 1). The model that I postulate whereby mitochondria are upstream of APOE predicts that, in an Alzheimer's mouse model, changes in expression of mitochondrial proteins should occur before AD-associated APOE upregulation. I tested this prediction in the 5xFAD mouse model where I found that mitochondrial defects indeed precede APOE upregulation. Thus, our findings suggest that mitochondria are potentially suitable targets early on in disease pathogenesis to avert or delay APOE-dependent disease progression.

Further work is needed to understand more details on the cell type/regional specificity of this mechanism in the brain and identify components of the mitochondria-nuclear pathway regulating APOE, which could serve as a promising drug target.
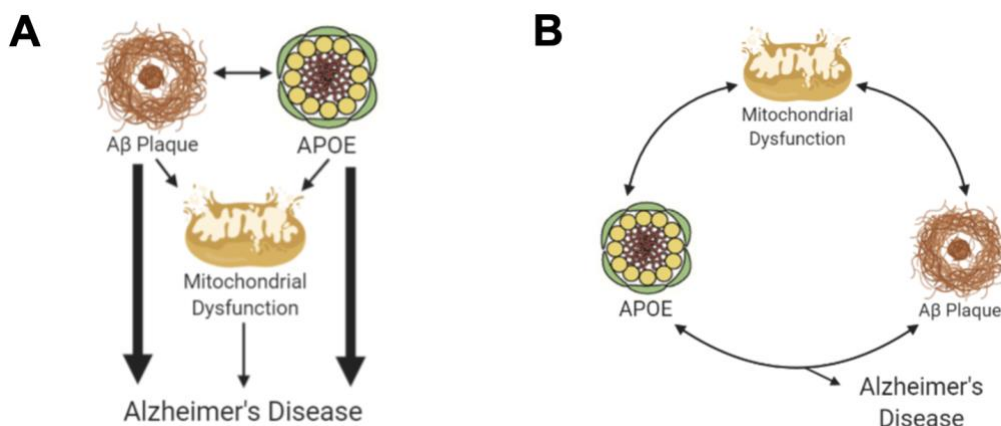


**Figure 1 Models of Alzheimer's disease pathogenesis.**

**A)** Conventional view of AD focuses on Aβ (and/or Tau) and APOE4 as primary disease drivers. Mitochondria are downstream bystanders that react to Aβ, Tau, and APOE. **B)** Our data pose an updated model in which mitochondria, Aβ, Tau, and APOE form a feedforward loop in which disturbances to any of these factors affect the others and drive disease. Mitochondria are thus capable of acting as upstream disease drivers in this model.

While we focused on Alzheimer's disease due to the outsized risk APOE4 plays in disease risk, our findings likely have relevance for understanding other diseases. APOE4 increases risk for dementia with Lewy bodies, frontotemporal lobar degeneration, cerebral amyloid angiopathy, proteinopathies involving α-synuclein, tau, and TDP-43, cardiovascular conditions including coronary artery disease and myocardial infarction, and cognitive decline in Down syndrome (Antonarakis et al., 2020; Belloy et al., 2019). Our results suggest mitochondrial-dependent APOE regulation could play a role in modulating progression or outcomes in these diseases as well, especially in APOE4 carriers. Beyond disease, our findings also likely have relevance for understanding neurodevelopmental processes. For example, cholesterol delivered in glial APOE

particles to neurons is crucial for synaptogenesis (Mauch et al., 2001). Moreover, a recent study found that APOE antagonizes axon growth in developing cortical neurons while promoting dendritic spine formation (Jin et al., 2023). Finally, APOE competes with Reelin for binding to the VLDL and ApoeR2 receptors and inhibits Reelin-induced downstream signaling (D'Arcangelo et al., 1999). Reelin-mediated signaling is important in neuronal migration and maturation, as well synaptic plasticity, learning, and memory (D'Arcangelo et al., 1995; Del Rio et al., 1997; Qiu and Weeber, 2007; Stranahan et al., 2013; Wedenoja et al., 2010; Weeber et al., 2002). Interestingly, genetic variations in Reelin also modify disease risk for schizophrenia, other neurodevelopmental disorders, and Alzheimer's disease (Chen et al., 2017; Di Donato et al., 2022; Lopera et al., 2023; Marzan et al., 2021). Thus, mitochondria may be capable of modulating synaptogenesis, neuronal migration, and synaptic plasticity through a plethora of APOE-dependent mechanisms. These hypotheses warrant further investigation.

Findings from this dissertation also add to knowledge on mitochondrial biology. We provide evidence to suggest that mitochondria extensively regulate protein secretion and provide the first example of mitochondria regulating the secretion of a lipoprotein. This builds on knowledge that mitochondria regulate the secretion of inflammatory cytokines and a handful of other proteins, such as the growth factor mitokines FGF21 and GDF15 (Durieux et al., 2011; Marchi et al., 2023). Our data add to growing evidence that mitochondria can regulate cellular function in a non-cell autonomous manner. We also provide further support for the hypothesis that mitochondrial dysfunction can induce neuroinflammation, thus positioning mitochondria as modulators of another important disease mechanism. Finally, this dissertation research provides an example of using genes associated with a rare neurodevelopmental disorder to better understand mechanisms of a common neurodegenerative disease. These results support the notion that neurodevelopment and neurodegeneration can share pathological mechanisms, and

rare disorders can provide models for understanding cellular mechanisms with importance to more common diseases (Hickman et al., 2022; Lee et al., 2020a).

# CHAPTER 2:
# APOE EXPRESSION AND SECRETION ARE MODULATED BY MITOCHONDRIAL DYSFUNCTION

Meghan E. Wynne[1], Oluwaseun Ogunbona[1-2], Alicia R. Lane[1], Avanti Gokhale[1], Stephanie Zlatic[1], Chongchong Xu[3], Zhexing Wen[1,3,9], Duc Duong[4], Sruti Rayaprolu[9]
Anna Ivanova[4], Eric A. Ortlund[4], Eric B. Dammer[4], Nicholas T. Seyfried[4], Blaine R. Roberts[4], Amanda Crocker[5], Vinit Shanbhag[6],
Michael Petris[6], Nanami Senoo[7], Selvaraju Kandasamy[7], Steven M. Claypool[7], Antoni Barrientos[8], Aliza P. Wingo[9], Thomas S. Wingo[9], Srikant Rangaraju[9], Allan Levey[9], Erica Werner[1*], Victor Faundez[1*].

Departments of Cell Biology[1], Pathology and Laboratory Medicine[2], Psychiatry and Behavioral Sciences[3], Biochemistry[4], and Neurology[9], and Human Genetics[9], USA, 30322, Emory University, Atlanta, Georgia, USA, 30322. Program in Neuroscience[5], Middlebury College, Middlebury, Vermont 05753. Department of Biochemistry[6], University of Missouri, Columbia, MO 65211. Department of Physiology[7], The Johns Hopkins University School of Medicine, Baltimore, MD 21205. Department of Neurology and Biochemistry & Molecular Biology[8], University of Miami Miller School of Medicine, FL 33136.

## 2.1 Abstract

Mitochondria influence cellular function through both cell-autonomous and non-cell autonomous mechanisms, such as production of paracrine and endocrine factors. Here, we demonstrate that mitochondrial regulation of the secretome is more extensive than previously appreciated, as both genetic and pharmacological disruption of the electron transport chain caused upregulation of the Alzheimer's disease risk factor apolipoprotein E (APOE) and other secretome components. Indirect disruption of the electron transport chain by gene editing of SLC25A mitochondrial membrane transporters as well as direct genetic and pharmacological disruption of either complexes I, III, or the copper-containing complex IV of the electron transport chain, elicited upregulation of APOE transcript, protein, and secretion, up to 49-fold. These APOE phenotypes were robustly expressed in diverse cell types and iPSC-derived human astrocytes as part of an inflammatory gene expression program. Moreover, age- and genotype-dependent decline in brain levels of respiratory complex I preceded an increase in APOE in the 5xFAD mouse model. We propose that mitochondria act as novel upstream regulators of APOE-dependent cellular processes in health and disease.

**2.2 Introduction**

Mitochondria are necessary for maintaining cellular and organismal health and function, by generating energy and serving as hubs for diverse metabolic and signaling pathways (Nunnari and Suomalainen, 2012). The majority of the mitochondrial functions described so far are cell-autonomous. However, mitochondria are also capable of influencing cellular function from a distance in a non-cell-autonomous manner. These non-cell-autonomous mechanisms, mostly elicited after cellular or mitochondrial damage, encompass intercellular transfer of mitochondria to secretion of endocrine and paracrine factors (D'Acunzo et al., 2021; Durieux et al., 2011; Hayakawa et al., 2016; Liu et al., 2021). These secreted factors include proteins encoded in the nuclear genome, such as alpha-fetoprotein, inflammatory cytokines and type I interferons, and growth factor mitokines (Bar-Ziv et al., 2020; Chung et al., 2017; Dhir et al., 2018; Durieux et al., 2011; Jett et al., 2022; Kim et al., 2013; Riley and Tait, 2020; Shimada et al., 2012; West et al., 2015). A second class of non-cell-autonomous factors are mitochondrially-derived peptides, encoded in the mitochondrial genome (Kim et al., 2017). Mitokines and mitochondrially-derived peptides modulate cell survival, metabolic and lipid homeostasis, body weight, longevity, and aging, a primary risk factor for cognitive decline in humans (Chung et al., 2017; Flippo and Potthoff, 2021; Klaus and Ost, 2020; Mullican et al., 2017; Tsai et al., 2018). In models of Alzheimer's disease, the mitochondrially-derived peptide humanin can reduce apoptosis, inflammation, accumulation of plaque-forming Aβ peptides, and cognitive deficits (Hashimoto et al., 2001; Tajima et al., 2005; Yen et al., 2013). The ability of factors encoded in the nuclear and mitochondrial genomes to regulate inflammation, lipid metabolism, aging, and Alzheimer's disease mechanisms suggests that mitochondrial-dependent modulation of protein secretion could modify neurological disease pathogenesis prior to cell death.

Here, we sought to identify proteins whose expression and secretion is modulated by mitochondrial function through an unbiased interrogation of human transcriptomes and proteomes. We focused our attention on factors whose expression is sensitive to mutations

affecting the inner mitochondrial membrane citrate transporter SLC25A1 and the ADP-ATP transporter SLC25A4 (ANT1). We chose these mitochondrial transporters because they have been genetically implicated in neurodevelopment, brain metabolism, psychiatric disease, and neurodegeneration (Balaraju et al., 2020; Chaouch et al., 2014; Edvardson et al., 2013; Gokhale et al., 2019; Kato et al., 2018; Lin-Hendel et al., 2016; Nota et al., 2013; Rigby et al., 2022; Siciliano et al., 2003). For example, SLC25A1 is a causal gene in two genetic diseases, a severe neurometabolic disease (combined D-2- and L-2-hydroxyglutaric aciduria) and a congenital myasthenic syndrome presenting with intellectual disability (Balaraju et al., 2020; Chaouch et al., 2014, Nota et al., 2013) (OMIM 615182- 618197). In addition, SLC25A1 is part of the chromosomal interval deleted in 22q11.2 deletion syndrome, a microdeletion syndrome associated with neurodevelopmental, psychiatric, and neurodegenerative diseases (Butcher et al., 2013; Schneider et al., 2014; Zinkstok et al., 2019). SLC25A1 has been implicated as a hub factor underlying a mitochondrial protein network, which includes SLC25A4, that is disrupted in 22q11.2 deletion syndrome cells (Gokhale et al., 2019). Since SLC25A1 and SLC25A4 coprecipitate (Gokhale et al., 2019), we hypothesized the existence of common downstream secretory and mitochondrial targets elicited by their mutation. We discovered that loss of SLC25A1 or SLC25A4 affected the secreted proteome as well as the mitochondrially annotated proteome. Apolipoprotein E (APOE) was among the secreted factors whose expression was increased in both SLC25A1 and SLC25A4 mutants. We focused on APOE since it is the main carrier of lipids and cholesterol in the brain (Mahley, 2016), and it is tied to cognitive function, neuroinflammation, and neurological disease risk (Belloy et al., 2019; Lanfranco et al., 2021; O'Donoghue et al., 2018; Parhizkar and Holtzman, 2022). Importantly, the APOE4 allele is known as the strongest genetic risk factor for sporadic Alzheimer's disease (Belloy et al., 2019). We found that APOE expression was increased by mutations of mitochondrial SLC25A transporters, which indirectly compromised the integrity of the electron transport chain, as well as by directly mutagenizing either assembly factors or subunits of complexes I, III, and IV of the electron

transport chain. While the APOE4 allele is thought to cause mitochondrial dysfunction in Alzheimer's disease (Area-Gomez et al., 2020; Chen et al., 2011; Mahley, 2023; Orr et al., 2019; Tambini et al., 2016; Yin et al., 2020), our study places mitochondria upstream of APOE, uncovering a novel function for these multifaceted organelles.

**2.3 Results**

**2.3.1 Genetic Disruption of Inner Mitochondrial Membrane Transporters Alters the Secretome**

Our goal was to identify secreted factors whose expression is modulated by genetic defects in nucleus-encoded mitochondrial genes. We hypothesized that changes in the secretome would affect the capacity of conditioned media to support cell growth in a genotype-dependent manner. Thus, we applied conditioned media from wild-type (*SLC25A1+*) and SLC25A1-null HAP1 cells (*SLC25A1Δ*) to cells from both genotypes and measured cell growth. We used this near-haploid human leukemia cell line since it has a short doubling time, and thus rapid protein turnover, making it well-suited to rapidly respond to changes in subproteomes, such as the secretome and mitoproteome. We dialyzed conditioned media from wild-type and *SLC25A1Δ* cells to exclude effects of metabolites, pH, and small peptides present in media (Fig. 2A). Dialyzed conditioned media from wild-type and *SLC25A1Δ* cells supported wild-type cell growth (Fig. 2A). Wild type cells similarly responded to dialyzed media from both genotypes, increasing growth by 50% as compared to non-dialyzed media (Fig. 2A compare columns 1, 3 and 2, 4). In contrast, while *SLC25A1Δ* cells fed with wild-type dialyzed conditioned media doubled in number (Fig. 2A, compare columns 5 and 7), dialyzed conditioned media from *SLC25A1Δ* cells fed onto themselves did not support their growth as compared to media from wild-type cells (Fig. 2A compare columns 7 to 8 and 6 to 8). These results suggest that wild-type cells and *SLC25A1Δ* cells condition media differently.

To identify compositional differences between wild-type and *SLC25A1Δ* conditioned media, we analyzed the proteome and transcriptome of *SLC25A1Δ* cells (Fig 2B, D-F, H-I). Fetal bovine serum in media prevented us from a direct analysis of the conditioned media by mass spectrometry. We annotated the *SLC25A1Δ* proteome and transcriptome with the human secretome database (Uhlen et al., 2019) and the Mitocarta 3.0 knowledgebase (Rath et al., 2021) to comprehensively identify differences in secreted factors and the consequences of the *SLC25A1*

mutation on mitochondria. We simultaneously analyzed the proteome and transcriptome of *SLC25A4Δ* cells to determine whether changes in the *SLC25A1Δ* proteome and transcriptome resulted specifically from the loss of SLC25A1, or could be generalized to another inner mitochondrial membrane transporter (Fig. 2C and G). We selected SLC25A4, as it encodes an ADP-ATP translocator that interacts with SLC25A1 (Gokhale et al., 2019). Tandem mass tagging mass spectrometry and RNAseq revealed that *SLC25A1Δ* cells underwent more extensive changes of their proteome and transcriptome than *SLC25A4Δ* cells (compare Fig. 2B with C and F with G). For example, 668 proteins significantly changed their expression in *SLC25A1Δ* cells compared to 110 proteins in *SLC25A4Δ* cells (log2 fold of change of 0.5 and p<0.05, Fig. 1B and C). Similarly, the *SLC25A1Δ* transcriptome was represented by 2433 transcripts whose expression was changed in *SLC25A1*-null cells, a 4-fold difference compared to the 560 transcripts found in *SLC25A4Δ* cells (log2 fold of change of 1 and p<0.001, Fig. 2F and G). Principal component analysis and 2D-tSNE analysis indicated that the whole measured proteome and transcriptome of *SLC25A1Δ* cells diverged strongly from wild-type cells, while *SLC25A4Δ* cells were more closely related to wild-type cells than *SLC25A1Δ* cells (Fig 2D and H). The same outcome was obtained by unsupervised clustering when considering proteins and transcripts significantly changed in at least one of these genotypes (Fig 2E and I), as *SLC25A4Δ* clustered with wild-type cells rather than *SLC25A1Δ* cells. Despite the abundance of altered gene products in these *SLC25A1Δ* and *SLC25A4Δ* datasets, there was limited overlap in proteomes and transcriptomes, with only 84 proteins and 385 mRNAs shared by both genotypes (Fig 2J). Notably, the congruency of the shared proteomes and transcriptomes reached only 0.9% of all the gene products whose expression was modified. This represents 27 proteins and transcripts similarly modified in *SLC25A1Δ* and *SLC25A4Δ* datasets (Fig 2J). Of these 27 common hits, one was annotated to mitochondria, FASTKD2, and five were annotated to the secreted human proteome, including soluble proteins such as apolipoprotein E (APOE) and cytokine receptor-like factor 1 (CRLF1) (Elson et al., 1998; Wernette-Hammond et al., 1989) (Fig 2J). APOE protein and

transcript were among the most upregulated factors in both *SLC25A1Δ* and *SLC25A4Δ* cells (Fig 2B-C and F-G).

Close to 10% of all the *SLC25A1Δ* and *SLC25A4Δ* proteome hits were proteins annotated to mitochondria, with a discrete overlap of 10 mitochondrial proteins between these two mutant genotypes, mostly downregulated constituents of complex III of the electron transport chain (Fig. 1K, UQCRB11, UQCRB, UQCRC2, and UQCRQ) as well as a factor required for the assembly of respiratory supercomplexes, COX7A2L (Fig. 2K) (Lobo-Jarne et al., 2018). The enrichment of secreted proteome annotated proteins was modest yet significant in *SLC25A1Δ* and *SLC25A4Δ* cells. Surprisingly, this degree of enrichment in components of the secretome was comparable to the enrichment of Mitocarta 3.0 annotated proteins in both mitochondrial mutants (Fig. 2L, M, and N). These results show that mutations affecting two inner mitochondrial membrane transporters, SLC25A1 and SLC25A4, similarly affect the secreted and mitochondrial proteomes.

We analyzed *SLC25A1Δ* and *SLC25A4Δ* datasets for additional commonalities at the ontological level, using the ClueGO tool to annotate datasets based on genotype and whether a factor was up- or down-regulated. The annotated datasets were used to simultaneously query the KEGG, REACTOME and GO CC databases. The proteome and transcriptome of both mutants identified developmental ontologies as shared terms, irrespective of whether factors were up- or down-regulated (Fig. 2O-P) gray nodes and supplementary file 1, (tissue development GO:0009888, Bonferroni corrected p=1.9E-26 and 2.3E-11 for the transcriptome and proteome, respectively). However, there were ontologies that stood out by their genotype- and up-regulation-dependent specificity. For instance, the most prominent ontology annotated to up-regulated *SLC25A1Δ* proteome and transcriptome hits was steroid biosynthesis (KEGG:00100, Bonferroni corrected p= 3.6E-8 and 1.9E-8 for the transcriptome and proteome, respectively. Fig. 2O-P). However, the expression of genes annotated to sterol biosynthesis ontologies was not modified in *SLC25A4Δ* mutants, even though the proteome and transcriptome of *SLC25A4Δ* cells showed increased expression of APOE, a cholesterol transport lipoprotein. These findings suggest that

expression of APOE and other hits common between these two mutant genotypes occurs independently from modifications in cholesterol synthesis pathways.
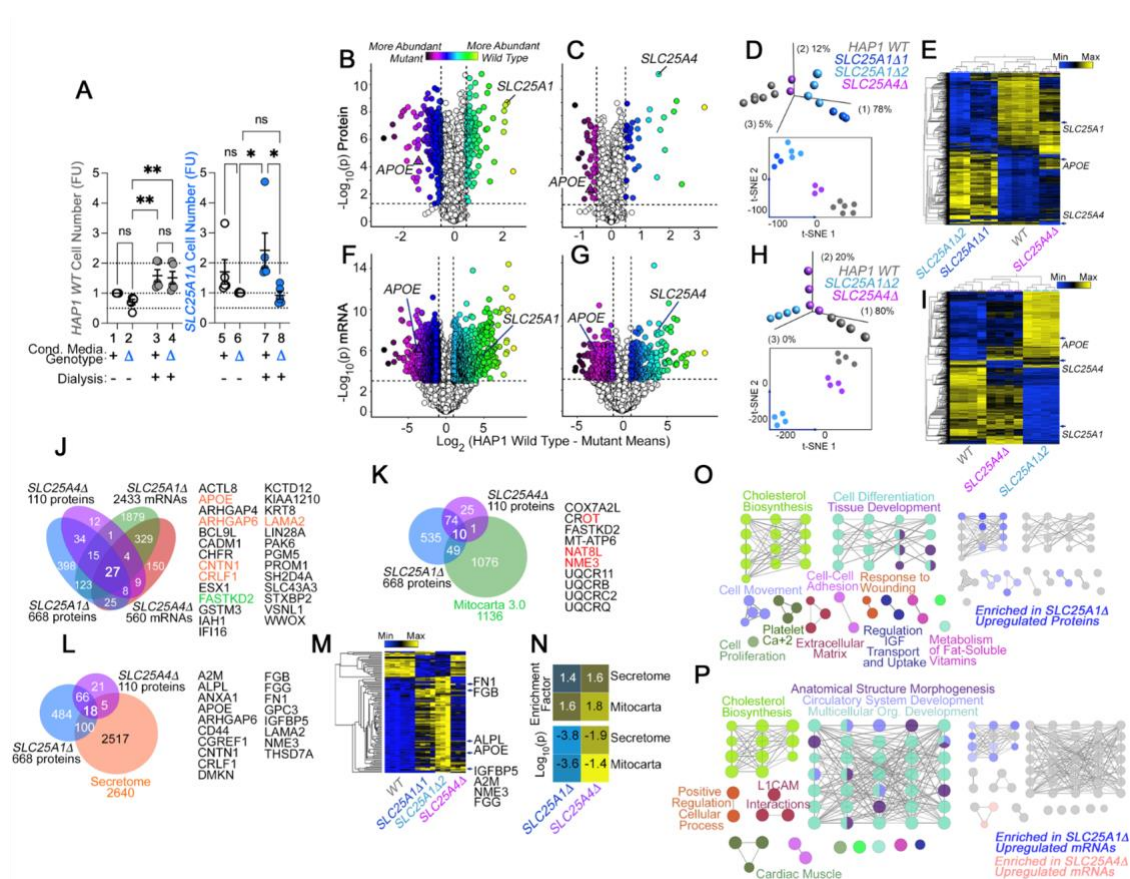


**Figure 2. The Secreted and Mitochondrial Proteomes are Modified by Inner Mitochondrial Membrane Transporter Mutants.**

**A**. Cell number determinations of wild-type (columns 1-4) and *SLC25A1*-null HAP1 cells (*SLC25A1Δ*, columns 5-8) grown in the presence of conditioned media from each genotype. Conditioned media was applied to cells for 48 hours before (columns 1, 2, 5 and 6) or after dialysis (columns 3, 4, 7, and 8). Cell number was determined by Alamar blue cell viability assay. FU, Normalized Alamar Blue Fluorescence Units. Mean± SEM, n=5, Two-Way ANOVA followed by Benjamini, Krieger and Yekutieli corrections. **B-C**. Volcano plots of TMT proteomic data from wild-type HAP1 cells (n=3), *SLC25A1Δ* (B, n=3 for two independent CRISPR clones), and *SLC25A4Δ* mutants (C, n=3), depicted are $\log_{10}$ p values and $\log_2$ fold of change. **D**. Principal component analysis and 2D-tSNE analyses of datasets in

B-C. **E**. Hierarchical clustering of all proteome hits where differential expression is significant with an $\alpha<0.001$ in at least one mutant genotype. **F-G**. Volcano plots of RNAseq data from wild-type HAP1 cells (n=4), *SLC25A1Δ* (B, n=4 for one independent CRISPR clone), and *SLC25A4Δ* mutants (C, n=4), depicted are $\log_{10}$ p values and $\log_2$ fold of change. **H**. PCA and 2D-tSNE analyses of datasets in F-G. Subject grouping was determined by k-means clustering. **I**. Hierarchical clustering of all RNAseq hits where differential expression is significant with an $\alpha=0.001$ in at least one mutant genotype. **J**. Venn diagram of protein and transcript hits shared by *SLC25A1Δ* and *SLC25A4Δ* mutants. 27 shared protein and RNA hits are annotated to either the human secretome (orange font) or annotated to Mitocarta 3.0 (green font). CROT was downregulated and upregulated in *SLC25A1Δ* and *SLC25A4Δ* mutants, respectively. **K.** Venn diagram of protein hits in *SLC25A1Δ* and *SLC25A4Δ* mutants annotated in Mitocarta 3.0. **L.** Venn diagram of protein hits in *SLC25A1Δ* and *SLC25A4Δ* mutants annotated in the Human Secretome (Uhlen et al., 2019). **M.** Hierarchical clustering of all proteins annotated to the human secretome across genotypes. **N.** Magnitude of compromise in secreted and mitochondrial proteomes in *SLC25A1Δ* and *SLC25A4Δ* mutants. p value was calculated with exact hypergeometric probability. **O-P.** Gene ontology analysis of proteome (O) and transcriptome (P) in *SLC25A1Δ* and *SLC25A4Δ* mutants. Overlapping and mutant-specific ontologies are color-coded by percent of contribution >50% to an ontological category. Gray represents ontologies where all three mutants similarly contribute hits.

### 2.3.2 APOE Expression is Uncoupled from Changes in Cholesterol Synthesis Pathways.

We focused on APOE and the sterol biosynthesis pathways to validate our proteome and transcriptome data. We also determined whether cholesterol synthesis pathways correlated with increased APOE expression in *SLC25A1Δ* and *SLC25A4Δ* cells. Electrochemical MesoScale ELISA determinations of APOE with a human-specific antibody revealed increased APOE in cell lysates and conditioned media from *SLC25A1Δ* and *SLC25A4Δ* cells (Fig. 3A and Fig. 3-figure supplement 1) (Chikkaveeraiah et al., 2012; Gaiottino et al., 2013). APOE protein expression and

secretion into media were increased ~5-20 times in two CRISPR *SLC25A1Δ* clones and *SLC25A4Δ* cells (Fig. 3A compare column 1 with 2-4 and Fig. 3-figure supplement 1 compare columns 1, 3, and 5 with 7, 9, and 11). APOE signal in complete media unexposed to cells was undetectable (Fig. 3A compare media columns 1 with 5). APOE present in media and cells was sensitive to protein synthesis inhibition with cycloheximide (Fig. 3-figure supplement 1 compare columns 1-2 and 7-8) and to disruption of the secretory pathway with brefeldin A (Fig. 3-figure supplement 1 compare columns 3-4 and 9-10). Additionally, the lysosome protease inhibitor E-64 minimally affected APOE levels; thus, making unlikely the contribution of lysosomes to the genotype-dependent differences in APOE levels (Fig. 3-figure supplement 1 compare columns 5-6 and 11-12). We confirmed the increased levels of APOE in cells by immunoblot with a different APOE antibody. We used recombinant human APOE as a standard (Fig. 3B). To exclude that an APOE expression increase was a haploid HAP1 cell peculiarity, we confirmed the increased levels of APOE in the diploid human neuroblastoma cell line SH-SY5Y where we CRISPRed out the SLC25A1 gene (Fig. 3C *SLC25A1Δ/Δ*). Much like HAP1 cells, *SLC25A1Δ/Δ* cells increased secretion of APOE by ~4-fold, in both cells and conditioned media, compared with wild-type cells (Fig. 3C, compare lanes 1 and 2). These results reveal a robust upregulation of both cellular and secreted APOE across mutant cell types.

If APOE expression depends on modifications in cholesterol pathways, then the expression of genes annotated to cholesterol metabolism and cholesterol content should be similarly modified in *SLC25A1Δ* and *SLC25A1Δ/Δ* cells. We measured the transcript levels of APOE and genes involved in cholesterol uptake and synthesis, in *SLC25A1Δ, SLC25A4Δ,* and *SLC25A1Δ/Δ* cells. We focused on the LDL receptor (LDLR), as well as cholesterol synthesis enzymes, ACAT2, MSMO1 and HMGCR, the latter the rate-limiting enzyme of the cholesterol synthesis pathway (Brown and Goldstein, 1980; Mazein et al., 2013). We chose these genes as upregulated hits from the transcriptome of *SLC25A1Δ* cells. We used VAMP2 and RPS20 as housekeeping gene controls (Fig. 3D-F). APOE mRNA increased ~3 fold in all three mutant cells.

In contrast, the expression of cholesterol synthesis pathway genes was increased in *SLC25A1Δ* (Fig. 3D)*,* but not in *SLC25A4Δ* and *SLC25A1Δ/Δ* cells (Fig. 3E and F). The upregulation of cholesterol synthesis pathway genes resulted in a significant increase of cholesterol and all cholesterol-ester species content in *SLC25A1Δ* cells, as determined by mass spectrometry (Fig. 3G and J). Triglyceride and other measured lipid families were similar in wild-type and *SLC25A1Δ* cells (Fig. 3G and J). In contrast, cholesterol and cholesterol-ester species were not modified in *SLC25A4Δ* (Fig. 3H and J) and *SLC25A1Δ/Δ* cells (Fig. 3I and K), even though the expression of APOE was upregulated to the same extent in all these mutant cells. These results make unlikely the hypothesis that increased APOE expression is coupled to an upregulation of cholesterol synthesis pathways.
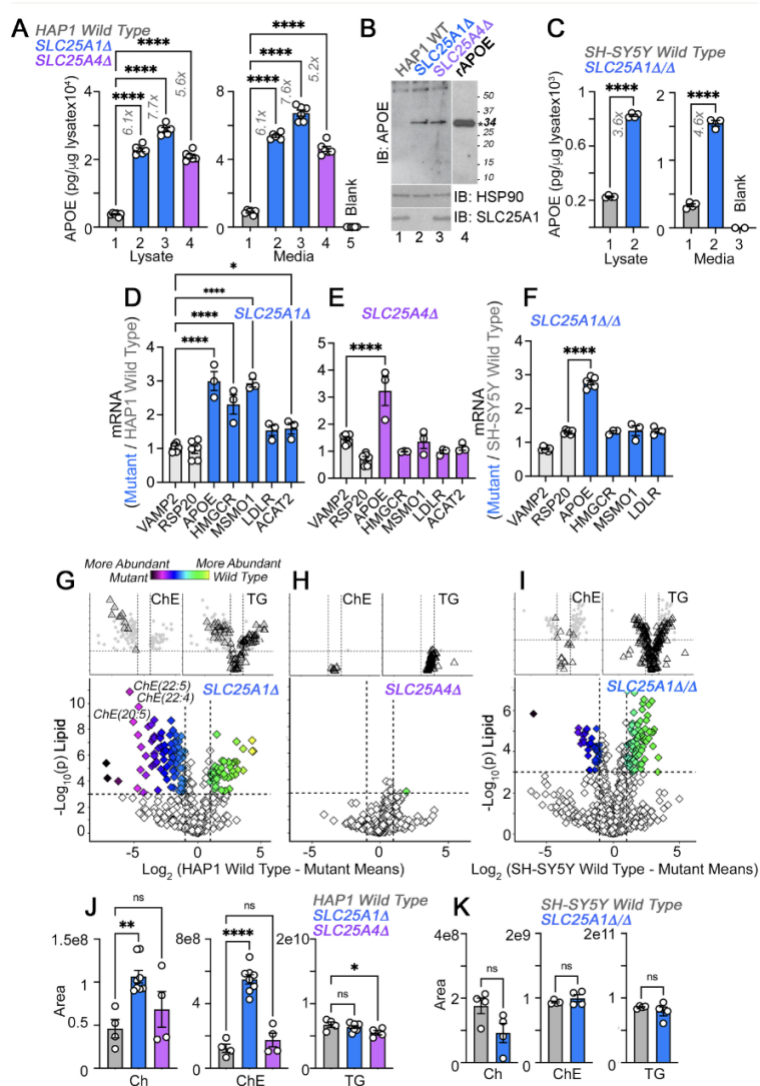
**Figure 3. APOE Transcripts and Protein Are Upregulated Independent from Cholesterol Levels in *SLC25A1* and *SLC25A4* Mutants.**

**A**. MesoScale electrochemiluminescence solid phase ELISA determinations of human APOE in wild-type (column 1), *SLC25A1Δ* (columns 2 and 3)*,* and *SLC25A4Δ* (column 4) HAP1 mutant cell lysates and conditioned media. Two independent *SLC25A1Δ* clones were tested (columns 2-3). Column 5 depicts complete media not exposed to cells.  n=4. **B**. APOE immunoblot of cellular extracts from wild-type, *SLC25A1Δ,* and *SLC25A4Δ* HAP1 mutant cells. HSP90 was used as a loading control. Lane 4 presents recombinant human APOE (rAPOE). In bold is the predicted molecular weight of rAPOE. **C**. MesoScale ELISA measurements of human APOE in wild-type and *SLC25A1Δ/Δ* SH-SY5Y mutant cell lysates and conditioned media. **D-F**. qRT-PCR quantification of APOE, sterol metabolism annotated genes, and housekeeping controls (VAMP2 and RPS20) in wild-type and diverse mutant

cell lines. **D** and **E** show transcript levels in *SLC25A1Δ* and *SLC25A4Δ* HAP1 mutant cells, respectively. **F** depicts transcript levels in *SLC25A1Δ/Δ* SH-SY5Y mutant cells. All data are expressed as transcript ratio between mutant and wild-type. n=3 for D-F. **G-I**. Volcano plots of positive mode untargeted lipidomics performed in *SLC25A1Δ*, *SLC25A4Δ,* and *SLC25A1Δ/Δ* mutant HAP1 and SH-SY5Y cells and their controls. Upper inserts present the distribution of cholesterol ester and triglyceride species marked by triangles. Depicted are $\log_{10}$ p values and $\log_2$ fold of change. n=4 per clone for the two *SLC25A1Δ* clones, n=4 for *SLC25A4Δ,* and n=4 for *SLC25A1Δ/Δ*. **J**. Total cellular levels of free cholesterol (Ch), cholesterol ester (ChE), and triglycerides (TG) in wild-type, *SLC25A1Δ*, and *SLC25A4Δ* HAP1 cells. **K**. Total cellular levels of free cholesterol (Ch), cholesterol ester (ChE), and triglycerides (TG) in wild-type and *SLC25A1Δ/Δ* SH-SY5Y cells. Average ± SEM, One-Way ANOVA followed by Bonferroni or Holm-Šydák's (D-F) multiple corrections, or unpaired t-test (K). See available source data for Figure 3B.
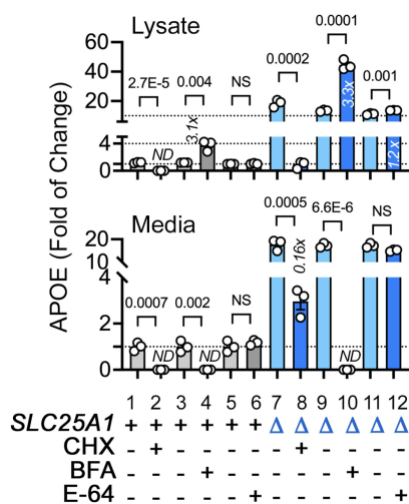


**Fig. 3 Fig Supplement 1. Effects of Diverse Non-Mitochondrial Inhibitors on APOE Expression and Secretion.**

APOE MesoScale ELISA in wild-type and *SLC25A1Δ* HAP1 cells treated with either vehicle (light colored columns 1, 3, and 5), cycloheximide (CHX 20µg/ml, columns 2 and 8), brefeldin A, (BFA 5 µg/ml, columns 4 and 10), or E-64 (50 µM, columns 6 and 12) for 8 h. Average ± SEM, Two-tailed t test. ND, not detected.

### 2.3.3 Perturbation of the Electron Transport Chain Complexes I and III Increases APOE Expression.

We turned our attention to common defects in *SLC25A1Δ* and *SLC25A4Δ* HAP1 cells that could explain the increased expression of APOE. A shared phenotype in both mutants was a drop in the levels of complex III subunits and the supercomplex III-IV assembly factor COX7A2L (Fig. 1K). We hypothesized that defects in the integrity of the electron transport chain could mediate the increased levels of APOE. To test this hypothesis, we first determined the effects of SLC25A1 and *SLC25A4* mutations on the organization of the electron transport chain by blue native electrophoresis. Second, we mutagenized assembly factors and subunits of complexes I (NDUFS3 and NDUFAF7), III (COX7A2L and HIGD1A), and IV of the electron transport chain (COX7A2L, HIGD1A, COX17, 18, 19, and 20) to then measure APOE levels (Lobo-Jarne et al., 2018; Nyvltova et al., 2022; Timon-Gomez et al., 2020a; Zurita Rendon et al., 2014). We determined the robustness of the increased APOE phenotype studying mutants in three human cell lines (HAP1, SH-SY5Y, and HEK293), which differ in several properties, including their genetic background, rate of growth, and tissue of origin.

We measured the expression of electron transport chain subunits by proteomics in HAP1 cells. We found even though complex III was affected in both *SLC25A1Δ* and *SLC25A4Δ* cells (Fig. 2K, 4A and Fig. 4-figure supplement 1A), the most pronounced defect was in the expression of complex I subunits in *SLC25A1Δ* cells (Fig. 4A). We scrutinized the integrity of respiratory chain complexes in *SLC25A1Δ* cells by SDS-PAGE, blue native electrophoresis, and bidimensional gel electrophoresis (Fig. 4B-D). We performed immunoblot analysis of SDS-PAGE resolved respiratory complex subunits with antibodies against subunits that undergo degradation in misassembled respiratory complexes (Civiletto et al., 2018; Ghazal et al., 2021). These experiments revealed that the most degraded subunits were those from complexes I and III (Fig. 4B).   We then analyzed respiratory complexes by blue native electrophoresis and found decreased expression of high molecular weight complexes containing NDUFS3, UQCRC2, and

COX4, which correspond to subunits of the respiratory complexes I, III and IV, respectively (Fig. 4C). Two-dimensional gel electrophoresis showed that high molecular weight respiratory complexes containing subunits of complexes I and III were diminished in *SLC25A1Δ* cells (Fig. 4D). Similarly, *SLC25A4Δ* HAP1 cells had reduced levels of complex III subunits (Fig. 4-figure supplement 1A), thus affecting the migration of complex III-containing supercomplexes in blue native electrophoresis (Fig. 4-figure supplement 1B). The effect of the *SLC25A4* mutation on APOE expression was not due to a defect in the SLC25A4 transport activity, as the SLC25A4 inhibitor bongkrekic acid did not increase the levels of APOE (Fig. 4-figure supplement 1C, compare columns 1 with 2 and 3), even at concentrations that inhibit mitochondrial respiration to the same extent as the *SLC25A4* mutation (Fig. 4-figure supplement 1D) (Gutierrez-Aguilar and Baines, 2013).

The loss of integrity in complexes I and III in *SLC25A1Δ* and *SLC25A4Δ* HAP1 cells suggest that respiratory chain defects could be responsible for the increased expression of APOE. We tested this hypothesis by targeting complexes I and III using genetic and pharmacological approaches (Fig. 4 and Fig. 4-figure supplement 2). We genetically perturbed complex I assembly and function by knocking-out either NDUFS3 or NDUFAF7 or by using the complex I inhibitor piericidin A (Fig. 4-figure supplement 2)(Bridges et al., 2020). NDUFS3 encodes NADH dehydrogenase [ubiquinone] iron-sulfur protein 3, a non-catalytic subunit of complex I necessary for complex I assembly and activity (Benit et al., 2004; D'Angelo et al., 2021). NDUFAF7 encodes NADH:ubiquinone oxidoreductase complex assembly factor 7, a methylase necessary for the early stages of complex I assembly (Zurita Rendon et al., 2014). We targeted NDUFS3 and NDUFAF7 because these genes localize to genetic loci associated with increased risk of Alzheimer's disease (de Rojas et al., 2021; Kunkle et al., 2019). Moreover, SLC25A1 and NDUFS3 share 91% of their proximity interactions (Antonicka et al., 2020), an observation we corroborated by co-immunoprecipitation of SLC25A1 and NDUFS3 (Fig. 4-figure supplement 3). NDUFS3 and NDUFAF7 CRISPR mutants compromised mitochondrial respiration, as shown by

Seahorse oximetry (Fig. 4E and H). Both mutants increased the expression of APOE mRNA, as compared to reference housekeeping transcripts, (Fig. 4F and I, RER1 and VAMP2) as well as APOE protein in cells and in conditioned media (Fig. 4G and J). These results demonstrate that the integrity and function of complex I regulate APOE expression and secretion.

We inhibited the function of complex III with the specific inhibitor antimycin I (von Jagow and Link, 1986). We inquired whether inhibition of complex III by antimycin would upregulate the expression of APOE in wild-type and in *SLC25A1Δ* cells. Since complex III levels were partially reduced in *SLC25A1Δ* cells (Fig 4A, B, and C), we reasoned that inhibition of residual complex III activity in *SLC25A1Δ* cells would reveal additive respiratory chain mechanisms affecting APOE expression. We measured respiration in wild-type and *SLC25A1Δ* cells in the absence and presence of increasing concentrations of antimycin (Fig. 4K). *SLC25A1Δ* cells were more sensitive to low doses of antimycin (Fig. 4K), a phenotype predicted for cells with reduced content of complex III. Antimycin addition increased APOE mRNA 3-fold in wild-type cells as compared to vehicle (Fig. 4L compare columns 9-10), whereas the expression of two housekeeping mRNAs, RER1 and PCBP1, was minimally affected by complex III inhibition (Fig. 4L compare columns 1-2 and 5-6). *SLC25A1Δ* cells doubled their APOE mRNA when treated with antimycin as compared to vehicle-treated *SLC25A1Δ* cells (Fig. 4L compare columns 11-12). Antimycin also increased APOE secretion in both wild-type and *SLC25A1Δ* cells by ~2-3-fold (Fig. 4M). No such increase was detectable in cell lysates in both genotypes (Fig. 4M). These data show that the effect of antimycin on APOE mRNA expression and protein secretion was additive with the *SLC25A1Δ* upregulation phenotype. Taken together, these results demonstrate that the expression of APOE is sensitive to complex III inhibition.
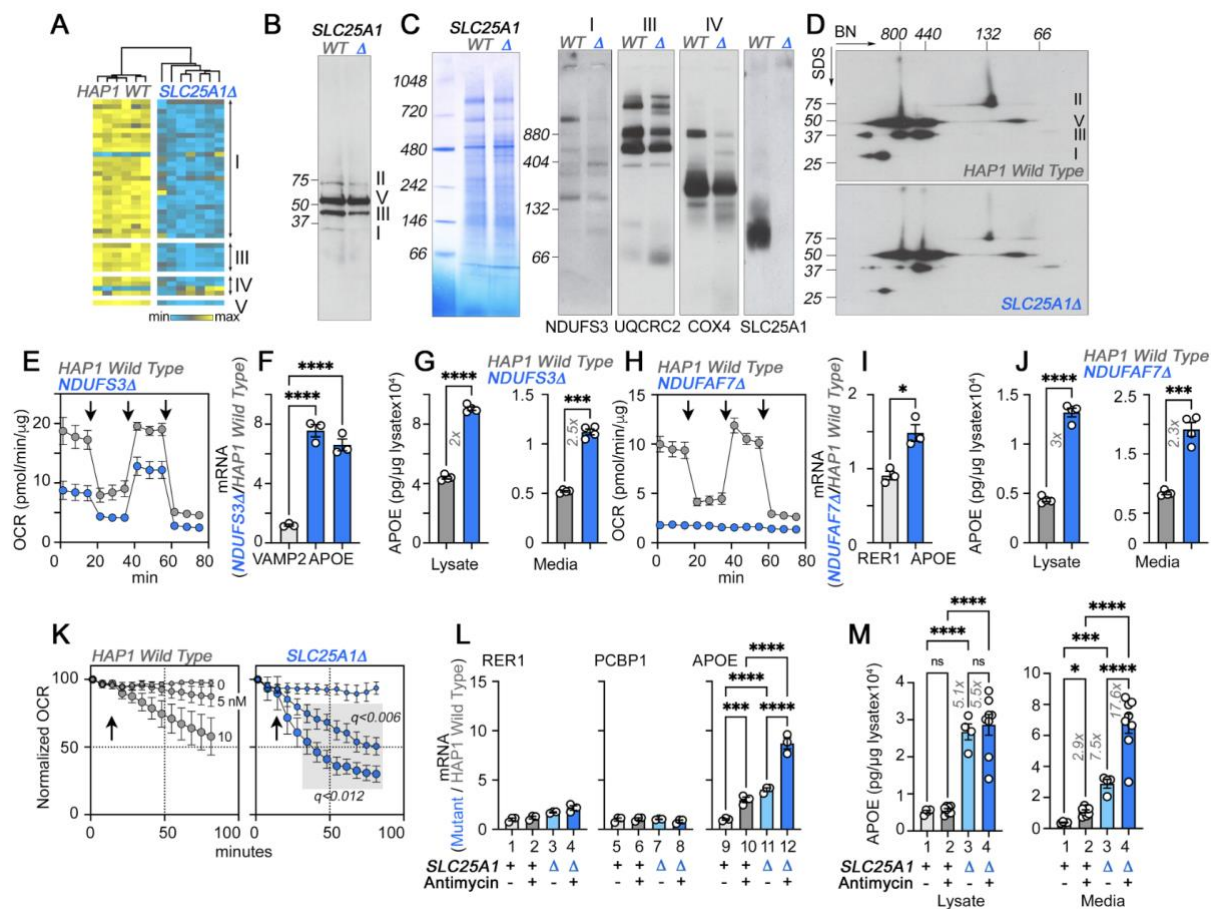
**Figure 4. The Integrity of Respiratory Chain Complex I is Required to Control APOE Expression.**

**A**. Expression of respiratory complex subunits in wild-type and *SLC25A1Δ* HAP1 cells quantified by TMT mass spectrometry. Kendal Tau hierarchical clustering analysis. **B**. Immunoblots with OxPhos antibody mix in mitochondrial fractions from wild-type and *SLC25A1Δ* cells. **C**. Blue native electrophoresis of mitochondrial fractions from wild-type and *SLC25A1Δ* cells. Shown are Coomassie stained native gel and immunoblots probed with antibodies against complex, I, III, IV, and SLC25A1. **D**. Blue native electrophoresis followed by SDS-PAGE then immunoblot with antibodies against complex, I, II, III, and V in mitochondrial fractions from wild-type and *SLC25A1Δ* cells. **E-G**. Seahorse stress test, APOE qRT-PCR, and APOE MesoScale ELISA analysis respectively in wild-type and *NDUFS3Δ* HAP1 cells. In F, APOE was measured with two primer sets. **H-J**. Seahorse stress test, APOE qRT-PCR, and APOE MesoScale ELISA analysis respectively in wild-type and *NDUFAF7Δ* HAP1 cells. VAMP2 or RER1 transcripts were used as controls in F and J. All qRT-PCR data are expressed as ratio between mutant and wild-type. E to M average ± SEM. One-Way ANOVA followed by Šydák's multiple correction (F), or

unpaired t-test with Welch's correction (G, I, and J). Arrows in E (n=4) and H (n=3) show sequential addition of oligomycin, FCCP, and rotenone-antimycin during the Seahorse stress test. **K**. *SLC25A1Δ* cells are more sensitive to antimycin than wild-type HAP1 cells. Wild type and *SLC25A1Δ* cells were exposed to vehicle or increasing concentrations of antimycin. Basal cellular respiration was measured for 90 min after additions (arrow) using Seahorse. Data are presented normalized to basal respiration in the absence of drug. Average ± SEM, n=3, Gray square shows significant differences between wild-type and *SLC25A1Δ* drug-treated cells as determined by multiple unpaired t-tests followed by corrections with the Benjamini-Krieger-Yekuiteli method (FDR=5%). **L-M**. APOE qRT-PCR and APOE MesoScale ELISA in wild-type and *SLC25A1Δ* HAP1 cells, respectively, treated with vehicle or antimycin. 20 nM antimycin was used in qPCR experiments. 20–80 nM was used in MesoScale ELISA experiments. RER1 (columns 1-4) and PCBP1 transcripts (columns 5-8) were used as housekeeping controls. All qRT-PCR data are expressed as ratio between mutant and wild-type. Average ± SEM, One-Way ANOVA followed by Benjamini-Krieger-Yekuiteli multiple comparison corrections (FDR=5%). See available source data for Figure 3B and C.
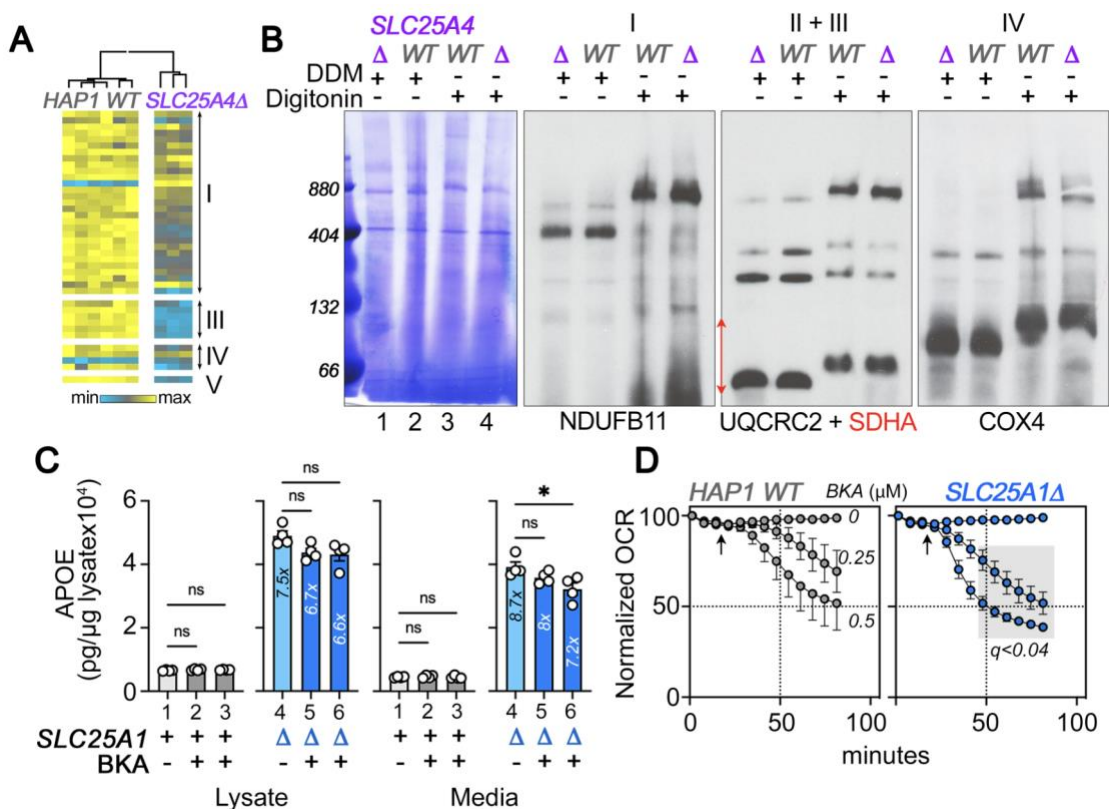
**Fig. 4 Fig Supplement 1. SLC25A4 Null HAP1 Cells Disrupt Complex III and Increase Expression of APOE.**

**A**. Expression of respiratory complex subunits in wild-type and *SLC25A4Δ* HAP1 cells quantified by TMT mass spectrometry. Kendal Tau hierarchical clustering analysis. **B**. Blue native electrophoresis followed by either Coomassie or immunoblotting with antibodies against complex, I, II, III, and IV in mitochondrial fractions from wild-type and *SLC25A4Δ* HAP1 cells. n-dodecyl-β-d-maltoside (DDM) was used to disrupt supercomplexes. **C.** APOE MesoScale ELISA in wild-type and *SLC25A1Δ* HAP1 cells treated with vehicle (columns 1 and 4) or bongkrekic acid 0.25 and 0.5 µM for 48 h (columns 2 and 5 and 3 and 6, respectively). Average ± SEM, One-Way ANOVA followed by Dunnett's multiple comparisons test. **D**. Wild type and *SLC25A1Δ* HAP1 cells were exposed to vehicle or increasing concentrations of bongkrekic acid (BKA). Basal cellular respiration was measured for 90 min after additions (arrow) using Seahorse. Data are presented normalized to basal respiration in the absence of drug. Average ± SEM, n=4 wild-type, n=8 for *SLC25A1Δ* mutants for treated and untreated cells. Gray square shows significant differences between wild-type and *SLC25A1Δ* drug-treated cells as determined by Two-Way ANOVA followed by Two-stage linear step-up procedure of Benjamini, Krieger and Yekutieli (FDR 5%).
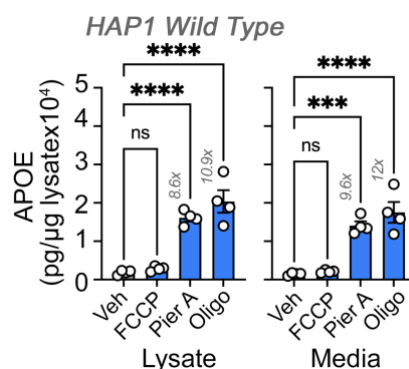
**Fig. 4 Fig Supplement 2. Effects of Inhibitors of the Electron Transport Chain on APOE Levels.**

HAP1 wild-type cells were treated with either piericidin A (2 µM), oligomycin (1 µM), and FCCP (0.125 µM) for 48h. Data is presented as a ratio between drug/vehicle. All figures depict average $\pm$ SEM. One-Way ANOVA followed by Dunnett's multiple correction.
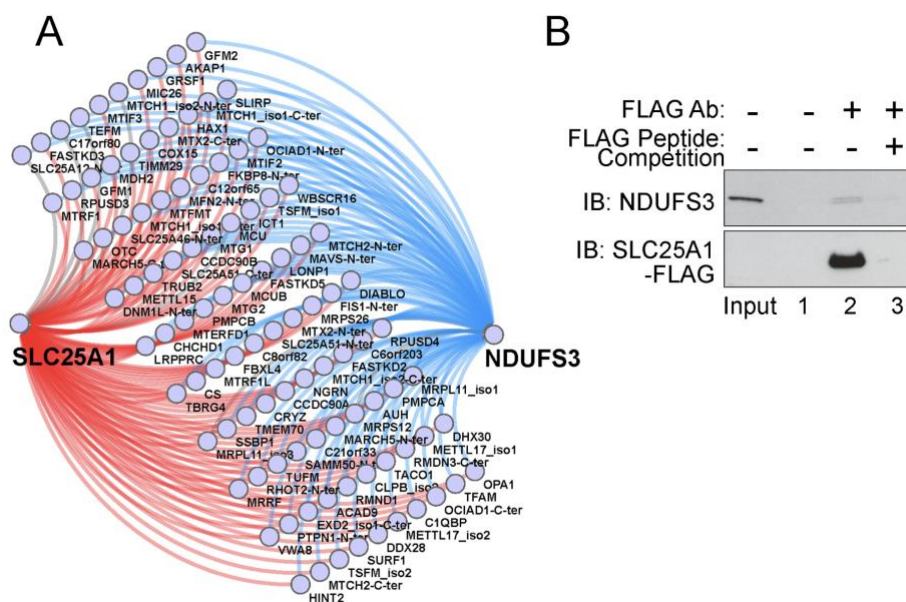


**Fig. 4 Fig Supplement 3. Interactions between SLC25A1 and NDUFS3.**

**A.** Proximity ligation map of interactions shared between SLC25A1 and NDUFS3.  **B.** SLC25A1-FLAG expressing SH-SY5Y cell lysates were immunoprecipitated with magnetic beads alone (lane 1) or FLAG antibodies (lanes 2-3), either in the absence or presence of an excess FLAG peptide for out-competition (Lanes 2 and 3, respectively). Immunoprecipitated complexes were probed by immunoblot with NDUSF3 antibody.

We tested the robustness of the increased APOE phenotype in HEK293 cells. We mutagenized *SLC25A4* alone or in conjunction with its two homologs, *SLC25A5* and *6*. *SLC25A4* is the main ADP/ATP carrier expressed in HAP1 cells (Fig. 5-figure supplement 1). In contrast, *SLC25A5* and *6* are the main species expressed by HEK293 cells (Lu et al., 2017). TMT proteomic analysis of whole cell extracts from *SLC25A4Δ/Δ* HEK293 cells revealed minimal changes in protein levels (Fig. 5A). In contrast, we found 223 differentially expressed proteins in *SLC25A4,5,6Δ/Δ* triple knock-out cells (Fig. 5A). Of these 223 proteins, 32 were annotated to the secretome, including APOE (Fig. 5B and C). We confirmed increased APOE levels by MesoScale ELISA in *SLC25A4,5,6Δ/Δ* triple knock-out cells, which increased APOE ~2-fold, in both cell extracts and conditioned media, as compared with wild-type and *SLC25A4Δ/Δ* HEK293 cells (Fig. 5D). Among the 223 differentially expressed proteins, we also identified 42 proteins annotated to Mitocarta 3.0 (Fig. 5B). These included increased levels of 4 of the 10 subunits in complex III (Fig. 5B and E). Formation of complex III supercomplexes was selectively compromised in *SLC25A4,5,6Δ/Δ* triple knock-out cells as determined by blue native electrophoresis (Fig. 5F). These mitochondrial proteome modifications and defective supercomplexes formation reduced mitochondrial respiration by 5-fold in triple knock-out cells (Fig. 5G). We conclude that increased APOE expression is robustly observed in diverse cell types where the integrity of complex III of the electron transport chain is compromised
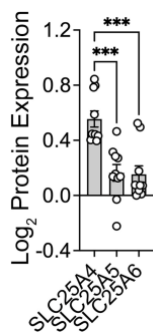
**Fig. 5 Fig Supplement 1. SLC25A4 Null HAP1 Cells Disrupt Complex III and Increase Expression of APOE.**

Expression of SLC25A4, 5 and 6 transporters in HAP1 cells obtained from TMT data in Fig. 1 and Supplementary File 1.
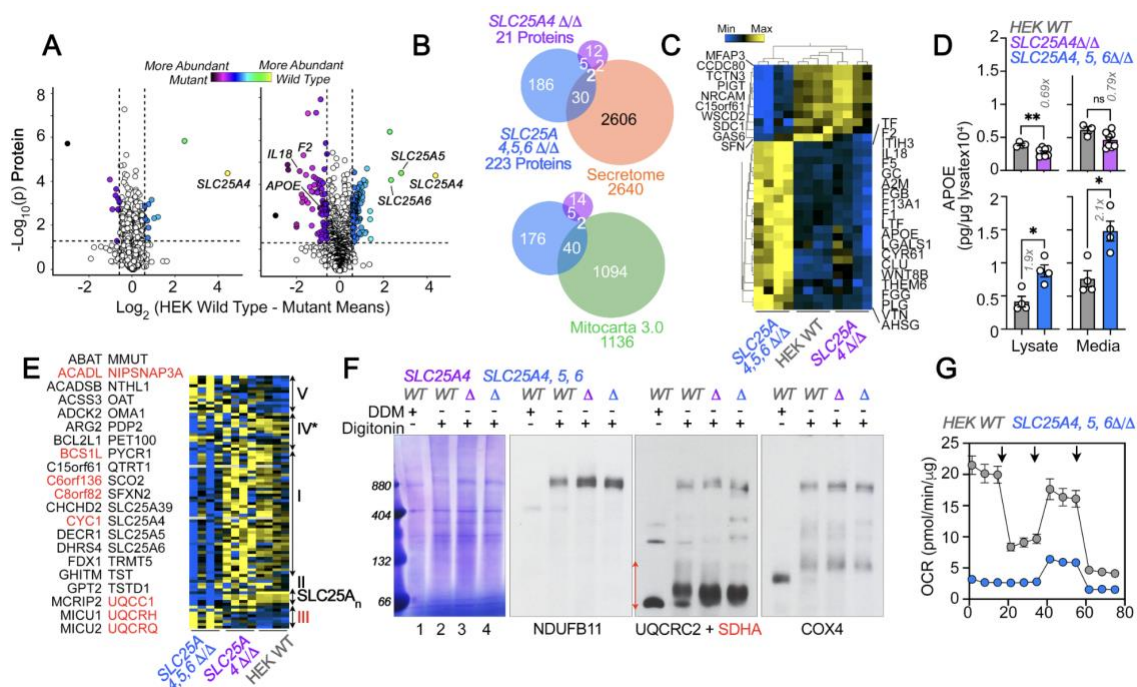


**Figure 5. Robustness and Redundancy of Adenine Nucleotide Translocators Regulating APOE Expression.**

**A.** Volcano plots of TMT proteomic data from wild-type HEK293 cells (n=4), *SLC25A4Δ/Δ* and triple knock-out *SLC25A4,5,6Δ/Δ* (B, n=4), depicted are $\log_{10}$ p values and $\log_2$ fold of change. **B**. Venn

diagram of protein hits in *SLC25A4Δ/Δ* and triple knock-out *SLC25A4,5,6Δ/Δ* mutants annotated in Mitocarta 3.0 or the Human Secretome (Uhlen et al., 2019). **C.** Hierarchical clustering of all proteins annotated to the human secretome across genotypes. **D**. MesoScale ELISA determinations of human APOE in wild-type and mutant HEK293 cells. Shown are APOE content in lysates and conditioned media. Mann-Whitney test. **E.** Mitocarta 3.0 annotated hits in the triple knock-out *SLC25A4,5,6Δ/Δ* proteome, see panel B. Red font indicates increased levels in mutant. Hierarchical clustering of all proteins annotated to electron transport chain subunits and SLC25A transporters across genotypes. **F.** Blue native electrophoresis followed by immunoblotting with antibodies against complex, I, II, III, and IV in mitochondrial fractions from wild-type and *SLC25A4Δ/Δ* and triple knock-out *SLC25A4,5,6Δ/Δ* cells. n-dodecyl-β-d-maltoside (DDM) was used to disrupt supercomplexes. Red arrow and font denote region blotted with SDHA antibodies . **G.** Seahorse stress test wild-type and triple knock-out *SLC25A4,5,6Δ/Δ* cells as in Fig. 3. N=3. See available source data for Figure 5F.

### 2.3.4 Direct and Indirect Mechanisms Affecting Complex IV Biogenesis Increases APOE Expression.

In order to address if the integrity of respiratory complexes, other than complexes I and III, could modulate APOE expression, we focused on complex IV in the electron transport chain. The assembly of this complex requires a pathway that begins at the plasma membrane to deliver copper, which is necessary for complex IV biogenesis (Fig. 6A)(Cobine et al., 2021; Garza et al., 2022). At mitochondria, complex IV requires assembly factors to generate the complex itself (HIGD1A, COX18, and COX20), factors to generate complex IV-containing supercomplexes (COX7A2L and HIGD1A), a copper transporter present in the inner mitochondrial membrane (SLC25A3), and metallochaperones that deliver copper I ions to complex IV (COX17 and COX19). In turn, the mitochondrial copper metallochaperone COX17 receives its copper from the plasma membrane copper uptake transporter SLC31A1 (Fig. 6A)(Cobine et al., 2021; Garza et al., 2022). We knocked out genes belonging to this pathway and assessed the expression of APOE in three cell models.

We mutated the mitochondrial factors COX7A2L, HIGD1A, COX18, COX19 or COX20 in HEK293 cells and measured APOE levels by MesoScale ELISA (Fig. 6B). We first focused on COX7A2L and HIGD1A as these two factors are required for the assembly of complex III-IV supercomplexes yet they differ in that COX7A2L does not affect the biogenesis of individual complexes, thus keeping mitochondrial respiration intact (Lobo-Jarne et al., 2018). In contrast, HIGD1A affects both supercomplex formation and the biogenesis of individual complexes III and IV (Timon-Gomez et al., 2020a). Mutagenesis of *COX7A2L* did not affect APOE expression but mutagenesis of *HIGD1A* increased APOE levels ~12-fold, both in cell lysates and conditioned media (Fig. 5B). We confirmed these findings with mutants in the complex IV assembly factors COX18 and 20 (Bourens and Barrientos, 2017; Nyvltova et al., 2022). *COX18* and *20* gene defects increased APOE expression to the same extent as HIGD1A (Fig. 6B).

Complex IV requires copper for its biogenesis and function. Thus, our model predicts that genetic disruption of proteins in the pathway that leads to delivery of copper to complex IV should increase APOE expression (Fig. 6A). Among the factors that help deliver copper into complex IV, we studied COX17 and COX19 (Banci et al., 2008; Cobine et al., 2021; Garza et al., 2022; Leary et al., 2013; Nyvltova et al., 2022; Oswald et al., 2009). Mutagenesis of COX19 in HEK293 cells increased the expression of APOE protein in both cells and conditioned media by ~40-fold (Fig. 6B). We confirmed this finding in two SH-SY5Y mutants of the metallochaperone COX17 (Fig. 6C, *COX17Δ/Δ*). We decreased cytoplasmic copper availability by either eliminating copper uptake via mutagenesis of the SLC31A1 transporter (Fig. 6D, *SLC31A1Δ/Δ* and Fig. 6-figure supplement 1), or by expressing in ATP7A-null SH-SY5Y cells (*ATP7AΔ/Δ* and Fig. 6-figure supplement 1) an ATP7A mutant that constitutively extrudes copper from cells due to mutagenesis of its endocytosis sorting signal (Fig. 6E and Fig. 6-figure supplement 1, *ATP7A-LL*) (Petris et al., 1998; Zhu et al., 2016). Both forms of cytoplasmic copper reduction increased APOE expression and secretion in two independent mutant or clonal isolates (Fig. 6D-E). Elimination of ATP7A alone did not increase APOE expression (Fig. 6F, *ATP7AΔ/Δ*). Mutagenesis of *SLC25A3*,

also increased the expression and secretion of APOE protein in HAP1 cells (Fig. 6G). We confirmed these results by measuring APOE mRNA levels with NanoString technology in two independent mutants of *COX17* and *SLC31A1,* as well as in wild-type cells incubated with a cell impermeant copper chelator, bathocuproinedisulfonic acid (Fig. 6H, BCS and Fig. 6-figure supplement 1). These pharmacological and genetic approaches to reduction of cytoplasmic copper robustly increased APOE mRNA as compared to wild-type cells (Fig. 6H), while levels of a housekeeping gene, TBP, were unchanged. These results demonstrate that impairing complex IV biogenesis, directly or indirectly, increases the expression of APOE transcript and protein in diverse cell lines. Along with our experiments targeting complexes I and III, these findings support the concept that diverse mechanisms converging on respiratory chain function and assembly can induce the expression and secretion of APOE.

To determine whether there was a relationship between the degree of respiratory chain compromise, glycolysis, and the extent of APOE secretion increase, we correlated the normalized secretion of APOE in diverse mitochondrial mutants to their normalized basal oxygen consumption rate, and the rate of extracellular acidification as a proxy for glycolysis (Fig. 6I-J). APOE negatively and significantly correlated with basal oxygen consumption (-0.62, Fig. 6J, r=-0.62, p=0.022). However, we identified an exception in mutants of the carnitine transporter SLC25A20 that increased APOE levels despite normal respiration (Fig. 6-figure supplement 2). The correlation of APOE expression with the rate of extracellular acidification did not differ from zero (Fig. 6J, p=0.2 and Fig. 6-figure supplement 3). These findings support the idea that respiratory chain integrity and activity rather than glycolytic adaptations in mutants affecting the electron transport chain modulate APOE expression.

We explored alternative mechanisms from electron transport chain assembly and activity required for increased APOE expression and secretion. We ruled out the possibility that either decreased cytoplasmic citrate levels (Fig. 6-figure supplement 4) or bioenergetic stress are responsible for the APOE increase in *SLC25A1Δ* cells, using activation of the AMPK pathway as

a read-out (Fig. 6-figure supplement 5). We ruled out accumulation of reactive oxygen species as a causal mechanism for increased APOE, as treatment with the antioxidant N-acetyl cysteine did not affect APOE mRNA levels in wild-type or *SLC25A1Δ* cells (Fig. 6-figure supplement 5). We also assessed whether activation of the mitochondrial stress response pathway caused APOE elevation (Fig. 6-figure supplement 5). We found that activation of the mitochondrial stress response with doxycycline (Quiros et al., 2017) modestly increased the secretion of APOE in *SLC25A1Δ* cells (Fig. 6-figure supplement 5 panel D columns 7-8) but not in wild-type cells (Fig. 6-figure supplement 5 panel D columns 5-6), even though wild-type cells robustly activated the mitochondrial stress response after doxycycline incubation (Fig. 6-figure supplement 5 panel E).
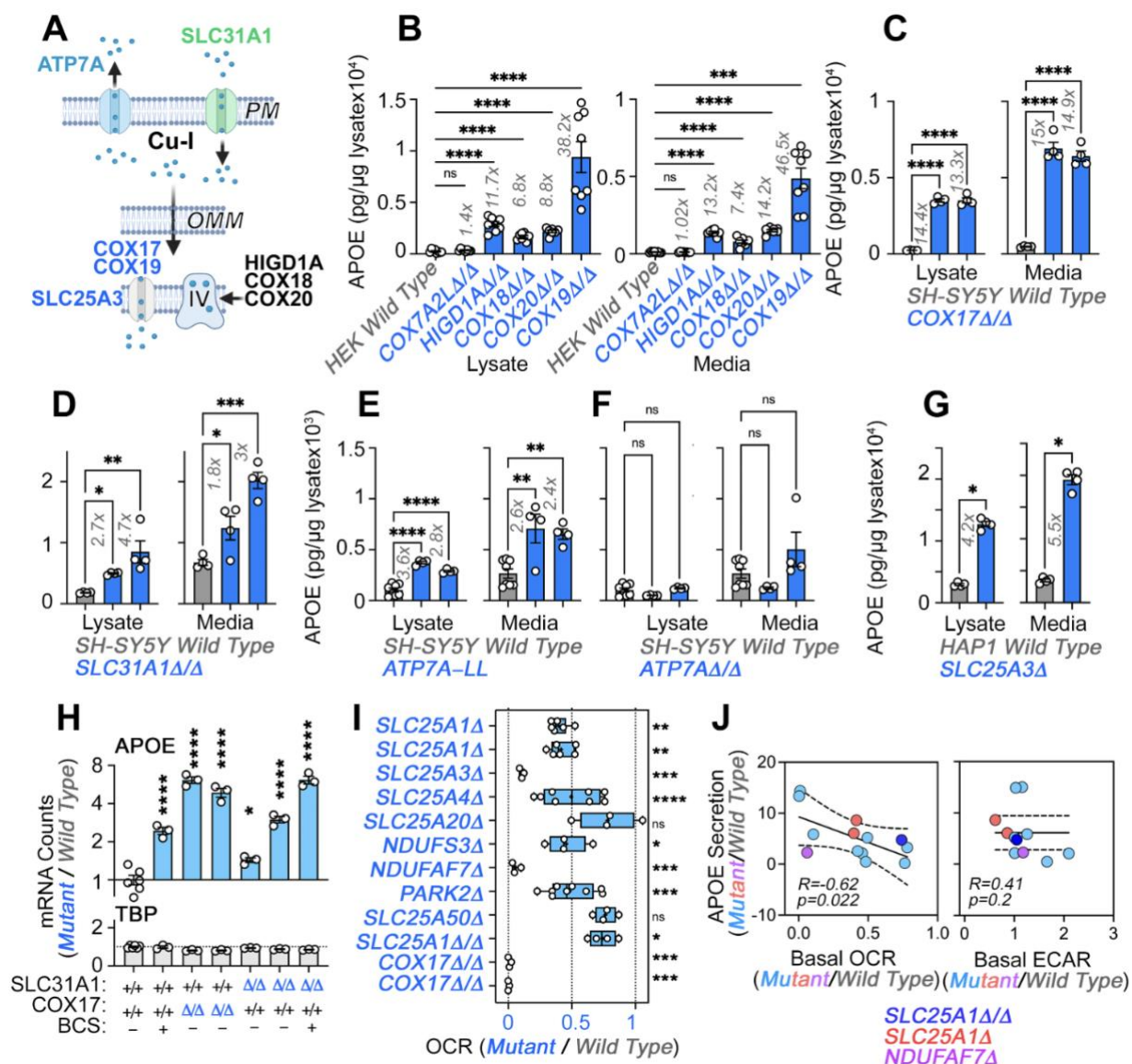
**Figure 6. Direct and Indirect Disruption of Complex IV Increases APOE Expression.**

**A**. Direct (COX17-20, HIGD1A) and indirect (SLC25A3, SLC31A1, ATP7A) mechanisms required for complex IV assembly. **B.** MesoScale ELISA determinations of human APOE in wild-type and HEK293 cell clones null for the genes indicated in blue font. Shown are APOE content in lysates and conditioned media. **C.** MesoScale ELISA determinations of human APOE in wild-type and two independent *COX17Δ/Δ* mutant SH-SY5Y cell clones. **D**. MesoScale ELISA determinations of human APOE in wild-type and two independent *SLC31A1Δ/Δ* mutant SH-SY5Y cell clones were studied. **E**. MesoScale ELISA determinations of human APOE in wild-type and two independent *ATP7AΔ/Δ* mutant SH-SY5Y cell clones transfected with the endocytosis-deficient ATP7A-LL construct. **F**. MesoScale ELISA determinations of

human APOE in wild-type and two independent *ATP7AΔ/Δ* mutant SH-SY5Y cell clones. **G**. MesoScale

ELISA determinations of human APOE in wild-type and *SLC25A3Δ* mutant HAP1 cells were studied.

N=8 for B and n=4 for C-G. **H**. NanoString mRNA quantification of human APOE and TBP transcripts

in wild-type, and two independent mutant clones of either *COX17Δ/Δ* or *SLC31A1Δ/Δ* mutant SH-SY5Y

cells. Wild type and *SLC31A1Δ/Δ* cells were treated with vehicle or 200 micromolar of the copper

chelator bathocuproinedisulfonic acid (BCS). TBP was used as a housekeeping control transcript. n=3.

**I**. Seahorse basal cellular respiration across different genotypes normalized to the corresponding wild-

type cell. **J.** Correlation between APOE in conditioned media with either basal cellular respiration (OCR)

or the extracellular acidification rate determined by Seahorse (ECAR, n=3-9). Simple linear regression

fit and 95% confidence interval is shown. All data are presented as average $\pm$ SEM. For B to F, and H

One-Way ANOVA followed by Benjamini-Krieger-Yekuiteli multiple comparison corrections (FDR=5%).

G unpaired t-test with Welch's correction.
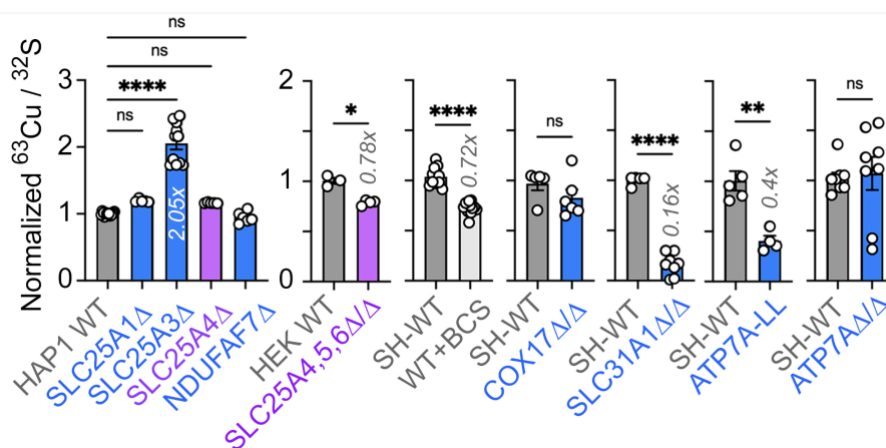


**Fig. 6 Fig Supplement 1. Total Cellular Copper in Wild Type and Diverse Mutant Cells.**

Copper and sulfur were measured by inductively coupled plasma mass spectrometry in wild-type and

mutant HAP1 and SH-SY5Y cells. Sulfur content was used as a loading control as described by Lane

et al. (Lane et al., 2022). Average $\pm$ SEM, One-Way ANOVA followed by Dunnett's multiple comparisons

test or unpaired t-test with Welch's correction.
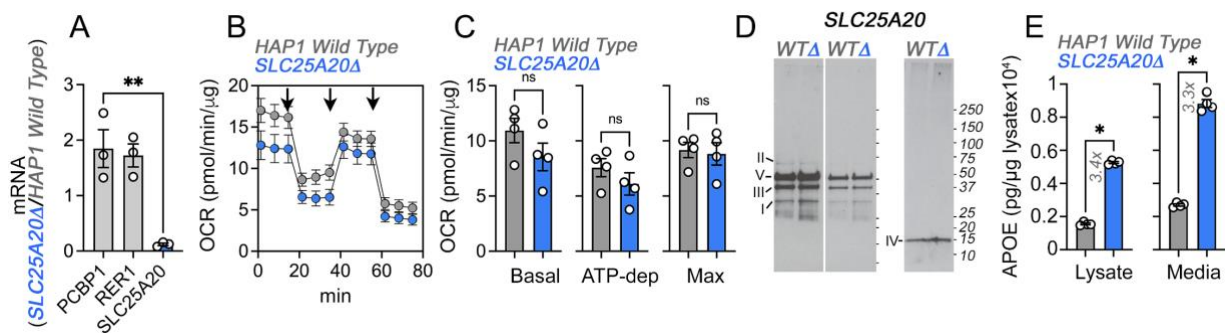
**Fig. 6 Fig Supplement 2. Upregulation of APOE Expression and Secretion in *SLC25A20* Mutant Cells.**

**A.** qRT-PCR quantification of SLC25A20 and housekeeping control genes (PCBP1 and RER1) in wild-type and *SLC25A20Δ* mutant cells. Average ± SEM, One-Way ANOVA followed by Dunnett's multiple comparisons test. **B**. Seahorse stress test in wild-type and *SLC25A20Δ* HAP1 cells. Arrows show sequential addition of oligomycin, FCCP, and rotenone-antimycin during the Seahorse stress test. **C**. Depicts basal, ATP-dependent and maximal oxygen consumption rates. p value, Mann-Whitney U test, n=4. **D**. Immunoblots with OxPhos antibody mix in mitochondrial fractions from wild-type and *SLC25A20Δ* cells. Left panels represent two exposures and right panel shows blot with COX4 antibodies. **E**. MesoScale ELISA determinations of human APOE in wild-type and *SLC25A20Δ* mutant cells. Shown are APOE content in lysates and conditioned media. p value, Mann-Whitney U test, n=4. All graphs depict average ± SEM.
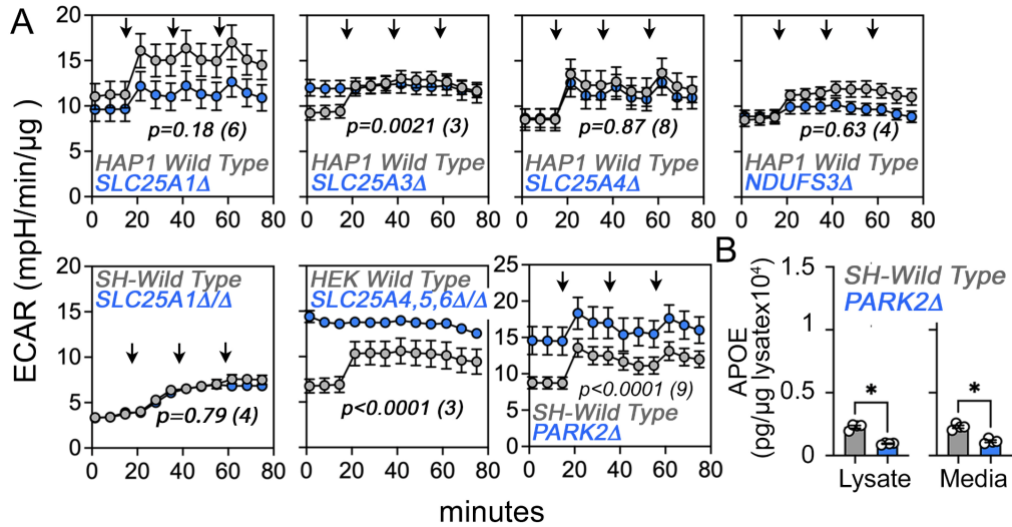
**Fig. 6 Fig Supplement 3. Extracellular Acidification Rate (ECAR) in Wild Type and Diverse Mutant Cells.**

**A.** ECAR was measured by Seahorse stress test in wild-type and mutant HAP1, SH-SY5Y, and HEK293 cells. Arrows mark the sequential addition of oligomycin, FCCP, and rotenone-antimycin during the Seahorse stress test. Average ± SEM, Two-Way ANOVA followed by Bonferroni multiple comparisons test, p value represents the effect of genotype, n of experiments is in parentheses. **B.** MesoScale ELISA determinations of human APOE in wild-type and *PARK2Δ/Δ* mutant SH-SY5Y cells. PARK2 mutants were selected as controls where there is strong acidification of media as measured by ECAR. Unpaired t-test with Welch's correction.

**Fig. 6 Fig Supplement 4. Citrate Effects on APOE Expression in HAP1 Cells.**

**A.** Diagram of citrate pathways and genes studied. **B**. Fireworks analysis of co-essentiality genes to identify genes connected to ACLY (Amici et al., 2021). Green denote hubs and purple marks MitoCarta annotated nodes. ACLY is a component of the SLC25A1 interactome, see Gokhale et al. (Gokhale et al., 2021). **C.** qRT-PCR quantification of citrate transporter SLC13A5 and a housekeeping control gene (PCBP1)  in wild-type and *SLC25A1Δ* HAP1 cells. **C.** MesoScale ELISA determinations of human APOE in wild-type and *SLC25A1Δ* HAP1 cells incubated with vehicle, 2.5 mM citrate for 48h. Average ± SEM, One-Way ANOVA followed by Dunnett's multiple comparisons test. **D.**  qRT-PCR quantification of ACLY and a housekeeping control gene (PCBP1) in wild-type and *ACLYΔ* mutant cells. Average ± SEM, One-Way ANOVA followed by Dunnett's multiple comparisons test. E. MesoScale ELISA determinations of human APOE in wild-type and *ACLYΔ* HAP1 cells. Unpaired t-test with Welch's correction.

**Fig. 6 Fig Supplement 5. AMPK, Mitochondrial Stress, and Redox Responses in Wild Type and**

***SLC25A1Δ* HAP1 cells.**

**A.** Activity of AMPK in wild-type (lanes 1-2) and *SLC25A1Δ* (lanes 3-4) HAP1 cells was assessed with

antibodies against AMPK, phospho-AMPK, and SLC25A1. Cells were treated with AICAR at 0.4 mM

concentration for 72 hours to induce the activation of AMPK (lanes 2 and 4). **B.** RNAseq determinations

of FGF21 and GDF21 as well ATF transcription factors in wild-type and mutant cells. **C.** Cis-regulatory

sequence analysis with iRegulon to infer transcriptional responses activated in the *SLC25A1Δ* and

*SLC25A4Δ* upregulated transcriptome (1429 transcripts p<0.001 and log2 fold of change=1) (Janky et

al., 2014). Significance threshold is set at 3. There are no ATF3, 4, or 5 target genes in the *SLC25A1Δ*

upregulated transcriptome. **D**. Activation of the mitochondrial stress response with doxycycline modestly

increases APOE in conditioned media from *SLC25A1Δ* cells but not in wild-type cells. MesoScale ELISA

determinations of human APOE in wild-type and *SLC25A1Δ* cells treated in the absence or presence of

doxycycline at a concentration of 9.75 micromolar for 48 hours. APOE was measured in cell lysates and media. **E-F**. Activation of the mitochondrial stress response with doxycycline in wild-type (D) and *SLC25A1Δ* (E) HAP1 cells. Doxycycline treatment was performed as in C. Gene expression was determined by qRT-PCR measuring the transcription factors ATF3-5 and their selected target genes ASNS, CHAC1, CHOP, PCK2 and WARS. RER1 and PCBP1 were used as housekeeping control transcripts. n=3. **G**. Cells were treated with 2 mM N-acetyl cysteine (NAC) for 48 hours, n=3. RER1 was used as a control gene and glutathione-disulfide reductase (GSR) as a NAC-sensitive gene reporter. E to G show data as a ratio between drug/vehicle. All figures depict average $\pm$ SEM. For F and G, One-Way ANOVA followed by Šydák's multiple correction. D and E One-Way ANOVA followed by Benjamini-Krieger-Yekuiteli multiple comparison corrections (FDR=5%).

## 2.3.5 Mitochondrial Dysfunction Induces APOE Expression and Inflammatory Responses in Immortalized Cells and Human Astrocytes.

The APOE4 allele is the strongest genetic risk factor for sporadic Alzheimer's disease and APOE-associated neuroinflammation is thought to play a prominent role in disease pathogenesis (Krasemann et al., 2017; Parhizkar and Holtzman, 2022; Tzioras et al., 2019; Zalocusky et al., 2021). We found that disruption of complex I subunit NDUFS3 and complex I assembly factor NDUFAF7 increases APOE expression (Fig. 4). The *NDUFS3* and *NDUFAF7* genes are encoded in loci that increase Alzheimer's disease risk (de Rojas et al., 2021; Kunkle et al., 2019). Moreover, the complex IV subunit COX7C is an additional electron transport gene encoded in a novel Alzheimer's risk locus (Bellenguez et al., 2022). These genetic associations between APOE and the respiratory chain with Alzheimer's disease risk prompted us to ask the following questions: 1) Do human brain cells modify the expression of APOE after disruption of the respiratory chain? 2) Is mitochondrially-induced APOE expression an isolated event, or does it co-occur in the context of inflammatory response?

To address the first question, we treated wild-type human iPSC-derived neurons and astrocytes with antimycin for 48 hours. Cells were treated with antimycin concentrations that

inhibit mitochondrial respiration in neurons and astrocytes, but do not affect cell viability (unpublished data). Astrocytes increased APOE protein expression two-fold after antimycin treatment (Fig. 7A). These astrocytic APOE increases were detected both in cell lysates and conditioned media (Fig. 7A). In contrast, neuronal cells failed to increase APOE expression after exposure to antimycin (Fig. 7A). We did not detect APOE in neuronal conditioned media (not shown). These findings show that APOE expression and secretion are modulated by intoxication of the electron transport chain in iPSC-derived human astrocytes but not neurons. To determine if APOE expression was coordinated with an inflammatory response, we analyzed the expression of 770 genes using a NanoString mRNA quantification panel. This neuroinflammatory panel reports the activity of 23 neuroinflammation pathways and processes across five brain cell types and 14 cell types of the peripheral immune system. We chose this approach since it is validated in Alzheimer's models, highly sensitive, and measures mRNAs without cDNA amplification (Das et al., 2021; Ramesha et al., 2021). We performed NanoString quantification in wild-type, *SLC25A1Δ*, and *SLC25A4Δ* HAP1 cells, as well as in iPSC-derived astrocytes treated for 48 hours with sublethal doses of antimycin (Fig. 6B). We identified upregulation of 3-10% of the genes in the panel across these three cellular models (Fig. 7B). Among these genes, APOE mRNA was upregulated 6-fold in mutant HAP1 cells and 1.5 times in antimycin-treated astrocytes as compared to a housekeeping control, TBP (Fig. 7C). The genes upregulated in antimycin-treated astrocytes were significantly enriched in genes annotated to the secretome, as compared to the content of secretome-annotated genes built into the panel (Fig. 7D, compare enrichment factors of 2.8 and 1.6, respectively). Like in *SLC25A1Δ* and *SLC25A4Δ* HAP1 cells, this enrichment of altered secretory transcripts induced by mitochondrial damage was similar to changes in mitochondrially-annotated transcripts.

We identified four upregulated mRNAs common to these three experimental conditions (Fig. 7E, APOE, TSPAN18, PTPN6, and LOX). The number of hits increased to 45 upregulated mRNAs when considering shared functional annotations (Fig. 7E). These functional annotations

were mostly related to cytokine signaling ontologies (Fig. 6F, R-HSA-1280215 and GO:0034097 Log q-value=-25.19 and -18.18). To explore whether the 85 upregulated genes in antimycin-treated astrocytes were part of a neurotoxic A1 reactive astrocyte phenotype associated with neurodegeneration, we compared the fold of induction of these transcripts with the changes in expression of these mRNAs in astrocytes after inflammatory LPS administration to elicit the A1 transcriptional phenotype (Liddelow et al., 2017). There was no correlation in gene expression among these datasets (Fig. 7-figure supplement 1). These results suggest that increased expression of APOE induced by disruption of mitochondria co-occurs with inflammatory mechanisms, which are distinct from known expression signatures of reactive astrocytes induced by LPS.
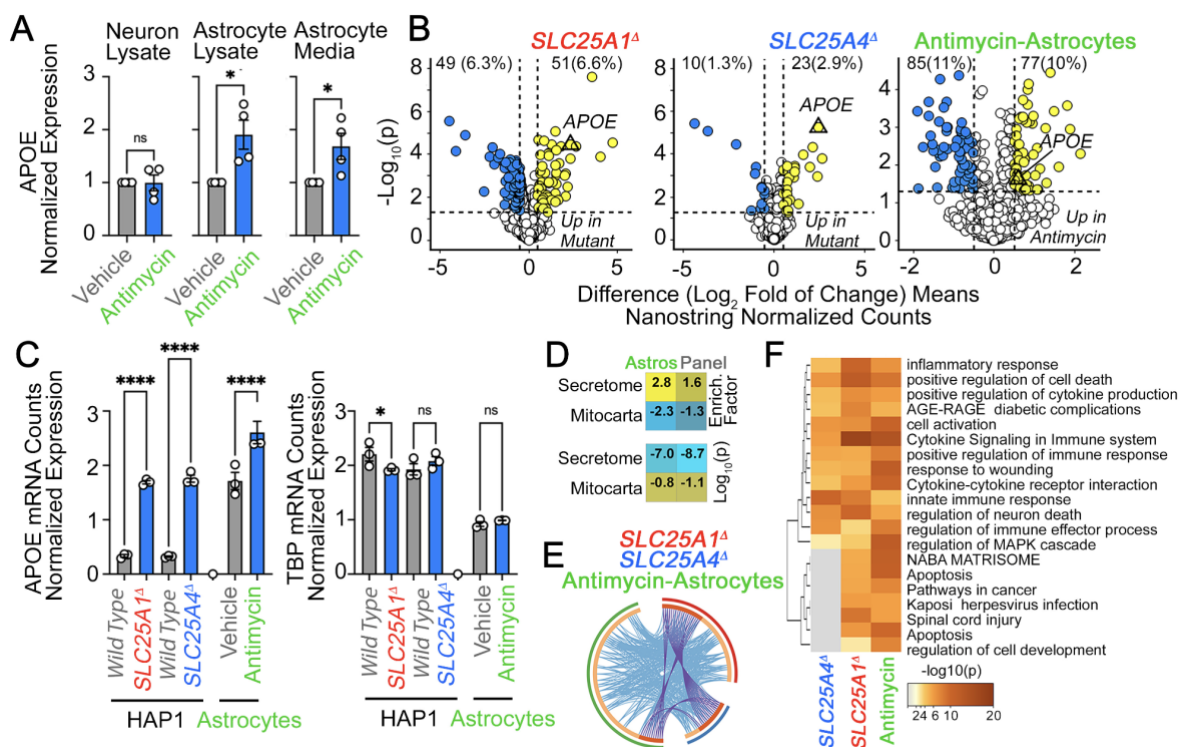


**Fig. 7. APOE Expression is Increased in Human Astrocytes after Complex III Inhibition.**

**A**. MesoScale ELISA determinations of human APOE in wild-type iPSC-derived human neurons and astrocytes treated with vehicle or 40-80 nM antimycin for 48h. APOE determinations were performed in

cell lysates and conditioned media and expressed normalized to a control value. n=4. *P* was obtained with two-sided estimation statistics. Untreated iPSC-derived astrocytes secrete ~70 x $10^4$ pg/μg lysate. **B-G**. Present analyses of changes in mRNA expression measured with NanoString Neuroinflammation panel. **B**. Volcano plots of wild-type, *SLC25A1Δ*, and *SLC25A4Δ* HAP1 cells (n=3 per genotype) and iPSC-derived astrocytes treated with vehicle or 80nM antimycin for 48h (n=3). Yellow symbols represent upregulated genes in mutant or drug treated cells. **C**. mRNA expression APOE and TBP was expressed as APOE /TADA2B or TBP/TADA2B ratios. TBP and TADA2B are both housekeeping control transcripts One-Way ANOVA followed by Benjamini-Krieger-Yekuiteli multiple comparison corrections (FDR=5%). **D.** Magnitude of compromise of significantly upregulated mRNAs annotated to secreted and mitochondrial proteomes in antimycin-treated astrocytes and compared to all genes present in the Neuroinflammation NanoString panel. p value was calculated with exact hypergeometric probability. **E.** Circos plot of shared upregulated hits in *SLC25A1Δ*, and *SLC25A4Δ* HAP1 cells and iPSC-derived astrocytes treated with 80nM antimycin. Outside arc represents the identity of each gene list. Inside arc represents a gene list, where each gene member of that list is assigned a spot on the arc. Dark orange color represents genes that are shared by multiple lists and light orange color represents genes that are unique to that gene list. Shared genes are presented by purple lines and different genes that belong to the same functional ontologies are connected by light blue lines. **F**. Metascape ontology analysis and clustering of genes upregulated in *SLC25A1Δ*, and *SLC25A4Δ* HAP1 cells and iPSC-derived astrocytes treated with 80nM antimycin. Accumulative hypergeometric p-values.
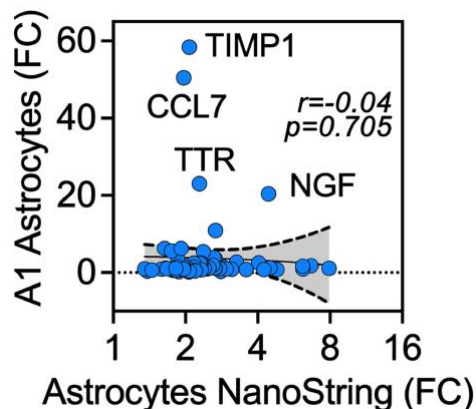
**Fig. 7 Fig Supplement 1. Human iPSC Astrocytes treated with Antimycin Differ in their Gene Expression as Compared to A1 Astrocytes.**

Correlation of fold of expression between the antimycin-upregulated genes in astrocytes obtained by NanoString (see Fig. 6) and the expression of the same genes in A1 reactive astrocytes induced by a neurotoxic stimulus constituted by C1IL1α (3 ng/ml), TNF (30 ng/ml), C1q (400 ng/ml) for 24 hours(Liddelow et al., 2017). Simple linear regression fit and 95% confidence interval is shown for n for x=85 and n for y axis=72. FC, fold of change.

### 2.3.6 The expression of APOE and respiratory chain subunits are inversely correlated in a mouse model of Alzheimer's disease

Increased expression of APOE coinciding with an inflammatory response is reminiscent of Alzheimer's pathology.   We hypothesized that if the expression of APOE and components of the electron transport chain were to be mechanistically linked, such an association should fulfill two predictions in a preclinical Alzheimer's brain model. First, there should be an inverse correlation in the protein levels of electron transport chain subunits and APOE if mitochondrial disruption were to induce increased APOE expression in diseased brains. Second, alterations in the levels of electron transport chain subunits should precede an APOE increase in diseased brains. To test this hypothesis, we used the 5xFAD mouse model of Alzheimer's disease that expresses human APP and presenilin 1 encoding five human pathogenic mutations that cause familial Alzheimer's disease (Oakley et al., 2006). Pathology in these mice progresses with aging

and these transgenes induce age-dependent expression of APOE and inflammatory gene products (Bai et al., 2020; Oakley et al., 2006). We analyzed a cohort of mice of both genotypes from ages 1.8 to 14.4 months (equally balanced for males and females per group), representing young adults to middle-age adult mice. Neuropathology begins at 2 months of age while cognitive impairment begins after 4 months of age in the 5xFAD mouse model (Girard et al., 2014; Oakley et al., 2006).

We performed TMT mass spectrometry on the cortex from 86 mice and quantified over 8,000 proteins from which we performed an analysis on APOE and 914 Mitocarta 3.0 proteins (Rath et al., 2021), including all subunits of the five complexes of the electron transport chain, and 33 of the SLC25A transporters present in mitochondria (Fig. 8A). We analyzed whether the expression of brain APOE correlated with the expression of these mitochondrial proteins and determined the effects of age, the 5xFAD genotype, and the interaction of these factors (Fig. 8A-C). We measured composite protein abundance of all subunits belonging to each one of the respiratory complexes, or composite SLC25An transporter protein abundance by calculating the first principal component of all proteins assigned to the complex or composite (Composite protein abundance, Fig. 8D). APOE expression across all ages inversely correlated with the expression of complex I, II, and IV subunits in 5xFAD but not in wild-type animals (Fig. 8B-C). We further examined the effects of age and genotype on the expression of APOE (Fig. 8D) and all complexes of the electron transport chain (Fig. 8D). The expression of respiratory complex subunits varied with age in wild-type animals (Fig. 8D, gray symbols). For example, complex I subunits increased to a plateau at 6 months of age in wild-type cortex (Fig. 8D, gray symbols). APOE expression remained constant with age in wild-type animals (Fig. 8D, gray symbols). However, APOE expression progressively increased 7-fold in 5xFAD animals (Fig. 8D, blue symbols) while most electron transport chain complexes decreased their expression with age in 5xFAD animals (Fig. 8C-D). We detected a significant decrease in the expression of complex I and one of three mitochondrial Alzheimer's disease risk factors, COX7C, in 5xFAD cortex (Bellenguez et al., 2022).

Importantly, these changes in respiratory chain protein levels preceded the APOE increase observed at 6 months of age in mutant animals (Fig. 8D). These results reveal that changes in the expression of complex I and COX7C are followed by later increases in APOE in diseased cortex.

### 2.3.7 *SLC25A1*-sensitive gene expression correlates with human cognitive trajectory during aging

We asked whether the expression of APOE, electron transport chain subunits, and SLC25A transporters correlates with age-dependent cognition in humans. We analyzed the Banner cohort of 106 individuals, of whom, 104 had normal cognitive performance at the time of enrollment (Beach et al., 2015). These adult brain donors were longitudinally assessed to determine their rate of change of cognitive performance over time (i.e., cognitive trajectory), irrespective of neuropathology. Cognitive trajectory refers to change of performance on the Mini-Mental State Exam (MMSE) over time (Folstein et al., 1975). The donor's quantitative brain proteomic profiles were obtained postmortem. In this and other cohorts, the expression of mitochondrial proteins, in particular complex I and III subunits, predicts cognitive preservation while proteins annotated to inflammatory ontologies predict a faster cognitive decline (Johnson et al., 2022; Wingo et al., 2019).

We assessed whether brain protein expression levels of gene products differentially expressed in SLC25A1-null cells, such as electron transport chain subunits (Fig. 2), correlated with cognitive trajectory in the Banner cohort subjects. We used three differentially expressed gene sets from SLC25A1-null cells: the downregulated *SLC25A1Δ* transcriptome dataset (Fig. 2F), which is enriched in genes associated with neuronal differentiation, axon guidance, and neurotransmission ontologies (Fig. 2P); the *SLC25A1Δ* upregulated mRNAs, which includes APOE and sterol synthesis genes (Fig. 2F and P); and the differentially expressed proteins in the *SLC25A1Δ* TMT proteome (Fig. 2B and O). These differentially expressed gene sets were

represented by the first principal component of their protein expression levels in each one of the 106 human subjects in the Banner cohort (Fig. 8E, PC1).

We confirmed the expression of some of the transcripts present in the downregulated *SLC25A1Δ* transcriptome by qRT-PCR, both in HAP1 cells and human neuroblastoma cells (Fig. 8-figure supplement 1), focusing on genes implicated in neurodevelopment and intellectual disability (Abidi et al., 2002; Akita et al., 2018; Ayalew et al., 2012; Bassani et al., 2012; Becker et al., 2009; Curto et al., 2019; Krocher et al., 2014; Kury et al., 2017; Lee et al., 2015; Leonardo et al., 1997; Picard et al., 2009; Shoukier et al., 2013; Srivastava et al., 2014; Tsuboyama and Iqbal, 2021; Vawter, 2000; Yan et al., 2018; Zemni et al., 2000; Zurek et al., 2016). In the Banner cohort, the brain protein expression representing the *SLC25A1Δ* upregulated mRNAs correlated with an accelerated cognitive decline (r=-0.607, p <1.03e-11, Fig. 8E). In contrast, the brain protein expression representing the downregulated mRNAs associated with a slower rate of cognitive decline in the Banner cohort proteomes (r=0.472, p<4.45e-07, Fig. 8E). Like the *SLC25A1Δ* upregulated mRNAs, increased brain expression of the differentially expressed proteins in the *SLC25A1Δ* TMT proteome (Fig. 2B) also correlated with accelerated cognitive decline (r=-0.537, p<4.45e-07, Fig. Fig. 8E). The *SLC25A1Δ* upregulated mRNAs and proteome shared APOE and sterol synthesis as a top ontology (Fig. 2O-P). These data suggest that genes and proteins sensitive to SLC25A1 expression regulate cellular processes important for cognition.

We used an orthogonal SLC25A1 dataset obtained from SH-SY5Y neuroblastoma cells to further test the hypothesis that the network of proteins regulated by SLC25A1 influences cognition. We focused on the SLC25A1 interactome, the proteins that co-precipitate with SLC25A1. We previously identified the SLC25A1 interactome using quantitative mass spectrometry and found that this network of proteins is enriched in some respiratory chain subunits as well as other SLC25A inner mitochondrial membrane transporters (Gokhale et al., 2021). We reasoned that if the SLC25A1 interactome converges on similar biological processes as the *SLC25A1Δ* proteome or transcriptomes, then the SLC25A1 interactome should also have

significant correlations with cognitive trajectory in the Banner cohort. In line with this reasoning, we found that greater expression of proteins belonging to the SLC25A1 interactome strongly correlated with a rapid cognitive decline in the Banner cohort (r=-0.527, p <9.92e-08, Fig. 8E). We used as controls the mitochondrial and cytoplasmic ribosomes subunit datasets consisting of ~80 subunits each (MitoCarta 3.0 and CORUM complex #306). The mitochondrial ribosome correlated poorly with cognitive decline in the Banner cohort as compared to the SLC25A1 datasets even though the SLC25A1 interactome dataset was of a similar size to the mitochondrial ribosome dataset (Fig. 8E, compare SLC25A1 interactome composed of 75 proteins and mitochondrial ribosome composed of 77 proteins). In addition, the expression of cytoplasmic ribosomal proteins did not correlate with the cognitive trajectory of the Banner subjects (r=-0.24 and p=0.249, Fig. 8E). Taken together, our data suggest that a network of mitochondrial proteins, including the respiratory chain and several members of the SLC25A transporter family, regulates APOE expression and other cellular processes modulating cognition during aging.
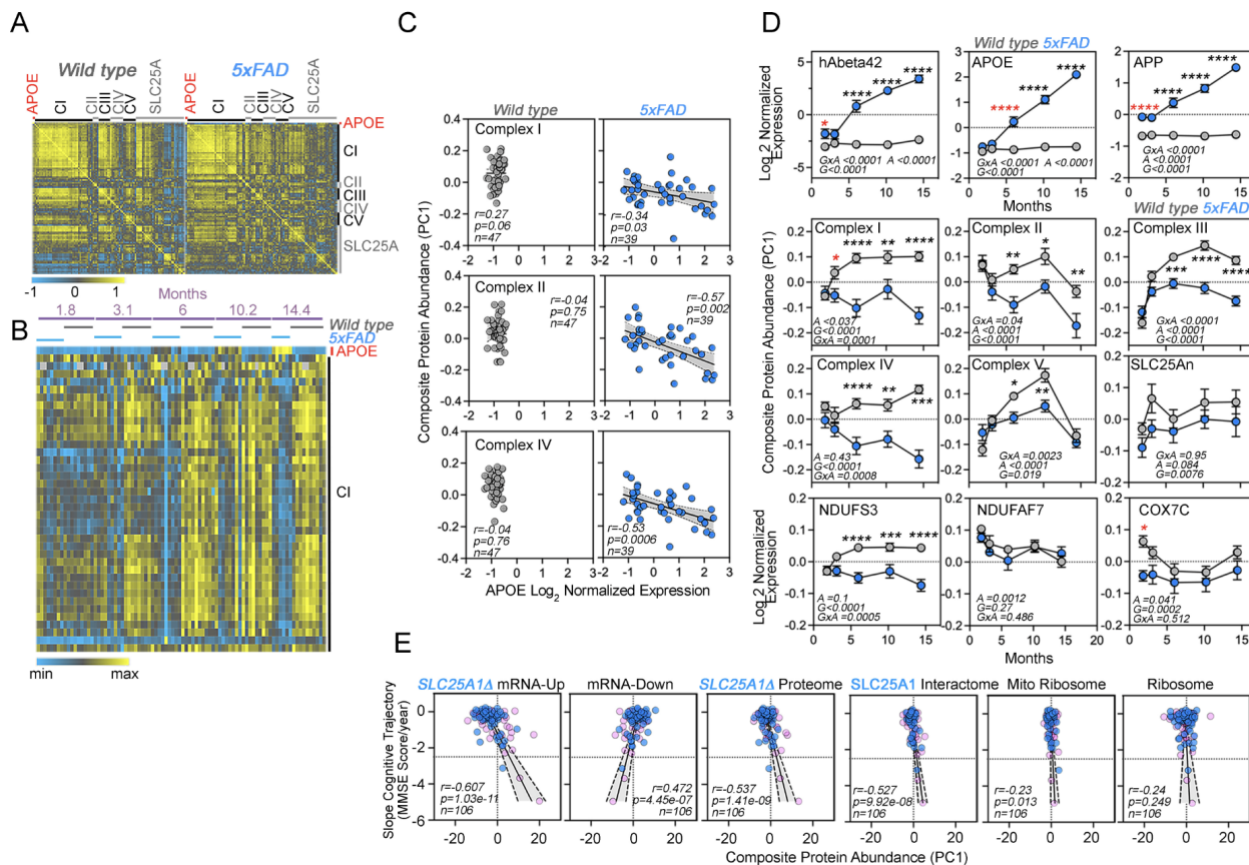
**Fig. 8. Correlative Studies of APOE Expression and Electron Transport Chain Subunits in an Alzheimer's mouse model and aging humans.**

**A**. Protein expression similarity matrix of APOE, complexes I to V (CI-CV) of the electron transport chain, and transporters of the SLC25A family in wild-type and 5xFAD mouse models. Data were obtained by TMT mass spectrometry from mouse cortices. Similarity was calculated with Spearman Rank correlation. **B.** Kendall Tau Hierarchical clustering of complex I subunits and APOE across ages and genotypes. **C.** Correlation of composite protein abundance for complexes I, II and IV in wild-type and 5xFAD mouse cortices with APOE levels. **D.** Quantification of human A beta 42 peptide, APP, APOE, three mitochondrial Alzheimer's risk factors (NDUFS3, NDUFAF7, and COX7C), and the composite protein abundance for complex I to V, as well as members of the SLC25A family of mitochondrial transporters in wild-type and 5xFAD mice (grey and blue symbols, respectively). Two-way ANOVA followed by Šídák's multiple comparisons tests. Factors are age (*A*), genotype (*G*), and their statistical interaction (*I*). Asterisks denote significant differences between genotypes at a defined age. Red asterisks denote the earliest age with

differences between genotypes. See supplementary file 1 for all Mitocarta hits in the 5xFAD mouse study. **E.** The SLC25A1 RNAseq, proteome, and interactome correlate with the cognitive trajectory of human subjects. Cytoplasmic and mitochondrial ribosome subunits were used as controls. Graphs depict the correlation between the cognitive trajectory (Mini-Mental State Examination (MMSE)) in subjects belonging to the Banner collection that were longitudinally followed for an average of 14 years (n=106) (Beach et al., 2015; Wingo et al., 2019). The *SLC25A1Δ* RNAseq, up and downregulated hits, proteome hits, as well as the SLC25A1 interactome hits principal components were derived by estimating eigenvectors of the expression matrix of protein abundance data. Best-fit regression line drawn in blue and the 99.9% confidence interval for the regression line shaded in gray. No covariate was applied because sex, age at enrollment, and education have been regressed out of cognitive trajectory (Wingo et al., 2019). Blue circles represent males, pink circles represent females (48.1%).
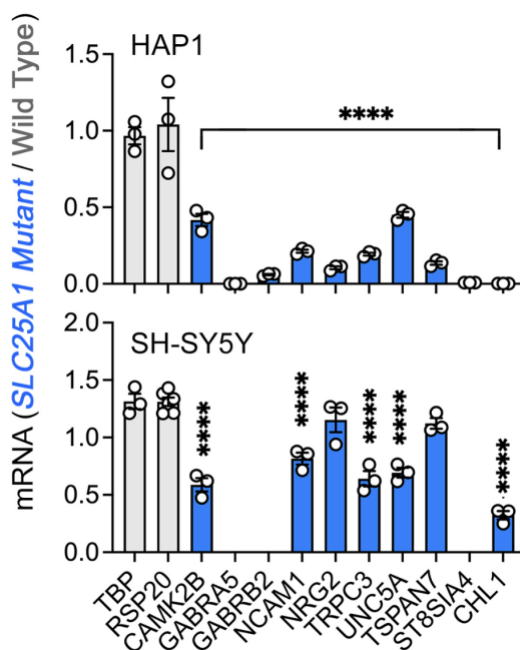


**Fig. 8 Fig Supplement 1. Interactions between SLC25A1 and NDUFS3 and Neuronal Ontology Annotated Genes Downregulated in *SLC25A1* Mutant Cells.**

qRT-PCR quantification of neuronal ontology annotated genes and housekeeping controls (TBP and RPS20) in wild-type and *SLC25A1* mutant HAP1 and SH-SY5Y cells. Average ± SEM, One-Way ANOVA followed by Holm-Šydák's multiple correction test. n=3.

**2.4 Discussion**

Here we report our discovery that mutations in nuclear-encoded mitochondrial transporter genes, *SLC25A1* and *SLC25A4*, modify the secretome and mitochondrially-annotated proteome to a similar extent. Intriguingly, mutations in either one of these mitochondrial transporters upregulated the expression and secretion of the lipoprotein APOE in diverse cellular systems. We focused on APOE, as it is the main risk factor for Alzheimer's disease, a disease associated with compromised mitochondrial function (Wang et al., 2020). We show that this mitochondrial-dependent APOE upregulation phenotype occurs in response to loss of integrity of the electron transport chain secondary to either *SLC25A1* or *SLC25A4* mutagenesis. We demonstrate that disruption of the assembly and function of electron transport chain complexes I, III, and IV also increases APOE, arguing that a main initiating event in a cascade that increases APOE levels is the disruption of electron transport chain integrity and function. Both mutations that directly or indirectly compromise the electron transport chain increase APOE levels. For example, genetic disruption of copper loading into complex IV with mutants directly targeting copper loading factors, such as COX17 and COX19, increased APOE levels. A similar APOE phenotype is obtained by indirectly disrupting cellular copper homeostasis at the plasma membrane (SLC31A1 and ATP7A), the mitochondrial inner membrane (SLC25A3), or by pharmacological copper chelation with BCS, all conditions that affect complex IV (Boulet et al., 2018; Cobine et al., 2021; Guthrie et al., 2020). The mitochondrial protein network modulating APOE expression includes proteins encoded by prioritized genes within Alzheimer's disease risk loci necessary for electron transport chain complex I assembly and function (de Rojas et al., 2021; Kunkle et al., 2019). Furthermore, we show that this mitochondrial regulation of APOE expression extends to brain cells, iPSC-derived human astrocytes, and co-occurs with an inflammatory gene expression response. Together, our data demonstrate that mitochondria robustly regulate APOE expression and secretion, placing them in a novel position upstream of APOE. We propose that this mitochondria-

to-APOE mechanism may operate in the pathogenesis of dementia, a proposition supported by our protein expression correlation studies in mouse Alzheimer's brains and aging human brains.

Our results support the idea that there are other intramitochondrial mechanisms connecting mitochondria to APOE expression and secretion beyond the loss of integrity of the electron transport chain. Mutagenesis of the mitochondrial carnitine transporter SLC25A20 also upregulated APOE, despite these cells respiring normally and having wild-type levels of respiratory chain subunits. Similarly, mutagenesis of a cytosolic enzyme that controls the synthesis of acetyl-CoA using citrate as a substrate also increases APOE expression. Thus, we postulate that in addition to the integrity of the electron transport chain there are other mitochondrial and cytoplasmic mechanisms regulating APOE expression.

We tested several alternative hypotheses that could account for a link between mitochondrial dysfunction and heightened nuclear expression of APOE. We measured the rates of oxygen consumption and extracellular acidification, the latter as a proxy for glycolysis (Zhang and Zhang, 2019). We found that while the oxygen consumption rate negatively correlated with APOE levels, the rate of extracellular acidification did not correlate with APOE expression (Fig. 6). These observations make it unlikely that glycolytic adaptations in the mitochondrial mutants used in our studies could account for the APOE phenotype. We also assessed whether decreased cytoplasmic ATP levels led to APOE upregulation. The AMPK pathway senses drops in ATP cytoplasmic levels and coordinates a response to increase ATP generation when cellular energy is depleted (Herzig and Shaw, 2018). If decreased ATP levels mediate increased APOE protein levels, SLC25A1-null cells should display activation of the AMPK pathway at baseline. We found that, while SLC25A1-null cells are sensitized to respond to an AMPK-activating drug, the pathway is minimally active in the cells at baseline (Fig. 6-figure supplement 5). This aligns with our previous finding that ATP levels between SLC25A1-null and wild-type cells do not differ (Gokhale et al., 2019). A second possible mechanism is that APOE expression is a coordinated response with an upregulation of cholesterol synthesis via SREBP transcription factors (Horton et al., 2002).

We found that SLC25A1-null HAP1 cells had increased expression of cholesterol synthesis pathway enzymes, accompanied by elevated free cholesterol and cholesterol esters, consistent with SREBP transcription factor activation. However, these phenotypes were not shared by SLC25A1-null neuroblastoma cells or SLC25A4-null cells, even though these cells also displayed increased APOE expression and secretion (Fig. 3). Thus, increased APOE resulting from mitochondrial dysfunction is not dependent on cholesterol synthesis pathways. A third mitochondria-to-nucleus pathway we investigated is mediated by activation of transcription factors ATF4 and CHOP (Quiros et al., 2017). These factors control the expression of mitokines in response to mitochondrial stress as part of the integrated stress response transcriptional pathway (Chung et al., 2017; Kim et al., 2013). Administration of doxycycline to trigger the stress response mounted an appropriate transcriptional response (Quiros et al., 2017) in both wild-type and SLC25A1-null cells (Fig. 6-figure supplement 5), although this response was somewhat blunted in the mutant cells, even at baseline (Fig. 6-figure supplement 5). Despite stress response activation, cellular and secreted levels of APOE protein were unaffected besides a mild increase in secretion in the SLC25A1-null cells (Fig. 6-figure supplement 5). Furthermore, FCCP, also a potent activator of the mitochondrial stress response (Quiros et al., 2017) failed to induce APOE expression in HAP1 cells, even though inhibition of either complexes I or V with piericidin A or oligomycin increased APOE levels (Fig. 4-figure supplement 2). Thus, the ATF4-dependent stress response alone cannot account for elevated APOE expression and secretion. A fourth mechanism that could account for the increased APOE expression is dependent on redox imbalance. We think this mechanism is unlikely because the antioxidant N-acetyl cysteine decreased the expression of the mitochondrial glutathione-disulfide reductase in both wild-type and SLC25A1-null cells, but it did not change APOE mRNA levels (Fig. 6-figure supplement 5). Finally, we looked for transcriptional signatures in the SLC25A1 and SLC25A4 upregulated transcriptomes and found neither common predicted transcription factors that could account for the changes in gene expression in both genotypes, nor transcription factors known to regulate APOE transcription such

as LXRs or C/EBPβ (Fig. S7C) (Laffitte et al., 2001; Xia et al., 2021). We suggest that a screen targeting large swaths of the genome in astrocytes and mutant cell lines used in this study would be an effective method for uncovering further mechanisms by which mitochondria contribute to APOE expression regulation.

Our findings expand previous work demonstrating that mitochondrial distress regulates the secretion of inflammatory cytokines and type I interferons (Dhir et al., 2018; Riley and Tait, 2020; Shimada et al., 2012; West et al., 2015), the growth factor mitokines GDF15 and FGF21 (Chung et al., 2017; Kim et al., 2013), the production of mitochondrially-derived peptides encoded in the mitochondrial genome (Kim et al., 2017), and alpha fetoprotein in hepatocytes (Jett et al., 2022). Our study makes two key contributions expanding on these non-cell autonomous mechanisms. First, we identified the first apolipoprotein whose expression and secretion are modulated by mutations affecting mitochondria. Second, while we focus on APOE, we think this apolipoprotein is a harbinger of an extended upregulation of the secreted proteome mediated by mitochondria (Uhlen et al., 2019). The importance of this secreted proteome change can be inferred from its extent and magnitude, which is on par with the changes we observed in the mitochondrially-annotated proteome. Our findings add to the growing notion that mitochondrial regulation of the secreted proteome is a more common process than previously appreciated (Jett et al., 2022; Sturm et al., 2023). We asked whether the APOE increase may be part of an inflammatory response by using NanoString mRNA quantification to assess the levels of activity of interleukin and interferon pathways in *SLC25A1Δ* and *SLC25A4Δ* cells and antimycin-treated astrocytes. Although *SLC25A4Δ* cells had a paucity of significant hits compared with *SLC25A1Δ* cells and antimycin-treated astrocytes, we found that all three experimental conditions converged on common hits whose number increased when considering hits belonging to shared ontologies. All cells showed increased levels of secreted cytokines and gene ontologies associated with their transcriptional profiles were enriched for cytokine signaling pathways. Thus, our data suggest that APOE upregulation in response to mitochondrial dysfunction could be part of an inflammatory

response initiated by mitochondria. Although mitochondria are often viewed as downstream targets of neuroinflammation, our results with antimycin-treated astrocytes add to growing evidence that mitochondria drive inflammatory signaling in the nervous system (Bader and Winklhofer, 2020; Joshi et al., 2019; Lin et al., 2022).

What role does increasing APOE expression and secretion in response to mitochondrial dysfunction serve for the cell? Increased APOE secretion induced by mitochondrial damage could be adaptive or maladaptive depending on the lipidation and contents of APOE. APOE-mediated lipid exchange between cells can alter the lipid microenvironments of cellular membranes, thereby influencing cell signaling and homeostasis (Martens et al., 2022; Tambini et al., 2016). APOE is a primary lipoprotein in the brain produced mainly by astrocytes, though neurons and other glia also express APOE (Belloy et al., 2019; Martens et al., 2022). APOE particles play necessary roles in handling toxic lipids by shuttling them between cell types, with differential effects depending on the cell type from which the APOE particle originated, the lipid species loaded in the particle, and the fate of the lipid-loaded particle (Guttenplan et al., 2021; Ioannou et al., 2019; Liu et al., 2017). We speculate that either APOE-dependent removal of toxic factors from *SLC25A1* mutant cells, or wild-type conditioned media delivering a factor missing from *SLC25A1* mutant media, could explain our finding that dialyzed conditioned media from SLC25A1 mutant cells cannot support their own growth. Astrocytes play a prominent role in carrying and processing toxic lipids in the brain through APOE-dependent mechanisms. Since we observed increased APOE secretion in astrocytes, but not neurons, in response to antimycin, we speculate that APOE released from astrocytes following antimycin administration may not sustain either astrocytes and/or neurons. Profiling the contents of antimycin-induced APOE particles released from astrocytes could further clarify their potential impact on the function and health of neighboring cells.

The APOE E4 allele is the strongest genetic risk factor for sporadic Alzheimer's disease and APOE, along with amyloidogenic processing of the amyloid precursor protein (APP) into Aβ,

is thought of as an initiating and driving factor in disease etiology (Frisoni et al., 2022; Huang and Mahley, 2014; Mahley, 2023; Martens et al., 2022). While mitochondrial dysfunction is acknowledged as an important factor in Alzheimer's disease, mitochondria are typically placed downstream of Aβ and APOE, with Aβ or the APOE4 allele perturbing mitochondrial function (Area-Gomez et al., 2020; Chen et al., 2011; Mahley, 2023; Orr et al., 2019; Tambini et al., 2016; Yin et al., 2020). Some have proposed that mitochondria act as upstream factors in Alzheimer's pathogenesis through metabolic and bioenergetic effects (Rangaraju et al., 2018; Swerdlow, 2018; Wang et al., 2020). We argue that mitochondria could also participate in Alzheimer's pathogenesis through modulation of APOE allele-dependent mechanisms. The increased expression of APOE, which is inversely correlated with the expression of respiratory chain subunits in the 5xFAD mouse model, supports this proposition (Fig. 8). For example, increased expression of APOE E4 downstream of mitochondrial dysfunction could either initiate or exacerbate the effects of the APOE4 allele in neurodegenerative processes, since APOE4 is prone to aggregation and poor lipidation (Gong et al., 2002; Hatters et al., 2006; Hubin et al., 2019). Our findings open the possibility that mitochondria could act as initiators or drivers of Alzheimer's pathogenesis through modulation of APOE-dependent disease processes. The correlation of expression levels in the prefrontal cortex of proteins dysregulated in the SLC25A1 proteome and transcriptome with human cognitive trajectory provides evidence for this conception. Together, our work supports the idea that mitochondria influence brain function and cognition in part through modulation of the secretome, including a novel role in regulation of APOE expression and secretion.

**2.5 Materials and Methods**

**Cell lines, gene editing, and culture conditions**

Human haploid (HAP1) isogenic cell lines were obtained from Horizon Discovery. In addition to the parental wild-type line (C631, RRID: CVCL_Y019), the following CRISPR/Cas9-edited knockout cell lines were used: SLC25A1 (HZGHC001753c010, RRID: CVCL_TM05 and HZGHC001753c003, RRID: CVCL_TM04), SLC25A3 (HZGHC000792c010, RRID:CVCL_TM31), SLC25A4 (HZGHC000778c011, RRID:CVCL_TM45), SLC25A20 (HZGHC000787c00, RRID:CVCL_TM21), SLC25A50/MTCH2 (HZGHC23788), NDUFS3 (HZGHC4722, RRID:CVCL_XQ89), NDUFAF7 (HZGHC55471), PARK2 (HZGHC003208c002, RRID:CVCL_TC07), and ACLY (HZGHC005811c011, RRID: CVCL_SB23 and HZGHC005811c002, RRID: CVCL_XK97). All HAP1 cells were grown in IMDM (Corning 10-016) with 10% Fetal Bovine Serum (FBS) (VWR, 97068-085) in a 10% CO2 incubator at 37°C, unless otherwise indicated. In experiments where a single clone of SLC25A1-null cells was used, the cell line HZGHC001753c010 (RRID: CVCL_TM05) was used. In experiments where a single clone of ACLY-null cells was used, the cell line HZGHC005811c002 (RRID: CVCL_XK97) was used. For each knockout cell line, an individual control line of the HAP1 parental line that was received with the particular knockout line was used. Mutants and their unique control line were cultured and handled as parallel pairs to avoid passage- and culture-induced variation.

Human neuroblastoma SH-SY5Y cells (ATCC, CRL-2266; RRID:CVCL_0019) were grown in DMEM media (Corning, 10-013) containing 10% FBS (VWR, 97068-085) at 37°C in 10% $CO_2$, unless otherwise indicated. SH-SY5Y cells deficient in SLC31A1 were genome edited using gRNA and Cas9 preassembled complexes by Synthego with a knock-out efficiency of 97%. The gRNAs used were UUGGUGAUCAAUACAGCUGG which targeted transcript ENST00000374212.5 exon 3. Wild-type and mutant cells were cloned by limited dilution and mutagenesis was confirmed by Sanger sequencing with the primer: 5'GGTGGGGGCCTAGTAGAATA. SH-SY5Y cells deficient in ATP7A were genome edited by

Synthego using gRNA and Cas9 preassembled complexes with a knock-out efficiency of 80%. The gRNAs used were ACAGACUCCAAAGACCCUAC which targeted transcript ENST00000341514 exon 3. Wild-type and mutant cells were cloned by limited dilution and mutagenesis was confirmed by Sanger sequencing with the primer: 5'TGCCTGATAGGTACCACAGTC. SH-SY5Y cells deficient in Cox17 were genome edited by Synthego using gRNA and Cas9 preassembled complexes with a knock-out efficiency of 94%. The gRNAs used were CCAAGAAGGCGCGCGAUGCG which targeted transcript ENST00000261070 exon 1. Wild-type and mutant cells were cloned by limited dilution and mutagenesis was confirmed by Sanger sequencing with the primer: 5'AGGCCCAATAATTATCTCCAGAGC. The Cox17-deficient cells were supplemented with 50ug/ml uridine (Sigma, U3003) in their growth media. SH-SY5Y cells deficient in SLC25A1 were genome edited by Synthego using gRNA and Cas9 preassembled complexes with a knock-out efficiency of 86%. The gRNAs used were GGGTTCCCGGTCCCTGCAGG which targeted transcript ENST00000215882 exon 2. Wild-type and mutant cells were cloned by limited dilution and mutagenesis was confirmed by Sanger sequencing with the primer: 5'GATGGAACCGTAGAGCAGGG. For each mutant cell line, an individual control line of the SH-SY5Y parental line that was received with the particular mutant line was used. In APOE protein measurement immunoassays, two separate clones of cells were used to exclude clonal or off-target effects.

ATP7A LL cells contained a di-leucine mutation generated by introducing alanine in L1750 and 1751 by the Emory Genomics Core into the SH-SY5Y ATP7A CRISPR KO cells. HA-tagged ATP7A cDNA in pQCXIP backbone vector was provided by Dr. Michael Petris. SH-SY5Y ATP7A LL and empty vector expressing cells were generated by transfecting ATP7A KO10 cells with lipofectamine 3000 (Invitrogen). Selection was started after 24 h with 0.5ug/ml Puromycin (Gibco). Growth of clones was boosted by supplementing the media with 1uM Copper until sufficient cells

grew to freeze down and passage well. All ATP7A and SLC31A1 KO cells were validated by measuring copper content using ICP mass spectrometry.

HEK293 ANT1 single knockout , ANT triple knockout and their wild-type control cells were grown in DMEM containing 10% FBS, supplemented with 2 mM L-glutamine (HyClone, SH30034.01), 100 µg/ml zeocin (Gibco, R25001), and 15 µg/ml Blasticidin S (Sigma, SBR00022). The ANT1, ANT2, ANT3 triple knockout cells were additionally supplemented with 1 mM sodium pyruvate (Sigma, S8636) and 50 µg/ml uridine (Sigma, U3003). gRNAs that targeted ANT1, ANT2, and ANT3 were separately cloned into PX459, a gift from Feng Zhang (Addgene). gRNA sequences are GATGGGCGCTACCGCCGTCT (for ANT1), GGGGAAGTAACGGATCACGT (for ANT2), CGGCCGTGGCTCCGATCGAG (for ANT3), respectively.  T-REx™ 293 cells (Invitrogen R71007) were transfected with the PX459 constructs individually in order of ANT3, ANT2, and ANT1. Cell lines lacking only ANT1 were transfected once only with the ANT1 PX459 construct. Following each transfection, cells were selected with puromycin (2 µg/ml) for 72 hours, single clones were isolated by ring cloning and the absence of the protein expression was analyzed by immunoblotting before proceeding to the next transfection.

HEK293 cells knockout cell lines for HIGD1A, COX7A2L, COX18, COX19, and COX20 and their control cell line were grown in DMEM media (Corning, 10-013) containing 10% FBS (VWR, 97068-085), 50 µg/ml uridine (Sigma, U3003), and 1x GlutaMAX (Gibco, 35050061) at 37°C in 10% $CO_2$. Details about the generation of the cell lines using TALEN can be found in Nývltová et al., 2022 ((Nyvltova et al., 2022), COX19), Bourens and Barrientos, 2017 ((Bourens and Barrientos, 2017), COX18), Lobo-Jarne et al., 2018 ((Lobo-Jarne et al., 2018), COX7A2L), Timón-Gómez  et al., 2017 ((Timon-Gomez et al., 2020a), HIGD1A), and Bourens et al., 2014 ((Bourens and Barrientos, 2017), COX20).

This work used cell lines which were obtained from ATCC and Horizon Discovery. Cell lines were authenticated by provider and were tested to be free of mycoplasma in house.

**Antibodies**

| Antibody | Dilution | Cat.No | RRID |
|----------|----------|--------|------|
| ACTIN | 1:5000 | A5441 | AB_476744 |
| AMPK | 1:1000 | 2532S | AB_330331 |
| APOE | 1:250 | 60531 | AB_920623 |
| COX4 | 1:1000 | 4850 | AB_2085424 |
| FLAG | 1:1000 | A190-102A | AB_67407 |
| HSP90 | 1:1000 | 610418 | AB_397798 |
| HSP90 | 1:1000 | 610418 | AB_397798 |
| mouse HRP | 1:5000 | A10668 | AB_2534058 |
| MT-ATP6 | 1:500 | 55313-1-AP | AB_2881305 |
| MTCO2 | 1:1000 | AB110258 | AB_10887758 |
| NDUFB11 | 1:1000 | ab183716 | |
| NDUFS3 | 1:200 | 15066-1-AP | AB_2151109 |
| OXPHOS mix | 1:250 | ab110412 | AB_2847807 |
| P-AMPK | 1:1000 | 2535T | AB_331250 |
| rabbit HRP | 1:5000 | G21234 | AB_2536530 |
| SDHA | 1:1000 | 11998 | AB_2750900 |
| SLC25A1 | 1:500 | 15235-1-AP | AB_2297856 |
| TFRC | 1:1000 | 13-6800 | AB_86623 |
| UQCRC2 | 1:500 | ab 14745 | AB_2213640 |
| Antibody | Dilution | Cat.No | RRID |

| | | | |
|---|---|---|---|
| SDHA | 1:1000 | 11998 | AB_2750900 |
| SLC25A1 | 1:500 | 15235-1-AP | AB_2297856 |
| HSP90 | 1:1000 | 610418 | AB_397798 |
| MT-ATP6 | 1:500 | 55313-1-AP | AB_2881305 |
| MTCO2 | 1:1000 | AB110258 | AB_10887758 |
| TFRC | 1:1000 | 13-6800 | AB_86623 |
| ACTIN | 1:5000 | A5441 | AB_476744 |
| COX4 | 1:1000 | 4850 | AB_2085424 |
| OXPHOS mix | 1:250 | ab110412 | AB_2847807 |
| NDUFS3 | 1:200 | 15066-1-AP | AB_2151109 |
| UQCRC2 | 1:500 | ab 14745 | AB_2213640 |
| HSP90 | 1:1000 | 610418 | AB_397798 |
| APOE | 1:250 | 60531 | AB_920623 |
| AMPK | 1:1000 | 2532S | AB_330331 |
| P-AMPK | 1:1000 | 2535T | AB_331250 |
| FLAG | 1:1000 | A190-102A | AB_67407 |
| mouse HRP | 1:5000 | A10668 | AB_2534058 |
| rabbit HRP | 1:5000 | G21234 | AB_2536530 |

**Primers**

| Primer | Forward Sequence | Reverse Sequence |
|---|---|---|
| ACAT2 | CCCAGAACAGGACAGAGAATG | AGCTTGGACATGGCTTCTATG |
| ACLY | CTCACTAAGCCCATCGTCTG | TCCTTCAAAGCCTGGTTCTTG |
| APOE | TGGGTCGCTTTTGGGATTAC | TTCAACTCCTTCATGGTCTCG |
| ASNS | ATCACTGTCGGGATGTACCC | TGATAAAAGGCAGCCAATCC |

| | | |
|---|---|---|
| ATF3 | GGAGCCTGGAGCAAAATGATG | AGGGCGTCAGGTTAGCAAAA |
| ATF4 | CAGCAAGGAGGATGCCTTCT | CCAACAGGGCATCCAAGTC |
| ATF5 | GAGCCCCTGGCAGGTGAT | CAGAGGGAGGAGAGCTGTGAA |
| CAMK2B | CAGCCAGAGATCACCAGAAG | CACCAGTGACCAGATCGAAG |
| CHAC1 | GTGGTGACGCTCCTTGAAGA | TTCAGGGCCTTGCTTACCTG |
| CHL1 | ATGGCTCCCCAGTTGACA | TGATTTGGTTGAAGGTTGGTAA |
| CHOP | AGCCAAAATCAGAGCTGGAA | TGGATCAGTCTGGAAAAGCA |
| GABRA5 | CCTCCATATTCACCTGCTTCA | CTGGTTGGCATCTGTGAAAAG |
| GABRB2 | ACTCAGAATCACAACCACAGC | CCACGCCAGTAAAACTCAATG |
| GSR | TTCCAGATGTTGACTGCCTG | GCCTTTGACGTTGGTATTCTG |
| HMGCR | ACAGATACTTGGGAATGCAGAG | CTGTCGGCGAATAGATACACC |
| LDLR | TTCACTCCATCTCAAGCATCG | ACTGAAAATGGCTTCGTTGATG |
| MSMO1 | TGAACTTCATTGGAAACTATGCTTC | TCTTTCAGGAAGGTTTACGTGAG |
| NCAM1 | TTGTTTTTCCTGGGAACTGC | ACTCTCCAACGCTGATCTCC |
| NRG2 | CACTCCTGTTCTCCTTCTCAC | TTTGCTGGTACCCACTGATG |
| PCBP1 | AAGACTTGACCACGTAACGAG | ATGCTTCCTACTTCCTTTCCG |
| PCK2 | CATCCGAAAGCTCCCCAAGT | GCTCTCTACTCGTGCCACAT |
| RER1 | CTTTCTTCGACGCTTTCAACG | CTGTACCTTCTCTTCCCATGTG |
| RPS20 | TGCTGACTTGATAAGAGGCG | GATCCCACGTCTTAGAACCTTC |
| SLC13A5 | AGAGGTTGTGTAAGGCCATG | AGCAAAGTTCACGAGGTCC |
| SLC25A20 | AGAAGCTGTACCAGGAGTTTG | ACTGACCCTCTTTCCCTCC |
| ST8SIA4 | CATTAGGAAGAGGTGGACGATC | AGAGCTATTGACAAGTGACCG |
| TBP | GAGAGTTCTGGGATTGTACCG | ATCCTCATGATTACCGCAGC |
| TRPC3 | CAAATGCAGAAGGAGAAGGC | CGTGTTGGCTGATTGAGAATG |
| TSPAN7 | CCTTATTGCCGAGAACTCCAC | ACACCAGGGACAGAAACATG |
| UNC5A | CTGTACCAGTGACCTCTGTG | AAACGAGGATGAGGACAAGC |
| VAMP2 | TCATCTTGGGAGTGATTTGCG | GGGCTGAAAGATATGGCTGAG |
| WARS | TCAGCAACTCATTCCCACAG | GCAGGGCTGGTTTAGGATAG |

**Generation of iNeurons from Human iPSCs**

Accutase (Gibco, A11105) was used to disassociate iPSC cells. On day -2, the cells were plated on a 12-well plate coated in matrigel (Corning, 354230) in mTeSR medium (StemCell Technologies, 85850) at a density of at 380,000 cells per well. On day −1, hNGN2 lentivirus (TetO-hNGN2-P2A-PuroR (RRID: Addgene_79049) or TetO-hNGN2-P2A-eGFP-T2A-PuroR (RRID: Addgene_79823)) together with FUdeltaGW-rtTA (RRID: Addgene_19780) lentivirus were added in fresh mTeSR medium containing 4µg/µl polybrene (Sigma, TR-1003). The lentiviruses were added at 1×106 pfu/ml per plasmid (multiplicity of infection (MOI) of 2). On day 0, the culture medium was replaced with fresh KSR, consisting of KnockOut DMEM (Gibco, 10829018), Knockout Replacement Serum (Gibco, 10828028), 1X Glutamax (Gibco, 35050061), 1 X MEM Non-essential Amino Acids (NEAA, Gibco, 11140050) and 100µM β-Mercaptoethanol (Gibco, 21985023). In addition, 2µg/ml doxycycline (Sigma, D9891) was added to the media, inducing TetO gene expression. Doxycycline was retained in the medium until the end of the experiment. Puromycin selection (5µg/ml) was started on day 1. On day 4, the culture medium was replaced with Neurobasal medium (Gibco, 21103049), supplemented with B27 supplement (Gibco, 17504044), 1 X Glutamax, 20% Dextrose (Sigma, D9434), 10ng/ml BDNF (Peprotech, 45002), 10ng/ml GDNF (PeproTech, 45010), 2µg/ml doxycycline (Sigma, D9891) and 5µg/mL puromycin (InvivoGen, ant-pr-1). Beginning on day 7, half of the medium in each well was replaced every week. On day 24, hNGN2-induced neurons were assayed (Zhang et al., 2013)**.**

**Differentiation of iPSCs into forebrain specific neural progenitors and astrocytes**

One hour of 1 mg/ml collagenase (Therm Fisher Scientific, 17104019) treatment was used to detach iPSC colonies. Following collagenase treatment, cells were suspended in embryoid body (EB) medium in non-treated polystyrene plates for 7 days. During this time, the medium was changed daily. EB medium consisted of DMEM/F12 (Gibco, 11330032), 20% Knockout Serum Replacement (Gibo, 10828028), 1 X Glutamax (Gibco, 35050061), 1 X MEM Non-essential Amino

Acids (NEAA, Gibco, 11140050), 100µM β-Mercaptoethanol (Gibco, 21985023), 2 µM dorsomorphin (Tocris, 3093) and 2 µM A-83 (Tocris, 692). After 7 days, EB medium was replaced by neural induction medium (hNPC medium), consisting of DMEM/F12, 1 X N2 supplement (Gibco, 17502048), B27 supplement, 1X NEAA, 1 X Glutamax, 2 µg/ml heparin (Sigma) and 2 µM cyclopamine (Tocris, 1623). On day 7, the floating EBs were then transferred to Matrigel-coated 6-well plates to form neural tube-like rosettes. The attached rosettes were kept for 15 days. During this time, the hNPC media of the rosettes was changed every other day. On day 22, the rosettes were picked mechanically and transferred to low attachment plates (Corning) in hNPC medium containing B27 supplement.

For astrocyte differentiation (Tcw et al., 2017), resuspended neural progenitor spheres were disassociated with accutase at 37°C for 10 min. After disassociation, they were placed on Matrigel coated 6 well plates. Forebrain NPCs were maintained at high density in hNPC medium. To differentiate NPCs to astrocytes, disassociated single cells were seeded at a density of 15,000 cells/cm$^2$ on Matrigel-coated plates and grown in astrocyte medium (ScienCell: 1801, astrocyte medium (1801-b), 2% fetal bovine serum (0010), astrocyte growth supplement (1852) and 10U/ml penicillin/streptomycin solution (0503)). From day 2, cells were fed every 48 hours for 20-30 days. Astrocytes were split when the cells reached 90-95% confluency (approximately every 6-7 days) and seeded again at their initial seeding density (15,000 cells/cm$^2$) as single cells in astrocyte medium.

**Seahorse metabolic oximetry**

Extracellular flux analysis was performed on the Seahorse XFe96 Analyzer (Seahorse Bioscience) following manufacturer recommendations. HAP1 cells and SH-SY5Y cells were seeded at a density of 40,000 cells/well and HEK293 cells were seeded at a density of 20,000 cells/well on Seahorse XF96 V3-PS Microplates (Agilent Technologies, 101085-004) after being trypsinized and counted (Bio-Rad TC20 automated Cell Counter) All Hap1 cells were grown in

normal growth media (IMDM) with 10% FBS except for Ndufaf7-null cells and their control line, which were also supplemented with uridine at 50ug/ml (Sigma, U3003). SH-SY5Y cells were grown in normal growth media (DMEM) with 10% FBS, except for COX17-deficient cells and their control line, which were also supplemented with uridine at 50 µg/ml (Sigma, U3003). XFe96 extracellular flux assay kit probes (Agilent Technologies, 102416-100) incubated with the included manufacturer calibration solution overnight at 37°C without $CO_2$ injection. The following day, wells were washed twice in Seahorse stress test media. The stress test media consisted of Seahorse XF base media (Agilent Technologies, 102353-100) with the addition of 2 mM L-glutamine (HyClone ,SH30034.01), 1 mM sodium pyruvate (Sigma, S8636), and 10 mM D-glucose (Sigma, G8769). After washes, cells incubated at 37°C without $CO_2$ injection for approximately 1 hour prior to the stress test. During this time, flux plate probes were loaded and calibrated. After calibration, the flux plate containing calibrant solution was exchanged for the Seahorse cell culture plate and equilibrated. Seahorse injection ports were filled with 10-fold concentrated solution of oligomycin A (Sigma, 75351), carbonyl cyanide-4-(trifluoromethoxy)phenylhydrazone (FCCP; Sigma, C2920), and rotenone (Sigma , R8875) mixed with antimycin A (Sigma, A8674) for final testing conditions of oligomycin (1.0 µM), FCCP (0.125 µM for Hap1 and HEK293, 0.25 µM for SH-SY5Y), rotenone (0.5 µM), and antimycin A (0.5 µM). In antimycin A sensitivity experiments, a separate solution of antimycin A was made at 100nm and 50nm concentrations to give a concentration of 10nm and 5nm in the well. In bongkrekic acid (BKA) sensitivity experiments,  ready-made BKA solution (Sigma, B6179) was added to seahorse media to obtain soluations at at 25 µM  and 50 µM , giving a final concentration of 0.25 µM and 0.5 µM in the well. Seahorse drugs were dissolved in DMSO and diluted in Seahorse stress test media for the Seahorse protocol. The flux analyzer protocol included three basal read cycles and three reads following injection of oligomycin A, FCCP, and rotenone plus antimycin A. In antimycin sensitivity experiments, antimycin A was injected following the basal read cycles and ten reads were taken before the protocol proceeded as usual with injections of oligomycin A, FCCP, and rotenone plus antimycin A. Each read cycle

included a 3 minute mix cycle followed by a 3 minute read cycle where oxygen consumption rate was determined over time. In all experiments, oxygen consumption rate readings in each well were normalized by protein concentration in the well. Protein concentration was measured using the Pierce BCA Protein Assay Kit (Thermo Fisher Scientific, 23227) according to manufacturer protocol. The BCA assay absorbance was read by a BioTek Synergy HT microplate reader using Gen5 software. For data analysis of oxygen consumption rates, the Seahorse Wave Software version 2.2.0.276 was used. Experiments were repeated at least in triplicate. Non-mitochondrial respiration was determined as the lowest oxygen consumption rate following injection of rotenone plus antimycin A. Basal respiration was calculated from the oxygen consumption rate just before oligomycin injection minus the non-mitochondrial respiration. Non-mitochondrial respiration was determined as the lowest oxygen consumption rate following injection of rotenone plus antimycin A. ATP-dependent respiration was calculated as the difference in oxygen consumption rates just before oligomycin injection to the minimum oxygen consumption rate following oligomycin injection but before FCCP injection. Maximal respiration was calculated as the maximum oxygen consumption rate of the three readings following FCCP injection minus non-mitochondrial respiration.

**Electrochemiluminescent immunoassays for APOE protein measurement**

HAP1, SH-SY5Y, and HEK293 cells were plated in 6 well dishes (Falcon, 353046). Each experimental condition was plated in three or four replicate wells. iPSC neurons and astrocytes were plated in 24 well dishes and grown to approximately 80% confluence. For iPSC cells, eight wells were used for each experimental condition and material from two wells was combined to generate an experimental replicate. For experiments where there was no drug treatment, cells were left overnight and samples were collected 22 – 26 hours later. In these experiments, Hap1 cells were plated at a density of 750,000 cells per well and SHYSY5Y and HEK293 cells were plated at a density of 1,000,000 cells per well. In experiments with doxycycline (Sigma, D9891)

or BKA (Sigma, B6179), cells were left incubating for 46-50 hours in drug or vehicle (cell culture grade water for doxycycline or 0.01 M Tris buffer at pH 7.5 for BKA) before sample collection, with fresh drug and vehicle media applied after approximately 24 hours. In these experiments, Hap1 cells were plated at a density of 300,000 cells per well and SH-SY5Y cells were plated at a density of 500,000 cells per well. In experiments with E-64 (Sigma E8640), brefeldin A (BFA, Sigma B6542) and cycloheximide (CHX, Thermo Scientific AC357420010), HAP1 cells were plated at a density of 750,000 cells/well in and left to grow overnight. The following day, growth media was exchanged for media containing the drug or vehicle (DMSO) and the cells were left for 8 hours before collection of the conditioned media and cell lysis. The following drug concentrations were used: E-64 – 50µm, BFA – 5 µg/mL, CHX – 20µg/mL.

To collect samples of cell lysate and conditioned media, cells were washed twice with ice-cold PBS containing 0.1 mM $CaCl_2$ and 1.0 mM $MgCl_2$, and then lysed on a rocker at 4°C in Buffer A (10mM HEPES, 0.15M NaCl, 1mM EGTA, and 100µM $MgCl_2$) + 0.5% Triton X-100 containing 10% protease inhibitor cocktail cOmplete (Roche, 118614500, prepared at 50x in distilled water). The lysis was spun down at 4°C at 13,000 rpm for 20 mins. The supernatant was collected and flash frozen for APOE protein measurement. Conditioned media was spun down at 4°C at 13,000 rpm for 15 mins to clarify before collecting and flash freezing for APOE protein measurement. Growth media unexposed to cells was incubated and collected in the same manner to serve as a control for APOE present in the media that might be detected by the antibody. Cell lysis and media samples were stored at -80°C for up to a month before APOE was measured. Media was spun down again at 4°C, 2000rpm for 5 mins to get rid of any precipitate after thawing. APOE measurements were conducted by the Emory Immunoassay Core facility using electrochemiluminescent detection of the APOE antibody (Meso Scale Diagnostics, F212I) according to manufacturer protocols with the suggested reagents (Diluent 37 (R50A), MSD GOLD Read Buffer A (R92TG), and MSD GOLD 96-well Small Spot Streptavidin SECTOR Plates

(L45SA-1)). Samples were not diluted for the electrochemiluminescence protocol (Chikkaveeraiah et al., 2012; Gaiottino et al., 2013).

**Conditioned media dialysis**

HAP1 SLC25A1-null cells and their control cell line were grown for approximately 48 hours to confluency before collecting their media. The conditioned media was spun down for 5 minutes at 800g and 4°C and then filtered with a syringe and 0.22 μm filter (Millipore, SLGV033RS) and stored at 4°C for no more than three days before being applied to cells. Conditioned media was dialyzed using 10K molecular weight cutoff cassettes (Thermo Scientific, 88252) according to manufacturer instructions. Cassettes were dialyzed 3 times consecutively with the volume in the cassette to the naïve media (IMDM, Corning 10-016) being 1:1000. The media was exchanged after 3 hours of dialysis for each cycle, with the final dialysis cycle occurring overnight. The dialyzed media was collected the next morning and stored at 4°C for no more than three days before being applied to cells. Viability of cells exposed to the conditioned media was assessed using an Alamar blue assay. For Alamar blue cell viability, HAP1 cells were plated at a density of 2000 cells/well in a 96 well plate and allowed to adhere for 30 mins in normal growth media, IMDM (Corning 10-016) with 10% FBS, before this media was swapped out with conditioned media (dialyzed or undialyzed) collected previously. Cells grew in conditioned media for approximately 48 hours, with fresh conditioned media being put on after approximately 24 hours. After 48 hours, viability was measured with the BioTek Synergy HT plate reader using Gen5 software after a 2 hour incubation in Alamar blue (R&D Systems, AR002). Wells without cells and incubated in Alamar blue were used as a background reading.

**RNA extraction, cDNA preparation, and qPCR**

In all experiments, cell growth media was changed approximately 24 hours before RNA extraction occurred. At least three replicate plates per experimental condition were used in each

experiment. For experiments with doxycycline (Sigma, D9891) and N-Acetyl-L-cysteine (Sigma, A9165), cells incubated in the drug or vehicle (cell culture grade water, Corning 25-055) for 48 hours and fresh drug or vehicle was applied in new media 24 hours before RNA extraction. Doxycycline was applied at 9.75µM and N-Acetyl-L-cysteine was applied at 2mM. RNA was extracted from cells using Trizol reagent (Invitrogen, 15596026). Cells were washed twice in ice-cold PBS containing 0.1 mM $CaCl_2$ and 1.0 mM $MgCl_2$ and then 1 ml of Trizol was added to the samples. A cell scraper was used before collecting the sample into a tube. The samples in Trizol incubated for 10 min at room temperature on an end-to-end rotator and then 200 µl of chloroform was added to each tube. After vigorous vortexing and a brief incubation, the chloroform mixture was centrifuged at 13,000 rpm at 4°C for 15 min. The aqueous layer was collected and 500 µl of isopropanol was added to it. The isopropanol mixture then rotated for 10 min at room temperature, followed by centrifugation at 13,000 rpm for 15 min at 4°C. The supernatant was discarded and the remaining pellet was washed with freshly prepared 75% ethanol in Milli-Q purified water using a brief vortex to lift the pellet. After washing, the pellet in ethanol was centrifuged again for 5 minutes at 13,000 rpm at 4°C. The ethanol was aspirated and the pellet was allowed to air dry. Lastly, the pellet was dissolved in 20-50 µl of molecular grade RNAase-free water and stored overnight at -20°C before the concentration and purity were checked using the Nanodrop One[C] (Thermo Fisher Scientific). cDNA was synthesized using 5 µg RNA as a template per reaction with the Superscript III First Strand Synthesis System Kit (Invitrogen, 18080-051) and its provided random hexamers. RNA was incubated with the random hexamers and dNTPs at 65°C for 5 min. The samples were then placed on ice while a cDNA synthesis mix was prepared according to the kit instructions. The cDNA synthesis mix was added to each of the tubes and the samples were then incubated at 25°C for 10 min, followed by 50 min at 50°C. The reaction was terminated at 85°C for 5 min. Finally, the samples were treated with kit-provided RNase H at 37°C for 20 min. A BioRad T100 thermal cycler was used to carry out this synthesis protocol.

For qPCR, the Real-Time qPCR Assay Entry on the IDT website was used to design primers. Primers were synthesized by Sigma-Aldrich Custom DNA Oligo service. Primer annealing and melting curves were used to confirm primer quality and specificity for single transcripts. qRT-PCR was performed using LightCycler 480 SYBR Green I Master (Roche, 04707516001) with 1 µl of the newly synthesized cDNA on the QuantStudio 6 Flex instrument (Applied Biosystems) in a 96 well format. The qRT-PCR protocol carried out by the QuantStudio 6 Flex consisted of initial denaturation at 95°C for 5 min, followed by 45 cycles of amplification with a 5 s hold at 95°C ramped at 4.4°C/s to 55°C. Temperature was maintained for 10 s at 55°C, then ramped up to 72°C at 2.2°C/s. Temperature was held at 72°C for 20 s and a single acquisition point was collected before ramping at 4.4°C/s to begin the cycle anew. The temperature was then held at 65°C for 1 min and ramped to 97°C at a rate of 0.11°C/s. Five acquisition points were collected per °C. Standard curves collected for each individual primer set were used to quantify data using QuantStudio RT-PCR Software version 1.2.

**Lipidomics**

HAP1 or SH-SY5Y cells were grown to 80 – 90% confluency on 15cm sterile dishes in normal growth media. Material from 2-4 plates was combined for a single replicate and four replicates were used for an experiment. The cells were washed three times in ice-cold PBS containing 10 mM EDTA and then incubated for approximately 30 minutes at 4°C. After incubation, the cells were lifted from the plate on ice and spun down at 800 rpm for 5 minutes at 4°C. Since SH-SY5Y cells lifted easily, the incubation step was skipped in these experiments. Cells were resuspended in ice-cold PBS and a cell count was then taken (Bio-Rad TC20 automated Cell Counter) for normalization and to ensure cells were at least 90% alive and at least 20 million cells would be present in each replicate sample. After counting, cells were again spun down at 800 rpm for 5 minutes at 4°C and the resulting cell pellets were flash-frozen and stored

at -80°C for a few weeks before lipidomic analysis was performed by the Emory Integrated Metabolomics and Lipidomics Core.

Briefly, for lipidomics HPLC grade water, chloroform, methanol, and acetonitrile were purchased from Fisher Scientific (Hampton, NH, USA). Formic acid and ammonium acetate were purchased from Sigma Aldrich (St. Louis, MO, USA). Lipid standards SPLASH® LIPIDOMIX® Mass Spec (cat# 330707) were purchased from Avanti Polar Lipids Inc. (Alabaster, AL, USA).

Prior to the lipid extraction samples were thawed on ice and spiked with SPLASH LIPIDOMIX deuterium-labeled internal standards (Avanti Polar Lipids Inc.). The lipids were extracted from samples using a modified Bligh and Dyer total lipid extraction method (Bligh and Dyer, 1959). Briefly, 2ml of the ice-cold mixture of methanol:chloroform (2:1, v/v) and 0.1% butylated hydroxytoluene (BHT) to prevent the auto-oxidation of polyunsaturated lipid species was added to the samples. The resulting monophasic mixtures were incubated at 4°C for 30 minutes. Then samples were centrifuged at 4000 rpm for 10 minutes and the supernatant was separated from the pellet by transferring to another tube. For the organic and aqueous phase separation 1ml of 0.5M sodium chloride solution was added and samples were vortexed for 10 minutes and centrifuged at 4000 rpm for 10 minutes. The organic fractions were separated and collected in glass vials. LC-MS/MS analysis was performed on Q Exactive HF mass spectrometer system coupled to the Ultimate 3000 liquid chromatography system (Thermo Scientific, USA) and reverse phase C18 column (2.1*50mm, 17mm particle size) (Waters, USA). The mobile phase A and B consisted of 40:60 water : acetonitrile (v/v) and 90:10 isopropanol : acetonitrile (v/v) respectively and both phases contain 10mM ammonium acetate and 0.1 % formic acid. The gradient flow parameters of mobile phase B were as follows: 0–1 min 40%–45%, 1.0–1.1 min 45%–50%, 1.1–5.0 min 50%–55%, 5.0–5.1 min 55%–70%, 5.1–8.0 min 70%–99%, 8.0–8.1 min 99%–40%, 8.1–9.5 min 40%. The flow rate was 0.4 mL/min during total 9.5 minutes run. The temperature for the autosampler and column was set for 4°C and 50°C respectively. Data acquisition was performed in positive electrospray ionization (ESI) mode and full and data-

dependent acquisition (DDA) scans data were collected. LC-MS data processing and lipid species identification were performed using LipidSearch software version 4.2 (Thermo Scientific).

### Preparing cell lysates for immunoblot

HAP1 cells were grown to 80-90% confluency in normal growth media (IMDM + 10%FBS). In experiments with the OXPHOS mix antibody (RRID: AB_2085424), cells were enriched for mitochondrial membranes as detailed below. The cells were washed 3 times with ice-cold PBS containing ice-cold PBS containing 10mM EDTA and then incubated for approximately 30 minutes at 4°C. After incubation, the cells were lifted from the plate on ice and spun down at 800 rpm for 5 minutes at 4°C. The resulting cell pellet was resuspended in a lysis buffer of Buffer A + 0.5% Triton X-100 containing 5% protease inhibitor cocktail cOmplete (Roche, 118614500, prepared at 50x in distilled water). Protein concentration was determined using the Bradford Assay (Bio-Rad, 5000006) and samples were diluted to 2ug/ul. Equal volumes of these cell lysate samples were combined with Laemmli buffer (SDS and 2-mercaptoethanol) reduced and denatured and heated for 5 min at 75°C. Samples were flash frozen and stored at -80°C until immunoblotting. In immunoblot experiments with the OXPHOS mix antibody and blue native gel electrophoresis experiments, cell lysates were enriched for mitochondrial membranes as follows. For each experimental condition, two 150mm dishes with HAP1 cells at 80-90% confluency were used. Trypsin was used to release the cells were and the cell pellet was washed by centrifugation with PBS.

### Immunoblots

HAP1 or SH-SY5Y cell lysates or one nanogram of recombinant APOE (Novus Biologicals, 99158) were suspended in Buffer A + 0.5% Tx-100 and Laemmli sample buffer. Along with protein ladder (BioRad, 161-0373), the cell lysates or recombinant protein were loaded on a 4-20% Criterion gel (BioRad, 3450032) for SDS-PAGE and transferred to PVDF membrane

(Millipore, IPFL00010) using the semidry transfer method. In experiments with AICAR (Sigma, A9978), cells were exposed to the drug at 0.4mM concentration for 72 hours before lysate preparation. Membranes were incubated in a blocking solution of TBS containing 5% nonfat milk and 0.05% Triton X-100. The membranes then incubated overnight with primary antibody solutions diluted in a buffer containing PBS with 3% BSA and 0.2% sodium azide. The following day, membranes were washed three times in TBS containing 0.05% Triton X-100 (TBST) and then incubated in secondary antibody (mouse HRP or rabbit HRP) diluted in blocking solution at room temperature for 30 minutes. The membranes were then rinsed in TBST 3 times and treated with Western Lightning Plus ECL reagent (PerkinElmer, NEL105001EA). Membranes were exposed to GE Healthcare Hyperfilm ECL (28906839) for visualization.

### Blue native gel electrophoresis

Procedures were performed according to established protocols (Diaz et al., 2009; Timon-Gomez et al., 2020b). Crude mitochondria were enriched according to an established protocol (Wieckowski et al., 2009). Briefly, cell homogenization took place in isolation buffer (225-mM mannitol (Sigma, M9647), 75-mM sucrose (Fisher S5-500), 0.1-mM EGTA, and 30-mM Tris–HCl pH 7.4) using 20 strokes in a Potter-Elvehjem homogenizer at 6,000rpm at 4ºC. Centrifugation at 600g for 5min was used to collect unbroken cells and nuclei and mitochondria were recovered from this supernatant by centrifugation at 7,000g for 10 min. After 1 wash of this pellet, membrane solubilization took place in 1.5 M 6-aminocaproic acid (Sigma A2504), 50 mM Bis-Tris pH 7.0 buffer with cOmplete antiprotease (Roche) and freshly prepared 4 g/g (digitonin/protein) (Miillipore, 300410). n-dodecyl-β-d-maltoside (DDM) was used at 4 g/g (DDM/protein). 3-12% gradient native gels (Invitrogen, BN2011BX10) were used to separate proteins by blue native gel electrophoresis. Molecular weight standards used were 10mg/ml Ferritin (404 and 880 kDa, Sigma F4503) and BSA (66 and 132kDa) (Roche, 03116956001). The first dimension was run at 150V for 30 min at room temperature with Coomassie blue (Serva, 17524), then at 250V for

150min at 4ºC in cathode buffer without Coomassie. For immunoblot, proteins were transferred to PVDF membranes and probed with the indicated antibodies, as detailed above. For separation in a second dimension, the lanes from the native gels were cut and loaded on a 10% denaturing SDS-PAGE gel with a single broad lane.

### Co-Immunoprecipitation

Stable cell lines expressing FLAG-tagged SLC25A1 were prepared by transfecting human neuroblastoma SH-SY5Y cells (ATCC, CRL-2266; RRID:CVCL_0019) with ORF expression clone containing N terminally tagged FLAG-SLC25A1 (GeneCopoeia, EX-A1932-Lv1020GS) (Gokhale et al., 2019). These cell lines were grown in DMEM containing 10% FBS, 100 µg/ml penicillin and streptomycin, and puromycin 2 µg/ml (Invitrogen, A1113803). For co-imunoprecipitation experiments, cells were grown in 10 cm dishes. On the day of the experiment, the plated cells were placed on ice and rinsed twice with cold PBS (Corning, 21-040) containing 0.1 mM $CaCl_2$ and 1.0 mm $MgCl_2$. Lysis buffer containing 150 mm NaCl, 10 mM HEPES, 1 mM EGTA, and 0.1 mM $MgCl_2$, pH 7.4 (Buffer A) with 0.5% Triton X-100 and Complete anti-protease (Roche, 11245200) was added to the plates and cells were scraped and put into Eppendorf tubes. Cell lysates were incubated on ice for 30 min and centrifuged at 16,100 × g for 10 min. Bradford Assay (Bio-Rad, 5000006) was used to determine protein concentration of the recovered clarified supernatant. 500µg of the soluble protein extract was incubated with 30 µl Dynal magnetic beads (Invitrogen, 110.31) coated with 1 µg of mouse monoclonal FLAG antibody (RRID: AB_259529). The beads combined with the cell lysates were incubated on an end-to-end rotator for 2 h at 4°C. In some cases, as controls, beads were incubated with the lysis buffer, without any antibodies or the immunoprecipitation was outcompeted with the 3XFLAG peptide (340 µm; Sigma, F4799). Beads were then washed 6 times with Buffer A with 0.1% Triton X-100 followed by elution with Laemmli buffer. Samples were then analyzed by SDS-PAGE, immunoblot using polyclonal antibodies against FLAG (RRID: AB_67407) and NDUFS3 (AB_2151109).

**NanoString mRNA Quantification**

HAP1 cells or SH-SY5Y cells were grown to confluency in a 10 cm sterile dish in normal growth media. SH-SY5Y SLC31A1 knockout cells were treated with vehicle (cell culture grade water) or BCS (Sigma, B1125) at 200μm for 24 hours. Three replicate plates were used for each experimental condition in experiments with HAP1 or SH-SY5Y cells. Astrocytes were seeded at a density of 15,000 cells/cm$^2$ on 6 well tissue culture dishes and grown until they reached 80% confluency. At least 500,000 cells per replicate were used. Astrocytes were treated either with a DMSO vehicle control or 80nM Antimycin A (Sigma, A8674) for 48 hours, with media being replaced every 24 hours. For preparation of samples, all cells were washed twice in ice-cold PBS containing 0.1 mM $CaCl_2$ and 1.0 mM $MgCl_2$. 1 ml of Trizol was added to the samples and the Trizol mixture was flash frozen and stored at -80°C for a few weeks until RNA Extraction and NanoString processing was completed by the Emory Integrated Genomics Core. The Core assessed RNA quality before proceeding with the NanoString protocol. The NanoString Neuroinflammation gene panel kit (115000230) or Metabolic Pathways Panel (115000367) was used for mRNA quantification. mRNA counts were normalized by the expression of the housekeeping gene TADA2B. Data were analyzed using Qlucore Omics Explorer Version 3.7(24) as indicated below.

**Preparation of cell pellets for proteomics and RNAseq**

Wild type or gene-edited HAP1 cells (SLC25A1 and SLC25A4) were grown in IMDM supplemented with 10% FBS and 100 μg/ml penicillin and streptomycin at 37°C in a 10% $CO_2$ incubator. Cells were grown on 10cm tissue culture dishes to 85% confluency. Cells were placed on ice, washed 3 times with ice cold PBS (Corning, 21-040), and then incubated with PBS with 10mM EDTA for 30 minutes at 4°C. Mechanical agitation with a 10ml pipette was used to remove cells from plates. The collected cells were then centrifuged at 800xg for 5 minutes at 4°C.

Following centrifugation, the supernatant was removed and the pellet was washed with ice cold PBS. The resuspended pellet was then spun at 16,100 x g for 5 minutes. The supernatant was aspirated away and the remaining pellet was flash frozen on dry ice for at least 5 minutes and stored at -80°C until further use. For proteomic and transcriptomic analysis, the experiment was conducted at least in triplicate.

**TMT mass spectrometry for proteomics**

Cell pellets were lysed in 200 µL of urea lysis buffer (8M urea, 100 mM NaH2PO4, pH 8.5), supplemented with 2 µL (100x stock) HALT protease and phosphatase inhibitor cocktail (Pierce). Lysates were then subjected to 3 rounds of probe sonication. Each round consisted of 5 seconds of activation at 30% amplitude and 15 of seconds of rest on ice. Protein concentration was determined by bicinchoninic acid (BCA) analysis and 100 ug of each lysate was aliquoted and volumes were equilibrated with additional lysis buffer. Aliquots were diluted with 50mM and was treated with 1mM DTT and 5mM IAA in sequential steps. Both steps were performed in room temperature with end to end rotation for 30 minutes. The alkylation step with IAA was performed in the dark. Lysyl endopeptidase (Wako) was added at a 1:50 (w/w) enzyme to protein ratio and the samples were digested for overnight. Samples were then diluted with 50mM triethylammonium bicarbonate (TEAB) to a urea concentration of 1M. Trypsin (Promega) was added at a 1:50 (w/w) enzyme to protein ratio and digestion proceeded overnight. Resulting peptides were desalted with a Sep-Pak C18 column (Waters). An aliquot equivalent to 20 ug of total protein was taken out of each sample and combined to obtain a global internal standard (GIS) use later for TMT labeling. All samples (16 individual and 4 GIS) were then dried under vacuum.

TMT labeling was performed according to the manufacturer's protocol. Briefly (Ping et al., 2018), the reagents were allowed to equilibrate to room temperature. Dried peptide samples (90 µg each) were resuspended in 100 µl of 100 mm TEAB buffer (supplied with the kit). Anhydrous

acetonitrile (41 µl) was added to each labeling reagent tube and the peptide solutions were transferred into their respective channel tubes. The reaction was incubated for 1 h and quenched for 15 min afterward with 8 µl of 5% hydroxylamine. All samples were combined and dried down. Peptides were resuspended in 100 µl of 90% acetonitrile and 0.01% acetic acid. The entire sample was loaded onto an offline electrostatic repulsion–hydrophilic interaction chromatography fractionation HPLC system and 96 fractions were collected. The fractions were combined into 24 fractions and dried down. Dried peptide fractions were resuspended in 100 µl of peptide loading buffer (0.1% formic acid, 0.03% trifluoroacetic acid, 1% acetonitrile). Peptide mixtures (2 µl) were separated on a self-packed C18 (1.9 µm Dr. Maisch, Germany) fused silica column (25 cm × 75 µm internal diameter; New Objective) by a Easy-nLC 1200 and monitored on a Fusion Lumos mass spectrometer (ThermoFisher Scientific). Elution was performed over a 140 min gradient at a rate of 350 nl/min with buffer B ranging from 3% to 90% (buffer A: 0.1% formic acid in water, buffer B: 0.1% formic in 80% acetonitrile). The mass spectrometer cycle was programmed to collect at the top speed for 3 s cycles. The MS scans (375-1500 m/z range, 400,000 AGC, 50 ms maximum ion time) were collected at a resolution of 120,000 at m/z 200 in profile mode. HCD MS/MS spectra (1.2 m/z isolation width, 36% collision energy, 50,000 AGC target, 86 ms maximum ion time) were collected in the Orbitrap at a resolution of 50000. Dynamic exclusion was set to exclude previous sequenced precursor ions for 15 s within a 10 ppm window. Precursor ions with +1 and +8 or higher charge states were excluded from sequencing.

MS/MS spectra were searched against human database from Uniprot (downloaded on 04/2015) with Proteome Discoverer 2.1.1.21 (ThermoFisher Scientific). Methionine oxidation (+15.9949 Da), asparagine, and glutamine deamidation (+0.9840 Da) and protein N-terminal acetylation (+42.0106 Da) were variable modifications (up to 3 allowed per peptide); static modifications included cysteine carbamidomethyl (+57.0215 Da), peptide n terminus TMT (+229.16293 Da), and lysine TMT (+229.16293 Da). Only fully tryptic peptides were considered with up to two miscleavages in the database search. A precursor mass tolerance of ±20 ppm and

a fragment mass tolerance of 0.6 Da were applied. Spectra matches were filtered by Percolator to a peptide-spectrum matches false discovery rate of <1%. Only razor and unique peptides were used for abundance calculations. Ratio of sample over the GIS of normalized channel abundances were used for comparison across all samples. Data files have been uploaded to ProteomeExchange**.**

Animal husbandry and euthanasia was carried out as approved by the Emory University Institutional Animal Care and Use Committees. For mouse brain proteomic studies, we performed TMT mass spectrometry on whole cortical brain homogenates from 43 WT and 43 5xFAD mice (MMRC#034848-JAX) and sampled age groups from 1.8 mo to 14.4 months. All groups contained equal numbers of males and females, with n=4 males and 4 females per age group. The methods used for these studies have been previously published (Johnson et al., 2022). Briefly, brain tissues were homogenized using a bullet blender along with sonication in 8M Urea lysis buffer containing HALT protease and phosphatase inhibitor (ThermoFisher). Proteins were reduced, alkylated and then digested with Lysyl endopeptidase and Trypsin, followed by peptide cleanup. TMT (16-plex kit) peptide labeling was performed as per manufacturer's instructions, with inclusion of one global internal standard (GIS) in each batch. All samples in a given batch were randomized across six TMT batches, while maintaining nearly-equal representation of age, sex and genotype across all six batches. A complete description of the TMT mass spectrometry study, including methods for sample preparation, mass spectrometry methodology and data processing, are available online (https://www.synapse.org/#!Synapse:syn27023828) and a comprehensive analysis of these data will be published separately. Mass spectrometry raw data were processed in Proteome Discover (Ver 2.1) and then searched against Uniprot mouse database (version 2020), and then processed downstream as described for human brain TMT mass spectrometry studies above. Batch effect was adjusted using bootstrap regression which modelled genotype, age, sex and batch, but covariance with batch only was removed (Wingo et al., 2020). From the

8,535 proteins identified in this mouse brain proteome, we analyzed data related to APOE and 914 proteins that were also found in the Mitocarta database (Rath et al., 2021).

### ICP Mass Spectrometry

Samples were prepared for ICP-MS, processed, and analyzed as described in (Lane et al., 2022). In brief, media was changed the day before samples were collected. Cells were detached using trypsin, centrifuged at 130 g (800 rpm) for 5 min at 4ºC, and resuspended in ice cold PBS. The cell suspension was distributed into microcentrifuge tubes and centrifuged at 210 g (1,500 rpm) for 5 min at 4ºC. The supernatant was removed and the cells were flash frozen in dry ice and stored at -80ºC. 24 hours before running samples on the ICP-MS instrument, samples were dissolved in 20 µL of 70% nitric acid and incubated at 95C for 10 min. Immediately prior to running samples, they were diluted 1:40 in 2% nitric acid in a deep 96 well plate (to a total volume of 800 µL). Quantitation of trace elements was performed using a Thermo iCAP-TQ series ICP-MS operated in oxygen reaction mode with detection of elements of interest with the third quadrupole. In experiments with BCS, cells were treated for 24 hours using 200 µM concentration. Detailed operating procedures and acquisition parameters are described in (Lane et al., 2022)

### RNAseq and data analysis

RNA isolation, library construction, and sequencing were performed by the Beijing Genomics Institute. Total RNA concentration was measured with Agilent 2100 Bio analyzer (Agilent RNA 6000 Nano Kit), QC metrics: RIN values, 28S/18S ratio and fragment length distribution. mRNA purification was achieved by poly-T oligo immobilized to magnetic beads. the mRNA was fragmented using divalent cations plus elevated temperature. RNA fragments were copied into first strand cDNA by reverse transcriptase and random primers. Second strand cDNA synthesis was performed with DNA Polymerase I and RNase H. A single 'A' base and subsequent ligation of adapter was done on cDNA fragments. Products were purified and enriched with PCR

amplification. The PCR yield was quantified using a Qubit and samples were pooled together to make a single strand DNA circle (ssDNA circle) producing the final library. DNA nanoballs were generated with the ssDNA circle by rolling circle replication to enlarge fluorescent signals during the sequencing process. DNA nanoballs were loaded into the patterned nanoarrays and pair-end reads of 100 bp were read through on the DNBseq platform. The DNBseq platform combined the DNA nanoball-based nanoarrays and stepwise sequencing using Combinational Probe-Anchor Synthesis Sequencing Method. On average, we produced ~4.41 Gb bases per sample. The average mapping ratio with reference genome was 92.56%, the average mapping ratio with gene was 72.22%; 17,240 genes were identified. 16,875 novel transcripts were identified. Read quality metrics: 4.56% of the total amount of reads contained more than 5% unknown N base; 5.92% of the total amount of reads which contained adaptors; 1.38% of the total reads were considered low quality meaning more than 20% of bases in the total read have quality score lower than 15. 88.14% of total amount of reads were considered clean reads and used for further analysis.

Sequencing reads were uploaded to the Galaxy web platform. We used the public server usegalaxy.eu to analyze the data (Afgan et al., 2018). FastQC was used to remove samples of suboptimal quality (Andrews, 2010). All mapping was performed using Galaxy server (v. 19.09) running Hisat2 (Galaxy Version 2.1.0+galaxy5), HTseq-Count (Galaxy Version 1.6.2), and DeSeq2 (Galaxy Version 2.11.40.2) (Anders et al., 2015; Kim et al., 2015; Love et al., 2014) . The Genome Reference Consortium build of the reference sequence (GRCh38/hg38) and the GTF files (NCBI) were used and can be acquired from iGenome (Illumina). Hisat2 was run with the following parameters: paired-end, unstranded, default settings were used except for a GTF file was used for transcript assembly. Alignments were visualized using IGV viewer (IGV-Web app version 1.7.0, igv.js version 2.10.5) with Ensembl v90 annotation file and Human (GRCh38/hg38) genome (Robinson et al., 2020; Robinson et al., 2011).

Aligned SAM/BAM files were processed using HTseq-count (Default settings except used GRCh38 GTF file and output for DESeq2 and gene length file). HTseq-count output files and raw

read files are publicly available (GEO with accession GSE201889). The HTseq-count compiled file is GSE201889_ RawHTseqCounts_ALL. Gene counts were normalized using DESeq2 (Love et al., 2014) followed by a regularized log transformation. Differential Expression was determined using DESeq2 with the following settings: Factors were cell type, pairwise comparisons between mutant cell lines versus control line was done, output all normalized tables, size estimation was the standard median ratio, fit type was parametric, outliers were filtered using a Cook's distance cutoff.

**Human Cognitive Trajectory and Proteome Correlations**

The Banner Sun Health Research Institute participants (Banner) project is a longitudinal clinicopathological study of normal aging, Alzheimer's disease (AD), and Parkinson's disease (PD). Most subjects were enrolled as cognitively normal volunteers from the retirement communities of the greater Phoenix, Arizona, USA (Beach et al., 2015). Recruitment efforts were also directed at subjects with AD and PD from the community and neurologists' offices. Subjects received standardized general medical, neurological, and neuropsychological tests annually during life and more than 90% received full pathological examinations after death (Beach et al., 2015).

Person-specific cognitive trajectory was estimated using a linear mixed model. In this model, the annual MMSE score was the longitudinal outcome, follow-up year as the independent variable, sex as the covariate, and with random intercept and random slope per subject using the lme4 R package (version 1.1-19).

Proteomic quantification from the dorsolateral prefrontal cortex of post-mortem brain tissue using mass spectrometry was described in detail here (Wingo et al., 2019). Raw data were analyzed using MaxQuant v1.5.2.8 with Thermo Foundation 2.0 for RAW file reading capability. Co-fragmented peptide search was enabled to deconvolute multiplex spectra. The false discovery rate (FDR) for peptide spectral matches, proteins, and site decoy fractions were set to 1%. Protein

quantification was estimated by label free quantification (LFQ) algorithm by MaxQuant and only considered razor plus unique peptides for each protein isoform. After label-free quantification, 3710 proteins were detected. Only proteins quantified in at least 90% of the samples were included in the analysis. $\log_2$ transformation of the proteomic profiles was performed. Effect of protein sequencing batch was removed using Combat (Johnson et al., 2007). Effects of sex, age at death, and post-mortem interval (PMI) were removed using bootstrap regression. Association between cognitive trajectory and datasets listed in Fig. 7E was examined using linear regression, in which cognitive trajectory was the outcome and the first principal component of the dataset was the predictor.

### Composite protein abundance calculations

Composite protein abundances of respiratory complexes and SLC25An paralogs in the 5xFAD mouse were calculated as the first principal component of individual protein abundances across 86 samples in the data set, using the WGCNA moduleEigengenes function with the standard imputation method allowed, similar to the calculation of synthetic eigengenes as described in (Johnson et al., 2022; Wingo et al., 2019). Given that protein abundances were $\log_2$-transformed, changes in composite values represent $\log_2$ fold change.

### Bioinformatic analyses and statistical analyses

Data from proteomes, RNAseq, NanoString, and lipidomics were processed with Qlucore Omics Explorer Version 3.6(33) normalizing log2 data to a mean of 0 and a variance of 1. Qlucore Omics was used to generate volcano plots, Euclidean hierarchical clustering, PCI and 2D- tSNE. 2D-tSNE was calculated with a perplexity of 5. All other statistical analyses were performed with Prism v9.2.0(283) using two tailed statistics and Alpha of 0.05 using test specified in each figure legend. No outlier identification and exclusion were applied. Asterisks denoting significance

followed Prism specifications. Estimation statistics in Fig. 5A was performed as described (Ho et al., 2019)**.**

Gene ontology analyses were carried out with Cluego. ClueGo v2.58 run on Cytoscape v3.8.2 (Bindea et al., 2009; Shannon et al., 2003). ClueGo was run querying GO BP, REACTOME, and KEGG considering all evidence, Medium Level of Network Specificity, and selecting pathways with a Bonferroni corrected p value <0.001. ClueGo was run with Go Term Fusion. Analysis of Nanostring Ontologies was performed with Metascape (Zhou et al., 2019). All statistically enriched terms based on the default choices under Express Analysis, cumulative hypergeometric p-values and enrichment factors were calculated and used for filtering. Remaining significant terms were then hierarchically clustered into a tree based on Kappa-statistical similarities among their gene memberships. Kappa score of 0.3 was applied as the threshold to cast the tree into term clusters (Zhou et al., 2019).

The interactome of NDUFS3 and SLC25A1 was generated from the proximity interaction datasets by Antonicka et al. (Antonicka et al., 2020). Data were imported into Cytoscape v3.8.2.

Enrichment (Representation Factor) and exact hypergeometric probability of gene set enrichments with hits from the Human Secretome (Uhlen et al., 2019) and Human Mitocarta 3.0 (Rath et al., 2021) in Figs. 1N and 5D were calculated with the engine nemates.org using the 20,577 gene count of the Uniprot Human Proteome Reference

**Data and Reagent Availability**

The mass spectrometry proteomics data have been deposited to the ProteomeXchange Consortium via the PRIDE (Deutsch et al., 2020) partner repository with dataset identifiers: PXD038974 and PXD017501.

RNAseq data were deposited in GEO with accession GSE201889

All reagents and cells are available upon request

**CHAPTER 3: DISCUSSION**

**3.1 Summary of findings**

In this dissertation, I tested the hypothesis that mutations in mitochondrial transporters linked to 22q11.2 deletion syndrome, SLC25A1 and SLC25A4, would alter the expression of secreted proteins, focusing on the secreted lipoprotein APOE. In support of my hypothesis, we show that mutations in nuclear-encoded mitochondrial transporter genes, SLC25A1 and SLC25A4, modify the secretome and mitochondrially-annotated proteome to a similar extent. Mutations in either of these mitochondrial transporters caused increased expression and secretion of the lipoprotein APOE in diverse cellular systems. We focused on APOE since it is a prominent risk factor for Alzheimer's disease, a disease associated with compromised mitochondrial function (Wang et al., 2020). We show that mitochondrial-dependent APOE upregulation occurs in response to mutagenesis of either SLC25A1 or SLC25A4 due to downstream loss of integrity of the electron transport chain. In addition to this indirect disruption of the electron transport chain, we demonstrate that genetic and pharmacological disruption of the assembly and function of electron transport chain complexes I, III, and IV also increases APOE. For example, complex IV depends on copper for its assembly and function. Genetic loss of factors that load copper into complex IV, such as COX17 and COX19, increased APOE levels. Moreover, indirectly disrupting cellular copper homeostasis at the plasma membrane (SLC31A1 and ATP7A), the mitochondrial inner membrane (SLC25A3), or by pharmacological copper chelation with BCS, all conditions that affect complex IV, also leads to APOE upregulation (Boulet et al., 2018; Cobine et al., 2021; Guthrie et al., 2020). The mitochondrial protein network modulating APOE expression also includes genes prioritized within Alzheimer's risk loci that encode proteins required for electron transport chain complex I assembly and function prioritized (de Rojas et al., 2021; Kunkle et al., 2019).These results support the hypothesis that a main initiating event in a cascade that increases APOE levels is disruption of electron transport chain integrity and function. Furthermore, we show that mitochondrial regulation of APOE expression occurs in brain cells, iPSC-derived human astrocytes, and is associated with an inflammatory

gene expression response. Together, our data demonstrate APOE expression and secretion is robustly regulated by mitochondria, placing them in a novel position upstream of APOE. We propose that this mitochondria-to-APOE mechanism may operate in the pathogenesis of dementia. This proposition is supported by our protein expression correlation studies in the cortex of an Alzheimer's mouse model and in aging human brains.

The findings from my dissertation expand previous work showing that mitochondrial distress regulates the secretion of inflammatory cytokines and type I interferons (Dhir et al., 2018; Riley and Tait, 2020; Shimada et al., 2012; West et al., 2015), the growth factor mitokines GDF15 and FGF21 (Chung et al., 2017; Kim et al., 2013), the production of mitochondrially-derived peptides encoded in the mitochondrial genome (Kim et al., 2017), and alpha fetoprotein in hepatocytes (Jett et al., 2022). My dissertation work makes two key contributions that expand on these non-cell autonomous mechanisms. First, we identified the first apolipoprotein whose expression and secretion is modulated by mitochondrial function. Second, while we focus on APOE, we think this apolipoprotein is a harbinger of more extensive regulation of the secreted proteome mediated by mitochondria (Uhlen et al., 2019). The importance of changes in gene expression of the secreted proteome occurring in response to mitochondrial dysfunction can be inferred from its extent and magnitude. We observed that changes in expression of secreted proteins were on par with the changes we observed in the mitochondrially-annotated proteome in response to mutagenesis of SLC25A1 or SLC25A4. Our findings add to growing recent evidence that mitochondrial regulation of the secreted proteome is a more common process than previously appreciated (Jett et al., 2022; Sturm et al., 2023).

Our results support the idea that intramitochondrial mechanisms beyond the loss of integrity of the electron transport chain connect mitochondria to APOE expression and secretion. For instance, mutagenesis of the mitochondrial carnitine transporter SLC25A20 caused APOE upregulation, despite these cells respiring normally and having wild-type levels of respiratory chain subunits. Similarly, mutagenesis of a cytosolic enzyme responsible for producing acetyl-

CoA using citrate as a substrate, ACLY, also increases APOE expression. Thus, we postulate that, in addition to the integrity of the electron transport chain, other mitochondrial and cytoplasmic mechanisms exist that regulate APOE expression.

## 3.2 Mechanisms of APOE upregulation

My thesis work raised an important yet unanswered question. What mechanisms connect mitochondrial dysfunction with changes in the expression and secretion of APOE? I propose these mechanisms involve upregulation of APOE gene expression. This idea is founded on my observation that APOE mRNA is increased after mitochondrial electron transport chain disruption and the sensitivity of APOE protein levels to protein synthesis inhibition.

We tested several alternative hypotheses that could account for the link between mitochondrial electron transport chain dysfunction and heightened nuclear expression of APOE. We measured oxygen consumption and extracellular acidification rates, the latter as a proxy for glycolysis (Zhang and Zhang, 2019). We found that the oxygen consumption rate negatively correlated with APOE levels, but the rate of extracellular acidification did not correlate with APOE expression (Fig. 5). These observations make it unlikely that glycolytic adaptations in the mitochondrial mutants used in our studies underly their APOE phenotype. We also assessed whether APOE upregulation occurred as a response to decreased cytoplasmic ATP levels, using the AMPK pathway as an indicator of ATP depletion. The AMPK pathway is a main sensor of drops in cytoplasmic ATP levels and coordinates a signaling and transcriptional response to increase ATP generation when more cellular energy is needed (Herzig and Shaw, 2018). If decreased ATP levels mediate increased APOE protein levels, the AMPK pathway should be activated at baseline in SLC25A1-null cells. We found that the pathway is minimally active at baseline in SLC25A1-null cells, even though they are sensitized to respond to an AMPK-activating drug (Fig. 5-figure supplement 5). This result aligns with our previous finding that ATP levels between SLC25A1-null and wild-type cells do not differ (Gokhale et al., 2019). A second possible

mechanism for increased APOE expression is that it is a coordinated response with an upregulation of cholesterol synthesis via SREBP transcription factors (Horton et al., 2002). We found that SLC25A1-null Hap1 cells increase expression of cholesterol synthesis pathway enzymes, leading to elevated levels of free cholesterol and cholesterol esterified species, which is consistent with SREBP transcription factor activation. However, these cholesterol phenotypes were not shared by SLC25A1-null neuroblastoma cells or SLC25A4-null cells, even though these cell lines also strongly upregulate APOE expression and secretion to levels comparable to SLC25A1 mutant cells (Fig. 3). Thus, increased APOE expression in response to mitochondrial dysfunction is not dependent on cholesterol synthesis pathways.

Another mechanism to explain APOE upregulation that we ruled out is the mitochondria-to-nucleus pathway mediated by activation of transcription factors ATF4 and CHOP (Quiros et al., 2017). These factors induce the expression of mitokines in response to mitochondrial stress as part of the integrated stress response transcriptional pathway (Chung et al., 2017; Kim et al., 2013). Administration of doxycycline to trigger the stress response led to an appropriate transcriptional response (Quiros et al., 2017) in both wild-type and SLC25A1-null cells (Fig. 6-figure supplement 5), although this response was somewhat blunted even at baseline in the mutant cells (Fig. 6-figure supplement 5). Despite stress response activation, cellular and secreted levels of APOE protein were unaffected with the exception of a mild increase in secretion in the SLC25A1-null cells (Fig. 6-figure supplement 5). Furthermore, FCCP, another potent activator of the mitochondrial stress response (Quiros et al., 2017), failed to induce APOE expression in HAP1 cells, even though inhibition of either complexes I or V with piericidin A or oligomycin, respectively, increased APOE levels (Fig. 4-figure supplement 2). Thus, elevated APOE expression and secretion cannot be explained by the ATF4-dependent stress response alone. A fourth mechanism that might account for increased APOE expression is altered oxidative stress occurring in response to mitochondrial dysfunction. We think this explanation is unlikely because the antioxidant N-acetyl cysteine decreased the expression of the mitochondrial

glutathione-disulfide reductase mRNA in both wild-type and SLC25A1-null cells, but it did not alter APOE mRNA levels (Fig. 6-figure supplement 5).

Finally, we looked for transcriptional signatures in the SLC25A1 and SLC25A4 upregulated transcriptomes that could account for APOE upregulation.  We found no changes in transcription factors known to regulate APOE transcription, such as LXRs or C/EBPβ. (Fig. 6 – figure supplement 5) (Laffitte et al., 2001; Xia et al., 2021). We also observed minimal changes in common in both cell lines that would account for shared changes in gene expression in both genotypes. Recent work shows that APOE secretion can be elevated in an LXR-independent manner through inhibition of class I histone deactylase enzymes (Dresselhaus et al., 2018). Additionally, SLC25A1 is involved in metabolism of acetyl groups, as citrate exported through the transporter to the cytoplasm is converted to acetyl-CoA (Majd et al., 2018; Ohanele et al., 2023). Thus, availability of acetyl groups could affect histone deactylase activity and consequently APOE transcription. Our results showing that knockout of ACLY, the enzyme responsible for converting citrate to acetyl-CoA, also causes APOE upregulation support the hypothesis that SLC25A1-mediated regulation of acetyl groups could play a role in APOE upregulation (Fig. 6-figure supplement 4). On the other hand, citrate supplementation in SLC25A1-null cells, which should increase the pool of acetyl-CoA, fails to reduce APOE upregulation (Fig. 6-figure supplement 4). In addition to acetyl groups, mitochondria may influence APOE transcription through metabolic regulation of the epigenome (Gut and Verdin, 2013; Kopinski et al., 2019; Picard et al., 2014; Schvartzman et al., 2018; Zhang et al., 2019). One example is the use of the TCA cycle metabolite α-ketoglutarate as a required enzymatic cofactor for the family of Jumonji domain-containing histone-lysine demethylase enzymes (Merkwirth et al., 2016). We suggest that a comprehensive epigenetic screen, employing tools such as ATACseq or an acetylated-histone CHIP analysis, in astrocytes and mutant cell lines used in this study would be an effective method to uncover further mechanisms by which mitochondria contribute to regulation of gene expression of APOE expression and other secretome components.

### 3.3 Mitochondria and Inflammation

Another hypothesis that we tested is that APOE upregulation may be part of an inflammatory response. We used a NanoString mRNA quantification panel to assess the levels of activity of interleukin and interferon pathways in SLC25A1-null and SLC25A4-null cells and antimycin-treated astrocytes. Though SLC25A1-null cells and antimycin-treated astrocytes showed more pronounced and numerous inflammatory gene expression changes than SLC25A4-null cells, we found that all three experimental conditions converged on common hits whose number increased when considering hits belonging to shared ontologies. All cells showed increased levels of transcripts encoding secreted cytokines. In line with this result, gene ontologies associated with their transcriptional profiles were enriched for cytokine signaling pathways. Thus, our data show that APOE upregulation in response to mitochondrial dysfunction co-occurs with an inflammatory response initiated by mitochondria. Although mitochondria are often viewed as downstream targets of neuroinflammation, our results showing changes in inflammatory gene expression in antimycin-treated astrocytes are consistent with growing evidence that mitochondria can drive inflammatory signaling in the nervous system (Bader and Winklhofer, 2020; Joshi et al., 2019; Lin et al., 2022). For instance, striatal neuronal dysfunction in a mouse model of Huntington's disease causes declining oxidative phosphorylation in disease-associated medium spiny neurons (Lee et al., 2020b). This decline in mitochondrial electron transport chain function causes release of mitochondrial RNA into the cytoplasm that elicits innate immune signaling (Lee et al., 2020b). This is one example of how mitochondrial molecules sensed in the cytoplasm or at the cell surface can act as inflammatory damage-associated molecular patterns (Nakahira et al., 2015; Riley and Tait, 2020; Tan and Finkel, 2020). Damage to the electron transport chain or other mitochondrial insults initiates release of molecules containing damage-associated molecular patterns, driving signaling through multiple pathways that lead to the secretion of inflammatory cytokines and type I interferons (Dhir et al., 2018; Riley and Tait,

2020; Shimada et al., 2012; West et al., 2015). This process is well defined in peripheral non-neural tissues but is just beginning to be appreciated in the central nervous system.

We asked whether the inflammatory gene expression program seen in astrocytes after exposure to antimycin resembled typical A1 inflammatory astrocyte gene expression induced by LPS and associated with neurodegeneration.  To answer this question, we compared the NanoString neuroinflammation panel profile of antimycin-treated astrocytes with the transcriptomic profile of neurotoxic A1 reactive astrocytes (Liddelow et al., 2017). Our results suggest antimycin-induced inflammatory gene programs differ from the A1 profile but future work is needed to confirm this finding. Further exploration of the functional changes occurring in astrocytes in response to mitochondrial toxicity will provide a greater understanding of how mitochondria modulate glial inflammatory signaling. For instance, our NanoString gene expression profile in astrocytes shows enrichment for complement cascade components in response to antimycin. Future work should test the hypothesis that mitochondrial dysfunction is capable of inducing complement signaling, given the importance of this pathway in synaptic pruning across diverse brain diseases (Presumey et al., 2017). Another recent finding that links APOE to neuroinflammation, which could potentially be modulated by mitochondria, is that neuronal APOE upregulation causes increased expression of immune major histocompatibility I complex (MHC-I) genes (Zalocusky et al., 2021). MHC-I expression in turn amplifies tau pathology and promotes neurodegeneration (Zalocusky et al., 2021).  An intriguing detail of this study that was not followed up on is that changes in gene expression of mitochondrial pathways, including TCA cycle, oxidative phosphorylation, and pyruvate metabolism, were highly correlated with neuronal APOE expression. While antimycin failed to induce APOE upregulation in iPSC-derived neurons in our study, our findings still suggest alternative manipulations of mitochondrial function or inhibition of neuronal mitochondrial function *in vivo* could regulate APOE expression. Thus, the hypothesis that mitochondria can induce MHC-I signaling through neuronal APOE upregulation warrants future investigation.

Another possibility worth exploring is whether mitochondrial dysfunction contributes to blood brain barrier breakdown and leakiness that can allow peripheral immune cell invasion into the central nervous system. Changes in blood brain barrier permeability appear important in many brain diseases and disorders, spanning neurodevelopment to neurodegeneration (Eshraghi et al., 2020; Kealy et al., 2020; Pollak et al., 2018; Prinz and Priller, 2017; Sweeney et al., 2018). APOE-mediated degeneration of the blood brain barrier contributes to neuroinflammation, synaptic dysfunction, and cognitive decline in Alzheimer's disease (Halliday et al., 2016; Montagne et al., 2020; Nation et al., 2019). Future work should determine whether mitochondrial regulation of APOE may modulate blood brain barrier function either in astrocytes, pericytes, or endothelial cells. Some evidence suggests this possibility. For instance, in a mouse model of the mitochondrial disease Leigh Syndrome where mice lack a subunit of complex I, it was shown that a key mechanism of disease pathogenesis is infiltration of peripheral leukocytes into the central nervous system. This study shows that mitochondrial electron transport chain function modulates blood brain barrier permeability, though the mechanisms by which this occurs is unclear (Stokes et al., 2022). Changes in mitochondrial function could alter blood brain barrier permeability through both cell-autonomous and non-cell autonomous mechanisms. For instance, mitochondrial perturbations in cells that make up the barrier may cause cellular dysfunction through different intrinsic mitochondrial mechanisms, such as bioenergetic deficit, elevated oxidative stress, mitochondrial-dependent apoptosis, or altered calcium regulation. Changes in mitochondrial function in cells of the blood brain barrier may also lead to alterations of the epigenome that cause dysfunction, such as altered expression of tight junction proteins or enzymes that degrade the extracellular matrix (Almutairi et al., 2016). On the other hand, mitochondrial dysfunction occurring in neurons or other cells not directly part of the barrier could also cause changes in protein secretion, such as upregulation of inflammatory cytokines, that affect barrier permeability indirectly (Almutairi et al., 2016).

Notably, 22q11.2 deletion syndrome, in which mitochondria are strongly implicated in disease pathogenesis, is also associated with increased blood brain barrier permeability. A recent study used an iPSC model of the blood brain barrier endothelium derived from cells of 22q11.2 deletion syndrome patients diagnosed with schizophrenia, as well as an *in vivo* 22q11.2 deletion syndrome mouse model, to show the blood brain barrier in 22q11.2 deletion syndrome has defective barrier integrity, leading to increased invasion of leukocytes and elevated glial activation (Crockett et al., 2021). These findings are very reminiscent of those of Stokes et al., in which a mitochondrial disorder causes glial activation and leukocyte invasion (Stokes et al., 2022). Thus, the notion that mitochondria could regulate barrier permeability is also a hypothesis worth testing in the context of 22q11.2 deletion syndrome. Since 22q11.2 deletion syndrome is associated with elevated oxidative stress, in part due to haploinsufficiency of TXNRD2, one possibility is that increased ROS signaling due to mitochondrial dysfunction impairs barrier integrity (Fernandez et al., 2019; Pun et al., 2009). Further work is needed to better understand the mechanisms that lead to changes in blood brain barrier permeability in disease and determine whether and how mitochondria play a role in this process (Almutairi et al., 2016).

## 3.4 Cellular functions of mitochondrial-mediated APOE upregulation

What role does upregulation of APOE expression and secretion in response to mitochondrial dysfunction serve for the cell? The lipidation and contents of APOE particles induced by mitochondrial damage may help to explain whether increased APOE levels in response to mitochondrial damage are adaptive or maladaptive. The lipid content of APOE influences APOE-mediated lipid exchange between cells that can alter the lipid microenvironments of cellular membranes, thereby influencing cell signaling and homeostasis (Martens et al., 2022; Tambini et al., 2016). APOE is a primary lipoprotein in the brain produced mainly by astrocytes, though neurons and other glia can also express APOE (Belloy et al., 2019; Martens et al., 2022). APOE particles play necessary roles in handling toxic lipids by shuttling

them between cell types, with differential effects depending on the cell type of origin of the APOE particle, the profile of lipid species loaded in the particle, and the fate of the lipid-loaded particle (Guttenplan et al., 2021; Ioannou et al., 2019; Liu et al., 2017). For instance, APOE particles shuttled from neurons to astrocytes can be loaded with peroxidated lipids, which are broken down as fuel for mitochondrial beta oxidation to prevent fatty acid toxicity in neurons (Ioannou et al., 2019; Liu et al., 2017). In contrast, astrocytic APOE can harbor neurotoxic long chain saturated fatty acids capable of inducing a lipid-mediated form of apoptosis in neighboring neurons and oligodendrocytes (Guttenplan et al., 2021; Liddelow et al., 2017). Interestingly, a recent study suggested that astrocytic APOE particles can also be loaded with miRNA that promotes histone acetylation to alter gene expression in neurons (Li et al., 2021). Since we observed increased APOE secretion in astrocytes, but not neurons, in response to antimycin, we speculate that APOE released from astrocytes following antimycin administration may not sustain either astrocytes and/or neurons, potentially due to toxic lipids or gene expression alterations resulting from delivery of the contents of APOE particles. Profiling the cargo of antimycin-induced APOE particles released from astrocytes could further clarify their potential impact on the function and health of neighboring cells.

In addition to the contents of APOE particles, cellular function can be influenced by the binding of APOE to several different cell surface receptors that play roles in lipid transport and metabolism, synaptic plasticity, inflammation, and processing and clearance of the Aβ protein found in Alzheimer's plaques (Holtzman et al., 2012; Jendresen et al., 2017; Lane-Donovan et al., 2014). Several APOE receptors have multiple ligands. Thus, increased APOE levels may cause APOE to outcompete other ligands for receptor binding and alter downstream signaling (D'Arcangelo et al., 1999; Holtzman et al., 2012; Kober and Brett, 2017). A surprising recent study showed that a form of early onset inherited Alzheimer's disease, caused by a mutation that drastically increases amyloid plaque generation, could be delayed in onset almost 20 years by a mutation that increased activation of the ApoeR2 signaling pathway by the ligand Reelin (Lopera

et al., 2023). Importantly, binding of APOE to ApoeR2 can antagonize activation of this pathway by Reelin, suggesting that APOE levels are capable of modulating Reelin-induced signaling (D'Arcangelo et al., 1999). In another study of resistance to early onset inherited Alzheimer's disease, an ultra-rare variant allele of APOE3 was shown to offset disease onset by nearly 30 years (Arboleda-Velasquez et al., 2019). The authors of this study concluded the ultra-rare APOE3 allele was protective in part due to its altered binding to the LDLR receptor and cell surface heparin sulfate proteoglycans, which are involved with lipoprotein and amyloid uptake (Arboleda-Velasquez et al., 2019; Fu et al., 2016; Ji et al., 1994). These findings show the importance of APOE receptors in maintaining brain health and suggest APOE upregulation may interfere with signaling of APOE receptors as a potential disease mechanism. Of note, we observed increased levels of the APOE receptor LDLR in SLC25A1-null Hap1 cells (Fig. 3). This LDLR upregulation could lead to increased cholesterol uptake through internalization of lipidated APOE particles, providing an explanation for why we observed elevated cholesterol levels in these cells. Knocking out APOE receptors in mitochondrial mutant cells or animals, or manipulating receptor signaling pathways downstream of APOE, and assessing how this affects cellular phenotypes is a strategy that could be used to determine whether the consequences of APOE upregulation in response to mitochondrial dysfunction depend on modulation of receptor signaling pathway activation by APOE.

## 3.5 Roles of APOE and mitochondria in Alzheimer's disease

The APOE4 allele is the strongest genetic risk factor for sporadic Alzheimer's disease and, in addition to amyloidogenic processing of the amyloid precursor protein (APP) into Aβ, APOE-mediated cellular processes are thought of as an initiating and driving factor in disease etiology (Frisoni et al., 2022; Huang and Mahley, 2014; Mahley, 2023; Martens et al., 2022). While mitochondrial dysfunction is viewed as an important factor in Alzheimer's disease, mitochondria are typically placed downstream of Aβ and APOE, with mitochondrial function being disrupted by

Aβ or the APOE4 allele (Area-Gomez et al., 2020; Chen et al., 2011; Mahley, 2023; Orr et al., 2019; Tambini et al., 2016; Yin et al., 2020). Some have argued that mitochondria act as driving factors in Alzheimer's pathogenesis through metabolic and bioenergetic effects (Rangaraju et al., 2018; Swerdlow, 2018; Wang et al., 2020). We argue that mitochondria could also participate in Alzheimer's pathogenesis through regulation of APOE-dependent cellular processes and modulation of APOE allele-dependent mechanisms. The inverse correlation of expression of respiratory chain subunits in the 5xFAD mouse model with increased expression of APOE supports this proposition (Fig. 7). We hypothesize that increased expression of APOE4 downstream of mitochondrial dysfunction could initiate or exacerbate molecular and cellular processes of neurodegeneration tied to the presence of the APOE4 allele. The APOE4 allele is prone to aggregation and poor lipidation compared with APOE3 (Gong et al., 2002; Hatters et al., 2006; Hubin et al., 2019). Evidence suggests that these biochemical properties of APOE4 ultimately trigger a cascade of cellular dysfunction, such as ER stress and impairments in mitochondrial and lipid metabolism, that promotes inflammation, plaque and tangle accumulation, and synaptic dysfunction to produce disease (Martens et al., 2022). In contrast to APOE4, the APOE2 allele may offer protection from the effects of mitochondrial damage. Mechanisms that explain the protective effect of APOE2 against Alzheimer's disease are poorly understood (Li et al., 2020; Martens et al., 2022). Thus, an experimental test of the hypothesis that the APOE2 allele confers resistance to damaged mitochondria would provide insight to better understanding the roles of APOE and mitochondria in Alzheimer's pathogenesis.

Our findings open the possibility that modulation of APOE-dependent disease processes promoting Alzheimer's pathogenesis could be initiated or driven by mitochondria. Importantly, decreasing APOE levels, through transgenic manipulation or anti-sense oligonucleotides, in mouse models of tauopathy greatly reduces tau-mediated neurodegeneration and neuroinflammation (Litvinchuk et al., 2021; Shi et al., 2017; Wang et al., 2021). Similar effects are seen targeting APOE in models of amyloidosis, where reduced APOE levels improve Aβ plaque

load, reduce neuroinflammation, and improve cognitive performance in memory assays (Liao et al., 2014; Mahan et al., 2022). These results show that targeting APOE has strong preclinical evidence of therapeutic potential. Thus, treatments that improve mitochondrial electron transport chain function may be capable of modulating APOE levels to decrease neuroinflammation and tau and/or Aβ neuropathology.   The correlation of expression levels in the prefrontal cortex of proteins dysregulated in the SLC25A1 proteome and transcriptome with human cognitive trajectory provides evidence for this proposition (Fig. 8). Together, the findings of my dissertation support the idea that mitochondria can influence brain function and cognition through modulation of the secretome, including a novel role in regulation of APOE expression and secretion.

**3.6 Influence of mitochondria on disease-associated regional and cell type vulnerabilities**

Neurodegenerative and neurodevelopmental disorders are often associated with regional and/or cell type specific vulnerabilities to the effects of risk genes or other pathologies (Hess et al., 2018; Jin et al., 2020; Pandya and Patani, 2021; Rajarajan et al., 2018; Seidlitz et al., 2020; Skene et al., 2018; Velmeshev et al., 2019). For instance, Parkinson's disease is associated with degeneration specifically of midbrain dopaminergic neurons in the substantia nigra pars compacta (Pandya and Patani, 2021). Alzheimer's disease is characterized by the spread of degeneration from the entorhinal cortex, to hippocampus, to temporal and prefrontal cortices (Braak and Braak, 1995; Braak et al., 1993). The locus coeruleus and cholinergic neurons also appear particularly vulnerable to degeneration in Alzheimer's disease (Hampel et al., 2018; Jacobs et al., 2021). Furthermore, single cell RNA sequencing of post mortem brain tissue of autism patients ties the disorder to dysfunction of upper layer excitatory neurons and microglia (Velmeshev et al., 2019). In schizophrenia, mapping genomic risk loci to brain cell types implicates glutamatergic pyramidal neurons, cortical interneurons, and medium spiny neurons of the striatum (Skene et al., 2018). While these disease-associated vulnerabilities of particular regions and cell types are well-

established, the underlying molecular mechanisms that lead to these vulnerabilities remain unclear.

One mechanism that could contribute to regional and cellular susceptibility is mitochondrial and metabolic specialization of different cell types and brain regions. Recent data demonstrate that mitochondria are specialized for different functions in different neuronal and glial cell types (Cserep et al., 2018; Fecher et al., 2019; Wynne et al., 2021). For instance, astrocytes are efficient in breaking down lipids through mitochondrial beta oxidation, while neurons struggle to do so (Eraso-Pichot et al., 2018; Fecher et al., 2019; Ioannou et al., 2019). We analyzed the expression of mitochondrial transcripts in publicly available single cell RNAseq data from the Allen Brain Institute and found that inhibitory neurons show higher expression of electron transport chain and mitoribosome genes than glutamatergic neurons (Wynne et al., 2021). These findings are consistent with other work showing that inhibitory neurons have greater energy demands than glutamatergic neurons (Cserep et al., 2018). We also observed that certain members of the SLC25A transporter family are preferentially expressed in inhibitory interneurons (Wynne et al., 2021). Findings from my dissertation provide another example of this mitochondrial cell type specificity in the case of sensitivity to antimycin, as the same antimycin treatment caused upregulation of APOE in iPSC-derived astrocytes but not neurons. Further investigation should examine how the sensitivity to mitochondrial perturbations affects APOE expression in additional glial cell types, such as microglia, oligodendrocytes, and pericytes, as cell type specific APOE-dependent processes mediated by these glial cells are implicated in various aspects of Alzheimer's disease. This includes inflammatory cytokine release and uptake and degradation of plaques by microglia, impaired myelination by oligodendrocytes, and changes in vascular and blood brain barrier function by pericytes (Bell et al., 2012; Blanchard et al., 2022; Halliday et al., 2016; Shi and Holtzman, 2018; Yeh et al., 2016).

Our lab also tested the hypothesis that mitochondria vary by brain region measuring proteomes from adult mice and analyzing the expression of mitochondrial genes. We found that

mitochondrial proteomes differ between the cortex, hippocampus, and striatum (Wynne et al., 2021). For example, we determined that mitoribosome and electron transport chain proteins show enrichment in the cortex compared with the hippocampus or striatum (Wynne et al., 2021). Together, these findings suggest the effects of mitochondrial perturbations could produce different consequences in the brain depending on the cell type or region affected. Moreover, certain regions or cell types could be more vulnerable to particular types of insults than others due to differences in the functional specialization of their mitochondria. For instance, it has been proposed that dopaminergic neurons of the substantia nigra pars compacta that degenerate in Parkinson's disease, as opposed to dopaminergic neurons of the ventral tegmental area, are particularly sensitive to mitochondrial toxins and the pro-oxidant nature of dopamine (Ricke et al., 2020). Higher energy demands, higher mitochondrial transport needs, reduced calcium buffering capacity, and relatively low antioxidant defenses have all been proposed to contribute to this sensitivity (Dryanovski et al., 2013; Neuhaus et al., 2014; Pacelli et al., 2015; Ricke et al., 2020). Another hypothesis that future experiments could investigate is whether regional sensitivity to mitochondrial perturbations differs over the course of Alzheimer's disease, which could help to explain the pattern and progression of regional degeneration.

**3.7 Future directions for this research**

The finding that assembly and function of the mitochondrial electron transport chain regulates APOE expression and secretion raises many questions for future investigation. Some of these are discussed above, such as determining whether APOE upregulation in response to mitochondrial dysfunction is a protective or harmful cellular response and determining what other brain cell types display upregulation of APOE in response to mitochondrial damage. We observed a pattern of mitochondrial and APOE gene expression in bulk proteomics of the cortex in a mouse model of Alzheimer's disease that is consistent with our model of mitochondria acting upstream of APOE. However, further work is needed *in vivo* to confirm that this mechanism operates in the

brain and understand which cell types may be more sensitive *in vivo.* A strategy to test this could be measuring APOE in isolated cell populations from the brain of a mouse model of mitochondrial dysfunction, such as mice lacking the complex I subunit NDUFS4 that model the neurodegenerative mitochondrial disease Leigh Syndrome. An alternative strategy could be assessing cellular APOE phenotypes after exposing wild type mice to a mitochondrial toxin, which is likely a more common pathway to mitochondrial dysfunction for humans than genetic defects.

Another important question to tackle is whether mitochondrial dysfunction leading to APOE upregulation has differential effects on Alzheimer's pathogenesis and outcomes for the different APOE alleles. The association of the APOE4 allele with mitochondrial dysfunction suggests that APOE4 carriers may be sensitized to mitochondrial perturbations due to poorer mitochondrial health at baseline. APOE4 upregulation is likely more harmful than upregulation of other APOE alleles due to the biochemical structure of APOE4 causing it to aggregate and transport lipids poorly, producing cellular stress (Martens et al., 2022). Since the molecular mechanisms that explain the protective effect of APOE2 on Alzheimer's risk are relatively understudied and poorly understood, future experiments should investigate whether carriers of the APOE2 allele may be more resistant to mitochondrial damage than APOE3 and/or APOE4 carriers (Li et al., 2020; Martens et al., 2022). This work would illuminate whether allele-dependent responses to mitochondrial function are in part responsible for the protective effects of APOE2. These hypotheses could be tested by perturbing mitochondrial function in Alzheimer's mouse models engineered to carry humanized versions of the different alleles of APOE, or in iPSC-derived patient cells carrying different APOE alleles.

Another intriguing area of future research in the link between mitochondria and APOE would be to explore how mitochondrial regulation of APOE may affect neurodevelopment. While the provision of cholesterol to neurons from glial APOE particles is known to be crucial during synaptogenesis (Mauch et al., 2001), the role of APOE in neurodevelopment is relatively understudied compared to the vast literature detailing its importance in neurodegeneration and

Alzheimer's disease. Given that diverse mitochondrial functions play important roles in neurogenesis and synaptogenesis, it is tempting to speculate that mitochondrial regulation of APOE also modulates neurodevelopmental processes (Cheng et al., 2012; Fame and Lehtinen, 2021; Iwata and Vanderhaeghen, 2021; Nguyen et al., 2023; Zehnder et al., 2021). Furthermore, evidence suggests that APOE allele status affects brain and cognitive development in humans, in part through gene-environment interactions where the APOE4 allele displays greater sensitivity to developmental toxin exposure (Dean et al., 2014; Guardia-Escote et al., 2019; Ng et al., 2013; Remer et al., 2020). Thus, our findings suggest adverse effects of toxins affecting mitochondria during neurodevelopment could be modulated by APOE allele genotype. Finally, APOE receptors play important roles in neurodevelopment (D'Arcangelo et al., 1999; Filipello et al., 2018; Jossin, 2020). Thus, future work should investigate whether upregulation of APOE in response to mitochondrial dysfunction in neurodevelopment modulates downstream signaling at these receptors to ultimately affect circuit function and behavior.

Lastly, it will be important to define the pathway and mechanisms that link changes in mitochondrial function to nuclear gene expression of APOE. Since we ruled out several potential mechanisms with a candidate approach, we suggest that a comprehensive genetic screen in mitochondrial mutants, or cells treated with mitochondrial toxins, would be the most robust method of approaching this question. Knowledge about the pathways that link mitochondria to APOE will be valuable in designing novel therapeutics that can target APOE-dependent disease processes.

**3.8 Conclusions**

In this dissertation research, I show a novel role for the mitochondrial electron transport chain in regulating the expression and secretion of the lipoprotein APOE, a protein strongly associated with Alzheimer's disease risk.  I also provide evidence that mitochondria can initiate changes in inflammatory gene expression in astrocytes. These findings have important implications for understanding the role of mitochondria in Alzheimer's disease and neurodegeneration. These

results support a model where mitochondria can act upstream of APOE-dependent cellular processes, such as neuroinflammation, to drive Alzheimer's pathogenesis. The results from my dissertation research also add to evidence of non-cell autonomous functions for mitochondria and bolster the evidence for an important role of mitochondria in regulating protein secretion. Finally, this dissertation research suggests that mitochondrial disorders and other rare genetic disorders where mitochondria are heavily implicated, such as 22q11.2 deletion syndrome, can serve as models to uncover novel functions of mitochondria with broad relevance to neurodevelopment and neurodegeneration.

**REFERENCES**

Abidi, F.E., E. Holinski-Feder, O. Rittinger, F. Kooy, H.A. Lubs, R.E. Stevenson, and C.E. Schwartz. 2002. A novel 2 bp deletion in the TM4SF2 gene is associated with MRX58. *J Med Genet.* 39:430-433.

Afgan, E., D. Baker, B. Batut, M. van den Beek, D. Bouvier, M. Cech, J. Chilton, D. Clements, N. Coraor, B.A. Gruning, A. Guerler, J. Hillman-Jackson, S. Hiltemann, V. Jalili, H. Rasche, N. Soranzo, J. Goecks, J. Taylor, A. Nekrutenko, and D. Blankenberg. 2018. The Galaxy platform for accessible, reproducible and collaborative biomedical analyses: 2018 update. *Nucleic Acids Res.* 46:W537-W544.

Akita, T., K. Aoto, M. Kato, M. Shiina, H. Mutoh, M. Nakashima, I. Kuki, S. Okazaki, S. Magara, T. Shiihara, K. Yokochi, K. Aiba, J. Tohyama, C. Ohba, S. Miyatake, N. Miyake, K. Ogata, A. Fukuda, N. Matsumoto, and H. Saitsu. 2018. De novo variants in CAMK2A and CAMK2B cause neurodevelopmental disorders. *Ann Clin Transl Neurol.* 5:280-296.

Al-Absi, A.R., P. Qvist, S. Okujeni, A.R. Khan, S. Glerup, C. Sanchez, and J.R. Nyengaard. 2020. Layers II/III of Prefrontal Cortex in Df(h22q11)/+ Mouse Model of the 22q11.2 Deletion Display Loss of Parvalbumin Interneurons and Modulation of Neuronal Morphology and Excitability. *Mol Neurobiol.* 57:4978-4988.

Al-Absi, A.R., S.K. Thambiappa, A.R. Khan, S. Glerup, C. Sanchez, A.M. Landau, and J.R. Nyengaard. 2022. Df(h22q11)/+ mouse model exhibits reduced binding levels of GABA(A) receptors and structural and functional dysregulation in the inhibitory and excitatory networks of hippocampus. *Mol Cell Neurosci.* 122:103769.

Almutairi, M.M., C. Gong, Y.G. Xu, Y. Chang, and H. Shi. 2016. Factors controlling permeability of the blood-brain barrier. *Cell Mol Life Sci.* 73:57-77.

Amici, D.R., J.M. Jackson, M.I. Truica, R.S. Smith, S.A. Abdulkadir, and M.L. Mendillo. 2021. FIREWORKS: a bottom-up approach to integrative coessentiality network analysis. *Life Sci Alliance.* 4.

Amin, H., F. Marinaro, D. De Pietri Tonelli, and L. Berdondini. 2017. Developmental excitatory-to-inhibitory GABA-polarity switch is disrupted in 22q11.2 deletion syndrome: a potential target for clinical therapeutics. *Sci Rep.* 7:15752.

Anders, S., P.T. Pyl, and W. Huber. 2015. HTSeq--a Python framework to work with high-throughput sequencing data. *Bioinformatics.* 31:166-169.

Andrews, S. 2010. FastQC: a quality control tool for high throughput sequence data.

Antonarakis, S.E., B.G. Skotko, M.S. Rafii, A. Strydom, S.E. Pape, D.W. Bianchi, S.L. Sherman, and R.H. Reeves. 2020. Down syndrome. *Nat Rev Dis Primers.* 6:9.

Antonicka, H., Z.Y. Lin, A. Janer, M.J. Aaltonen, W. Weraarpachai, A.C. Gingras, and E.A. Shoubridge. 2020. A High-Density Human Mitochondrial Proximity Interaction Network. *Cell Metab.* 32:479-497 e479.

Arboleda-Velasquez, J.F., F. Lopera, M. O'Hare, S. Delgado-Tirado, C. Marino, N. Chmielewska, K.L. Saez-Torres, D. Amarnani, A.P. Schultz, R.A. Sperling, D. Leyton-Cifuentes, K. Chen, A. Baena, D. Aguillon, S. Rios-Romenets, M. Giraldo, E. Guzman-Velez, D.J. Norton, E. Pardilla-Delgado, A. Artola, J.S. Sanchez, J. Acosta-Uribe, M. Lalli, K.S. Kosik, M.J. Huentelman, H. Zetterberg, K. Blennow, R.A. Reiman, J. Luo, Y. Chen, P. Thiyyagura, Y. Su, G.R. Jun, M. Naymik, X. Gai, M. Bootwalla, J. Ji, L. Shen, J.B. Miller, L.A. Kim, P.N. Tariot, K.A. Johnson, E.M.

Reiman, and Y.T. Quiroz. 2019. Resistance to autosomal dominant Alzheimer's disease in an APOE3 Christchurch homozygote: a case report. *Nat Med*. 25:1680-1683.

Area-Gomez, E., D. Larrea, M. Pera, R.R. Agrawal, D.N. Guilfoyle, L. Pirhaji, K. Shannon, H.A. Arain, A. Ashok, Q. Chen, A.A. Dillman, H.Y. Figueroa, M.R. Cookson, S.S. Gross, E. Fraenkel, K.E. Duff, and T. Nuriel. 2020. APOE4 is Associated with Differential Regional Vulnerability to Bioenergetic Deficits in Aged APOE Mice. *Sci Rep*. 10:4277.

Armando, M., F. Papaleo, and S. Vicari. 2012. COMT implication in cognitive and psychiatric symptoms in chromosome 22q11 microdeletion syndrome: a selective review. *CNS Neurol Disord Drug Targets*. 11:273-281.

Association, A.s. 2023. 2023 Alzheimer's disease facts and figures. *Alzheimers Dement*. 19:1598-1695.

Ayalew, M., H. Le-Niculescu, D.F. Levey, N. Jain, B. Changala, S.D. Patel, E. Winiger, A. Breier, A. Shekhar, R. Amdur, D. Koller, J.I. Nurnberger, A. Corvin, M. Geyer, M.T. Tsuang, D. Salomon, N.J. Schork, A.H. Fanous, M.C. O'Donovan, and A.B. Niculescu. 2012. Convergent functional genomics of schizophrenia: from comprehensive understanding to genetic risk prediction. *Mol Psychiatry*. 17:887-905.

Bader, V., and K.F. Winklhofer. 2020. Mitochondria at the interface between neurodegeneration and neuroinflammation. *Semin Cell Dev Biol*. 99:163-171.

Bagni, C., and R.S. Zukin. 2019. A Synaptic Perspective of Fragile X Syndrome and Autism Spectrum Disorders. *Neuron*. 101:1070-1088.

Bai, B., X. Wang, Y. Li, P.C. Chen, K. Yu, K.K. Dey, J.M. Yarbro, X. Han, B.M. Lutz, S. Rao, Y. Jiao, J.M. Sifford, J. Han, M. Wang, H. Tan, T.I. Shaw, J.H. Cho, S. Zhou, H. Wang, M. Niu, A. Mancieri, K.A. Messler, X. Sun, Z. Wu, V. Pagala, A.A. High, W. Bi, H. Zhang, H. Chi, V. Haroutunian, B. Zhang, T.G. Beach, G. Yu, and J. Peng. 2020. Deep Multilayer Brain Proteomics Identifies Molecular Networks in Alzheimer's Disease Progression. *Neuron*. 105:975-991 e977.

Balaraju, S., A. Topf, G. McMacken, V.P. Kumar, A. Pechmann, H. Roper, S. Vengalil, K. Polavarapu, S. Nashi, N.P. Mahajan, I.A. Barbosa, C. Deshpande, R.W. Taylor, J. Cossins, D. Beeson, S. Laurie, J. Kirschner, R. Horvath, R. McFarland, A. Nalini, and H. Lochmuller. 2020. Congenital myasthenic syndrome with mild intellectual disability caused by a recurrent SLC25A1 variant. *Eur J Hum Genet*. 28:373-377.

Banci, L., I. Bertini, S. Ciofi-Baffoni, T. Hadjiloi, M. Martinelli, and P. Palumaa. 2008. Mitochondrial copper(I) transfer from Cox17 to Sco1 is coupled to electron transfer. *Proc Natl Acad Sci U S A*. 105:6803-6808.

Bar-Ziv, R., T. Bolas, and A. Dillin. 2020. Systemic effects of mitochondrial stress. *EMBO Rep*. 21:e50094.

Barisano, G., K. Kisler, B. Wilkinson, A.M. Nikolakopoulou, A.P. Sagare, Y. Wang, W. Gilliam, M.T. Huuskonen, S.T. Hung, J.K. Ichida, F. Gao, M.P. Coba, and B.V. Zlokovic. 2022. A "multi-omics" analysis of blood-brain barrier and synaptic dysfunction in APOE4 mice. *J Exp Med*. 219.

Barnat, M., M. Capizzi, E. Aparicio, S. Boluda, D. Wennagel, R. Kacher, R. Kassem, S. Lenoir, F. Agasse, B.Y. Braz, J.P. Liu, J. Ighil, A. Tessier, S.O. Zeitlin, C.

Duyckaerts, M. Dommergues, A. Durr, and S. Humbert. 2020. Huntington's disease alters human neurodevelopment. *Science*. 369:787-793.

Barthet, G., and C. Mulle. 2020. Presynaptic failure in Alzheimer's disease. *Prog Neurobiol*. 194:101801.

Bassani, S., L.A. Cingolani, P. Valnegri, A. Folci, J. Zapata, A. Gianfelice, C. Sala, Y. Goda, and M. Passafaro. 2012. The X-linked intellectual disability protein TSPAN7 regulates excitatory synapse development and AMPAR trafficking. *Neuron*. 73:1143-1158.

Beach, T.G., C.H. Adler, L.I. Sue, G. Serrano, H.A. Shill, D.G. Walker, L. Lue, A.E. Roher, B.N. Dugger, C. Maarouf, A.C. Birdsill, A. Intorcia, M. Saxon-Labelle, J. Pullen, A. Scroggins, J. Filon, S. Scott, B. Hoffman, A. Garcia, J.N. Caviness, J.G. Hentz, E. Driver-Dunckley, S.A. Jacobson, K.J. Davis, C.M. Belden, K.E. Long, M. Malek-Ahmadi, J.J. Powell, L.D. Gale, L.R. Nicholson, R.J. Caselli, B.K. Woodruff, S.Z. Rapscak, G.L. Ahern, J. Shi, A.D. Burke, E.M. Reiman, and M.N. Sabbagh. 2015. Arizona Study of Aging and Neurodegenerative Disorders and Brain and Body Donation Program. *Neuropathology*. 35:354-389.

Becker, E.B., P.L. Oliver, M.D. Glitsch, G.T. Banks, F. Achilli, A. Hardy, P.M. Nolan, E.M. Fisher, and K.E. Davies. 2009. A point mutation in TRPC3 causes abnormal Purkinje cell development and cerebellar ataxia in moonwalker mice. *Proc Natl Acad Sci U S A*. 106:6706-6711.

Bell, R.D., E.A. Winkler, I. Singh, A.P. Sagare, R. Deane, Z. Wu, D.M. Holtzman, C. Betsholtz, A. Armulik, J. Sallstrom, B.C. Berk, and B.V. Zlokovic. 2012. Apolipoprotein E controls cerebrovascular integrity via cyclophilin A. *Nature*. 485:512-516.

Bellenguez, C., F. Kucukali, I.E. Jansen, L. Kleineidam, S. Moreno-Grau, N. Amin, A.C. Naj, R. Campos-Martin, B. Grenier-Boley, V. Andrade, P.A. Holmans, A. Boland, V. Damotte, S.J. van der Lee, M.R. Costa, T. Kuulasmaa, Q. Yang, I. de Rojas, J.C. Bis, A. Yaqub, I. Prokic, J. Chapuis, S. Ahmad, V. Giedraitis, D. Aarsland, P. Garcia-Gonzalez, C. Abdelnour, E. Alarcon-Martin, D. Alcolea, M. Alegret, I. Alvarez, V. Alvarez, N.J. Armstrong, A. Tsolaki, C. Antunez, I. Appollonio, M. Arcaro, S. Archetti, A.A. Pastor, B. Arosio, L. Athanasiu, H. Bailly, N. Banaj, M. Baquero, S. Barral, A. Beiser, A.B. Pastor, J.E. Below, P. Benchek, L. Benussi, C. Berr, C. Besse, V. Bessi, G. Binetti, A. Bizarro, R. Blesa, M. Boada, E. Boerwinkle, B. Borroni, S. Boschi, P. Bossu, G. Brathen, J. Bressler, C. Bresner, H. Brodaty, K.J. Brookes, L.I. Brusco, D. Buiza-Rueda, K. Burger, V. Burholt, W.S. Bush, M. Calero, L.B. Cantwell, G. Chene, J. Chung, M.L. Cuccaro, A. Carracedo, R. Cecchetti, L. Cervera-Carles, C. Charbonnier, H.H. Chen, C. Chillotti, S. Ciccone, J. Claassen, C. Clark, E. Conti, A. Corma-Gomez, E. Costantini, C. Custodero, D. Daian, M.C. Dalmasso, A. Daniele, E. Dardiotis, J.F. Dartigues, P.P. de Deyn, K. de Paiva Lopes, L.D. de Witte, S. Debette, J. Deckert, T. Del Ser, et al. 2022. New insights into the genetic etiology of Alzheimer's disease and related dementias. *Nat Genet*.

Belloy, M.E., V. Napolioni, and M.D. Greicius. 2019. A Quarter Century of APOE and Alzheimer's Disease: Progress to Date and the Path Forward. *Neuron*. 101:820-838.

Benit, P., A. Slama, F. Cartault, I. Giurgea, D. Chretien, S. Lebon, C. Marsac, A. Munnich, A. Rotig, and P. Rustin. 2004. Mutant NDUFS3 subunit of mitochondrial complex I causes Leigh syndrome. *J Med Genet*. 41:14-17.

Bie, B., J. Wu, J.F. Foss, and M. Naguib. 2019. Activation of mGluR1 Mediates C1q-Dependent Microglial Phagocytosis of Glutamatergic Synapses in Alzheimer's Rodent Models. *Mol Neurobiol*. 56:5568-5585.

Bindea, G., B. Mlecnik, H. Hackl, P. Charoentong, M. Tosolini, A. Kirilovsky, W.H. Fridman, F. Pages, Z. Trajanoski, and J. Galon. 2009. ClueGO: a Cytoscape plug-in to decipher functionally grouped gene ontology and pathway annotation networks. *Bioinformatics*. 25:1091-1093.

Blanchard, J.W., L.A. Akay, J. Davila-Velderrain, D. von Maydell, H. Mathys, S.M. Davidson, A. Effenberger, C.Y. Chen, K. Maner-Smith, I. Hajjar, E.A. Ortlund, M. Bula, E. Agbas, A. Ng, X. Jiang, M. Kahn, C. Blanco-Duque, N. Lavoie, L. Liu, R. Reyes, Y.T. Lin, T. Ko, L. R'Bibo, W.T. Ralvenius, D.A. Bennett, H.P. Cam, M. Kellis, and L.H. Tsai. 2022. APOE4 impairs myelination via cholesterol dysregulation in oligodendrocytes. *Nature*. 611:769-779.

Bligh, E.G., and W.J. Dyer. 1959. A rapid method of total lipid extraction and purification. *Can J Biochem Physiol*. 37:911-917.

Boot, E., A.S. Bassett, and C. Marras. 2019. 22q11.2 Deletion Syndrome-Associated Parkinson's Disease. *Mov Disord Clin Pract*. 6:11-16.

Borsche, M., S.L. Pereira, C. Klein, and A. Grunewald. 2021. Mitochondria and Parkinson's Disease: Clinical, Molecular, and Translational Aspects. *J Parkinsons Dis*. 11:45-60.

Boulet, A., K.E. Vest, M.K. Maynard, M.G. Gammon, A.C. Russell, A.T. Mathews, S.E. Cole, X. Zhu, C.B. Phillips, J.Q. Kwong, S.C. Dodani, S.C. Leary, and P.A. Cobine. 2018. The mammalian phosphate carrier SLC25A3 is a mitochondrial copper transporter required for cytochrome c oxidase biogenesis. *J Biol Chem*. 293:1887-1896.

Bour, A., J. Grootendorst, E. Vogel, C. Kelche, J.C. Dodart, K. Bales, P.H. Moreau, P.M. Sullivan, and C. Mathis. 2008. Middle-aged human apoE4 targeted-replacement mice show retention deficits on a wide range of spatial memory tasks. *Behav Brain Res*. 193:174-182.

Bourens, M., and A. Barrientos. 2017. Human mitochondrial cytochrome c oxidase assembly factor COX18 acts transiently as a membrane insertase within the subunit 2 maturation module. *J Biol Chem*. 292:7774-7783.

Braak, H., and E. Braak. 1995. Staging of Alzheimer's disease-related neurofibrillary changes. *Neurobiol Aging*. 16:271-278; discussion 278-284.

Braak, H., E. Braak, and J. Bohl. 1993. Staging of Alzheimer-related cortical destruction. *Eur Neurol*. 33:403-408.

Bridges, H.R., J.G. Fedor, J.N. Blaza, A. Di Luca, A. Jussupow, O.D. Jarman, J.J. Wright, A.A. Agip, A.P. Gamiz-Hernandez, M.M. Roessler, V.R.I. Kaila, and J. Hirst. 2020. Structure of inhibitor-bound mammalian complex I. *Nat Commun*. 11:5261.

Brown, M.S., and J.L. Goldstein. 1980. Multivalent feedback regulation of HMG CoA reductase, a control mechanism coordinating isoprenoid synthesis and cell growth. *J Lipid Res*. 21:505-517.

Bu, G. 2009. Apolipoprotein E and its receptors in Alzheimer's disease: pathways, pathogenesis and therapy. *Nat Rev Neurosci*. 10:333-344.

Bulow, P., A. Patgiri, and V. Faundez. 2022. Mitochondrial protein synthesis and the bioenergetic cost of neurodevelopment. *iScience*. 25:104920.

Butcher, N.J., T.R. Kiehl, L.N. Hazrati, E.W. Chow, E. Rogaeva, A.E. Lang, and A.S. Bassett. 2013. Association between early-onset Parkinson disease and 22q11.2 deletion syndrome: identification of a novel genetic form of Parkinson disease and its clinical implications. *JAMA Neurol*. 70:1359-1366.

Butcher, N.J., C. Marras, M. Pondal, P. Rusjan, E. Boot, L. Christopher, G.M. Repetto, R. Fritsch, E.W.C. Chow, M. Masellis, A.P. Strafella, A.E. Lang, and A.S. Bassett. 2017. Neuroimaging and clinical features in adults with a 22q11.2 deletion at risk of Parkinson's disease. *Brain*. 140:1371-1383.

Campbell, P.D., I. Lee, S. Thyme, and M. Granato. 2023. Mitochondrial genes in the 22q11.2 deleted region regulate neural stem and progenitor cell proliferation. *bioRxiv*.

Chandra, R., M. Engeln, C. Schiefer, M.H. Patton, J.A. Martin, C.T. Werner, L.M. Riggs, T.C. Francis, M. McGlincy, B. Evans, H. Nam, S. Das, K. Girven, P. Konkalmatt, A.M. Gancarz, S.A. Golden, S.D. Iniguez, S.J. Russo, G. Turecki, B.N. Mathur, M. Creed, D.M. Dietz, and M.K. Lobo. 2017. Drp1 Mitochondrial Fission in D1 Neurons Mediates Behavioral and Cellular Plasticity during Early Cocaine Abstinence. *Neuron*. 96:1327-1341 e1326.

Chang, S., T. ran Ma, R.D. Miranda, M.E. Balestra, R.W. Mahley, and Y. Huang. 2005. Lipid- and receptor-binding regions of apolipoprotein E4 fragments act in concert to cause mitochondrial dysfunction and neurotoxicity. *Proc Natl Acad Sci U S A*. 102:18694-18699.

Chaouch, A., V. Porcelli, D. Cox, S. Edvardson, P. Scarcia, A. De Grassi, C.L. Pierri, J. Cossins, S.H. Laval, H. Griffin, J.S. Muller, T. Evangelista, A. Topf, A. Abicht, A. Huebner, M. von der Hagen, K. Bushby, V. Straub, R. Horvath, O. Elpeleg, J. Palace, J. Senderek, D. Beeson, L. Palmieri, and H. Lochmuller. 2014. Mutations in the Mitochondrial Citrate Carrier SLC25A1 are Associated with Impaired Neuromuscular Transmission. *J Neuromuscul Dis*. 1:75-90.

Chen, H.K., Z.S. Ji, S.E. Dodson, R.D. Miranda, C.I. Rosenblum, I.J. Reynolds, S.B. Freedman, K.H. Weisgraber, Y. Huang, and R.W. Mahley. 2011. Apolipoprotein E4 domain interaction mediates detrimental effects on mitochondria and is a potential therapeutic target for Alzheimer disease. *J Biol Chem*. 286:5215-5221.

Chen, N., Y. Bao, Y. Xue, Y. Sun, D. Hu, S. Meng, L. Lu, and J. Shi. 2017. Meta-analyses of RELN variants in neuropsychiatric disorders. *Behav Brain Res*. 332:110-119.

Chen, Y., M.S. Durakoglugil, X. Xian, and J. Herz. 2010. ApoE4 reduces glutamate receptor function and synaptic plasticity by selectively impairing ApoE receptor recycling. *Proc Natl Acad Sci U S A*. 107:12011-12016.

Cheng, A., R. Wan, J.L. Yang, N. Kamimura, T.G. Son, X. Ouyang, Y. Luo, E. Okun, and M.P. Mattson. 2012. Involvement of PGC-1alpha in the formation and maintenance of neuronal dendritic spines. *Nat Commun*. 3:1250.

Cheroni, C., N. Caporale, and G. Testa. 2020. Autism spectrum disorder at the crossroad between genes and environment: contributions, convergences, and interactions in ASD developmental pathophysiology. *Mol Autism*. 11:69.

Chikkaveeraiah, B.V., A.A. Bhirde, N.Y. Morgan, H.S. Eden, and X. Chen. 2012. Electrochemical immunosensors for detection of cancer protein biomarkers. *ACS Nano*. 6:6546-6561.

Choi, S.J., J. Mukai, M. Kvajo, B. Xu, A. Diamantopoulou, P.M. Pitychoutis, B. Gou, J.A. Gogos, and H. Zhang. 2018. A Schizophrenia-Related Deletion Leads to KCNQ2-Dependent Abnormal Dopaminergic Modulation of Prefrontal Cortical Interneuron Activity. *Cereb Cortex*. 28:2175-2191.

Chun, S., F. Du, J.J. Westmoreland, S.B. Han, Y.D. Wang, D. Eddins, I.T. Bayazitov, P. Devaraju, J. Yu, M.M. Mellado Lagarde, K. Anderson, and S.S. Zakharenko. 2017. Thalamic miR-338-3p mediates auditory thalamocortical disruption and its late onset in models of 22q11.2 microdeletion. *Nat Med*. 23:39-48.

Chun, S., J.J. Westmoreland, I.T. Bayazitov, D. Eddins, A.K. Pani, R.J. Smeyne, J. Yu, J.A. Blundon, and S.S. Zakharenko. 2014. Specific disruption of thalamic inputs to the auditory cortex in schizophrenia models. *Science*. 344:1178-1182.

Chung, H.K., D. Ryu, K.S. Kim, J.Y. Chang, Y.K. Kim, H.S. Yi, S.G. Kang, M.J. Choi, S.E. Lee, S.B. Jung, M.J. Ryu, S.J. Kim, G.R. Kweon, H. Kim, J.H. Hwang, C.H. Lee, S.J. Lee, C.E. Wall, M. Downes, R.M. Evans, J. Auwerx, and M. Shong. 2017. Growth differentiation factor 15 is a myomitokine governing systemic energy homeostasis. *J Cell Biol*. 216:149-165.

Civiletto, G., S.A. Dogan, R. Cerutti, G. Fagiolari, M. Moggio, C. Lamperti, C. Beninca, C. Viscomi, and M. Zeviani. 2018. Rapamycin rescues mitochondrial myopathy via coordinated activation of autophagy and lysosomal biogenesis. *EMBO Mol Med*. 10.

Cobine, P.A., S.A. Moore, and S.C. Leary. 2021. Getting out what you put in: Copper in mitochondria and its impacts on human disease. *Biochim Biophys Acta Mol Cell Res*. 1868:118867.

Corder, E.H., A.M. Saunders, N.J. Risch, W.J. Strittmatter, D.E. Schmechel, P.C. Gaskell, Jr., J.B. Rimmler, P.A. Locke, P.M. Conneally, K.E. Schmader, and et al. 1994. Protective effect of apolipoprotein E type 2 allele for late onset Alzheimer disease. *Nat Genet*. 7:180-184.

Corder, E.H., A.M. Saunders, W.J. Strittmatter, D.E. Schmechel, P.C. Gaskell, G.W. Small, A.D. Roses, J.L. Haines, and M.A. Pericak-Vance. 1993. Gene dose of apolipoprotein E type 4 allele and the risk of Alzheimer's disease in late onset families. *Science*. 261:921-923.

Crabtree, G.W., and J.A. Gogos. 2014. Synaptic plasticity, neural circuits, and the emerging role of altered short-term information processing in schizophrenia. *Front Synaptic Neurosci*. 6:28.

Crabtree, G.W., A.J. Park, J.A. Gordon, and J.A. Gogos. 2016. Cytosolic Accumulation of L-Proline Disrupts GABA-Ergic Transmission through GAD Blockade. *Cell Rep*. 17:570-582.

Crockett, A.M., S.K. Ryan, A.H. Vasquez, C. Canning, N. Kanyuch, H. Kebir, G. Ceja, J. Gesualdi, E. Zackai, D. McDonald-McGinn, A. Viaene, R. Kapoor, N. Benallegue, R. Gur, S.A. Anderson, and J.I. Alvarez. 2021. Disruption of the blood-brain barrier in 22q11.2 deletion syndrome. *Brain*. 144:1351-1360.

Cserep, C., B. Posfai, A.D. Schwarcz, and A. Denes. 2018. Mitochondrial Ultrastructure Is Coupled to Synaptic Performance at Axonal Release Sites. *eNeuro*. 5.

Curto, Y., J. Alcaide, I. Rockle, H. Hildebrandt, and J. Nacher. 2019. Effects of the Genetic Depletion of Polysialyltransferases on the Structure and Connectivity of Interneurons in the Adult Prefrontal Cortex. *Front Neuroanat*. 13:6.

D'Acunzo, P., R. Perez-Gonzalez, Y. Kim, T. Hargash, C. Miller, M.J. Alldred, H. Erdjument-Bromage, S.C. Penikalapati, M. Pawlik, M. Saito, M. Saito, S.D. Ginsberg, T.A. Neubert, C.N. Goulbourne, and E. Levy. 2021. Mitovesicles are a novel population of extracellular vesicles of mitochondrial origin altered in Down syndrome. *Sci Adv*. 7.

D'Angelo, L., E. Astro, M. De Luise, I. Kurelac, N. Umesh-Ganesh, S. Ding, I.M. Fearnley, G. Gasparre, M. Zeviani, A.M. Porcelli, E. Fernandez-Vizarra, and L. Iommarini. 2021. NDUFS3 depletion permits complex I maturation and reveals TMEM126A/OPA7 as an assembly factor binding the ND4-module intermediate. *Cell Rep*. 35:109002.

D'Arcangelo, G., R. Homayouni, L. Keshvara, D.S. Rice, M. Sheldon, and T. Curran. 1999. Reelin is a ligand for lipoprotein receptors. *Neuron*. 24:471-479.

D'Arcangelo, G., G.G. Miao, S.C. Chen, H.D. Soares, J.I. Morgan, and T. Curran. 1995. A protein related to extracellular matrix proteins deleted in the mouse mutant reeler. *Nature*. 374:719-723.

Das, M., W. Mao, E. Shao, S. Tamhankar, G.Q. Yu, X. Yu, K. Ho, X. Wang, J. Wang, and L. Mucke. 2021. Interdependence of neural network dysfunction and microglial alterations in Alzheimer's disease-related models. *iScience*. 24:103245.

de Rojas, I., S. Moreno-Grau, N. Tesi, B. Grenier-Boley, V. Andrade, I.E. Jansen, N.L. Pedersen, N. Stringa, A. Zettergren, I. Hernandez, L. Montrreal, C. Antunez, A. Antonell, R.M. Tankard, J.C. Bis, R. Sims, C. Bellenguez, I. Quintela, A. Gonzalez-Perez, M. Calero, E. Franco-Macias, J. Macias, R. Blesa, L. Cervera-Carles, M. Menendez-Gonzalez, A. Frank-Garcia, J.L. Royo, F. Moreno, R. Huerto Vilas, M. Baquero, M. Diez-Fairen, C. Lage, S. Garcia-Madrona, P. Garcia-Gonzalez, E. Alarcon-Martin, S. Valero, O. Sotolongo-Grau, A. Ullgren, A.C. Naj, A.W. Lemstra, A. Benaque, A. Perez-Cordon, A. Benussi, A. Rabano, A. Padovani, A. Squassina, A. de Mendonca, A. Arias Pastor, A.A.L. Kok, A. Meggy, A.B. Pastor, A. Espinosa, A. Corma-Gomez, A. Martin Montes, A. Sanabria, A.L. DeStefano, A. Schneider, A. Haapasalo, A. Kinhult Stahlbom, A. Tybjaerg-Hansen, A.M. Hartmann, A. Spottke, A. Corbaton-Anchuelo, A. Rongve, B. Borroni, B. Arosio, B. Nacmias, B.G. Nordestgaard, B.W. Kunkle, C. Charbonnier, C. Abdelnour, C. Masullo, C. Martinez Rodriguez, C. Munoz-Fernandez, C. Dufouil, C. Graff, C.B. Ferreira, C. Chillotti, C.A. Reynolds, C. Fenoglio, C. Van Broeckhoven, C. Clark, C. Pisanu, C.L. Satizabal, C. Holmes, D. Buiza-Rueda, D. Aarsland, D. Rujescu, D. Alcolea, D. Galimberti, D. Wallon, D. Seripa, E. Grunblatt, E. Dardiotis, E. Duzel, E. Scarpini, E. Conti, E. Rubino, E. Gelpi, E. Rodriguez-Rodriguez, et al. 2021. Common variants in Alzheimer's disease and risk stratification by polygenic risk scores. *Nat Commun*. 12:3417.

Dean, D.C., 3rd, B.A. Jerskey, K. Chen, H. Protas, P. Thiyyagura, A. Roontiva, J. O'Muircheartaigh, H. Dirks, N. Waskiewicz, K. Lehman, A.L. Siniard, M.N. Turk, X. Hua, S.K. Madsen, P.M. Thompson, A.S. Fleisher, M.J. Huentelman, S.C. Deoni, and E.M. Reiman. 2014. Brain differences in infants at differential genetic risk for

late-onset Alzheimer disease: a cross-sectional imaging study. *JAMA Neurol*. 71:11-22.

Dejanovic, B., T. Wu, M.C. Tsai, D. Graykowski, V.D. Gandham, C.M. Rose, C.E. Bakalarski, H. Ngu, Y. Wang, S. Pandey, M.G. Rezzonico, B.A. Friedman, R. Edmonds, A. De Maziere, R. Rakosi-Schmidt, T. Singh, J. Klumperman, O. Foreman, M.C. Chang, L. Xie, M. Sheng, and J.E. Hanson. 2022. Complement C1q-dependent excitatory and inhibitory synapse elimination by astrocytes and microglia in Alzheimer's disease mouse models. *Nat Aging*. 2:837-850.

Del Rio, J.A., B. Heimrich, V. Borrell, E. Forster, A. Drakew, S. Alcantara, K. Nakajima, T. Miyata, M. Ogawa, K. Mikoshiba, P. Derer, M. Frotscher, and E. Soriano. 1997. A role for Cajal-Retzius cells and reelin in the development of hippocampal connections. *Nature*. 385:70-74.

DeMaio, A., S. Mehrotra, K. Sambamurti, and S. Husain. 2022. The role of the adaptive immune system and T cell dysfunction in neurodegenerative diseases. *J Neuroinflammation*. 19:251.

Desplats, P., A.M. Gutierrez, M.C. Antonelli, and M.G. Frasch. 2020. Microglial memory of early life stress and inflammation: Susceptibility to neurodegeneration in adulthood. *Neurosci Biobehav Rev*. 117:232-242.

Deutsch, E.W., N. Bandeira, V. Sharma, Y. Perez-Riverol, J.J. Carver, D.J. Kundu, D. Garcia-Seisdedos, A.F. Jarnuczak, S. Hewapathirana, B.S. Pullman, J. Wertz, Z. Sun, S. Kawano, S. Okuda, Y. Watanabe, H. Hermjakob, B. MacLean, M.J. MacCoss, Y. Zhu, Y. Ishihama, and J.A. Vizcaino. 2020. The ProteomeXchange consortium in 2020: enabling 'big data' approaches in proteomics. *Nucleic Acids Res*. 48:D1145-D1152.

Devaraju, P., J. Yu, D. Eddins, M.M. Mellado-Lagarde, L.R. Earls, J.J. Westmoreland, G. Quarato, D.R. Green, and S.S. Zakharenko. 2017. Haploinsufficiency of the 22q11.2 microdeletion gene Mrpl40 disrupts short-term synaptic plasticity and working memory through dysregulation of mitochondrial calcium. *Mol Psychiatry*. 22:1313-1326.

Devaraju, P., and S.S. Zakharenko. 2017. Mitochondria in complex psychiatric disorders: Lessons from mouse models of 22q11.2 deletion syndrome: Hemizygous deletion of several mitochondrial genes in the 22q11.2 genomic region can lead to symptoms associated with neuropsychiatric disease. *Bioessays*. 39.

Dhir, A., S. Dhir, L.S. Borowski, L. Jimenez, M. Teitell, A. Rotig, Y.J. Crow, G.I. Rice, D. Duffy, C. Tamby, T. Nojima, A. Munnich, M. Schiff, C.R. de Almeida, J. Rehwinkel, A. Dziembowski, R.J. Szczesny, and N.J. Proudfoot. 2018. Mitochondrial double-stranded RNA triggers antiviral signalling in humans. *Nature*. 560:238-242.

Di Donato, N., R. Guerrini, C.J. Billington, A.J. Barkovich, P. Dinkel, E. Freri, M. Heide, E.S. Gershon, T.S. Gertler, R.J. Hopkin, S. Jacob, S.K. Keedy, D. Kooshavar, P.J. Lockhart, D.R. Lohmann, I.G. Mahmoud, E. Parrini, E. Schrock, G. Severi, A.E. Timms, R.I. Webster, M.J.H. Willis, M.S. Zaki, J.G. Gleeson, R.J. Leventer, and W.B. Dobyns. 2022. Monoallelic and biallelic mutations in RELN underlie a graded series of neurodevelopmental disorders. *Brain*. 145:3274-3287.

Diaz, F., A. Barrientos, and F. Fontanesi. 2009. Evaluation of the mitochondrial respiratory chain and oxidative phosphorylation system using blue native gel electrophoresis. *Curr Protoc Hum Genet*. Chapter 19:Unit19 14.

Dietschy, J.M., and S.D. Turley. 2001. Cholesterol metabolism in the brain. *Curr Opin Lipidol*. 12:105-112.

Douglas, R.J., and K.A. Martin. 2007. Recurrent neuronal circuits in the neocortex. *Curr Biol*. 17:R496-500.

Dragicevic, N., M. Mamcarz, Y. Zhu, R. Buzzeo, J. Tan, G.W. Arendash, and P.C. Bradshaw. 2010. Mitochondrial amyloid-beta levels are associated with the extent of mitochondrial dysfunction in different brain regions and the degree of cognitive impairment in Alzheimer's transgenic mice. *J Alzheimers Dis*. 20 Suppl 2:S535-550.

Dresselhaus, E., J.M. Duerr, F. Vincent, E.K. Sylvain, M. Beyna, L.F. Lanyon, E. LaChapelle, M. Pettersson, K.R. Bales, and G. Ramaswamy. 2018. Class I HDAC inhibition is a novel pathway for regulating astrocytic apoE secretion. *PLoS One*. 13:e0194661.

Dryanovski, D.I., J.N. Guzman, Z. Xie, D.J. Galteri, L.A. Volpicelli-Daley, V.M. Lee, R.J. Miller, P.T. Schumacker, and D.J. Surmeier. 2013. Calcium entry and alpha-synuclein inclusions elevate dendritic mitochondrial oxidant stress in dopaminergic neurons. *J Neurosci*. 33:10154-10164.

Dumanis, S.B., J.A. Tesoriero, L.W. Babus, M.T. Nguyen, J.H. Trotter, M.J. Ladu, E.J. Weeber, R.S. Turner, B. Xu, G.W. Rebeck, and H.S. Hoe. 2009. ApoE4 decreases spine density and dendritic complexity in cortical neurons in vivo. *J Neurosci*. 29:15317-15322.

Durieux, J., S. Wolff, and A. Dillin. 2011. The cell-non-autonomous nature of electron transport chain-mediated longevity. *Cell*. 144:79-91.

Earls, L.R., I.T. Bayazitov, R.G. Fricke, R.B. Berry, E. Illingworth, G. Mittleman, and S.S. Zakharenko. 2010. Dysregulation of presynaptic calcium and synaptic plasticity in a mouse model of 22q11 deletion syndrome. *J Neurosci*. 30:15843-15855.

Edelmann, L., R.K. Pandita, and B.E. Morrow. 1999. Low-copy repeats mediate the common 3-Mb deletion in patients with velo-cardio-facial syndrome. *Am J Hum Genet*. 64:1076-1086.

Edvardson, S., V. Porcelli, C. Jalas, D. Soiferman, Y. Kellner, A. Shaag, S.H. Korman, C.L. Pierri, P. Scarcia, N.D. Fraenkel, R. Segel, A. Schechter, A. Frumkin, O. Pines, A. Saada, L. Palmieri, and O. Elpeleg. 2013. Agenesis of corpus callosum and optic nerve hypoplasia due to mutations in SLC25A1 encoding the mitochondrial citrate transporter. *J Med Genet*. 50:240-245.

Elson, G.C., P. Graber, C. Losberger, S. Herren, D. Gretener, L.N. Menoud, T.N. Wells, M.H. Kosco-Vilbois, and J.F. Gauchat. 1998. Cytokine-like factor-1, a novel soluble protein, shares homology with members of the cytokine type I receptor family. *J Immunol*. 161:1371-1379.

Eom, T.Y., I.T. Bayazitov, K. Anderson, J. Yu, and S.S. Zakharenko. 2017. Schizophrenia-Related Microdeletion Impairs Emotional Memory through MicroRNA-Dependent Disruption of Thalamic Inputs to the Amygdala. *Cell Rep*. 19:1532-1544.

Eraso-Pichot, A., M. Braso-Vives, A. Golbano, C. Menacho, E. Claro, E. Galea, and R. Masgrau. 2018. GSEA of mouse and human mitochondriomes reveals fatty acid oxidation in astrocytes. *Glia*. 66:1724-1735.

Eshraghi, R.S., C. Davies, R. Iyengar, L. Perez, R. Mittal, and A.A. Eshraghi. 2020. Gut-Induced Inflammation during Development May Compromise the Blood-Brain Barrier and Predispose to Autism Spectrum Disorder. *J Clin Med*. 10.

Exner, N., A.K. Lutz, C. Haass, and K.F. Winklhofer. 2012. Mitochondrial dysfunction in Parkinson's disease: molecular mechanisms and pathophysiological consequences. *EMBO J*. 31:3038-3062.

Fame, R.M., and M.K. Lehtinen. 2021. Mitochondria in Early Forebrain Development: From Neurulation to Mid-Corticogenesis. *Front Cell Dev Biol*. 9:780207.

Farmer, B.C., H.C. Williams, N.A. Devanney, M.A. Piron, G.K. Nation, D.J. Carter, A.E. Walsh, R. Khanal, L.E.A. Young, J.C. Kluemper, G. Hernandez, E.J. Allenger, R. Mooney, L.R. Golden, C.T. Smith, J.A. Brandon, V.A. Gupta, P.A. Kern, M.S. Gentry, J.M. Morganti, R.C. Sun, and L.A. Johnson. 2021. APOEpsilon4 lowers energy expenditure in females and impairs glucose oxidation by increasing flux through aerobic glycolysis. *Mol Neurodegener*. 16:62.

Farrer, L.A., L.A. Cupples, J.L. Haines, B. Hyman, W.A. Kukull, R. Mayeux, R.H. Myers, M.A. Pericak-Vance, N. Risch, and C.M. van Duijn. 1997. Effects of age, sex, and ethnicity on the association between apolipoprotein E genotype and Alzheimer disease. A meta-analysis. APOE and Alzheimer Disease Meta Analysis Consortium. *JAMA*. 278:1349-1356.

Fecher, C., L. Trovo, S.A. Muller, N. Snaidero, J. Wettmarshausen, S. Heink, O. Ortiz, I. Wagner, R. Kuhn, J. Hartmann, R.M. Karl, A. Konnerth, T. Korn, W. Wurst, D. Merkler, S.F. Lichtenthaler, F. Perocchi, and T. Misgeld. 2019. Cell-type-specific profiling of brain mitochondria reveals functional and molecular diversity. *Nat Neurosci*. 22:1731-1742.

Fenelon, K., J. Mukai, B. Xu, P.K. Hsu, L.J. Drew, M. Karayiorgou, G.D. Fischbach, A.B. Macdermott, and J.A. Gogos. 2011. Deficiency of Dgcr8, a gene disrupted by the 22q11.2 microdeletion, results in altered short-term plasticity in the prefrontal cortex. *Proc Natl Acad Sci U S A*. 108:4447-4452.

Fenelon, K., B. Xu, C.S. Lai, J. Mukai, S. Markx, K.L. Stark, P.K. Hsu, W.B. Gan, G.D. Fischbach, A.B. MacDermott, M. Karayiorgou, and J.A. Gogos. 2013. The pattern of cortical dysfunction in a mouse model of a schizophrenia-related microdeletion. *J Neurosci*. 33:14825-14839.

Fernandez, A., D.W. Meechan, B.A. Karpinski, E.M. Paronett, C.A. Bryan, H.L. Rutz, E.A. Radin, N. Lubin, E.R. Bonner, A. Popratiloff, L.A. Rothblat, T.M. Maynard, and A.S. LaMantia. 2019. Mitochondrial Dysfunction Leads to Cortical Under-Connectivity and Cognitive Impairment. *Neuron*. 102:1127-1142 e1123.

Ferrari, A., S. Del'Olio, and A. Barrientos. 2021. The Diseased Mitoribosome. *FEBS Lett*. 595:1025-1061.

Fiksinski, A.M., G.D. Hoftman, J.A.S. Vorstman, and C.E. Bearden. 2023. A genetics-first approach to understanding autism and schizophrenia spectrum disorders: the 22q11.2 deletion syndrome. *Mol Psychiatry*. 28:341-353.

Fiksinski, A.M., M. Schneider, C.M. Murphy, M. Armando, S. Vicari, J.M. Canyelles, D. Gothelf, S. Eliez, E.J. Breetvelt, C. Arango, and J.A.S. Vorstman. 2018. Understanding the pediatric psychiatric phenotype of 22q11.2 deletion syndrome. *Am J Med Genet A*. 176:2182-2191.

Fiksinski, A.M., M. Schneider, J. Zinkstok, D. Baribeau, S. Chawner, and J.A.S. Vorstman. 2021. Neurodevelopmental Trajectories and Psychiatric Morbidity: Lessons Learned From the 22q11.2 Deletion Syndrome. *Curr Psychiatry Rep*. 23:13.

Filipello, F., R. Morini, I. Corradini, V. Zerbi, A. Canzi, B. Michalski, M. Erreni, M. Markicevic, C. Starvaggi-Cucuzza, K. Otero, L. Piccio, F. Cignarella, F. Perrucci, M. Tamborini, M. Genua, L. Rajendran, E. Menna, S. Vetrano, M. Fahnestock, R.C. Paolicelli, and M. Matteoli. 2018. The Microglial Innate Immune Receptor TREM2 Is Required for Synapse Elimination and Normal Brain Connectivity. *Immunity*. 48:979-991 e978.

Flippo, K.H., and M.J. Potthoff. 2021. Metabolic Messengers: FGF21. *Nat Metab*. 3:309-317.

Folstein, M.F., S.E. Folstein, and P.R. McHugh. 1975. "Mini-mental state". A practical method for grading the cognitive state of patients for the clinician. *J Psychiatr Res*. 12:189-198.

Forrest, M.P., E. Parnell, and P. Penzes. 2018. Dendritic structural plasticity and neuropsychiatric disease. *Nat Rev Neurosci*. 19:215-234.

Frisoni, G.B., D. Altomare, D.R. Thal, F. Ribaldi, R. van der Kant, R. Ossenkoppele, K. Blennow, J. Cummings, C. van Duijn, P.M. Nilsson, P.Y. Dietrich, P. Scheltens, and B. Dubois. 2022. The probabilistic model of Alzheimer disease: the amyloid hypothesis revised. *Nat Rev Neurosci*. 23:53-66.

Fu, Y., J. Zhao, Y. Atagi, H.M. Nielsen, C.C. Liu, H. Zheng, M. Shinohara, T. Kanekiyo, and G. Bu. 2016. Apolipoprotein E lipoprotein particles inhibit amyloid-beta uptake through cell surface heparan sulphate proteoglycan. *Mol Neurodegener*. 11:37.

Gaiottino, J., N. Norgren, R. Dobson, J. Topping, A. Nissim, A. Malaspina, J.P. Bestwick, A.U. Monsch, A. Regeniter, R.L. Lindberg, L. Kappos, D. Leppert, A. Petzold, G. Giovannoni, and J. Kuhle. 2013. Increased neurofilament light chain blood levels in neurodegenerative neurological diseases. *PLoS One*. 8:e75091.

Galea, E., L.D. Weinstock, R. Larramona-Arcas, A.F. Pybus, L. Gimenez-Llort, C. Escartin, and L.B. Wood. 2022. Multi-transcriptomic analysis points to early organelle dysfunction in human astrocytes in Alzheimer's disease. *Neurobiol Dis*. 166:105655.

Gambardella, S., R. Ferese, S. Scala, S. Carboni, F. Biagioni, E. Giardina, S. Zampatti, N. Modugno, F. Fabbiano, F. Fornai, D. Centonze, and S. Ruggieri. 2018. Mitochondrial Serine Protease HTRA2 p.G399S in a Female with Di George Syndrome and Parkinson's Disease. *Parkinsons Dis*. 2018:5651435.

Garza, N.M., A.B. Swaminathan, K.P. Maremanda, M. Zulkifli, and V.M. Gohil. 2022. Mitochondrial copper in human genetic disorders. *Trends in Endocrinology & Metabolism*.

Gauvrit, T., H. Benderradji, L. Buee, D. Blum, and D. Vieau. 2022. Early-Life Environment Influence on Late-Onset Alzheimer's Disease. *Front Cell Dev Biol*. 10:834661.

Gebara, E., O. Zanoletti, S. Ghosal, J. Grosse, B.L. Schneider, G. Knott, S. Astori, and C. Sandi. 2021. Mitofusin-2 in the Nucleus Accumbens Regulates Anxiety and Depression-like Behaviors Through Mitochondrial and Neuronal Actions. *Biol Psychiatry*. 89:1033-1044.

Ghazal, N., J.N. Peoples, T.A. Mohiuddin, and J.Q. Kwong. 2021. Mitochondrial functional resilience after TFAM ablation in the adult heart. *Am J Physiol Cell Physiol*. 320:C929-C942.

Gibney, S.M., and H.A. Drexhage. 2013. Evidence for a dysregulated immune system in the etiology of psychiatric disorders. *J Neuroimmune Pharmacol*. 8:900-920.

Girard, S.D., M. Jacquet, K. Baranger, M. Migliorati, G. Escoffier, A. Bernard, M. Khrestchatisky, F. Feron, S. Rivera, F.S. Roman, and E. Marchetti. 2014. Onset of hippocampus-dependent memory impairments in 5XFAD transgenic mouse model of Alzheimer's disease. *Hippocampus*. 24:762-772.

Gogos, J.A., M. Santha, Z. Takacs, K.D. Beck, V. Luine, L.R. Lucas, J.V. Nadler, and M. Karayiorgou. 1999. The gene encoding proline dehydrogenase modulates sensorimotor gating in mice. *Nat Genet*. 21:434-439.

Gokhale, A., C. Hartwig, A.A.H. Freeman, J.L. Bassell, S.A. Zlatic, C. Sapp Savas, T. Vadlamudi, F. Abudulai, T.T. Pham, A. Crocker, E. Werner, Z. Wen, G.M. Repetto, J.A. Gogos, S.M. Claypool, J.K. Forsyth, C.E. Bearden, J. Glausier, D.A. Lewis, N.T. Seyfried, J.Q. Kwong, and V. Faundez. 2019. Systems Analysis of the 22q11.2 Microdeletion Syndrome Converges on a Mitochondrial Interactome Necessary for Synapse Function and Behavior. *J Neurosci*. 39:3561-3581.

Gokhale, A., C.E. Lee, S.A. Zlatic, A.A.H. Freeman, N. Shearing, C. Hartwig, O. Ogunbona, J.L. Bassell, M.E. Wynne, E. Werner, C. Xu, Z. Wen, D. Duong, N.T. Seyfried, C.E. Bearden, V.J. Olah, M.J.M. Rowan, J.R. Glausier, D.A. Lewis, and V. Faundez. 2021. Mitochondrial Proteostasis Requires Genes Encoded in a Neurodevelopmental Syndrome Locus. *J Neurosci*. 41:6596-6616.

Gong, J.S., M. Kobayashi, H. Hayashi, K. Zou, N. Sawamura, S.C. Fujita, K. Yanagisawa, and M. Michikawa. 2002. Apolipoprotein E (ApoE) isoform-dependent lipid release from astrocytes prepared from human ApoE3 and ApoE4 knock-in mice. *J Biol Chem*. 277:29919-29926.

Gothelf, D., S. Eliez, T. Thompson, C. Hinard, L. Penniman, C. Feinstein, H. Kwon, S. Jin, B. Jo, S.E. Antonarakis, M.A. Morris, and A.L. Reiss. 2005. COMT genotype predicts longitudinal cognitive decline and psychosis in 22q11.2 deletion syndrome. *Nat Neurosci*. 8:1500-1502.

Guardia-Escote, L., P. Basaure, F. Peris-Sampedro, J. Biosca-Brull, M. Cabre, F. Sanchez-Santed, J.L. Domingo, and M.T. Colomina. 2019. APOE genetic background and sex confer different vulnerabilities to postnatal chlorpyrifos exposure and modulate the response to cholinergic drugs. *Behav Brain Res*. 376:112195.

Guna, A., N.J. Butcher, and A.S. Bassett. 2015. Comparative mapping of the 22q11.2 deletion region and the potential of simple model organisms. *J Neurodev Disord*. 7:18.

Gut, P., and E. Verdin. 2013. The nexus of chromatin regulation and intermediary metabolism. *Nature*. 502:489-498.

Guthrie, L.M., S. Soma, S. Yuan, A. Silva, M. Zulkifli, T.C. Snavely, H.F. Greene, E. Nunez, B. Lynch, C. De Ville, V. Shanbhag, F.R. Lopez, A. Acharya, M.J. Petris, B.E. Kim, V.M. Gohil, and J.C. Sacchettini. 2020. Elesclomol alleviates Menkes pathology and mortality by escorting Cu to cuproenzymes in mice. *Science*. 368:620-625.

Gutierrez-Aguilar, M., and C.P. Baines. 2013. Physiological and pathological roles of mitochondrial SLC25 carriers. *Biochem J*. 454:371-386.

Guttenplan, K.A., M.K. Weigel, P. Prakash, P.R. Wijewardhane, P. Hasel, U. Rufen-Blanchette, A.E. Munch, J.A. Blum, J. Fine, M.C. Neal, K.D. Bruce, A.D. Gitler, G. Chopra, S.A. Liddelow, and B.A. Barres. 2021. Neurotoxic reactive astrocytes induce cell death via saturated lipids. *Nature*. 599:102-107.

Hall, C.N., M.C. Klein-Flugge, C. Howarth, and D. Attwell. 2012. Oxidative phosphorylation, not glycolysis, powers presynaptic and postsynaptic mechanisms underlying brain information processing. *J Neurosci*. 32:8940-8951.

Halliday, M.R., S.V. Rege, Q. Ma, Z. Zhao, C.A. Miller, E.A. Winkler, and B.V. Zlokovic. 2016. Accelerated pericyte degeneration and blood-brain barrier breakdown in apolipoprotein E4 carriers with Alzheimer's disease. *J Cereb Blood Flow Metab*. 36:216-227.

Hamm, J.P., D.S. Peterka, J.A. Gogos, and R. Yuste. 2017. Altered Cortical Ensembles in Mouse Models of Schizophrenia. *Neuron*. 94:153-167 e158.

Hammond, T.R., S.E. Marsh, and B. Stevens. 2019. Immune Signaling in Neurodegeneration. *Immunity*. 50:955-974.

Hampel, H., M.M. Mesulam, A.C. Cuello, M.R. Farlow, E. Giacobini, G.T. Grossberg, A.S. Khachaturian, A. Vergallo, E. Cavedo, P.J. Snyder, and Z.S. Khachaturian. 2018. The cholinergic system in the pathophysiology and treatment of Alzheimer's disease. *Brain*. 141:1917-1933.

Harper, K.M., T. Hiramoto, K. Tanigaki, G. Kang, G. Suzuki, W. Trimble, and N. Hiroi. 2012. Alterations of social interaction through genetic and environmental manipulation of the 22q11.2 gene Sept5 in the mouse brain. *Hum Mol Genet*. 21:3489-3499.

Hartman, R.E., D.F. Wozniak, A. Nardi, J.W. Olney, L. Sartorius, and D.M. Holtzman. 2001. Behavioral phenotyping of GFAP-apoE3 and -apoE4 transgenic mice: apoE4 mice show profound working memory impairments in the absence of Alzheimer's-like neuropathology. *Exp Neurol*. 170:326-344.

Hashimoto, Y., T. Niikura, H. Tajima, T. Yasukawa, H. Sudo, Y. Ito, Y. Kita, M. Kawasumi, K. Kouyama, M. Doyu, G. Sobue, T. Koide, S. Tsuji, J. Lang, K. Kurokawa, and I. Nishimoto. 2001. A rescue factor abolishing neuronal cell death by a wide spectrum of familial Alzheimer's disease genes and Abeta. *Proc Natl Acad Sci U S A*. 98:6336-6341.

Hatters, D.M., N. Zhong, E. Rutenber, and K.H. Weisgraber. 2006. Amino-terminal domain stability mediates apolipoprotein E aggregation into neurotoxic fibrils. *J Mol Biol*. 361:932-944.

Hayakawa, K., E. Esposito, X. Wang, Y. Terasaki, Y. Liu, C. Xing, X. Ji, and E.H. Lo. 2016. Transfer of mitochondria from astrocytes to neurons after stroke. *Nature*. 535:551-555.

He, K., L. Nie, Q. Zhou, S.U. Rahman, J. Liu, X. Yang, and S. Li. 2019. Proteomic Profiles of the Early Mitochondrial Changes in APP/PS1 and ApoE4 Transgenic Mice Models of Alzheimer's Disease. *J Proteome Res*. 18:2632-2642.

Herzig, S., and R.J. Shaw. 2018. AMPK: guardian of metabolism and mitochondrial homeostasis. *Nat Rev Mol Cell Biol*. 19:121-135.

Hess, J.L., G.C. Akutagava-Martins, J.D. Patak, S.J. Glatt, and S.V. Faraone. 2018. Why is there selective subcortical vulnerability in ADHD? Clues from postmortem brain gene expression data. *Mol Psychiatry*. 23:1787-1793.

Hickman, R.A., S.A. O'Shea, M.F. Mehler, and W.K. Chung. 2022. Neurogenetic disorders across the lifespan: from aberrant development to degeneration. *Nat Rev Neurol*. 18:117-124.

Hiramoto, T., G. Kang, G. Suzuki, Y. Satoh, R. Kucherlapati, Y. Watanabe, and N. Hiroi. 2011. Tbx1: identification of a 22q11.2 gene as a risk factor for autism spectrum disorder in a mouse model. *Hum Mol Genet*. 20:4775-4785.

Ho, J., T. Tumkaya, S. Aryal, H. Choi, and A. Claridge-Chang. 2019. Moving beyond P values: data analysis with estimation graphics. *Nat Methods*. 16:565-566.

Hoftman, G.D., D. Datta, and D.A. Lewis. 2017. Layer 3 Excitatory and Inhibitory Circuitry in the Prefrontal Cortex: Developmental Trajectories and Alterations in Schizophrenia. *Biol Psychiatry*. 81:862-873.

Hollis, F., M.A. van der Kooij, O. Zanoletti, L. Lozano, C. Canto, and C. Sandi. 2015. Mitochondrial function in the brain links anxiety with social subordination. *Proc Natl Acad Sci U S A*. 112:15486-15491.

Holtzman, D.M., J. Herz, and G. Bu. 2012. Apolipoprotein E and apolipoprotein E receptors: normal biology and roles in Alzheimer disease. *Cold Spring Harb Perspect Med*. 2:a006312.

Hong, S., V.F. Beja-Glasser, B.M. Nfonoyim, A. Frouin, S. Li, S. Ramakrishnan, K.M. Merry, Q. Shi, A. Rosenthal, B.A. Barres, C.A. Lemere, D.J. Selkoe, and B. Stevens. 2016. Complement and microglia mediate early synapse loss in Alzheimer mouse models. *Science*. 352:712-716.

Horton, J.D., J.L. Goldstein, and M.S. Brown. 2002. SREBPs: activators of the complete program of cholesterol and fatty acid synthesis in the liver. *J Clin Invest*. 109:1125-1131.

Huang, Y., and R.W. Mahley. 2014. Apolipoprotein E: structure and function in lipid metabolism, neurobiology, and Alzheimer's diseases. *Neurobiol Dis*. 72 Pt A:3-12.

Hubin, E., P.B. Verghese, N. van Nuland, and K. Broersen. 2019. Apolipoprotein E associated with reconstituted high-density lipoprotein-like particles is protected from aggregation. *FEBS Lett*. 593:1144-1153.

Hunt, A., P. Schonknecht, M. Henze, U. Seidl, U. Haberkorn, and J. Schroder. 2007. Reduced cerebral glucose metabolism in patients at risk for Alzheimer's disease. *Psychiatry Res*. 155:147-154.

Ignatenko, O., D. Chilov, I. Paetau, E. de Miguel, C.B. Jackson, G. Capin, A. Paetau, M. Terzioglu, L. Euro, and A. Suomalainen. 2018. Loss of mtDNA activates astrocytes and leads to spongiotic encephalopathy. *Nat Commun*. 9:70.

Ioannou, M.S., J. Jackson, S.H. Sheu, C.L. Chang, A.V. Weigel, H. Liu, H.A. Pasolli, C.S. Xu, S. Pang, D. Matthies, H.F. Hess, J. Lippincott-Schwartz, and Z. Liu. 2019. Neuron-Astrocyte Metabolic Coupling Protects against Activity-Induced Fatty Acid Toxicity. *Cell*. 177:1522-1535 e1514.

Ivashko-Pachima, Y., A. Hadar, I. Grigg, V. Korenkova, O. Kapitansky, G. Karmon, M. Gershovits, C.L. Sayas, R.F. Kooy, J. Attems, D. Gurwitz, and I. Gozes. 2021. Discovery of autism/intellectual disability somatic mutations in Alzheimer's brains:

mutated ADNP cytoskeletal impairments and repair as a case study. *Mol Psychiatry*. 26:1619-1633.

Iwata, R., and P. Vanderhaeghen. 2021. Regulatory roles of mitochondria and metabolism in neurogenesis. *Curr Opin Neurobiol*. 69:231-240.

Jacobs, H.I.L., J.A. Becker, K. Kwong, N. Engels-Dominguez, P.C. Prokopiou, K.V. Papp, M. Properzi, O.L. Hampton, F. d'Oleire Uquillas, J.S. Sanchez, D.M. Rentz, G. El Fakhri, M.D. Normandin, J.C. Price, D.A. Bennett, R.A. Sperling, and K.A. Johnson. 2021. In vivo and neuropathology data support locus coeruleus integrity as indicator of Alzheimer's disease pathology and cognitive decline. *Sci Transl Med*. 13:eabj2511.

Jalal, R., A. Nair, A. Lin, A. Eckfeld, L. Kushan, J. Zinberg, K.H. Karlsgodt, T.D. Cannon, and C.E. Bearden. 2021. Social cognition in 22q11.2 deletion syndrome and idiopathic developmental neuropsychiatric disorders. *J Neurodev Disord*. 13:15.

Janky, R., A. Verfaillie, H. Imrichova, B. Van de Sande, L. Standaert, V. Christiaens, G. Hulselmans, K. Herten, M. Naval Sanchez, D. Potier, D. Svetlichnyy, Z. Kalender Atak, M. Fiers, J.C. Marine, and S. Aerts. 2014. iRegulon: from a gene list to a gene regulatory network using large motif and track collections. *PLoS Comput Biol*. 10:e1003731.

Jeanne, M., M.L. Vuillaume, D.C. Ung, V.E. Vancollie, C. Wagner, S.C. Collins, S. Vonwill, D. Haye, N. Chelloug, R. Pfundt, J. Kummeling, M.P. Moizard, S. Marouillat, T. Kleefstra, B. Yalcin, F. Laumonnier, and A. Toutain. 2021. Haploinsufficiency of the HIRA gene located in the 22q11 deletion syndrome region is associated with abnormal neurodevelopment and impaired dendritic outgrowth. *Hum Genet*. 140:885-896.

Jendresen, C., V. Arskog, M.R. Daws, and L.N. Nilsson. 2017. The Alzheimer's disease risk factors apolipoprotein E and TREM2 are linked in a receptor signaling pathway. *J Neuroinflammation*. 14:59.

Jett, K.A., Z.N. Baker, A. Hossain, A. Boulet, P.A. Cobine, S. Ghosh, P. Ng, O. Yilmaz, K. Barreto, J. DeCoteau, K. Mochoruk, G.N. Ioannou, C. Savard, S. Yuan, O.H. Abdalla, C. Lowden, B.E. Kim, H.M. Cheng, B.J. Battersby, V.M. Gohil, and S.C. Leary. 2022. Mitochondrial dysfunction reactivates alpha-fetoprotein expression that drives copper-dependent immunosuppression in mitochondrial disease models. *J Clin Invest*.

Ji, Y., Y. Gong, W. Gan, T. Beach, D.M. Holtzman, and T. Wisniewski. 2003. Apolipoprotein E isoform-specific regulation of dendritic spine morphology in apolipoprotein E transgenic mice and Alzheimer's disease patients. *Neuroscience*. 122:305-315.

Ji, Z.S., S. Fazio, and R.W. Mahley. 1994. Variable heparan sulfate proteoglycan binding of apolipoprotein E variants may modulate the expression of type III hyperlipoproteinemia. *J Biol Chem*. 269:13421-13428.

Jin, S., X. Chen, Y. Tian, R. Jarvis, V. Promes, and Y. Yang. 2023. Astroglial exosome HepaCAM signaling and ApoE antagonization coordinates early postnatal cortical pyramidal neuronal axon growth and dendritic spine formation. *bioRxiv*.

Jin, X., S.K. Simmons, A. Guo, A.S. Shetty, M. Ko, L. Nguyen, V. Jokhi, E. Robinson, P. Oyler, N. Curry, G. Deangeli, S. Lodato, J.Z. Levin, A. Regev, F. Zhang, and P.

Arlotta. 2020. In vivo Perturb-Seq reveals neuronal and glial abnormalities associated with autism risk genes. *Science*. 370.

Johnson, E.C.B., E.K. Carter, E.B. Dammer, D.M. Duong, E.S. Gerasimov, Y. Liu, J. Liu, R. Betarbet, L. Ping, L. Yin, G.E. Serrano, T.G. Beach, J. Peng, P.L. De Jager, V. Haroutunian, B. Zhang, C. Gaiteri, D.A. Bennett, M. Gearing, T.S. Wingo, A.P. Wingo, J.J. Lah, A.I. Levey, and N.T. Seyfried. 2022. Large-scale deep multi-layer analysis of Alzheimer's disease brain reveals strong proteomic disease-related changes not observed at the RNA level. *Nat Neurosci*. 25:213-225.

Johnson, W.E., C. Li, and A. Rabinovic. 2007. Adjusting batch effects in microarray expression data using empirical Bayes methods. *Biostatistics*. 8:118-127.

Jonas, R.K., C.A. Montojo, and C.E. Bearden. 2014. The 22q11.2 deletion syndrome as a window into complex neuropsychiatric disorders over the lifespan. *Biol Psychiatry*. 75:351-360.

Joshi, A.U., P.S. Minhas, S.A. Liddelow, B. Haileselassie, K.I. Andreasson, G.W. Dorn, 2nd, and D. Mochly-Rosen. 2019. Fragmented mitochondria released from microglia trigger A1 astrocytic response and propagate inflammatory neurodegeneration. *Nat Neurosci*. 22:1635-1648.

Jossin, Y. 2020. Reelin Functions, Mechanisms of Action and Signaling Pathways During Brain Development and Maturation. *Biomolecules*. 10.

Kahn, J.B., R.G. Port, S.A. Anderson, and D.A. Coulter. 2020. Modular, Circuit-Based Interventions Rescue Hippocampal-Dependent Social and Spatial Memory in a 22q11.2 Deletion Syndrome Mouse Model. *Biol Psychiatry*. 88:710-718.

Kalia, L.V., and A.E. Lang. 2015. Parkinson's disease. *Lancet*. 386:896-912.

Kanellopoulos, A.K., V. Mariano, M. Spinazzi, Y.J. Woo, C. McLean, U. Pech, K.W. Li, J.D. Armstrong, A. Giangrande, P. Callaerts, A.B. Smit, B.S. Abrahams, A. Fiala, T. Achsel, and C. Bagni. 2020. Aralar Sequesters GABA into Hyperactive Mitochondria, Causing Social Behavior Deficits. *Cell*. 180:1178-1197 e1120.

Karayiorgou, M., M.A. Morris, B. Morrow, R.J. Shprintzen, R. Goldberg, J. Borrow, A. Gos, G. Nestadt, P.S. Wolyniec, V.K. Lasseter, and et al. 1995. Schizophrenia susceptibility associated with interstitial deletions of chromosome 22q11. *Proc Natl Acad Sci U S A*. 92:7612-7616.

Karayiorgou, M., T.J. Simon, and J.A. Gogos. 2010. 22q11.2 microdeletions: linking DNA structural variation to brain dysfunction and schizophrenia. *Nat Rev Neurosci*. 11:402-416.

Karpinski, B.A., T.M. Maynard, C.A. Bryan, G. Yitsege, A. Horvath, N.H. Lee, S.A. Moody, and A.S. LaMantia. 2022. Selective disruption of trigeminal sensory neurogenesis and differentiation in a mouse model of 22q11.2 deletion syndrome. *Dis Model Mech*. 15.

Kasahara, T., M. Kubota, T. Miyauchi, Y. Noda, A. Mouri, T. Nabeshima, and T. Kato. 2006. Mice with neuron-specific accumulation of mitochondrial DNA mutations show mood disorder-like phenotypes. *Mol Psychiatry*. 11:577-593, 523.

Kato, T.M., M. Kubota-Sakashita, N. Fujimori-Tonou, F. Saitow, S. Fuke, A. Masuda, S. Itohara, H. Suzuki, and T. Kato. 2018. Ant1 mutant mice bridge the mitochondrial and serotonergic dysfunctions in bipolar disorder. *Mol Psychiatry*. 23:2039-2049.

Kealy, J., C. Greene, and M. Campbell. 2020. Blood-brain barrier regulation in psychiatric disorders. *Neurosci Lett*. 726:133664.

Keren-Shaul, H., A. Spinrad, A. Weiner, O. Matcovitch-Natan, R. Dvir-Szternfeld, T.K. Ulland, E. David, K. Baruch, D. Lara-Astaiso, B. Toth, S. Itzkovitz, M. Colonna, M. Schwartz, and I. Amit. 2017. A Unique Microglia Type Associated with Restricting Development of Alzheimer's Disease. *Cell*. 169:1276-1290 e1217.

Keser, V., J.B. Lachance, S.S. Alam, Y. Lim, E. Scarlata, A. Kaur, T.F. Zhang, S. Lv, P. Lachapelle, C. O'Flaherty, J.A. Golden, and L.A. Jerome-Majewska. 2019. Snap29 mutant mice recapitulate neurological and ophthalmological abnormalities associated with 22q11 and CEDNIK syndrome. *Commun Biol*. 2:375.

Khan, T.A., O. Revah, A. Gordon, S.J. Yoon, A.K. Krawisz, C. Goold, Y. Sun, C.H. Kim, Y. Tian, M.Y. Li, J.M. Schaepe, K. Ikeda, N.D. Amin, N. Sakai, M. Yazawa, L. Kushan, S. Nishino, M.H. Porteus, J.L. Rapoport, J.A. Bernstein, R. O'Hara, C.E. Bearden, J.F. Hallmayer, J.R. Huguenard, D.H. Geschwind, R.E. Dolmetsch, and S.P. Pasca. 2020. Neuronal defects in a human cellular model of 22q11.2 deletion syndrome. *Nat Med*. 26:1888-1898.

Kim, D., B. Langmead, and S.L. Salzberg. 2015. HISAT: a fast spliced aligner with low memory requirements. *Nat Methods*. 12:357-360.

Kim, K.H., Y.T. Jeong, H. Oh, S.H. Kim, J.M. Cho, Y.N. Kim, S.S. Kim, D.H. Kim, K.Y. Hur, H.K. Kim, T. Ko, J. Han, H.L. Kim, J. Kim, S.H. Back, M. Komatsu, H. Chen, D.C. Chan, M. Konishi, N. Itoh, C.S. Choi, and M.S. Lee. 2013. Autophagy deficiency leads to protection from obesity and insulin resistance by inducing Fgf21 as a mitokine. *Nat Med*. 19:83-92.

Kim, S.H., K.D. Nichols, E.N. Anderson, Y. Liu, N. Ramesh, W. Jia, C.J. Kuerbis, M. Scalf, L.M. Smith, U.B. Pandey, and R.S. Tibbetts. 2023. Axon guidance genes modulate neurotoxicity of ALS-associated UBQLN2. *Elife*. 12.

Kim, S.J., J. Xiao, J. Wan, P. Cohen, and K. Yen. 2017. Mitochondrially derived peptides as novel regulators of metabolism. *J Physiol*. 595:6613-6621.

Kisby, G.E., and P.S. Spencer. 2021. Genotoxic Damage During Brain Development Presages Prototypical Neurodegenerative Disease. *Front Neurosci*. 15:752153.

Klaus, S., and M. Ost. 2020. Mitochondrial uncoupling and longevity - A role for mitokines? *Exp Gerontol*. 130:110796.

Kober, D.L., and T.J. Brett. 2017. TREM2-Ligand Interactions in Health and Disease. *J Mol Biol*. 429:1607-1629.

Kopinski, P.K., K.A. Janssen, P.M. Schaefer, S. Trefely, C.E. Perry, P. Potluri, J.A. Tintos-Hernandez, L.N. Singh, K.R. Karch, S.L. Campbell, M.T. Doan, H. Jiang, I. Nissim, E. Nakamaru-Ogiso, K.E. Wellen, N.W. Snyder, B.A. Garcia, and D.C. Wallace. 2019. Regulation of nuclear epigenome by mitochondrial DNA heteroplasmy. *Proc Natl Acad Sci U S A*. 116:16028-16035.

Kovacs, G.G., H. Adle-Biassette, I. Milenkovic, S. Cipriani, J. van Scheppingen, and E. Aronica. 2014. Linking pathways in the developing and aging brain with neurodegeneration. *Neuroscience*. 269:152-172.

Krasemann, S., C. Madore, R. Cialic, C. Baufeld, N. Calcagno, R. El Fatimy, L. Beckers, E. O'Loughlin, Y. Xu, Z. Fanek, D.J. Greco, S.T. Smith, G. Tweet, Z. Humulock, T. Zrzavy, P. Conde-Sanroman, M. Gacias, Z. Weng, H. Chen, E. Tjon, F. Mazaheri, K. Hartmann, A. Madi, J.D. Ulrich, M. Glatzel, A. Worthmann, J. Heeren, B. Budnik, C. Lemere, T. Ikezu, F.L. Heppner, V. Litvak, D.M. Holtzman, H. Lassmann, H.L. Weiner, J. Ochando, C. Haass, and O. Butovsky. 2017. The TREM2-APOE

Pathway Drives the Transcriptional Phenotype of Dysfunctional Microglia in Neurodegenerative Diseases. *Immunity*. 47:566-581 e569.

Krocher, T., I. Rockle, U. Diederichs, B. Weinhold, H. Burkhardt, Y. Yanagawa, R. Gerardy-Schahn, and H. Hildebrandt. 2014. A crucial role for polysialic acid in developmental interneuron migration and the establishment of interneuron densities in the mouse prefrontal cortex. *Development*. 141:3022-3032.

Kunkle, B.W., B. Grenier-Boley, R. Sims, J.C. Bis, V. Damotte, A.C. Naj, A. Boland, M. Vronskaya, S.J. van der Lee, A. Amlie-Wolf, C. Bellenguez, A. Frizatti, V. Chouraki, E.R. Martin, K. Sleegers, N. Badarinarayan, J. Jakobsdottir, K.L. Hamilton-Nelson, S. Moreno-Grau, R. Olaso, R. Raybould, Y. Chen, A.B. Kuzma, M. Hiltunen, T. Morgan, S. Ahmad, B.N. Vardarajan, J. Epelbaum, P. Hoffmann, M. Boada, G.W. Beecham, J.G. Garnier, D. Harold, A.L. Fitzpatrick, O. Valladares, M.L. Moutet, A. Gerrish, A.V. Smith, L. Qu, D. Bacq, N. Denning, X. Jian, Y. Zhao, M. Del Zompo, N.C. Fox, S.H. Choi, I. Mateo, J.T. Hughes, H.H. Adams, J. Malamon, F. Sanchez-Garcia, Y. Patel, J.A. Brody, B.A. Dombroski, M.C.D. Naranjo, M. Daniilidou, G. Eiriksdottir, S. Mukherjee, D. Wallon, J. Uphill, T. Aspelund, L.B. Cantwell, F. Garzia, D. Galimberti, E. Hofer, M. Butkiewicz, B. Fin, E. Scarpini, C. Sarnowski, W.S. Bush, S. Meslage, J. Kornhuber, C.C. White, Y. Song, R.C. Barber, S. Engelborghs, S. Sordon, D. Voijnovic, P.M. Adams, R. Vandenberghe, M. Mayhaus, L.A. Cupples, M.S. Albert, P.P. De Deyn, W. Gu, J.J. Himali, D. Beekly, A. Squassina, A.M. Hartmann, A. Orellana, D. Blacker, E. Rodriguez-Rodriguez, S. Lovestone, M.E. Garcia, R.S. Doody, C. Munoz-Fernadez, R. Sussams, H. Lin, T.J. Fairchild, Y.A. Benito, et al. 2019. Genetic meta-analysis of diagnosed Alzheimer's disease identifies new risk loci and implicates Abeta, tau, immunity and lipid processing. *Nat Genet*. 51:414-430.

Kury, S., G.M. van Woerden, T. Besnard, M. Proietti Onori, X. Latypova, M.C. Towne, M.T. Cho, T.E. Prescott, M.A. Ploeg, S. Sanders, H.A.F. Stessman, A. Pujol, B. Distel, L.A. Robak, J.A. Bernstein, A.S. Denomme-Pichon, G. Lesca, E.A. Sellars, J. Berg, W. Carre, O.L. Busk, B.W.M. van Bon, J.L. Waugh, M. Deardorff, G.E. Hoganson, K.B. Bosanko, D.S. Johnson, T. Dabir, O.L. Holla, A. Sarkar, K. Tveten, J. de Bellescize, G.J. Braathen, P.A. Terhal, D.K. Grange, A. van Haeringen, C. Lam, G. Mirzaa, J. Burton, E.J. Bhoj, J. Douglas, A.B. Santani, A.I. Nesbitt, K.L. Helbig, M.V. Andrews, A. Begtrup, S. Tang, K.L.I. van Gassen, J. Juusola, K. Foss, G.M. Enns, U. Moog, K. Hinderhofer, N. Paramasivam, S. Lincoln, B.H. Kusako, P. Lindenbaum, E. Charpentier, C.B. Nowak, E. Cherot, T. Simonet, C.A.L. Ruivenkamp, S. Hahn, C.A. Brownstein, F. Xia, S. Schmitt, W. Deb, D. Bonneau, M. Nizon, D. Quinquis, J. Chelly, G. Rudolf, D. Sanlaville, P. Parent, B. Gilbert-Dussardier, A. Toutain, V.R. Sutton, J. Thies, L. Peart-Vissers, P. Boisseau, M. Vincent, A.M. Grabrucker, C. Dubourg, N. Undiagnosed Diseases, W.H. Tan, N.E. Verbeek, M. Granzow, G.W.E. Santen, J. Shendure, B. Isidor, L. Pasquier, R. Redon, Y. Yang, M.W. State, T. Kleefstra, B. Cogne, H. Gem, S. Deciphering Developmental Disorders, S. Petrovski, K. Retterer, et al. 2017. De Novo Mutations in Protein Kinase Genes CAMK2A and CAMK2B Cause Intellectual Disability. *Am J Hum Genet*. 101:768-788.

Kuzniewska, B., D. Cysewski, M. Wasilewski, P. Sakowska, J. Milek, T.M. Kulinski, M. Winiarski, P. Kozielewicz, E. Knapska, M. Dadlez, A. Chacinska, A. Dziembowski,

and M. Dziembowska. 2020. Mitochondrial protein biogenesis in the synapse is supported by local translation. *EMBO Rep*. 21:e48882.

Laffitte, B.A., J.J. Repa, S.B. Joseph, D.C. Wilpitz, H.R. Kast, D.J. Mangelsdorf, and P. Tontonoz. 2001. LXRs control lipid-inducible expression of the apolipoprotein E gene in macrophages and adipocytes. *Proc Natl Acad Sci U S A*. 98:507-512.

Lake, N.J., B.D. Webb, D.A. Stroud, T.R. Richman, B. Ruzzenente, A.G. Compton, H.S. Mountford, J. Pulman, C. Zangarelli, M. Rio, N. Boddaert, Z. Assouline, M.D. Sherpa, E.E. Schadt, S.M. Houten, J. Byrnes, E.M. McCormick, Z. Zolkipli-Cunningham, K. Haude, Z. Zhang, K. Retterer, R. Bai, S.E. Calvo, V.K. Mootha, J. Christodoulou, A. Rotig, A. Filipovska, I. Cristian, M.J. Falk, M.D. Metodiev, and D.R. Thorburn. 2017. Biallelic Mutations in MRPS34 Lead to Instability of the Small Mitoribosomal Subunit and Leigh Syndrome. *Am J Hum Genet*. 101:239-254.

Lambert, J.C., S. Heath, G. Even, D. Campion, K. Sleegers, M. Hiltunen, O. Combarros, D. Zelenika, M.J. Bullido, B. Tavernier, L. Letenneur, K. Bettens, C. Berr, F. Pasquier, N. Fievet, P. Barberger-Gateau, S. Engelborghs, P. De Deyn, I. Mateo, A. Franck, S. Helisalmi, E. Porcellini, O. Hanon, I. European Alzheimer's Disease Initiative, M.M. de Pancorbo, C. Lendon, C. Dufouil, C. Jaillard, T. Leveillard, V. Alvarez, P. Bosco, M. Mancuso, F. Panza, B. Nacmias, P. Bossu, P. Piccardi, G. Annoni, D. Seripa, D. Galimberti, D. Hannequin, F. Licastro, H. Soininen, K. Ritchie, H. Blanche, J.F. Dartigues, C. Tzourio, I. Gut, C. Van Broeckhoven, A. Alperovitch, M. Lathrop, and P. Amouyel. 2009. Genome-wide association study identifies variants at CLU and CR1 associated with Alzheimer's disease. *Nat Genet*. 41:1094-1099.

Lane, A., A. Gokhale, E. Werner, A. Roberts, A. Freeman, B. Roberts, and V. Faundez. 2022. Sulfur- and phosphorus-standardized metal quantification of biological specimens using inductively coupled plasma mass spectrometry. *STAR Protoc*. 3:101334.

Lane-Donovan, C., G.T. Philips, and J. Herz. 2014. More than cholesterol transporters: lipoprotein receptors in CNS function and neurodegeneration. *Neuron*. 83:771-787.

Lanfranco, M.F., J. Sepulveda, G. Kopetsky, and G.W. Rebeck. 2021. Expression and secretion of apoE isoforms in astrocytes and microglia during inflammation. *Glia*. 69:1478-1493.

Lau, C.G., and R.S. Zukin. 2007. NMDA receptor trafficking in synaptic plasticity and neuropsychiatric disorders. *Nat Rev Neurosci*. 8:413-426.

Leary, S.C., P.A. Cobine, T. Nishimura, R.M. Verdijk, R. de Krijger, R. de Coo, M.A. Tarnopolsky, D.R. Winge, and E.A. Shoubridge. 2013. COX19 mediates the transduction of a mitochondrial redox signal from SCO1 that regulates ATP7A-mediated cellular copper efflux. *Mol Biol Cell*. 24:683-691.

Lee, C.E., K.S. Singleton, M. Wallin, and V. Faundez. 2020a. Rare Genetic Diseases: Nature's Experiments on Human Development. *iScience*. 23:101123.

Lee, H., R.J. Fenster, S.S. Pineda, W.S. Gibbs, S. Mohammadi, J. Davila-Velderrain, F.J. Garcia, M. Therrien, H.S. Novis, F. Gao, H. Wilkinson, T. Vogt, M. Kellis, M.J. LaVoie, and M. Heiman. 2020b. Cell Type-Specific Transcriptomics Reveals that Mutant Huntingtin Leads to Mitochondrial RNA Release and Neuronal Innate Immune Activation. *Neuron*. 107:891-908 e898.

Lee, K.H., H. Lee, C.H. Yang, J.S. Ko, C.H. Park, R.S. Woo, J.Y. Kim, W. Sun, J.H. Kim, W.K. Ho, and S.H. Lee. 2015. Bidirectional Signaling of Neuregulin-2 Mediates Formation of GABAergic Synapses and Maturation of Glutamatergic Synapses in Newborn Granule Cells of Postnatal Hippocampus. *J Neurosci*. 35:16479-16493.

Lemmon, M.A., and J. Schlessinger. 2010. Cell signaling by receptor tyrosine kinases. *Cell*. 141:1117-1134.

Leonardo, E.D., L. Hinck, M. Masu, K. Keino-Masu, S.L. Ackerman, and M. Tessier-Lavigne. 1997. Vertebrate homologues of C. elegans UNC-5 are candidate netrin receptors. *Nature*. 386:833-838.

Li, J., S.K. Ryan, E. Deboer, K. Cook, S. Fitzgerald, H.M. Lachman, D.C. Wallace, E.M. Goldberg, and S.A. Anderson. 2019. Mitochondrial deficits in human iPSC-derived neurons from patients with 22q11.2 deletion syndrome and schizophrenia. *Transl Psychiatry*. 9:302.

Li, X., J. Zhang, D. Li, C. He, K. He, T. Xue, L. Wan, C. Zhang, and Q. Liu. 2021. Astrocytic ApoE reprograms neuronal cholesterol metabolism and histone-acetylation-mediated memory. *Neuron*. 109:957-970 e958.

Li, Z., F. Shue, N. Zhao, M. Shinohara, and G. Bu. 2020. APOE2: protective mechanism and therapeutic implications for Alzheimer's disease. *Mol Neurodegener*. 15:63.

Liao, F., Y. Hori, E. Hudry, A.Q. Bauer, H. Jiang, T.E. Mahan, K.B. Lefton, T.J. Zhang, J.T. Dearborn, J. Kim, J.P. Culver, R. Betensky, D.F. Wozniak, B.T. Hyman, and D.M. Holtzman. 2014. Anti-ApoE antibody given after plaque onset decreases Abeta accumulation and improves brain function in a mouse model of Abeta amyloidosis. *J Neurosci*. 34:7281-7292.

Liddelow, S.A., K.A. Guttenplan, L.E. Clarke, F.C. Bennett, C.J. Bohlen, L. Schirmer, M.L. Bennett, A.E. Munch, W.S. Chung, T.C. Peterson, D.K. Wilton, A. Frouin, B.A. Napier, N. Panicker, M. Kumar, M.S. Buckwalter, D.H. Rowitch, V.L. Dawson, T.M. Dawson, B. Stevens, and B.A. Barres. 2017. Neurotoxic reactive astrocytes are induced by activated microglia. *Nature*. 541:481-487.

Lin, M.M., N. Liu, Z.H. Qin, and Y. Wang. 2022. Mitochondrial-derived damage-associated molecular patterns amplify neuroinflammation in neurodegenerative diseases. *Acta Pharmacol Sin*.

Lin-Hendel, E.G., M.J. McManus, D.C. Wallace, S.A. Anderson, and J.A. Golden. 2016. Differential Mitochondrial Requirements for Radially and Non-radially Migrating Cortical Neurons: Implications for Mitochondrial Disorders. *Cell Rep*. 15:229-237.

Litvinchuk, A., T.V. Huynh, Y. Shi, R.J. Jackson, M.B. Finn, M. Manis, C.M. Francis, A.C. Tran, P.M. Sullivan, J.D. Ulrich, B.T. Hyman, T. Cole, and D.M. Holtzman. 2021. Apolipoprotein E4 Reduction with Antisense Oligonucleotides Decreases Neurodegeneration in a Tauopathy Model. *Ann Neurol*. 89:952-966.

Liu, C.C., C.C. Liu, T. Kanekiyo, H. Xu, and G. Bu. 2013. Apolipoprotein E and Alzheimer disease: risk, mechanisms and therapy. *Nat Rev Neurol*. 9:106-118.

Liu, D., Y. Gao, J. Liu, Y. Huang, J. Yin, Y. Feng, L. Shi, B.P. Meloni, C. Zhang, M. Zheng, and J. Gao. 2021. Intercellular mitochondrial transfer as a means of tissue revitalization. *Signal Transduct Target Ther*. 6:65.

Liu, L., K.R. MacKenzie, N. Putluri, M. Maletic-Savatic, and H.J. Bellen. 2017. The Glia-Neuron Lactate Shuttle and Elevated ROS Promote Lipid Synthesis in Neurons and Lipid Droplet Accumulation in Glia via APOE/D. *Cell Metab*. 26:719-737 e716.

Lobo-Jarne, T., E. Nyvltova, R. Perez-Perez, A. Timon-Gomez, T. Molinie, A. Choi, A. Mourier, F. Fontanesi, C. Ugalde, and A. Barrientos. 2018. Human COX7A2L Regulates Complex III Biogenesis and Promotes Supercomplex Organization Remodeling without Affecting Mitochondrial Bioenergetics. *Cell Rep*. 25:1786-1799 e1784.

Loisy, M., G. Bouisset, S. Lopez, M. Muller, A. Spitsyn, J. Duval, R.A. Piskorowski, L. Verret, and V. Chevaleyre. 2022. Sequential inhibitory plasticities in hippocampal area CA2 and social memory formation. *Neuron*. 110:2854-2866 e2854.

Lopera, F., C. Marino, A.S. Chandrahas, M. O'Hare, N.D. Villalba-Moreno, D. Aguillon, A. Baena, J.S. Sanchez, C. Vila-Castelar, L. Ramirez Gomez, N. Chmielewska, G.M. Oliveira, J.L. Littau, K. Hartmann, K. Park, S. Krasemann, M. Glatzel, D. Schoemaker, L. Gonzalez-Buendia, S. Delgado-Tirado, S. Arevalo-Alquichire, K.L. Saez-Torres, D. Amarnani, L.A. Kim, R.C. Mazzarino, H. Gordon, Y. Bocanegra, A. Villegas, X. Gai, M. Bootwalla, J. Ji, L. Shen, K.S. Kosik, Y. Su, Y. Chen, A. Schultz, R.A. Sperling, K. Johnson, E.M. Reiman, D. Sepulveda-Falla, J.F. Arboleda-Velasquez, and Y.T. Quiroz. 2023. Resilience to autosomal dominant Alzheimer's disease in a Reelin-COLBOS heterozygous man. *Nat Med*. 29:1243-1252.

Love, M.I., W. Huber, and S. Anders. 2014. Moderated estimation of fold change and dispersion for RNA-seq data with DESeq2. *Genome Biol*. 15:550.

Lu, Y.W., M.G. Acoba, K. Selvaraju, T.C. Huang, R.S. Nirujogi, G. Sathe, A. Pandey, and S.M. Claypool. 2017. Human adenine nucleotide translocases physically and functionally interact with respirasomes. *Mol Biol Cell*. 28:1489-1506.

Mahan, T.E., C. Wang, X. Bao, A. Choudhury, J.D. Ulrich, and D.M. Holtzman. 2022. Selective reduction of astrocyte apoE3 and apoE4 strongly reduces Abeta accumulation and plaque-related pathology in a mouse model of amyloidosis. *Mol Neurodegener*. 17:13.

Mahapatra, G., Z. Gao, J.R. Bateman, 3rd, S.N. Lockhart, J. Bergstrom, A.R. DeWitt, J.E. Piloso, P.A. Kramer, J.L. Gonzalez-Armenta, K.A. Amick, R. Casanova, S. Craft, and A.J.A. Molina. 2023. Blood-based bioenergetic profiling reveals differences in mitochondrial function associated with cognitive performance and Alzheimer's disease. *Alzheimers Dement*. 19:1466-1478.

Mahley, R.W. 2016. Central Nervous System Lipoproteins: ApoE and Regulation of Cholesterol Metabolism. *Arterioscler Thromb Vasc Biol*. 36:1305-1315.

Mahley, R.W. 2023. Apolipoprotein E4 targets mitochondria and the mitochondria-associated membrane complex in neuropathology, including Alzheimer's disease. *Curr Opin Neurobiol*. 79:102684.

Majd, H., M.S. King, A.C. Smith, and E.R.S. Kunji. 2018. Pathogenic mutations of the human mitochondrial citrate carrier SLC25A1 lead to impaired citrate export required for lipid, dolichol, ubiquinone and sterol synthesis. *Biochim Biophys Acta Bioenerg*. 1859:1-7.

Mansur, F., E.S.A.L. Teles, A.K.S. Gomes, J. Magdalon, J.S. de Souza, K. Griesi-Oliveira, M.R. Passos-Bueno, and A.L. Sertie. 2021. Complement C4 Is Reduced in iPSC-Derived Astrocytes of Autism Spectrum Disorder Subjects. *Int J Mol Sci*. 22.

Marchi, S., E. Guilbaud, S.W.G. Tait, T. Yamazaki, and L. Galluzzi. 2023. Mitochondrial control of inflammation. *Nat Rev Immunol*. 23:159-173.

Marissal, T., R.F. Salazar, C. Bertollini, S. Mutel, M. De Roo, I. Rodriguez, D. Muller, and A. Carleton. 2018. Restoring wild-type-like CA1 network dynamics and behavior during adulthood in a mouse model of schizophrenia. *Nat Neurosci*. 21:1412-1420.

Martens, Y.A., N. Zhao, C.C. Liu, T. Kanekiyo, A.J. Yang, A.M. Goate, D.M. Holtzman, and G. Bu. 2022. ApoE Cascade Hypothesis in the pathogenesis of Alzheimer's disease and related dementias. *Neuron*.

Marzan, S., M.A. Aziz, and M.S. Islam. 2021. Association Between REELIN Gene Polymorphisms (rs7341475 and rs262355) and Risk of Schizophrenia: an Updated Meta-analysis. *J Mol Neurosci*. 71:675-690.

Mauch, D.H., K. Nagler, S. Schumacher, C. Goritz, E.C. Muller, A. Otto, and F.W. Pfrieger. 2001. CNS synaptogenesis promoted by glia-derived cholesterol. *Science*. 294:1354-1357.

Mazein, A., S. Watterson, W.Y. Hsieh, W.J. Griffiths, and P. Ghazal. 2013. A comprehensive machine-readable view of the mammalian cholesterol biosynthesis pathway. *Biochem Pharmacol*. 86:56-66.

McDonald-McGinn, D.M., and K.E. Sullivan. 2011. Chromosome 22q11.2 deletion syndrome (DiGeorge syndrome/velocardiofacial syndrome). *Medicine (Baltimore)*. 90:1-18.

McDonald-McGinn, D.M., K.E. Sullivan, B. Marino, N. Philip, A. Swillen, J.A. Vorstman, E.H. Zackai, B.S. Emanuel, J.R. Vermeesch, B.E. Morrow, P.J. Scambler, and A.S. Bassett. 2015. 22q11.2 deletion syndrome. *Nat Rev Dis Primers*. 1:15071.

McLaughlin, R.L., D. Schijven, W. van Rheenen, K.R. van Eijk, M. O'Brien, R.S. Kahn, R.A. Ophoff, A. Goris, D.G. Bradley, A. Al-Chalabi, L.H. van den Berg, J.J. Luykx, O. Hardiman, J.H. Veldink, E.G.C. Project Min, and C. Schizophrenia Working Group of the Psychiatric Genomics. 2017. Genetic correlation between amyotrophic lateral sclerosis and schizophrenia. *Nat Commun*. 8:14774.

Meechan, D.W., H.L. Rutz, M.S. Fralish, T.M. Maynard, L.A. Rothblat, and A.S. LaMantia. 2015. Cognitive ability is associated with altered medial frontal cortical circuits in the LgDel mouse model of 22q11.2DS. *Cereb Cortex*. 25:1143-1151.

Meechan, D.W., E.S. Tucker, T.M. Maynard, and A.S. LaMantia. 2009. Diminished dosage of 22q11 genes disrupts neurogenesis and cortical development in a mouse model of 22q11 deletion/DiGeorge syndrome. *Proc Natl Acad Sci U S A*. 106:16434-16445.

Meechan, D.W., E.S. Tucker, T.M. Maynard, and A.S. LaMantia. 2012. Cxcr4 regulation of interneuron migration is disrupted in 22q11.2 deletion syndrome. *Proc Natl Acad Sci U S A*. 109:18601-18606.

Meng, J., L. Han, N. Zheng, T. Wang, H. Xu, Y. Jiang, Z. Wang, Z. Liu, Q. Zheng, X. Zhang, H. Luo, D. Can, J. Lu, H. Xu, and Y.W. Zhang. 2022. Microglial Tmem59 Deficiency Impairs Phagocytosis of Synapse and Leads to Autism-Like Behaviors in Mice. *J Neurosci*. 42:4958-4979.

Meredith, R.M., J. Dawitz, and I. Kramvis. 2012. Sensitive time-windows for susceptibility in neurodevelopmental disorders. *Trends Neurosci*. 35:335-344.

Merkwirth, C., V. Jovaisaite, J. Durieux, O. Matilainen, S.D. Jordan, P.M. Quiros, K.K. Steffen, E.G. Williams, L. Mouchiroud, S.U. Tronnes, V. Murillo, S.C. Wolff, R.J. Shaw, J. Auwerx, and A. Dillin. 2016. Two Conserved Histone Demethylases Regulate Mitochondrial Stress-Induced Longevity. *Cell*. 165:1209-1223.

Mi, Y., G. Qi, F. Vitali, Y. Shang, A.C. Raikes, T. Wang, Y. Jin, R.D. Brinton, H. Gu, and F. Yin. 2023. Loss of fatty acid degradation by astrocytic mitochondria triggers neuroinflammation and neurodegeneration. *Nat Metab*. 5:445-465.

Modgil, S., D.K. Lahiri, V.L. Sharma, and A. Anand. 2014. Role of early life exposure and environment on neurodegeneration: implications on brain disorders. *Transl Neurodegener*. 3:9.

Mok, K.Y., U. Sheerin, J. Simon-Sanchez, A. Salaka, L. Chester, V. Escott-Price, K. Mantripragada, K.M. Doherty, A.J. Noyce, N.E. Mencacci, S.J. Lubbe, C. International Parkinson's Disease Genomics, C.H. Williams-Gray, R.A. Barker, K.D. van Dijk, H.W. Berendse, P. Heutink, J.C. Corvol, F. Cormier, S. Lesage, A. Brice, K. Brockmann, C. Schulte, T. Gasser, T. Foltynie, P. Limousin, K.E. Morrison, C.E. Clarke, S. Sawcer, T.T. Warner, A.J. Lees, H.R. Morris, M.A. Nalls, A.B. Singleton, J. Hardy, A.Y. Abramov, V. Plagnol, N.M. Williams, and N.W. Wood. 2016. Deletions at 22q11.2 in idiopathic Parkinson's disease: a combined analysis of genome-wide association data. *Lancet Neurol*. 15:585-596.

Montagne, A., D.A. Nation, A.P. Sagare, G. Barisano, M.D. Sweeney, A. Chakhoyan, M. Pachicano, E. Joe, A.R. Nelson, L.M. D'Orazio, D.P. Buennagel, M.G. Harrington, T.L.S. Benzinger, A.M. Fagan, J.M. Ringman, L.S. Schneider, J.C. Morris, E.M. Reiman, R.J. Caselli, H.C. Chui, J. Tcw, Y. Chen, J. Pa, P.S. Conti, M. Law, A.W. Toga, and B.V. Zlokovic. 2020. APOE4 leads to blood-brain barrier dysfunction predicting cognitive decline. *Nature*. 581:71-76.

Montesanto, A., P. Crocco, M. Anfossi, N. Smirne, G. Puccio, R. Colao, R. Maletta, G. Passarino, A.C. Bruni, and G. Rose. 2016. The Genetic Variability of UCP4 Affects the Individual Susceptibility to Late-Onset Alzheimer's Disease and Modifies the Disease's Risk in APOE-varepsilon4 Carriers. *J Alzheimers Dis*. 51:1265-1274.

Mostafa, G.A., and A.A. Shehab. 2010. The link of C4B null allele to autism and to a family history of autoimmunity in Egyptian autistic children. *J Neuroimmunol*. 223:115-119.

Motahari, Z., T.M. Maynard, A. Popratiloff, S.A. Moody, and A.S. LaMantia. 2020. Aberrant early growth of individual trigeminal sensory and motor axons in a series of mouse genetic models of 22q11.2 deletion syndrome. *Hum Mol Genet*. 29:3081-3093.

Motahari, Z., S.A. Moody, T.M. Maynard, and A.S. LaMantia. 2019. In the line-up: deleted genes associated with DiGeorge/22q11.2 deletion syndrome: are they all suspects? *J Neurodev Disord*. 11:7.

Mukai, J., M. Tamura, K. Fenelon, A.M. Rosen, T.J. Spellman, R. Kang, A.B. MacDermott, M. Karayiorgou, J.A. Gordon, and J.A. Gogos. 2015. Molecular substrates of altered axonal growth and brain connectivity in a mouse model of schizophrenia. *Neuron*. 86:680-695.

Mukherjee, A., F. Carvalho, S. Eliez, and P. Caroni. 2019. Long-Lasting Rescue of Network and Cognitive Dysfunction in a Genetic Schizophrenia Model. *Cell*. 178:1387-1402 e1314.

Mullican, S.E., X. Lin-Schmidt, C.N. Chin, J.A. Chavez, J.L. Furman, A.A. Armstrong, S.C. Beck, V.J. South, T.Q. Dinh, T.D. Cash-Mason, C.R. Cavanaugh, S. Nelson, C. Huang, M.J. Hunter, and S.M. Rangwala. 2017. GFRAL is the receptor for GDF15

and the ligand promotes weight loss in mice and nonhuman primates. *Nat Med*. 23:1150-1157.

Munoz-Pujol, G., J.D. Ortigoza-Escobar, A.J. Paredes-Fuentes, C. Jou, O. Ugarteburu, L. Gort, D. Yubero, A. Garcia-Cazorla, M. O'Callaghan, J. Campistol, J. Muchart, V.A. Yepez, M. Gusic, J. Gagneur, H. Prokisch, R. Artuch, A. Ribes, R. Urreizti, and F. Tort. 2023. Leigh syndrome is the main clinical characteristic of PTCD3 deficiency. *Brain Pathol*. 33:e13134.

Murphy, K.C. 2002. Schizophrenia and velo-cardio-facial syndrome. *Lancet*. 359:426-430.

Murphy, K.C., L.A. Jones, and M.J. Owen. 1999. High rates of schizophrenia in adults with velo-cardio-facial syndrome. *Arch Gen Psychiatry*. 56:940-945.

Murru, S., S. Hess, E. Barth, E.R. Almajan, D. Schatton, S. Hermans, S. Brodesser, T. Langer, P. Kloppenburg, and E.I. Rugarli. 2019. Astrocyte-specific deletion of the mitochondrial m-AAA protease reveals glial contribution to neurodegeneration. *Glia*. 67:1526-1541.

Naj, A.C., G. Jun, G.W. Beecham, L.S. Wang, B.N. Vardarajan, J. Buros, P.J. Gallins, J.D. Buxbaum, G.P. Jarvik, P.K. Crane, E.B. Larson, T.D. Bird, B.F. Boeve, N.R. Graff-Radford, P.L. De Jager, D. Evans, J.A. Schneider, M.M. Carrasquillo, N. Ertekin-Taner, S.G. Younkin, C. Cruchaga, J.S. Kauwe, P. Nowotny, P. Kramer, J. Hardy, M.J. Huentelman, A.J. Myers, M.M. Barmada, F.Y. Demirci, C.T. Baldwin, R.C. Green, E. Rogaeva, P. St George-Hyslop, S.E. Arnold, R. Barber, T. Beach, E.H. Bigio, J.D. Bowen, A. Boxer, J.R. Burke, N.J. Cairns, C.S. Carlson, R.M. Carney, S.L. Carroll, H.C. Chui, D.G. Clark, J. Corneveaux, C.W. Cotman, J.L. Cummings, C. DeCarli, S.T. DeKosky, R. Diaz-Arrastia, M. Dick, D.W. Dickson, W.G. Ellis, K.M. Faber, K.B. Fallon, M.R. Farlow, S. Ferris, M.P. Frosch, D.R. Galasko, M. Ganguli, M. Gearing, D.H. Geschwind, B. Ghetti, J.R. Gilbert, S. Gilman, B. Giordani, J.D. Glass, J.H. Growdon, R.L. Hamilton, L.E. Harrell, E. Head, L.S. Honig, C.M. Hulette, B.T. Hyman, G.A. Jicha, L.W. Jin, N. Johnson, J. Karlawish, A. Karydas, J.A. Kaye, R. Kim, E.H. Koo, N.W. Kowall, J.J. Lah, A.I. Levey, A.P. Lieberman, O.L. Lopez, W.J. Mack, D.C. Marson, F. Martiniuk, D.C. Mash, E. Masliah, W.C. McCormick, S.M. McCurry, A.N. McDavid, A.C. McKee, M. Mesulam, B.L. Miller, et al. 2011. Common variants at MS4A4/MS4A6E, CD2AP, CD33 and EPHA1 are associated with late-onset Alzheimer's disease. *Nat Genet*. 43:436-441.

Nakahira, K., S. Hisata, and A.M. Choi. 2015. The Roles of Mitochondrial Damage-Associated Molecular Patterns in Diseases. *Antioxid Redox Signal*. 23:1329-1350.

Nakamura, T., A. Watanabe, T. Fujino, T. Hosono, and M. Michikawa. 2009. Apolipoprotein E4 (1-272) fragment is associated with mitochondrial proteins and affects mitochondrial function in neuronal cells. *Mol Neurodegener*. 4:35.

Nation, D.A., M.D. Sweeney, A. Montagne, A.P. Sagare, L.M. D'Orazio, M. Pachicano, F. Sepehrband, A.R. Nelson, D.P. Buennagel, M.G. Harrington, T.L.S. Benzinger, A.M. Fagan, J.M. Ringman, L.S. Schneider, J.C. Morris, H.C. Chui, M. Law, A.W. Toga, and B.V. Zlokovic. 2019. Blood-brain barrier breakdown is an early biomarker of human cognitive dysfunction. *Nat Med*. 25:270-276.

Nehme, R., O. Pietilainen, M. Artomov, M. Tegtmeyer, V. Valakh, L. Lehtonen, C. Bell, T. Singh, A. Trehan, J. Sherwood, D. Manning, E. Peirent, R. Malik, E.J. Guss, D.

Hawes, A. Beccard, A.M. Bara, D.Z. Hazelbaker, E. Zuccaro, G. Genovese, A.A. Loboda, A. Neumann, C. Lilliehook, O. Kuismin, E. Hamalainen, M. Kurki, C.M. Hultman, A.K. Kahler, J.A. Paulo, A. Ganna, J. Madison, B. Cohen, D. McPhie, R. Adolfsson, R. Perlis, R. Dolmetsch, S. Farhi, S. McCarroll, S. Hyman, B. Neale, L.E. Barrett, W. Harper, A. Palotie, M. Daly, and K. Eggan. 2022. The 22q11.2 region regulates presynaptic gene-products linked to schizophrenia. *Nat Commun.* 13:3690.

Neuhaus, J.F., O.R. Baris, S. Hess, N. Moser, H. Schroder, S.J. Chinta, J.K. Andersen, P. Kloppenburg, and R.J. Wiesner. 2014. Catecholamine metabolism drives generation of mitochondrial DNA deletions in dopaminergic neurons. *Brain.* 137:354-365.

Ng, S., C.C. Lin, Y.H. Hwang, W.S. Hsieh, H.F. Liao, and P.C. Chen. 2013. Mercury, APOE, and children's neurodevelopment. *Neurotoxicology.* 37:85-92.

Nguyen, T.T.M., R. Gadet, M. Lanfranchi, R.A. Lahaye, S. Yandiev, O. Lohez, I. Mikaelian, L. Jabbour, R. Rimokh, J. Courchet, F. Saudou, N. Popgeorgiev, and G. Gillet. 2023. Mitochondrial Bcl-xL promotes brain synaptogenesis by controlling non-lethal caspase activation. *iScience.* 26:106674.

Nota, B., E.A. Struys, A. Pop, E.E. Jansen, M.R. Fernandez Ojeda, W.A. Kanhai, M. Kranendijk, S.J. van Dooren, M.R. Bevova, E.A. Sistermans, A.W. Nieuwint, M. Barth, T. Ben-Omran, G.F. Hoffmann, P. de Lonlay, M.T. McDonald, A. Meberg, A.C. Muntau, J.M. Nuoffer, R. Parini, M.H. Read, A. Renneberg, R. Santer, T. Strahleck, E. van Schaftingen, M.S. van der Knaap, C. Jakobs, and G.S. Salomons. 2013. Deficiency in SLC25A1, encoding the mitochondrial citrate carrier, causes combined D-2- and L-2-hydroxyglutaric aciduria. *Am J Hum Genet.* 92:627-631.

Nowacki, J.C., A.M. Fields, and M.M. Fu. 2022. Emerging cellular themes in leukodystrophies. *Front Cell Dev Biol.* 10:902261.

Nunnari, J., and A. Suomalainen. 2012. Mitochondria: in sickness and in health. *Cell.* 148:1145-1159.

Nyvltova, E., J.V. Dietz, J. Seravalli, O. Khalimonchuk, and A. Barrientos. 2022. Coordination of metal center biogenesis in human cytochrome c oxidase. *Nat Commun.* 13:3615.

O'Donoghue, M.C., S.E. Murphy, G. Zamboni, A.C. Nobre, and C.E. Mackay. 2018. APOE genotype and cognition in healthy individuals at risk of Alzheimer's disease: A review. *Cortex.* 104:103-123.

Oakley, H., S.L. Cole, S. Logan, E. Maus, P. Shao, J. Craft, A. Guillozet-Bongaarts, M. Ohno, J. Disterhoft, L. Van Eldik, R. Berry, and R. Vassar. 2006. Intraneuronal beta-amyloid aggregates, neurodegeneration, and neuron loss in transgenic mice with five familial Alzheimer's disease mutations: potential factors in amyloid plaque formation. *J Neurosci.* 26:10129-10140.

Odell, D., A. Maciulis, A. Cutler, L. Warren, W.M. McMahon, H. Coon, G. Stubbs, K. Henley, and A. Torres. 2005. Confirmation of the association of the C4B null allelle in autism. *Hum Immunol.* 66:140-145.

Ohanele, C., J.N. Peoples, A. Karlstaedt, J.T. Geiger, A.D. Gayle, N. Ghazal, F. Sohani, M.E. Brown, M.E. Davis, G.A. Porter, V. Faundez, and J.Q. Kwong. 2023.

Mitochondrial citrate carrier SLC25A1 is a dosage-dependent regulator of metabolic reprogramming and morphogenesis in the developing heart. *bioRxiv*.

Orr, A.L., C. Kim, D. Jimenez-Morales, B.W. Newton, J.R. Johnson, N.J. Krogan, D.L. Swaney, and R.W. Mahley. 2019. Neuronal Apolipoprotein E4 Expression Results in Proteome-Wide Alterations and Compromises Bioenergetic Capacity by Disrupting Mitochondrial Function. *J Alzheimers Dis*. 68:991-1011.

Oswald, C., U. Krause-Buchholz, and G. Rodel. 2009. Knockdown of human COX17 affects assembly and supramolecular organization of cytochrome c oxidase. *J Mol Biol*. 389:470-479.

Owen, M.J., and J.L. Doherty. 2016. What can we learn from the high rates of schizophrenia in people with 22q11.2 deletion syndrome? *World Psychiatry*. 15:23-25.

Pacelli, C., N. Giguere, M.J. Bourque, M. Levesque, R.S. Slack, and L.E. Trudeau. 2015. Elevated Mitochondrial Bioenergetics and Axonal Arborization Size Are Key Contributors to the Vulnerability of Dopamine Neurons. *Curr Biol*. 25:2349-2360.

Padula, M.C., M. Schaer, E. Scariati, M. Schneider, D. Van De Ville, M. Debbane, and S. Eliez. 2015. Structural and functional connectivity in the default mode network in 22q11.2 deletion syndrome. *J Neurodev Disord*. 7:23.

Pandya, V.A., and R. Patani. 2021. Region-specific vulnerability in neurodegeneration: lessons from normal ageing. *Ageing Res Rev*. 67:101311.

Parhizkar, S., and D.M. Holtzman. 2022. APOE mediated neuroinflammation and neurodegeneration in Alzheimer's disease. *Semin Immunol*:101594.

Paronett, E.M., D.W. Meechan, B.A. Karpinski, A.S. LaMantia, and T.M. Maynard. 2015. Ranbp1, Deleted in DiGeorge/22q11.2 Deletion Syndrome, is a Microcephaly Gene That Selectively Disrupts Layer 2/3 Cortical Projection Neuron Generation. *Cereb Cortex*. 25:3977-3993.

Paterlini, M., S.S. Zakharenko, W.S. Lai, J. Qin, H. Zhang, J. Mukai, K.G. Westphal, B. Olivier, D. Sulzer, P. Pavlidis, S.A. Siegelbaum, M. Karayiorgou, and J.A. Gogos. 2005. Transcriptional and behavioral interaction between 22q11.2 orthologs modulates schizophrenia-related phenotypes in mice. *Nat Neurosci*. 8:1586-1594.

Patterson, P.H. 2009. Immune involvement in schizophrenia and autism: etiology, pathology and animal models. *Behav Brain Res*. 204:313-321.

Petris, M.J., J. Camakaris, M. Greenough, S. LaFontaine, and J.F. Mercer. 1998. A C-terminal di-leucine is required for localization of the Menkes protein in the trans-Golgi network. *Hum Mol Genet*. 7:2063-2071.

Picard, M., M.J. McManus, J.D. Gray, C. Nasca, C. Moffat, P.K. Kopinski, E.L. Seifert, B.S. McEwen, and D.C. Wallace. 2015. Mitochondrial functions modulate neuroendocrine, metabolic, inflammatory, and transcriptional responses to acute psychological stress. *Proc Natl Acad Sci U S A*. 112:E6614-6623.

Picard, M., R.J. Petrie, J. Antoine-Bertrand, E. Saint-Cyr-Proulx, J.F. Villemure, and N. Lamarche-Vane. 2009. Spatial and temporal activation of the small GTPases RhoA and Rac1 by the netrin-1 receptor UNC5a during neurite outgrowth. *Cell Signal*. 21:1961-1973.

Picard, M., J. Zhang, S. Hancock, O. Derbeneva, R. Golhar, P. Golik, S. O'Hearn, S. Levy, P. Potluri, M. Lvova, A. Davila, C.S. Lin, J.C. Perin, E.F. Rappaport, H. Hakonarson, I.A. Trounce, V. Procaccio, and D.C. Wallace. 2014. Progressive

increase in mtDNA 3243A>G heteroplasmy causes abrupt transcriptional reprogramming. *Proc Natl Acad Sci U S A*. 111:E4033-4042.

Pietrocola, F., L. Galluzzi, J.M. Bravo-San Pedro, F. Madeo, and G. Kroemer. 2015. Acetyl coenzyme A: a central metabolite and second messenger. *Cell Metab*. 21:805-821.

Ping, L., D.M. Duong, L. Yin, M. Gearing, J.J. Lah, A.I. Levey, and N.T. Seyfried. 2018. Global quantitative analysis of the human brain proteome in Alzheimer's and Parkinson's Disease. *Sci Data*. 5:180036.

Piskorowski, R.A., K. Nasrallah, A. Diamantopoulou, J. Mukai, S.I. Hassan, S.A. Siegelbaum, J.A. Gogos, and V. Chevaleyre. 2016. Age-Dependent Specific Changes in Area CA2 of the Hippocampus and Social Memory Deficit in a Mouse Model of the 22q11.2 Deletion Syndrome. *Neuron*. 89:163-176.

Pollak, T.A., S. Drndarski, J.M. Stone, A.S. David, P. McGuire, and N.J. Abbott. 2018. The blood-brain barrier in psychosis. *Lancet Psychiatry*. 5:79-92.

Presumey, J., A.R. Bialas, and M.C. Carroll. 2017. Complement System in Neural Synapse Elimination in Development and Disease. *Adv Immunol*. 135:53-79.

Prinz, M., and J. Priller. 2017. The role of peripheral immune cells in the CNS in steady state and disease. *Nat Neurosci*. 20:136-144.

Pun, P.B., J. Lu, and S. Moochhala. 2009. Involvement of ROS in BBB dysfunction. *Free Radic Res*. 43:348-364.

Qi, G., Y. Mi, X. Shi, H. Gu, R.D. Brinton, and F. Yin. 2021. ApoE4 Impairs Neuron-Astrocyte Coupling of Fatty Acid Metabolism. *Cell Rep*. 34:108572.

Qiu, S., and E.J. Weeber. 2007. Reelin signaling facilitates maturation of CA1 glutamatergic synapses. *J Neurophysiol*. 97:2312-2321.

Quiros, P.M., M.A. Prado, N. Zamboni, D. D'Amico, R.W. Williams, D. Finley, S.P. Gygi, and J. Auwerx. 2017. Multi-omics analysis identifies ATF4 as a key regulator of the mitochondrial stress response in mammals. *J Cell Biol*. 216:2027-2045.

Rajarajan, P., T. Borrman, W. Liao, N. Schrode, E. Flaherty, C. Casino, S. Powell, C. Yashaswini, E.A. LaMarca, B. Kassim, B. Javidfar, S. Espeso-Gil, A. Li, H. Won, D.H. Geschwind, S.M. Ho, M. MacDonald, G.E. Hoffman, P. Roussos, B. Zhang, C.G. Hahn, Z. Weng, K.J. Brennand, and S. Akbarian. 2018. Neuron-specific signatures in the chromosomal connectome associated with schizophrenia risk. *Science*. 362.

Ramesha, S., S. Rayaprolu, C.A. Bowen, C.R. Giver, S. Bitarafan, H.M. Nguyen, T. Gao, M.J. Chen, N. Nwabueze, E.B. Dammer, A.K. Engstrom, H. Xiao, A. Pennati, N.T. Seyfried, D.J. Katz, J. Galipeau, H. Wulff, E.K. Waller, L.B. Wood, A.I. Levey, and S. Rangaraju. 2021. Unique molecular characteristics and microglial origin of Kv1.3 channel-positive brain myeloid cells in Alzheimer's disease. *Proc Natl Acad Sci U S A*. 118.

Rangaraju, S., E.B. Dammer, S.A. Raza, T. Gao, H. Xiao, R. Betarbet, D.M. Duong, J.A. Webster, C.M. Hales, J.J. Lah, A.I. Levey, and N.T. Seyfried. 2018. Quantitative proteomics of acutely-isolated mouse microglia identifies novel immune Alzheimer's disease-related proteins. *Mol Neurodegener*. 13:34.

Rangaraju, V., M. Lauterbach, and E.M. Schuman. 2019. Spatially Stable Mitochondrial Compartments Fuel Local Translation during Plasticity. *Cell*. 176:73-84 e15.

Rath, S., R. Sharma, R. Gupta, T. Ast, C. Chan, T.J. Durham, R.P. Goodman, Z. Grabarek, M.E. Haas, W.H.W. Hung, P.R. Joshi, A.A. Jourdain, S.H. Kim, A.V. Kotrys, S.S. Lam, J.G. McCoy, J.D. Meisel, M. Miranda, A. Panda, A. Patgiri, R. Rogers, S. Sadre, H. Shah, O.S. Skinner, T.L. To, M.A. Walker, H. Wang, P.S. Ward, J. Wengrod, C.C. Yuan, S.E. Calvo, and V.K. Mootha. 2021. MitoCarta3.0: an updated mitochondrial proteome now with sub-organelle localization and pathway annotations. *Nucleic Acids Res*. 49:D1541-D1547.

Raulin, A.C., S.V. Doss, Z.A. Trottier, T.C. Ikezu, G. Bu, and C.C. Liu. 2022. ApoE in Alzheimer's disease: pathophysiology and therapeutic strategies. *Mol Neurodegener*. 17:72.

Reh, R.K., B.G. Dias, C.A. Nelson, 3rd, D. Kaufer, J.F. Werker, B. Kolb, J.D. Levine, and T.K. Hensch. 2020. Critical period regulation across multiple timescales. *Proc Natl Acad Sci U S A*. 117:23242-23251.

Reichardt, L.F. 2006. Neurotrophin-regulated signalling pathways. *Philos Trans R Soc Lond B Biol Sci*. 361:1545-1564.

Reiman, E.M., K. Chen, G.E. Alexander, R.J. Caselli, D. Bandy, D. Osborne, A.M. Saunders, and J. Hardy. 2005. Correlations between apolipoprotein E epsilon4 gene dose and brain-imaging measurements of regional hypometabolism. *Proc Natl Acad Sci U S A*. 102:8299-8302.

Remer, J., D.C. Dean, 3rd, K. Chen, R.A. Reiman, M.J. Huentelman, E.M. Reiman, and S.C.L. Deoni. 2020. Longitudinal white matter and cognitive development in pediatric carriers of the apolipoprotein epsilon4 allele. *Neuroimage*. 222:117243.

Ricke, K.M., T. Pass, S. Kimoloi, K. Fahrmann, C. Jungst, A. Schauss, O.R. Baris, M. Aradjanski, A. Trifunovic, T.M. Eriksson Faelker, M. Bergami, and R.J. Wiesner. 2020. Mitochondrial Dysfunction Combined with High Calcium Load Leads to Impaired Antioxidant Defense Underlying the Selective Loss of Nigral Dopaminergic Neurons. *J Neurosci*. 40:1975-1986.

Rigby, M.J., N.S. Orefice, A.J. Lawton, M. Ma, S.L. Shapiro, S.Y. Yi, I.A. Dieterich, A. Frelka, H.N. Miles, R.A. Pearce, J.P.J. Yu, L. Li, J.M. Denu, and L. Puglielli. 2022. Increased expression of SLC25A1/CIC causes an autistic-like phenotype with altered neuron morphology. *Brain*.

Riley, J.S., and S.W. Tait. 2020. Mitochondrial DNA in inflammation and immunity. *EMBO Rep*. 21:e49799.

Robinson, J.T., H. Thorvaldsdóttir, D. Turner, and J.P. Mesirov. 2020. igv.js: an embeddable JavaScript implementation of the Integrative Genomics Viewer (IGV). *bioRxiv*.

Robinson, J.T., H. Thorvaldsdottir, W. Winckler, M. Guttman, E.S. Lander, G. Getz, and J.P. Mesirov. 2011. Integrative genomics viewer. *Nat Biotechnol*. 29:24-26.

Romme, I.A., M.A. de Reus, R.A. Ophoff, R.S. Kahn, and M.P. van den Heuvel. 2017. Connectome Disconnectivity and Cortical Gene Expression in Patients With Schizophrenia. *Biol Psychiatry*. 81:495-502.

Rosenberg, A., M. Saggar, P. Rogu, A. Limoges, A. Junker, C. Sandi, E. Mosharov, D. Dumitriu, C. Anacker, and M. Picard. 2022. A Network Approach to Mapping Mouse Brain-wide Mitochondrial Respiratory Chain Capacity in Relation to Behavior. *bioRxiv*.

Saitta, S.C., S.E. Harris, A.P. Gaeth, D.A. Driscoll, D.M. McDonald-McGinn, M.K. Maisenbacher, J.M. Yersak, P.K. Chakraborty, A.M. Hacker, E.H. Zackai, T. Ashley, and B.S. Emanuel. 2004. Aberrant interchromosomal exchanges are the predominant cause of the 22q11.2 deletion. *Hum Mol Genet*. 13:417-428.

Schmukler, E., S. Solomon, S. Simonovitch, Y. Goldshmit, E. Wolfson, D.M. Michaelson, and R. Pinkas-Kramarski. 2020. Altered mitochondrial dynamics and function in APOE4-expressing astrocytes. *Cell Death Dis*. 11:578.

Schneider, M., M. Debbane, A.S. Bassett, E.W. Chow, W.L. Fung, M. van den Bree, M. Owen, K.C. Murphy, M. Niarchou, W.R. Kates, K.M. Antshel, W. Fremont, D.M. McDonald-McGinn, R.E. Gur, E.H. Zackai, J. Vorstman, S.N. Duijff, P.W. Klaassen, A. Swillen, D. Gothelf, T. Green, A. Weizman, T. Van Amelsvoort, L. Evers, E. Boot, V. Shashi, S.R. Hooper, C.E. Bearden, M. Jalbrzikowski, M. Armando, S. Vicari, D.G. Murphy, O. Ousley, L.E. Campbell, T.J. Simon, S. Eliez, B. International Consortium on, and S. Behavior in 22q11.2 Deletion. 2014. Psychiatric disorders from childhood to adulthood in 22q11.2 deletion syndrome: results from the International Consortium on Brain and Behavior in 22q11.2 Deletion Syndrome. *Am J Psychiatry*. 171:627-639.

Schor, N.F., and D.W. Bianchi. 2021. Neurodevelopmental Clues to Neurodegeneration. *Pediatr Neurol*. 123:67-76.

Schreiner, M., J.K. Forsyth, K.H. Karlsgodt, A.E. Anderson, N. Hirsh, L. Kushan, L.Q. Uddin, L. Mattiacio, I.L. Coman, W.R. Kates, and C.E. Bearden. 2017. Intrinsic Connectivity Network-Based Classification and Detection of Psychotic Symptoms in Youth With 22q11.2 Deletions. *Cereb Cortex*. 27:3294-3306.

Schvartzman, J.M., C.B. Thompson, and L.W.S. Finley. 2018. Metabolic regulation of chromatin modifications and gene expression. *J Cell Biol*. 217:2247-2259.

Seidlitz, J., A. Nadig, S. Liu, R.A.I. Bethlehem, P.E. Vertes, S.E. Morgan, F. Vasa, R. Romero-Garcia, F.M. Lalonde, L.S. Clasen, J.D. Blumenthal, C. Paquola, B. Bernhardt, K. Wagstyl, D. Polioudakis, L. de la Torre-Ubieta, D.H. Geschwind, J.C. Han, N.R. Lee, D.G. Murphy, E.T. Bullmore, and A. Raznahan. 2020. Transcriptomic and cellular decoding of regional brain vulnerability to neurogenetic disorders. *Nat Commun*. 11:3358.

Sekar, A., A.R. Bialas, H. de Rivera, A. Davis, T.R. Hammond, N. Kamitaki, K. Tooley, J. Presumey, M. Baum, V. Van Doren, G. Genovese, S.A. Rose, R.E. Handsaker, C. Schizophrenia Working Group of the Psychiatric Genomics, M.J. Daly, M.C. Carroll, B. Stevens, and S.A. McCarroll. 2016. Schizophrenia risk from complex variation of complement component 4. *Nature*. 530:177-183.

Sellgren, C.M., J. Gracias, B. Watmuff, J.D. Biag, J.M. Thanos, P.B. Whittredge, T. Fu, K. Worringer, H.E. Brown, J. Wang, A. Kaykas, R. Karmacharya, C.P. Goold, S.D. Sheridan, and R.H. Perlis. 2019. Increased synapse elimination by microglia in schizophrenia patient-derived models of synaptic pruning. *Nat Neurosci*. 22:374-385.

Shannon, P., A. Markiel, O. Ozier, N.S. Baliga, J.T. Wang, D. Ramage, N. Amin, B. Schwikowski, and T. Ideker. 2003. Cytoscape: a software environment for integrated models of biomolecular interaction networks. *Genome Res*. 13:2498-2504.

Sharpley, M.S., C. Marciniak, K. Eckel-Mahan, M. McManus, M. Crimi, K. Waymire, C.S. Lin, S. Masubuchi, N. Friend, M. Koike, D. Chalkia, G. MacGregor, P. Sassone-Corsi, and D.C. Wallace. 2012. Heteroplasmy of mouse mtDNA is genetically unstable and results in altered behavior and cognition. *Cell*. 151:333-343.

Shi, Y., and D.M. Holtzman. 2018. Interplay between innate immunity and Alzheimer disease: APOE and TREM2 in the spotlight. *Nat Rev Immunol*. 18:759-772.

Shi, Y., K. Yamada, S.A. Liddelow, S.T. Smith, L. Zhao, W. Luo, R.M. Tsai, S. Spina, L.T. Grinberg, J.C. Rojas, G. Gallardo, K. Wang, J. Roh, G. Robinson, M.B. Finn, H. Jiang, P.M. Sullivan, C. Baufeld, M.W. Wood, C. Sutphen, L. McCue, C. Xiong, J.L. Del-Aguila, J.C. Morris, C. Cruchaga, I. Alzheimer's Disease Neuroimaging, A.M. Fagan, B.L. Miller, A.L. Boxer, W.W. Seeley, O. Butovsky, B.A. Barres, S.M. Paul, and D.M. Holtzman. 2017. ApoE4 markedly exacerbates tau-mediated neurodegeneration in a mouse model of tauopathy. *Nature*. 549:523-527.

Shimada, K., T.R. Crother, J. Karlin, J. Dagvadorj, N. Chiba, S. Chen, V.K. Ramanujan, A.J. Wolf, L. Vergnes, D.M. Ojcius, A. Rentsendorj, M. Vargas, C. Guerrero, Y. Wang, K.A. Fitzgerald, D.M. Underhill, T. Town, and M. Arditi. 2012. Oxidized mitochondrial DNA activates the NLRP3 inflammasome during apoptosis. *Immunity*. 36:401-414.

Shin, S.H., and Y.K. Kim. 2023. Early Life Stress, Neuroinflammation, and Psychiatric Illness of Adulthood. *Adv Exp Med Biol*. 1411:105-134.

Shoukier, M., S. Fuchs, E. Schwaibold, M. Lingen, J. Gartner, K. Brockmann, and B. Zirn. 2013. Microduplication of 3p26.3 in nonsyndromic intellectual disability indicates an important role of CHL1 for normal cognitive function. *Neuropediatrics*. 44:268-271.

Siciliano, G., A. Tessa, S. Petrini, M. Mancuso, C. Bruno, G.S. Grieco, A. Malandrini, L. DeFlorio, B. Martini, A. Federico, G. Nappi, F.M. Santorelli, and L. Murri. 2003. Autosomal dominant external ophthalmoplegia and bipolar affective disorder associated with a mutation in the ANT1 gene. *Neuromuscul Disord*. 13:162-165.

Sigurdsson, T., K.L. Stark, M. Karayiorgou, J.A. Gogos, and J.A. Gordon. 2010. Impaired hippocampal-prefrontal synchrony in a genetic mouse model of schizophrenia. *Nature*. 464:763-767.

Silverman, D.H., G.W. Small, C.Y. Chang, C.S. Lu, M.A. Kung De Aburto, W. Chen, J. Czernin, S.I. Rapoport, P. Pietrini, G.E. Alexander, M.B. Schapiro, W.J. Jagust, J.M. Hoffman, K.A. Welsh-Bohmer, A. Alavi, C.M. Clark, E. Salmon, M.J. de Leon, R. Mielke, J.L. Cummings, A.P. Kowell, S.S. Gambhir, C.K. Hoh, and M.E. Phelps. 2001. Positron emission tomography in evaluation of dementia: Regional brain metabolism and long-term outcome. *JAMA*. 286:2120-2127.

Simonovitch, S., E. Schmukler, E. Masliah, R. Pinkas-Kramarski, and D.M. Michaelson. 2019. The Effects of APOE4 on Mitochondrial Dynamics and Proteins in vivo. *J Alzheimers Dis*. 70:861-875.

Skene, N.G., J. Bryois, T.E. Bakken, G. Breen, J.J. Crowley, H.A. Gaspar, P. Giusti-Rodriguez, R.D. Hodge, J.A. Miller, A.B. Munoz-Manchado, M.C. O'Donovan, M.J. Owen, A.F. Pardinas, J. Ryge, J.T.R. Walters, S. Linnarsson, E.S. Lein, C. Major Depressive Disorder Working Group of the Psychiatric Genomics, P.F. Sullivan, and J. Hjerling-Leffler. 2018. Genetic identification of brain cell types underlying schizophrenia. *Nat Genet*. 50:825-833.

Smeland, O.B., A. Shadrin, S. Bahrami, I. Broce, M. Tesli, O. Frei, K.V. Wirgenes, K.S. O'Connell, F. Krull, F. Bettella, N.E. Steen, L. Sugrue, Y. Wang, P. Svenningsson, M. Sharma, L. Pihlstrom, M. Toft, M. O'Donovan, S. Djurovic, R. Desikan, A.M. Dale, and O.A. Andreassen. 2021. Genome-wide Association Analysis of Parkinson's Disease and Schizophrenia Reveals Shared Genetic Architecture and Identifies Novel Risk Loci. *Biol Psychiatry*. 89:227-235.

Srivastava, S., J. Cohen, J. Pevsner, S. Aradhya, D. McKnight, E. Butler, M. Johnston, and A. Fatemi. 2014. A novel variant in GABRB2 associated with intellectual disability and epilepsy. *Am J Med Genet A*. 164A:2914-2921.

Stark, K.L., B. Xu, A. Bagchi, W.S. Lai, H. Liu, R. Hsu, X. Wan, P. Pavlidis, A.A. Mills, M. Karayiorgou, and J.A. Gogos. 2008. Altered brain microRNA biogenesis contributes to phenotypic deficits in a 22q11-deletion mouse model. *Nat Genet*. 40:751-760.

Stokes, J.C., R.L. Bornstein, K. James, K.Y. Park, K.A. Spencer, K. Vo, J.C. Snell, B.M. Johnson, P.G. Morgan, M.M. Sedensky, N.A. Baertsch, and S.C. Johnson. 2022. Leukocytes mediate disease pathogenesis in the Ndufs4(KO) mouse model of Leigh syndrome. *JCI Insight*. 7.

Stranahan, A.M., J.R. Erion, and M. Wosiski-Kuhn. 2013. Reelin signaling in development, maintenance, and plasticity of neural networks. *Ageing Res Rev*. 12:815-822.

Strittmatter, W.J., A.M. Saunders, D. Schmechel, M. Pericak-Vance, J. Enghild, G.S. Salvesen, and A.D. Roses. 1993. Apolipoprotein E: high-avidity binding to beta-amyloid and increased frequency of type 4 allele in late-onset familial Alzheimer disease. *Proc Natl Acad Sci U S A*. 90:1977-1981.

Sturm, G., K.R. Karan, A.S. Monzel, B. Santhanam, T. Taivassalo, C. Bris, S.A. Ware, M. Cross, A. Towheed, A. Higgins-Chen, M.J. McManus, A. Cardenas, J. Lin, E.S. Epel, S. Rahman, J. Vissing, B. Grassi, M. Levine, S. Horvath, R.G. Haller, G. Lenaers, D.C. Wallace, M.P. St-Onge, S. Tavazoie, V. Procaccio, B.A. Kaufman, E.L. Seifert, M. Hirano, and M. Picard. 2023. OxPhos defects cause hypermetabolism and reduce lifespan in cells and in patients with mitochondrial diseases. *Commun Biol*. 6:22.

Styr, B., and I. Slutsky. 2018. Imbalance between firing homeostasis and synaptic plasticity drives early-phase Alzheimer's disease. *Nat Neurosci*. 21:463-473.

Sumitomo, A., K. Horike, K. Hirai, N. Butcher, E. Boot, T. Sakurai, F.C. Nucifora, Jr., A.S. Bassett, A. Sawa, and T. Tomoda. 2018. A mouse model of 22q11.2 deletions: Molecular and behavioral signatures of Parkinson's disease and schizophrenia. *Sci Adv*. 4:eaar6637.

Sweeney, M.D., A.P. Sagare, and B.V. Zlokovic. 2018. Blood-brain barrier breakdown in Alzheimer disease and other neurodegenerative disorders. *Nat Rev Neurol*. 14:133-150.

Swerdlow, R.H. 2018. Mitochondria and Mitochondrial Cascades in Alzheimer's Disease. *J Alzheimers Dis*. 62:1403-1416.

Swillen, A., and D. McDonald-McGinn. 2015. Developmental trajectories in 22q11.2 deletion. *Am J Med Genet C Semin Med Genet*. 169:172-181.

Tajima, H., M. Kawasumi, T. Chiba, M. Yamada, K. Yamashita, M. Nawa, Y. Kita, K. Kouyama, S. Aiso, M. Matsuoka, T. Niikura, and I. Nishimoto. 2005. A humanin

derivative, S14G-HN, prevents amyloid-beta-induced memory impairment in mice. *J Neurosci Res*. 79:714-723.

Tambini, M.D., M. Pera, E. Kanter, H. Yang, C. Guardia-Laguarta, D. Holtzman, D. Sulzer, E. Area-Gomez, and E.A. Schon. 2016. ApoE4 upregulates the activity of mitochondria-associated ER membranes. *EMBO Rep*. 17:27-36.

Tan, E.K., Y.X. Chao, A. West, L.L. Chan, W. Poewe, and J. Jankovic. 2020. Parkinson disease and the immune system - associations, mechanisms and therapeutics. *Nat Rev Neurol*. 16:303-318.

Tan, J.X., and T. Finkel. 2020. Mitochondria as intracellular signaling platforms in health and disease. *J Cell Biol*. 219.

Tang, S.X., J.J. Yi, M.E. Calkins, D.A. Whinna, C.G. Kohler, M.C. Souders, D.M. McDonald-McGinn, E.H. Zackai, B.S. Emanuel, R.C. Gur, and R.E. Gur. 2014. Psychiatric disorders in 22q11.2 deletion syndrome are prevalent but undertreated. *Psychol Med*. 44:1267-1277.

Tartaglione, A.M., A. Venerosi, and G. Calamandrei. 2016. Early-Life Toxic Insults and Onset of Sporadic Neurodegenerative Diseases-an Overview of Experimental Studies. *Curr Top Behav Neurosci*. 29:231-264.

Taylor, E.B. 2017. Functional Properties of the Mitochondrial Carrier System. *Trends Cell Biol*. 27:633-644.

Tcw, J., M. Wang, A.A. Pimenova, K.R. Bowles, B.J. Hartley, E. Lacin, S.I. Machlovi, R. Abdelaal, C.M. Karch, H. Phatnani, P.A. Slesinger, B. Zhang, A.M. Goate, and K.J. Brennand. 2017. An Efficient Platform for Astrocyte Differentiation from Human Induced Pluripotent Stem Cells. *Stem Cell Reports*. 9:600-614.

Terada, T., T. Obi, T. Bunai, T. Matsudaira, E. Yoshikawa, I. Ando, M. Futatsubashi, H. Tsukada, and Y. Ouchi. 2020. In vivo mitochondrial and glycolytic impairments in patients with Alzheimer disease. *Neurology*. 94:e1592-e1604.

Therriault, J., A.L. Benedet, T.A. Pascoal, S. Mathotaarachchi, M. Chamoun, M. Savard, E. Thomas, M.S. Kang, F. Lussier, C. Tissot, M. Parsons, M.N.I. Qureshi, P. Vitali, G. Massarweh, J.P. Soucy, S. Rej, P. Saha-Chaudhuri, S. Gauthier, and P. Rosa-Neto. 2020. Association of Apolipoprotein E epsilon4 With Medial Temporal Tau Independent of Amyloid-beta. *JAMA Neurol*. 77:470-479.

Timon-Gomez, A., J. Garlich, R.A. Stuart, C. Ugalde, and A. Barrientos. 2020a. Distinct Roles of Mitochondrial HIGD1A and HIGD2A in Respiratory Complex and Supercomplex Biogenesis. *Cell Rep*. 31:107607.

Timon-Gomez, A., R. Perez-Perez, E. Nyvltova, C. Ugalde, F. Fontanesi, and A. Barrientos. 2020b. Protocol for the Analysis of Yeast and Human Mitochondrial Respiratory Chain Complexes and Supercomplexes by Blue Native Electrophoresis. *STAR Protoc*. 1.

Toritsuka, M., S. Kimoto, K. Muraki, M.A. Landek-Salgado, A. Yoshida, N. Yamamoto, Y. Horiuchi, H. Hiyama, K. Tajinda, N. Keni, E. Illingworth, T. Iwamoto, T. Kishimoto, A. Sawa, and K. Tanigaki. 2013. Deficits in microRNA-mediated Cxcr4/Cxcl12 signaling in neurodevelopmental deficits in a 22q11 deletion syndrome mouse model. *Proc Natl Acad Sci U S A*. 110:17552-17557.

Tripathi, A., M. Spedding, E. Schenker, M. Didriksen, A. Cressant, and T.M. Jay. 2020. Cognition- and circuit-based dysfunction in a mouse model of 22q11.2 microdeletion syndrome: effects of stress. *Transl Psychiatry*. 10:41.

Tsai, V.W.W., Y. Husaini, A. Sainsbury, D.A. Brown, and S.N. Breit. 2018. The MIC-1/GDF15-GFRAL Pathway in Energy Homeostasis: Implications for Obesity, Cachexia, and Other Associated Diseases. *Cell Metab.* 28:353-368.

Tse, L.H., and Y.H. Wong. 2019. GPCRs in Autocrine and Paracrine Regulations. *Front Endocrinol (Lausanne).* 10:428.

Tsuboyama, M., and M.A. Iqbal. 2021. CHL1 deletion is associated with cognitive and language disabilities - Case report and review of literature. *Mol Genet Genomic Med.* 9:e1725.

Tzioras, M., C. Davies, A. Newman, R. Jackson, and T. Spires-Jones. 2019. Invited Review: APOE at the interface of inflammation, neurodegeneration and pathological protein spread in Alzheimer's disease. *Neuropathol Appl Neurobiol.* 45:327-346.

Uhlen, M., M.J. Karlsson, A. Hober, A.S. Svensson, J. Scheffel, D. Kotol, W. Zhong, A. Tebani, L. Strandberg, F. Edfors, E. Sjostedt, J. Mulder, A. Mardinoglu, A. Berling, S. Ekblad, M. Dannemeyer, S. Kanje, J. Rockberg, M. Lundqvist, M. Malm, A.L. Volk, P. Nilsson, A. Manberg, T. Dodig-Crnkovic, E. Pin, M. Zwahlen, P. Oksvold, K. von Feilitzen, R.S. Haussler, M.G. Hong, C. Lindskog, F. Ponten, B. Katona, J. Vuu, E. Lindstrom, J. Nielsen, J. Robinson, B. Ayoglu, D. Mahdessian, D. Sullivan, P. Thul, F. Danielsson, C. Stadler, E. Lundberg, G. Bergstrom, A. Gummesson, B.G. Voldborg, H. Tegel, S. Hober, B. Forsstrom, J.M. Schwenk, L. Fagerberg, and A. Sivertsson. 2019. The human secretome. *Sci Signal.* 12.

Valla, J., R. Yaari, A.B. Wolf, Y. Kusne, T.G. Beach, A.E. Roher, J.J. Corneveaux, M.J. Huentelman, R.J. Caselli, and E.M. Reiman. 2010. Reduced posterior cingulate mitochondrial activity in expired young adult carriers of the APOE epsilon4 allele, the major late-onset Alzheimer's susceptibility gene. *J Alzheimers Dis.* 22:307-313.

Van Battum, E.Y., S. Brignani, and R.J. Pasterkamp. 2015. Axon guidance proteins in neurological disorders. *Lancet Neurol.* 14:532-546.

Vanderhaeghen, P., and H.J. Cheng. 2010. Guidance molecules in axon pruning and cell death. *Cold Spring Harb Perspect Biol.* 2:a001859.

Vawter, M.P. 2000. Dysregulation of the neural cell adhesion molecule and neuropsychiatric disorders. *Eur J Pharmacol.* 405:385-395.

Velmeshev, D., L. Schirmer, D. Jung, M. Haeussler, Y. Perez, S. Mayer, A. Bhaduri, N. Goyal, D.H. Rowitch, and A.R. Kriegstein. 2019. Single-cell genomics identifies cell type-specific molecular changes in autism. *Science.* 364:685-689.

Venkataraman, A.V., A. Mansur, G. Rizzo, C. Bishop, Y. Lewis, E. Kocagoncu, A. Lingford-Hughes, M. Huiban, J. Passchier, J.B. Rowe, H. Tsukada, D.J. Brooks, L. Martarello, R.A. Comley, L. Chen, A.J. Schwarz, R. Hargreaves, R.N. Gunn, E.A. Rabiner, and P.M. Matthews. 2022. Widespread cell stress and mitochondrial dysfunction occur in patients with early Alzheimer's disease. *Sci Transl Med.* 14:eabk1051.

von Jagow, G., and T.A. Link. 1986. Use of specific inhibitors on the mitochondrial bc1 complex. *Methods Enzymol.* 126:253-271.

Wadhwani, A.R., A. Affaneh, S. Van Gulden, and J.A. Kessler. 2019. Neuronal apolipoprotein E4 increases cell death and phosphorylated tau release in alzheimer disease. *Ann Neurol.* 85:726-739.

Wang, C., W.A. Wilson, S.D. Moore, B.E. Mace, N. Maeda, D.E. Schmechel, and P.M. Sullivan. 2005. Human apoE4-targeted replacement mice display synaptic deficits in the absence of neuropathology. *Neurobiol Dis*. 18:390-398.

Wang, C., M. Xiong, M. Gratuze, X. Bao, Y. Shi, P.S. Andhey, M. Manis, C. Schroeder, Z. Yin, C. Madore, O. Butovsky, M. Artyomov, J.D. Ulrich, and D.M. Holtzman. 2021. Selective removal of astrocytic APOE4 strongly protects against tau-mediated neurodegeneration and decreases synaptic phagocytosis by microglia. *Neuron*. 109:1657-1674 e1657.

Wang, W., F. Zhao, X. Ma, G. Perry, and X. Zhu. 2020. Mitochondria dysfunction in the pathogenesis of Alzheimer's disease: recent advances. *Mol Neurodegener*. 15:30.

Wedenoja, J., A. Tuulio-Henriksson, J. Suvisaari, A. Loukola, T. Paunio, T. Partonen, T. Varilo, J. Lonnqvist, and L. Peltonen. 2010. Replication of association between working memory and Reelin, a potential modifier gene in schizophrenia. *Biol Psychiatry*. 67:983-991.

Weeber, E.J., U. Beffert, C. Jones, J.M. Christian, E. Forster, J.D. Sweatt, and J. Herz. 2002. Reelin and ApoE receptors cooperate to enhance hippocampal synaptic plasticity and learning. *J Biol Chem*. 277:39944-39952.

Wernette-Hammond, M.E., S.J. Lauer, A. Corsini, D. Walker, J.M. Taylor, and S.C. Rall, Jr. 1989. Glycosylation of human apolipoprotein E. The carbohydrate attachment site is threonine 194. *J Biol Chem*. 264:9094-9101.

West, A.P., W. Khoury-Hanold, M. Staron, M.C. Tal, C.M. Pineda, S.M. Lang, M. Bestwick, B.A. Duguay, N. Raimundo, D.A. MacDuff, S.M. Kaech, J.R. Smiley, R.E. Means, A. Iwasaki, and G.S. Shadel. 2015. Mitochondrial DNA stress primes the antiviral innate immune response. *Nature*. 520:553-557.

Westmark, C.J., D.K. Sokol, B. Maloney, and D.K. Lahiri. 2016. Novel roles of amyloid-beta precursor protein metabolites in fragile X syndrome and autism. *Mol Psychiatry*. 21:1333-1341.

Wieckowski, M.R., C. Giorgi, M. Lebiedzinska, J. Duszynski, and P. Pinton. 2009. Isolation of mitochondria-associated membranes and mitochondria from animal tissues and cells. *Nat Protoc*. 4:1582-1590.

Wingo, A.P., E.B. Dammer, M.S. Breen, B.A. Logsdon, D.M. Duong, J.C. Troncosco, M. Thambisetty, T.G. Beach, G.E. Serrano, E.M. Reiman, R.J. Caselli, J.J. Lah, N.T. Seyfried, A.I. Levey, and T.S. Wingo. 2019. Large-scale proteomic analysis of human brain identifies proteins associated with cognitive trajectory in advanced age. *Nat Commun*. 10:1619.

Wingo, A.P., W. Fan, D.M. Duong, E.S. Gerasimov, E.B. Dammer, Y. Liu, N.V. Harerimana, B. White, M. Thambisetty, J.C. Troncoso, N. Kim, J.A. Schneider, I.M. Hajjar, J.J. Lah, D.A. Bennett, N.T. Seyfried, A.I. Levey, and T.S. Wingo. 2020. Shared proteomic effects of cerebral atherosclerosis and Alzheimer's disease on the human brain. *Nat Neurosci*. 23:696-700.

Wingo, T.S., Y. Liu, E.S. Gerasimov, S.M. Vattathil, M.E. Wynne, J. Liu, A. Lori, V. Faundez, D.A. Bennett, N.T. Seyfried, A.I. Levey, and A.P. Wingo. 2022. Shared mechanisms across the major psychiatric and neurodegenerative diseases. *Nat Commun*. 13:4314.

Wynne, M.E., A.R. Lane, K.S. Singleton, S.A. Zlatic, A. Gokhale, E. Werner, D. Duong, J.Q. Kwong, A.J. Crocker, and V. Faundez. 2021. Heterogeneous Expression of

Nuclear Encoded Mitochondrial Genes Distinguishes Inhibitory and Excitatory Neurons. *eNeuro*. 8.

Xia, Y., Z.H. Wang, J. Zhang, X. Liu, S.P. Yu, K.X. Ye, J.Z. Wang, K. Ye, and X.C. Wang. 2021. C/EBPbeta is a key transcription factor for APOE and preferentially mediates ApoE4 expression in Alzheimer's disease. *Mol Psychiatry*. 26:6002-6022.

Xu, B., P.K. Hsu, K.L. Stark, M. Karayiorgou, and J.A. Gogos. 2013. Derepression of a neuronal inhibitor due to miRNA dysregulation in a schizophrenia-related microdeletion. *Cell*. 152:262-275.

Xu, B., J.L. Roos, S. Levy, E.J. van Rensburg, J.A. Gogos, and M. Karayiorgou. 2008. Strong association of de novo copy number mutations with sporadic schizophrenia. *Nat Genet*. 40:880-885.

Yan, L., A. Shamir, M. Skirzewski, E. Leiva-Salcedo, O.B. Kwon, I. Karavanova, D. Paredes, O. Malkesman, K.R. Bailey, D. Vullhorst, J.N. Crawley, and A. Buonanno. 2018. Neuregulin-2 ablation results in dopamine dysregulation and severe behavioral phenotypes relevant to psychiatric disorders. *Mol Psychiatry*. 23:1233-1243.

Yao, J., R.W. Irwin, L. Zhao, J. Nilsen, R.T. Hamilton, and R.D. Brinton. 2009. Mitochondrial bioenergetic deficit precedes Alzheimer's pathology in female mouse model of Alzheimer's disease. *Proc Natl Acad Sci U S A*. 106:14670-14675.

Yeh, F.L., Y. Wang, I. Tom, L.C. Gonzalez, and M. Sheng. 2016. TREM2 Binds to Apolipoproteins, Including APOE and CLU/APOJ, and Thereby Facilitates Uptake of Amyloid-Beta by Microglia. *Neuron*. 91:328-340.

Yen, K., C. Lee, H. Mehta, and P. Cohen. 2013. The emerging role of the mitochondrial-derived peptide humanin in stress resistance. *J Mol Endocrinol*. 50:R11-19.

Yilmaz, M., E. Yalcin, J. Presumey, E. Aw, M. Ma, C.W. Whelan, B. Stevens, S.A. McCarroll, and M.C. Carroll. 2021. Overexpression of schizophrenia susceptibility factor human complement C4A promotes excessive synaptic loss and behavioral changes in mice. *Nat Neurosci*. 24:214-224.

Yin, J., E.M. Reiman, T.G. Beach, G.E. Serrano, M.N. Sabbagh, M. Nielsen, R.J. Caselli, and J. Shi. 2020. Effect of ApoE isoforms on mitochondria in Alzheimer disease. *Neurology*. 94:e2404-e2411.

Zalocusky, K.A., R. Najm, A.L. Taubes, Y. Hao, S.Y. Yoon, N. Koutsodendris, M.R. Nelson, A. Rao, D.A. Bennett, J. Bant, D.J. Amornkul, Q. Xu, A. An, O. Cisne-Thomson, and Y. Huang. 2021. Neuronal ApoE upregulates MHC-I expression to drive selective neurodegeneration in Alzheimer's disease. *Nat Neurosci*. 24:786-798.

Zaremba, J.D., A. Diamantopoulou, N.B. Danielson, A.D. Grosmark, P.W. Kaifosh, J.C. Bowler, Z. Liao, F.T. Sparks, J.A. Gogos, and A. Losonczy. 2017. Impaired hippocampal place cell dynamics in a mouse model of the 22q11.2 deletion. *Nat Neurosci*. 20:1612-1623.

Zehnder, T., F. Petrelli, J. Romanos, E.C. De Oliveira Figueiredo, T.L. Lewis, Jr., N. Deglon, F. Polleux, M. Santello, and P. Bezzi. 2021. Mitochondrial biogenesis in developing astrocytes regulates astrocyte maturation and synapse formation. *Cell Rep*. 35:108952.

Zemni, R., T. Bienvenu, M.C. Vinet, A. Sefiani, A. Carrie, P. Billuart, N. McDonell, P. Couvert, F. Francis, P. Chafey, F. Fauchereau, G. Friocourt, V. des Portes, A.

Cardona, S. Frints, A. Meindl, O. Brandau, N. Ronce, C. Moraine, H. van Bokhoven, H.H. Ropers, R. Sudbrak, A. Kahn, J.P. Fryns, C. Beldjord, and J. Chelly. 2000. A new gene involved in X-linked mental retardation identified by analysis of an X;2 balanced translocation. *Nat Genet*. 24:167-170.

Zhang, D., Z. Tang, H. Huang, G. Zhou, C. Cui, Y. Weng, W. Liu, S. Kim, S. Lee, M. Perez-Neut, J. Ding, D. Czyz, R. Hu, Z. Ye, M. He, Y.G. Zheng, H.A. Shuman, L. Dai, B. Ren, R.G. Roeder, L. Becker, and Y. Zhao. 2019. Metabolic regulation of gene expression by histone lactylation. *Nature*. 574:575-580.

Zhang, J., and Q. Zhang. 2019. Using Seahorse Machine to Measure OCR and ECAR in Cancer Cells. *Methods Mol Biol*. 1928:353-363.

Zhang, Y., C. Pak, Y. Han, H. Ahlenius, Z. Zhang, S. Chanda, S. Marro, C. Patzke, C. Acuna, J. Covy, W. Xu, N. Yang, T. Danko, L. Chen, M. Wernig, and T.C. Sudhof. 2013. Rapid single-step induction of functional neurons from human pluripotent stem cells. *Neuron*. 78:785-798.

Zhou, Y., B. Zhou, L. Pache, M. Chang, A.H. Khodabakhshi, O. Tanaseichuk, C. Benner, and S.K. Chanda. 2019. Metascape provides a biologist-oriented resource for the analysis of systems-level datasets. *Nat Commun*. 10:1523.

Zhu, S., V. Shanbhag, V.L. Hodgkinson, and M.J. Petris. 2016. Multiple di-leucines in the ATP7A copper transporter are required for retrograde trafficking to the trans-Golgi network. *Metallomics*. 8:993-1001.

Zinkstok, J.R., E. Boot, A.S. Bassett, N. Hiroi, N.J. Butcher, C. Vingerhoets, J.A.S. Vorstman, and T. van Amelsvoort. 2019. Neurobiological perspective of 22q11.2 deletion syndrome. *Lancet Psychiatry*. 6:951-960.

Zurek, A.A., S.W. Kemp, Z. Aga, S. Walker, M. Milenkovic, A.J. Ramsey, E. Sibille, S.W. Scherer, and B.A. Orser. 2016. alpha5GABAA receptor deficiency causes autism-like behaviors. *Ann Clin Transl Neurol*. 3:392-398.

Zurita Rendon, O., L. Silva Neiva, F. Sasarman, and E.A. Shoubridge. 2014. The arginine methyltransferase NDUFAF7 is essential for complex I assembly and early vertebrate embryogenesis. *Hum Mol Genet*. 23:5159-5170.